UNIVERSITY OF CALIFORNIA, SAN DIEGO

Syndecan-1, a Clearance Receptor for Triglyceride-Rich Lipoproteins

A dissertation submitted in partial satisfaction of the requirements
of the degree Doctor of Philosophy

in

Biomedical Sciences

by

Erin Marie Foley

Committee in Charge:

Professor Jeffrey D. Esko, Chair
Professor Susan Ferro-Novick
Professor Richard L. Gallo
Professor Randolph Y. Hampton
Professor Joseph L. Witztum

2012

The dissertation of Erin Marie Foley is approved, and it is acceptable in quality and form for publication on microfilm and electronically:

_____

_____

_____

_____

_____

Chair

University of California, San Diego

2012

DEDICATION

I dedicate this dissertation to my silly and wonderful family:

To my mom, Ruth, who always taught me
that my best is everyone else's medium,

To my dad, Mark, who is either a stellar wakeboarder
or an epic racecar driver, or, umm, both dude,

and

To my sister, Katie, who is not a witch.

Love ya mean it.

EPIGRAPH

Success is never final,
Failure is never fatal.
It's courage that counts.

~John Wooden
Legendary UCLA Basketball Coach

TABLE OF CONTENTS

LIST OF ABBREVIATIONS

AdSdc1	adenovirus containing syndecan-1 cDNA
AlbCre	Cre transgene driven by rat albumin promoter
APO/Apo	apolipoprotein
APOE/ApoE	apolipoprotein E
APOB/ApoB	apolipoprotein B
APOA/ApoA	apolipoprotein A
APOC/ApoC	apolipoprotein C
APOAV/ApoAV	apolipoprotein AV
AUC	area under the curve
CR	chylomicron remnant
CS	chondroitin sulfate
FPLC	fast-phase liquid chromatography
GAG	glycosaminoglycan
GlcA	*D*-glucuronic acid
GlcNAc	*N*-acetyl-*D*-glucosamine
HDL	high density lipoprotein
HS	heparan sulfate
HSPG	heparan sulfate proteoglycan
IDL	intermediate density lipoprotein
IdoA	*L*-iduronic acid
LDL	low density lipoprotein
LDLR/Ldlr	LDL receptor
LPL/Lpl	lipoprotein lipase
LRP1/Lrp1	LDL receptor-related protein
NDST/Ndst	*N*-deacetylase *N*-sulfotransferase
OST/Ost	*O*-sulfotranferase
SDC/Sdc	syndecan
Tie2Cre	Cre transgene driven by the Tie2 promoter
TRL	triglyceride-rich lipoprotein
TC	total cholesterol
TG	triglyceride
VLDL	very low density lipoprotein

LIST OF FIGURES AND TABLES

ACKNOWLEDGEMENTS

The past six years have been a tremendous learning experience, and I could not have made it through without the help of several incredibly generous individuals. First, I'd like to thank my advisor Jeff Esko for his patience, his time, his unwavering support, and his insights into the meaning behind ABC's *Lost*. I also thank my thesis committee members, Susan Ferro-Novick, Richard Gallo, Randy Hampton, and Joseph Witztum for their advice and guidance during this process. I am grateful to Marilyn Farquhar for providing me with financial support through the Predoctoral and Postdoctoral Training in Cancer Cell Biology grant (5T32CA067754-17).

I would also like to thank past and present members of the Esko lab, especially Kristin Stanford, Jon Gonzales, Philip Gordts, Rusty Bishop, Roger Lawrence and Yiping Deng for their collaborative help with the work presented in this thesis. Danyin Song, Ding Xu, Patrick Secrest, Adam Cadwallader, Emylie Seamen, Angie Trieu and Carlos Lameda-Diaz have also provided invaluable support in the planning and execution of my experiments. I'd also like to thank GRTC manager Peili Hsu for taking such good care of us (the kids).

Many others at UCSD assisted with my research. Qiongyu Chen and David Ditto in the Hematology Core collected blood samples from my mice and helped with serum chemistry analysis. From the Witztum laboratory, Joe Juliano and Jennifer Pattison assisted with lipoprotein analysis. Timo Merloo in the EM Core trained me to use the electron microscope and assisted with lipoprotein sizing studies. From the Varki Lab, Sandra Diaz taught me how to use numerous pieces of equipment. Pyong

Park (Harvard) assisted with adenovirus creation, and Anne Zaiss (UCLA) taught me how to purify and titer viruses.

Chapter 1 is reprinted with minor modifications from *Progress in Molecular Biology and Translational Science,* Volume 93, Erin M. Foley and Jeffrey D. Esko, "Hepatic heparan sulfate proteoglycans and endocytic clearance of triglyceride-rich lipoproteins", Pages 213-33, Copyright © (2010), with permission from Elsevier.

Section 2.2, section 2.4, and appendix A contain material reprinted from The Journal of Clinical Investigation, Volume 119, Issue 11, Kristin I. Stanford, Joseph R. Bishop, Erin M. Foley, Jon C. Gonzales, Ingrid R. Niesman, Joseph L. Witztum, Jeffrey D. Esko, "Syndecan-1 is the primary heparan sulfate proteoglycan mediating hepatic clearance of triglyceride-rich lipoproteins in mice", Pages 3236-45, Copyright © (2009), The American Society for Clinical Investigation.

Sections 2.3, section 2.5, and appendix C contain material reprinted from Hepatology, Volume 55, Issue 1, Yiping Deng, Erin M. Foley, Jon C. Gonzales, Philip Gordts, Yulin Li, and Jeffrey D. Esko, "Shedding of syndecan-1 from human hepatocytes alters VLDL clearance", Pages 277-86, Copyright © (2009) with permission from John Wiley and Sons.

Section 2.5 and appendix B contain material reprinted from The Journal of Biological Chemistry, Volume 285, Issue 19, Joseph R. Bishop, Erin Foley, Roger Lawrence, and Jeffrey D. Esko, "Insulin-dependent diabetes mellitus in mice does not alter liver heparan sulfate", Pages 14658-62, Copyright © (2010), American Society for Biochemistry and Molecular Biology.

Work presented in chapter 3 will be submitted for publication to the Journal of Biological Chemistry with coauthors Kristin I. Stanford, Philip P.L.S.M Gordts, Jon C. Gonzales, Roger Lawrence, and Jeffrey D. Esko. The dissertation author was the primary author of this work. Together with her coauthors, the dissertation author would like to thank Jennifer Pattison and Joe Juliano for their assistance with FPLC and lipid analysis. We would also like to thank Timo Merloo and Marilyn Farquhar for technical assistance with electron microscopy. We acknowledge Carlos Lameda Diaz for his kind assistance with glycosaminoglycan isolation. We are grateful to Joe Witztum for helpful discussions. This work was supported by NIH grant GM33063 (to J.D. Esko) and training grant 5T32CA067754-17 (to E.M. Foley). Work was conducted within the department of Cellular and Molecular Medicine, and the Glycobiology Research and Training Center, University of California, San Diego, La Jolla, California.

CURRICULUM VITAE

Education:

2006 Bachelor of Science, Biochemistry
University of California Los Angeles

2012 Doctor of Philosophy, Biomedical Sciences
University of California, San Diego

Publications:

Foley, E.M., Stanford, K.I., Gordts, P.L.S.M., Gonzales, J.C., Lawrence, R. and Esko, J.D. Heparan sulfate proteoglycans mediate hepatic clearance of triglyceride-rich lipoproteins of unique size and composition. *In preparation.*

Deng, Y., **Foley, E.M.,** Gonzales, J.C., Gordts, P.L., Li, Y., and Esko, J.D. 2012. Shedding of syndecan-1 from human hepatocytes alters VLDL clearance. *Hepatology* 55: 277-86.

Foley, E.M., and Esko, J.D. 2010. Hepatic heparan sulfate proteoglycans and endocytic clearance of triglyceride-rich lipoproteins. *Progress in Molecular Biology and Translational Science* 93:213-233.

Bishop, J.R., **Foley, E.,** Lawrence, R., and Esko, J.D. 2010. Insulin-dependent diabetes mellitus in mice does not alter liver heparan sulfate. *The Journal of Biological Chemistry* 285:14658-14662.

Stanford, K.I., Bishop, J.R., **Foley, E.M.,** Gonzales, J.C., Niesman, I.R., Witztum, J.L., and Esko, J.D. 2009. Syndecan-1 is the primary heparan sulfate proteoglycan mediating hepatic clearance of triglyceride-rich lipoproteins in mice. *The Journal of Clinical Investigation* 119:3236-3245.

ABSTRACT OF THE DISSERTATION

Syndecan-1, a Clearance Receptor for Triglyceride-Rich Lipoproteins

by

Erin Marie Foley

Doctor of Philosophy in Biomedical Sciences

University of California, San Diego, 2012

Professor Jeffrey D. Esko, Chair

Triglyceride-rich remnant lipoproteins are cleared from the circulation by hepatic receptors including the low density lipoprotein receptor (Ldlr), the Ldlr-related protein, and heparan sulfate proteoglycans (HSPGs). This dissertation describes the identification of syndecan-1 as the primary heparan sulfate proteoglycan receptor for remnant lipoproteins in the liver, characterizes its function as a receptor, and defines its relative contribution to clearance in the context of other known receptors. Chapter 1 serves as a primer on lipoprotein metabolism, provides background information about sydecan-1 structure, function and regulation, and reviews relevant literature

implicating syndecan-1 in lipoprotein clearance. Chapter 2 demonstrates the contribution of syndecan-1 to clearance in mice and in human hepatocytes, analyzes elements of syndecan-1 structure that are important for its function as an endocytic receptor, and discusses the influence of syndecan-1 in disease-associated hypertriglyceridemia. Chapter 3 introduces a new mouse model in which three hepatocyte lipoprotein receptors – Ldlr, Lrp1, and HSPGs – have been inactivated. Using this model, it is shown that HSPGs mediate clearance of triglyceride-rich lipoproteins of unique size and apolipoprotein composition. Chapter 4 reviews ongoing and future studies of syndecan-1 as a clearance receptor for triglyceride-rich lipoprotein remnants and discusses the broader implications of this work.

CHAPTER 1

Introduction: Hepatic heparan sulfate proteoglycans and endocytic clearance of triglyceride-rich lipoproteins

1.1 Summary

Hypertriglyceridemia, characterized by the accumulation of triglyceride-rich lipoproteins in the blood, affects 10–20% of the population in western countries and increases the risk of atherosclerosis, coronary artery disease, and pancreatitis. The etiology of hypertriglyceridemia is complex, and much interest exists in identifying and characterizing the biological and environmental factors that affect the synthesis and turnover of plasma triglycerides. Genetic studies in mice have recently identified heparan sulfate proteoglycans as a class of receptors that mediates the clearance of triglyceride-rich lipoproteins in the liver. Heparan sulfate proteoglycans are expressed by endothelial cells that line the hepatic sinusoids and the underlying hepatocytes, and are present in the perisinusoidal space (space of Disse).

The purpose of this thesis is to characterize the heparan sulfate proteoglycan syndecan-1 as a clearance receptor for triglyceride-rich lipoproteins. This introductory chapter will describe syndecan-1 structure and regulation, provide background information about the identification of syndecan-1 as the primary proteoglycan that mediates triglyceride-rich lipoprotein clearance, and discuss the dependence of lipoprotein binding on heparan sulfate fine structure.

1.2 Lipoprotein metabolism

Lipoproteins transport triglycerides, cholesterol, and phospholipids through the blood for distribution and use throughout the body. These particles consist of noncovalent associations of lipid and protein and contain a hydrophobic core of cholesterol ester and triglyceride enveloped by a monolayer of phospholipids, unesterified cholesterol, and apolipoproteins. Lipoprotein classes differ in density, size, function, and lipid and apolipoprotein content.

The triglyceride-rich lipoproteins are functionally defined as the fraction of plasma lipoproteins that have a density of less than 1.006 g/mL. Triglyceride-rich lipoproteins arise from both exogenous (dietary) and endogenous (liver) sources. Dietary triglyceride is packaged into large, buoyant chylomicrons, which contain APOB48, APOCII, and APOE, by the mucosal cells that line the intestine. In circulation, chylomicrons encounter lipoprotein lipase (LPL), which is anchored to the endothelial surface by its receptor GPIHBP1 (1). LPL hydrolyzes the triglycerides in the core of these particles into free fatty acids, which can then be used for energy production or storage. The inner core is partially depleted of triglycerides by lipolysis, resulting in the formation of chylomicron remnants. These smaller remnant particles pass through the fenestrated endothelium of the liver sinusoids and are sequestered in the space of Disse. Here, the remnant lipoproteins become enriched in APOE, undergo further processing by LPL and hepatic lipase (HL), and are cleared by one of several endocytic receptors (2).

The liver packages endogenous fats into very low density lipoproteins (VLDLs) that contain APOB100 (and ApoB48 in the mouse). VLDLs also encounter

LPL in the circulation and, after hydrolysis, are converted into VLDL remnants and intermediate density lipoproteins (IDLs). Like chylomicron remnants, VLDL remnants enter into the hepatic space of Disse and may be cleared from the circulation. IDLs that remain in the circulation are further processed by HL and, in humans, by the cholesterol ester transfer protein (CETP), resulting in the formation of cholesterol-rich low density lipoproteins (LDL). The liver also synthesizes high density lipoproteins (HDL) that transport surplus cholesterol from the periphery back to the liver (3). This process is called reverse cholesterol transport.

In the liver, several endocytic receptors mediate the clearance of triglyceride-rich lipoproteins from circulation. The first to be identified was the LDL receptor (LDLR), initially described by Brown and Goldstein (4). Mice, rabbits, and humans with inactivating mutations in the LDLR gene have high levels of cholesterol and exhibit a modest accumulation of triglycerides (5-7), suggesting that LDLR is responsible for some, but not all, triglyceride-rich lipoprotein clearance. Herz and colleagues later identified another group of endocytic receptors bearing structural homology to LDLR, the LDLR-related proteins (LRPs) (8, 9). Though LRPs bind and internalize remnants enriched in APOE (10), they also have diverse functions in signaling, neurotransmission, and cellular entry of toxins and viruses (11). The liver makes LRP1 and LRP5, but these proteins are also widely expressed in other tissues (9, 12). Systemic LRP1 null mice are not viable (13). Liver-specific ablation of LRP1 does not result in remnant particle accumulation unless compounded with LDLR deficiency (14, Chapter 3). Systemic LRP5 null mice are viable, but do not accumulate remnant particles unless they are subjected to a high fat diet (15). VLDLR, another

member of the LRP family, mediates clearance of APOE-rich triglyceride-rich lipoproteins in the periphery (heart, muscle, adipose tissue, macrophages) but is not expressed in the liver (16). *Vldlr*$^{-/-}$ mice have normal levels of plasma lipids, and the role of VLDLR in triglyceride-rich lipoprotein clearance becomes apparent only after severely stressing triglyceride metabolism (17-19).

The lipolysis-stimulated lipoprotein receptor (LSR) is also a candidate receptor, though its exact role in triglyceride-rich lipoprotein clearance is still under study. Upon activation by free fatty acids, LSR undergoes a conformational change and binds to APOB- and APOE-containing lipoproteins (20, 21). Liver-specific knockdown of LSR expression leads to hypertriglyceridemia in the fed state, but fasting triglyceride levels are normal (22). Heterozygous *Lsr*$^{+/-}$ mice have delayed postprandial clearance of triglyceride-rich lipoproteins (23), but systemic inactivation of LSR leads to embryonic lethality (24), alluding to perhaps other roles for this protein. Other receptors of note include the Scavenger Receptor BI (SR-B1). Though some evidence suggests that SR-B1 can mediate clearance of VLDLs and chylomicrons in vivo (25-27), its major role is in HDL clearance (28).

1.3 Syndecan-1 and remnant lipoprotein clearance

A large body of work has suggested that heparan sulfate proteoglycans act in the clearance of triglyceride-rich lipoproteins. These studies, pioneered in the laboratories of K.J. Williams and R.W. Mahley, reported decreased lipoprotein uptake in cells treated with heparinases that degrade heparan sulfate chains, pharmacological agents that manipulate glycosaminoglycan biosynthesis, or in Chinese hamster ovary

(CHO) cell mutants lacking specific heparan sulfate biosynthetic enzymes (29-37). Upon infusion of mice with lactoferrin, heparinase, or heparan sulfate mimetics, which bind, degrade, or compete with heparan sulfate respectively, reduced plasma clearance rates and hepatic uptake of labeled VLDL were observed as well (38-40). Furthermore, it was shown that heparan sulfate was localized on hepatocyte basal membranes facing the space of Disse in the liver by using immunoelectron microscopy (41, 42).

In tissue culture models, lipoproteins can bind to several proteoglycans. Fuki *et al*. have described increased cell association and uptake of LPL-enriched lipoproteins by CHO cells transfected with expression constructs for the transmembrane proteoglycans syndecan-1, -2, and -4, though the greatest effect was seen in the syndecan-1 expressing cells (43). They also showed that WiDr cells, a variant colon carcinoma line expressing only the secreted proteoglycan perlecan, were able to bind, internalize, and degrade LPL-enriched lipoproteins (44). In another study, transfection of an antisense oligonucleotide to syndecan-1 and treatment with an antibody against syndecan-1 decreased the binding of remnant particles to human HepG2 hepatoma cells by 50–70% (45).

A recent study in syndecan-1 knockout mice (*Sdc1*$^{-/-}$) has provided genetic evidence that syndecan-1 is the primary heparan sulfate proteoglycan that mediates the clearance of triglyceride-rich lipoproteins *in vivo* (46). In the fasted state, Sdc1-deficient mice accumulate triglycerides in approximately twofold excess compared to the wild type, but have normal cholesterol levels (Table 1-1). The accumulated particles consist of chylomicron remnants, VLDLs, and IDLs containing ApoB100,

ApoB48, ApoE, ApoAI, and ApoCs. The clearance of intestinally derived chylomicrons is delayed in *Sdc1*$^{-/-}$ mice, and restoring syndecan-1 expression in the liver, using adenovirus, corrects the postprandial clearance defect *in vivo*. Though these results disagree with a previous study in which infection with an adenovirus containing syndecan-1 caused hypertriglyceridemia (47), the disparity may have been caused by differences in viral load between the two studies, timing of lipid analysis relative to viral infection, or acute liver injury caused by the virus. Importantly, syndecan-1 facilitates uptake and degradation of labeled VLDL in cultured hepatocytes. Taken together, these findings suggest that syndecan-1 is the long sought-after receptor that works in parallel with Ldlr in the clearance of triglyceride-rich lipoproteins *in vivo*.

Table 1-1: *Fasting lipid levels in heparan sulfate biosynthetic and proteoglycan mutant mice.*

Genotype	Triglycerides (mg/dL)	Cholesterol (mg/dL)	Reference
Wildtype	38 - 58	70 - 98	(46, 48, 49)
Ndst1$^{f/f}$*AlbCre*$^{+}$	91.7 ± 35.0	81.4 ± 9.1	(48)
Hs2st$^{f/f}$*AlbCre*$^{+}$	100 ± 10	98 ± 4	(49)
Hs6st1$^{f/f}$*AlbCre*$^{+}$	80 ± 27		(49)
Sdc1$^{-/-}$	95 ± 11	70 ± 1	(46)
Sdc3$^{-/-}$	49 ± 8		(46)
Sdc4$^{-/-}$	59 ± 11		(46)

Abbreviations: *Ndst1*, *N*-acetyl-*D*-glucosamine *N*-deacetylase/*N*-sulfotransferase 1; *Alb*, albumin; *Cre*, Cre recombinase; *Sdc*, syndecan; *Hs2st*, uronyl 2-O-sulfotransferase; *Hs6st1*, glucosaminyl 6-*O*-sulfotransferase 1.

1.4 Syndecan-1 structure and regulation

Syndecan-1 is a type-I transmembrane proteoglycan, containing three extracellular attachment sites for heparan sulfate and two for chondroitin sulfate (Figure 1-1; Ref. (50)). Occupation levels of these sites varies in different cell types (51), but its most active form contains heparan sulfate at all three N-terminal sites (52, 53). Syndecan-1 was first described by Bernfield and colleagues in mammary epithelial cells (54, 55) and has diverse functions in cell adhesion and motility (56), tumorigenesis (57), and microbial infection (58). Syndecan-1 contains a juxtamembrane cleavage site (59), allowing protease-mediated shedding of the ectodomain and glycosaminoglycan chains (60).

As syndecan-1 plays a major role in the clearance of triglycerides, the regulation of its expression and activity are of great interest. Syndecan-1 expression is partially controlled by nuclear hormone receptors. These receptors are activated by small, lipophilic ligands and subsequently translocate into the nucleus to alter gene expression (62). The farnesoid-X-receptor (FXR) has been shown to bind a nonconsensus DR-1 element in the syndecan-1 promoter and to increase expression of the SDC1 gene in HepG2 human hepatoma cells (63). FXR agonists increased binding, uptake, and degradation of radiolabeled methylated LDL, a chemically modified form of LDL that no longer binds to LDLR or LRP. Though FXR modulates expression of other factors involved in lipoprotein metabolism, including APOCII (64) and APOE (65), regulation of syndecan-1 by FXR might also contribute to lipoprotein uptake in humans. Syndecan-1 expression in prostate cells is also controlled by peroxisome proliferator-activated receptor gamma (PPARγ), another nuclear hormone

receptor (66). Syndecan-1 mRNA was increased in the prostate gland of animals fed an n-3 polyunsaturated fatty acid-enriched diet. Similar effects were noted in the human prostate cancer cell line, PC-3. This effect was mimicked by a PPARγ agonist, troglitazone, and inhibited in the presence of a PPARγ antagonist. PPARγ-mediated regulation of syndecan-1 was also seen in human breast cancer cells treated with n-3 fatty acid-enriched LDLs (67). Whether PPARs influence syndecan-1 expression in hepatocytes is not known. These findings suggest that the ability of dietary n-3 fatty acids to ameliorate hypertriglyceridemia in patients may be partially due to the enhanced expression of syndecan-1.

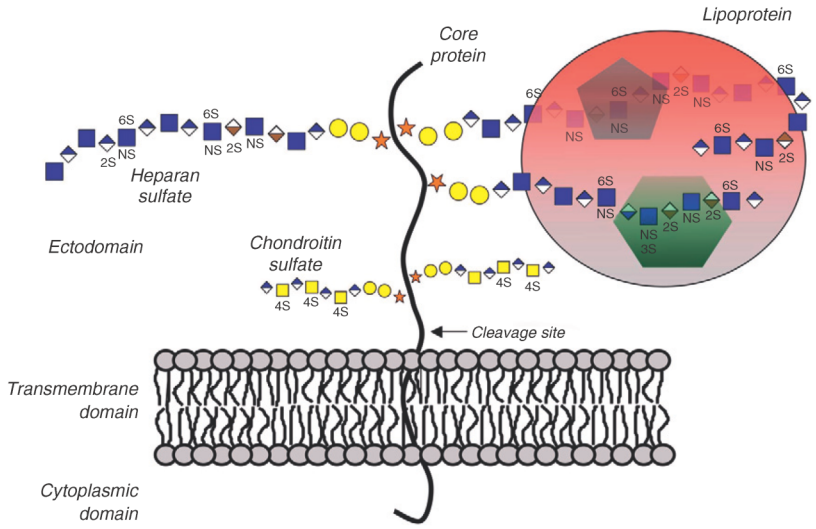

Figure 1-1: *Syndecan-1*. Syndecan-1 is a type-1 transmembrane protein bearing up to three heparan sulfate and two chondroitin/dermatan sulfate chains. It undergoes proteolytic cleavage, resulting in shedding of the large extracellular domain bearing the GAG chains. The short cytoplasmic tail interacts with a number of cytosolic proteins and may play a role in Sdc1 endocytosis. A lipoprotein is shown binding to the heparan sulfate chains via the interaction of short sulfated domains with apolipoproteins or lipases depicted by the large hexagon and pentagon. The GAG chains were rendered using the symbol nomenclature described in Ref. (61).

Syndecan-1 function is also regulated by proteolytic shedding. Proteolysis of syndecan-1 at a specific juxtamembrane cleavage site between amino acids A243 and S244 releases the extracellular ectodomain containing the glycosaminoglycan chains (59). Various metalloproteinases mediate syndecan-1 ectodomain shedding, including MMP-7 in lung epithelial cells (68), MMP-9 in HeLa cells and primary macrophages (69), and MMP-14 in HEK293T and HT1080 cells (70). Even though syndecan-1 shedding can occur constitutively, shedding is induced following the activation of both G-protein coupled receptors and protein tyrosine kinases by specific agonists, including thrombin and epidermal growth factor (71). Other shedding agonists include bacterial virulence factors (72) and phorbol esters such as phorbol myristic acid (PMA) (73). Although the biological significance of syndecan-1 shedding is unclear, it is often thought to attenuate syndecan-1 function. For example, syndecan-1 shedding protects against tissue damage during the inflammatory response by modulating the availability of chemokines (74).

Although syndecan-1 shedding has not been characterized in the liver, syndecan-1 ectodomains accumulate in conditioned media from cultured primary hepatocytes (75). Syndecan-1 shedding from hepatocytes may be a mechanism to downregulate its activity as a cell-surface endocytic receptor, but this process would increase the local concentration of free ectodomains in the space of Disse. Such free ectodomains might sequester triglyceride-rich lipoproteins in circulation and prevent their diffusion out of the space, or they might compete with cell-surface syndecan-1 or other receptors for lipoprotein binding. Thus, the functional significance of syndecan-1 shedding in the liver and the identification of the hepatic ‘‘sheddase’’ require further

study. Small molecules or antibodies that inhibit syndecan shedding may prove to be useful research tools or may have pharmacological relevance in the treatment of dyslipidemias. Syndecan-1 shedding is discussed further in Chapter 2.

Syndecan-1 is also regulated in an ‘‘inside-to-outside’’ manner via its cytoplasmic domain. The 34-amino acid cytoplasmic domain consists of two constant regions (C1 and C2) that are conserved among the four syndecan family members (50). The membrane-proximal region (C1) is thought to mediate syndecan dimerization and ligand binding (76, 77). The C2 region interacts with cytoskeletal proteins (78) and terminates in an EYFA domain that can bind the PDZ (postsynaptic density protein, Drosophila disc large tumor suppressor, and zonula occludens-1 protein) domain-containing proteins (79, 80). C1 and C2 flank a syndecan-specific variable region (V) that is believed to direct individual functions of the family members. The cytoplasmic domains of all syndecans contain four invariant tyrosine residues. Some studies have suggested that tyrosine phosphorylation promotes syndecan-1 shedding (81, 82). Another study reported that mutations in the tyrosine residues abrogates shedding, but that this inhibition occurred in a phosphorylation-independent manner (83). Also, these investigators found that the small GTPase Rab5 directly interacts with the cytoplasmic domain and acts as a molecular switch that regulates syndecan-1 shedding. It remains to be determined if cytoplasmic domain signaling regulates syndecan-1 endocytosis as well.

1.5 Structural features of heparan sulfate required for lipoprotein binding and clearance

Liver heparan sulfate is unique in its structure. The chains contain approximately 1.34 sulfates per disaccharide (84), which is roughly twice the amount observed in other mouse and human tissues but less than heparin (2–2.5 sulfates per disaccharide) (85). Liver heparan sulfate is rich in N-sulfated glucosamine and 2-O-sulfated iduronic acid, and contains a high proportion of trisulfated disaccharides (D2S6, disaccharide code described in Ref. (86)). The average chain is approximately 40–60 disaccharides long (Mr 14,000–22,000) (84, 87), which is shorter than heparan sulfate chains found in other tissues. These modified sugar residues are not equally dispersed throughout the chain and the highly sulfated disaccharides are clustered furthest (distal) from the protein core (84).

Studies using mutant mice with defects in heparan sulfate biosynthesis have identified structural features of the chains that are required for lipoprotein binding. One study focused on the enzyme *N*-acetylglucosamine *N*-deacetylase/*N*-sulfotransferase-1 (NDST1), which removes acetyl groups from subsets of N-acetylglucosamine residues and adds sulfate to the free amino groups. Systemic inactivation of Ndst1 in mice results in perinatal lethality due to brain, lung and other defects (88-90). To study the effect of inactivating Ndst1 in triglyceride-rich lipoprotein clearance, a mouse bearing a conditional allele of *Ndst1* was cross-bred to mice expressing the bacterial Cre recombinase under the control of the liver specific albumin promoter (*AlbCre*). $Ndst1^{f/f}AlbCre^{+}$ mice were viable and fertile (48) and have a phenotype that is essentially identical to $Sdc1^{-/-}$ mice (49); they accumulate

fasting triglycerides approximately two-fold (Table 1-1) and show delayed clearance of postprandial chylomicrons and injected human VLDL.

The deletion of Ndst1 in hepatocytes decreased overall sulfation of heparan sulfate by approximately 50% (48). Significant changes in disaccharide composition were also observed, as initial N-deacetylation and N-sulfation of N-acetylglucosamine residues are coupled to subsequent uronyl 2-O-sulfation and glucosaminyl 6-O-sulfation (91). N- and 2-O-sulfation of heparan sulfate isolated from highly purified *Ndst1*$^{f/f}$*AlbCre*$^{+}$ hepatocytes was decreased significantly compared to wildtype cells (decreased from 38 sulfate groups/100 disaccharides to 18 for N-sulfates and 17 sulfate groups/100 disaccharides to 4 for 2-O-sulfate groups, respectively). However, the abundance of 6-O-sulfated disaccharides was not significantly affected (31 sulfate groups/100 disaccharides in mutants vs. 26 in the wild type).

Accumulation of triglyceride-rich lipoproteins in *Ndst1*$^{f/f}$*Cre*$^{+}$ mice might have been caused by specific changes in heparan sulfate fine structure or simply by an overall reduction in charge. To address this question, plasma triglyceride levels were measured in mice with hepatocyte specific inactivation of either uronyl 2-O-sulfotransferase (*Hs2st*$^{f/f}$*AlbCre*$^{+}$) or glucosaminyl 6-O-sulfotransferase-1 (*Hs6st1*$^{f/f}$*AlbCre*$^{+}$) (49). As expected, *Hs2st*$^{f/f}$*AlbCre*$^{+}$ mice have dramatically reduced levels of 2-O-sulfated disaccharides (4 sulfate groups/100 disaccharides in mutants vs. 21 in wild-type littermates). These mice accumulate plasma triglycerides (Table 1-1) and have delayed clearance of intestinally derived chylomicrons and injected human VLDLs to approximately the same extent as observed in *Ndst1*$^{f/f}$*AlbCre*$^{+}$ and *Sdc1*$^{-/-}$ mice. In contrast, the *Hs6st1*$^{f/f}$*AlbCre*$^{+}$ mice do not exhibit any changes in plasma

triglycerides. The lack of phenotype might reflect a partial reduction in glucosamine 6-O-sulfation in *Hs6st1*$^{f/f}$*AlbCre*$^{+}$ hepatocytes due to the expression of other Hs6st isoforms or the enrichment of trisulfated disaccharides (92). However, 6-O-desulfated heparin competed for lipoprotein binding, at the surface of primary hepatocytes, to the same extent as unmodified heparin, whereas heparinoids lacking N-sulfate and 2-O-sulfate groups did not block binding. Taken together, these data demonstrate that plasma triglyceride-rich lipoprotein binding and uptake depends less on overall charge of the chains, and more on uronic acid 2-O-sulfation and glucosamine N-sulfation, with overall glucosamine 6-O-sulfation making little contribution. However, it has been suggested that specific 6-O-sulfate groups might be important (93).

1.6 Apolipoprotein and lipase interactions with heparan sulfate

The binding of heparan sulfate to protein ligands occurs through electrostatic interactions between the negatively charged sulfates and carboxyl groups on the polysaccharide with their complementary positively charged domains in the protein. These interactions are often highly specific; binding sites usually consist of 8–12 sugar residues with patterned arrangements of sulfated sugars and uronic acid epimers (91). This raises the question as to the identity of the apolipoprotein ligand on remnant lipoproteins that mediates binding to heparan sulfate. The binding sequences for LPL and APOE have been identified (Table 1-2) (94-97). However, care must be taken in interpreting these findings, since the physiological relevance of these interactions to remnant clearance has not been established in vivo through the study of mutants.

Table 1-2: *Apolipoproteins and lipases that bind heparin/heparan sulfate (from (98)).*

Ligand	Binding Specificity	References
APOE	Sequences rich in GlcNS6S-IdoA2s; heparin binding domains mapped	(94, 95, 98, 99)
APOB	Unknown, but interacts with heparan sulfate and heparin; heparin binding domains mapped	(100-102)
Hepatic Lipase	Heparin oligosaccharides; heparin binding domains mapped	(103-105)
Lipoprotein Lipase	Affinity for sequences rich in GlcNS6S-IdoA2S, modestly sulfated sequences	(96, 106)
Endothelial Lipase	Interacts with heparan sulfate	(107, 108)
APOAV	Interacts with heparin	(109)

Interestingly, the diameter of a remnant triglyceride-rich lipoprotein particle is 40–80 nm (84, 87), and is approximately equal to the extended length of a heparan sulfate chain in the liver. Given their relatively large size, it is possible that lipoproteins require multiple interactions with heparan sulfate to bind with sufficient affinity to stabilize the lipoprotein–proteoglycan complex before endocytosis. This might be achieved by simultaneous engagement with multiple heparan sulfate chains—a ‘‘proteoglycan hug’’ (Figure 1-1). The unique ability of syndecan- 1 to bind and internalize remnant lipoproteins might therefore stem from the fact that its ectodomain contains three sites for heparan sulfate attachment. Syndecan- 1 can also multimerize (77), and thus increase the local concentration of heparan sulfate chains around a ligand. Notably, several studies have reported that syndecan-1 clustering precedes endocytosis (43, 110), suggesting that lipoproteins may bind to and cluster multiple syndecan-1 molecules before internalization.

Many triglyceride-rich lipoprotein-associated proteins, including APOE, APOB100, APOB48, LPL, and HL bind heparin. Whether the binding of lipoproteins to heparan sulfate is mediated by a specific protein ligand has not been conclusively demonstrated. One theory, known as the ‘‘secretion-capture’’ hypothesis, suggests that APOE produced by hepatocytes enriches lipoproteins in the space of Disse and acts as a ligand for clearance through proteoglycans (111). Indeed, heparan sulfate chains isolated from proteoglycans produced by $Ndst1^{f/f}AlbCre^{+}$ hepatocytes show decreased binding to APOE. However, some genetic studies do not support the conclusion that APOE is the primary ligand for heparan sulfate-mediated clearance. ApoE deficient mice have elevated levels of triglyceride-rich lipoproteins, but interbreeding these mice with $Ldlr^{-/-}$ mice showed that nonfasting plasma triglyceride levels were similar in $Ldlr^{-/-}ApoE^{-/-}$ compound mutants and single mutants deficient in Ldlr or ApoE (112). The lack of an additive effect in these compound mutants suggests that ApoE-dependent clearance of remnant particles was mediated mostly via Ldlr.

APOB, a key structural component of both the intestine- and liver-derived lipoproteins, might also serve as a ligand for syndecan-1-mediated uptake. In humans, full length APOB100 is made by the liver while truncated APOB48 is made in enterocytes of the small intestine as a result of mRNA editing. In mice, both these forms are made in the liver. Veniant and colleagues made mutant mice that expressed only one of the ApoB isoforms (113). Both ‘‘ApoB48-only’’ and ‘‘ApoB100-only’’ mice produced and cleared VLDLs and chylomicrons. However, when each of these mice was bred with Ldlr-deficient mice, fasting plasma triglyceride accumulated to a greater extent when ApoB48 was lacking (i.e., in the ApoB100-only mice). Thus,

syndecan-1 may mediate clearance via ApoB48, an idea that can be tested by breeding syndecan-1 deficient mice with ApoB48-only mice.

LPL is thought to have a ‘‘bridging function,’’ independent of its enzymatic activity. LPL is made by muscle and adipose tissue, transported to the capillary lumen, and anchored there by GPIHBP1 (1). LPL can become associated with lipoproteins in the blood whence it travels with them back to the liver. Heeren *et al.* showed that triglyceride-rich lipoproteins isolated from patients with catalytically inactive LPL were cleared after injection into mice and enrichment with inactive LPL further enhanced hepatic clearance by 35%. Furthermore, catalytically inactive LPL expressed in muscle in transgenic mice also caused greater hepatic uptake by a comparable amount (114). In other studies, LPL-enriched chylomicrons were shown to bind to HepG2 cells 30-fold better than nonenriched particles, and heparan lyase treatment abolished this enhanced binding (115, 116). Similar observations have been made in syndecan-1 transfected CHO cells using methylated LDL enriched with LPL. Further genetic studies using mice deficient in various combinations of the lipoprotein receptors and ligands will be necessary to characterize interactions between heparan sulfate and lipoproteins.

1.7 Syndecan-1 is the primary proteoglycan receptor in the liver

Mouse hepatocytes contain mRNA for eight heparan sulfate proteoglycans including the membrane proteoglycans syndecan-1, -2, and -4, glypican-1 and -4, and the secreted proteoglycans perlecan, agrin, and collagen XVIII (46). Of the available mutant mice, only syndecan-1 (46) and collagen XVIII deficient mice accumulate

fasting triglycerides (117). Crossbreeding mutants deficient for syndecan-1 and Ndst1 (*Sdc1*$^{-/-}$*Ndst1*$^{f/f}$*AlbCre*$^{+}$) did not accentuate triglyceride accumulation beyond levels observed in each single mutant, indicating that syndecan-1 is the primary proteoglycan receptor mediating binding, uptake, and degradation of triglyceride-rich lipoproteins in the liver (46). Characterization of the systemic collagen XVIII null mouse supports this conclusion, as hyperchylomicronemia in this mouse is not caused by clearance defects in the liver, but instead by the altered secretion of Lpl and altered lipolysis in peripheral tissues (117).

Though selective ablation of liver heparan sulfate causes a twofold accumulation of triglyceride-rich lipoproteins, mice with an endothelial deficiency in Ndst1 expression (*Ndst1*$^{f/f}$*Tie2Cre*$^{+}$) do not accumulate triglycerides (48). This finding supports the idea that only hepatocyte heparan sulfate binds to lipoprotein particles and mediates their clearance. The liver contains other cell types, including stellate cells and Kupffer cells. Both cell types produce heparan sulfate proteoglycans (118-120), but their contribution to lipoprotein sequestration, processing, and eventual clearance is unknown.

As syndecan-1 is found in other cell types, we wondered why hepatic syndecan-1 mediates clearance, while syndecan-1 in other tissues does not. On the hepatocyte surface, syndecan-1 is specifically localized to the space of Disse (41, 42, 46). Thus, it is poised in a unique environment where the relative concentration of both lipoproteins and ligands is high. The local concentration of syndecan-1 may be substantially higher here, than in other tissues. Another possibility is that the relatively high levels of sulfation observed in liver heparan sulfate create more binding sites for

the triglyceride-rich lipoproteins. Liver HS is especially rich in N- and 2-O-sulfation, modifications that are required for lipoprotein binding and uptake (48, 49). The degree of substitution of the core protein could also be a variable.

1.8 Relative contribution of syndecan-1 to clearance

As noted above, there are at least three major receptors involved in the hepatic clearance of triglyceride-rich lipoproteins: LDLR, LRP1, and syndecan-1. The relative contribution of each receptor to lipoprotein clearance has not been determined *in vivo*. Before the identification of syndecan-1 as a receptor, pharmacological inhibition of LDLR family members was used to address this question. Mice injected with a LDLR-blocking antibody exhibited a 45% decrease in rapid removal of remnant particles from the plasma and also a 45% decrease in liver uptake (121). Treatment with exogenous receptor associated protein (RAP), which blocks binding to LRP1, decreased remnant clearance by about 55% and reduced liver uptake by 70%. However, RAP also binds to heparan sulfate proteoglycans and with low affinity to the LDLR, making these results hard to interpret. Indeed, co-treatment with both the LDLR-blocking antibody and RAP did not result in an additive accumulation, suggesting that RAP may have decreased uptake by blocking multiple receptors.

Additional insight has been gained by the analyses of mice bearing paired mutations in triglyceride-rich lipoprotein receptors. Crossbreeding $Ndst1^{f/f}AlbCre^{+}$ mice with $Ldlr^{-/-}$ mice resulted in a larger accumulation of triglycerides than observed in either of the individual mutant mice (48), suggesting that these two receptors work independently and may partially compensate for one another. Furthermore, cholesterol

levels were accentuated in the compound mutant compared to mice lacking only the Ldlr. Thus, HSPGs may participate in the clearance of cholesterol-rich lipoproteins, independent of LDLR. The relative contribution of HSPGs, LDLR, and LRP1 is addressed by new studies presented in Chapter 3.

The number of proteoglycan binding sites for VLDL on the hepatocyte surface is approximately 100-times greater than the number of LDLR molecules (46). Based on this difference in receptor number, it seems as though syndecan-1 may have a greater contribution to clearance. However, endocytosis of LDLR occurs by clathrin-mediated pathways and is rapid, with receptors having a half-life of approximately 5–10 minutes on the cell surface (122). Syndecan-1 lacks the hallmarks of a classical clathrin-mediated receptor, and has been reported to enter the cell by a lipid raft pathway with relatively slow kinetics ($t_{1/2}$ ~ 20–60 minutes) (110, 123-125). Thus, compared to LDLR, syndecan-1 constitutes a low-affinity, high-capacity uptake system. The fact that both *Sdc1*$^{-/-}$ and *Ldlr*$^{-/-}$ mice accumulate triglycerides suggests that they cannot fully compensate for one another, possibly because they recognize different subsets of particles which differ in their apolipoprotein composition or size. Nevertheless, the synergistic effect of compounding mutations in Ldlr and Sdc1 would suggest that they also clear a common pool of triglyceride-rich lipoproteins. The differences in receptor preference and the nature of the subsets of particles remain unknown.

Several groups have proposed that proteoglycans mediate a multi-step internalization process involving triglyceride-rich lipoprotein binding and subsequent transfer to the LRP1 before endocytosis (126, 127). It is still unclear whether such

‘‘lipoprotein handoff’’ occurs, but ample evidence suggests that syndecan-1 and other heparan sulfate proteoglycans can act independently as endocytic receptors for a variety of natural and synthetic ligands (128-130). Syndecan-1 has been shown to mediate uptake of APOE-VLDL, independently of LRP1, in a LDLR-deficient cell line (124), and LRP1 mediates endocytosis of non-lipoprotein ligands independent of heparan sulfate proteoglycans (131). Additionally, mice with a liver specific ablation of Lrp1 do not accumulate triglycerides unless stressed with a high fat diet (14), but syndecan-1 deficient mice fed normal chow accumulate triglycerides (46). It is likely, therefore, that the two receptors work independently to clear triglycerides under normal conditions.

1.9 Conclusion

Hypertriglyceridemia increases the risk of atherosclerosis, coronary artery disease, and pancreatitis and thus much interest exists in understanding the genetic and environmental factors that contribute to dyslipidemia (132-137). Genetic data showing that heparan sulfate proteoglycans act as independent receptors for the clearance of triglyceride-rich lipoproteins in the liver provides new insights into the role of hepatic receptors and opens up many new avenues for research. For example, changes in heparan sulfate abundance and structure may be an underlying cause of human dyslipidemias caused by hormone therapy, drug treatment, obesity, and metabolic syndrome. Some familial human dyslipidemias may be explained by polymorphisms in genes encoding proteoglycan core proteins and enzymes involved in heparan sulfate biosynthesis. Based on the findings that have emerged from studies of syndecan-1 and

heparan sulfate-deficient mice, we predict that studies of other genes in the system will yield new insights into the role of heparan sulfate proteoglycans in lipid clearance and other aspects of lipid metabolism in extrahepatic tissues.

1.10 Acknowledgements

This chapter is reprinted with minor modifications from *Progress in Molecular Biology and Translational Science,* Volume 93, Erin M. Foley and Jeffrey D. Esko, "Hepatic heparan sulfate proteoglycans and endocytic clearance of triglyceride-rich lipoproteins", Pages 213-33, Copyright © (2010), with permission from Elsevier. The dissertation author is the primary author of this chapter, and would like to thank Kristin Stanford for helpful discussions.

1.11 References

1. Beigneux, A.P., Davies, B.S., Gin, P., Weinstein, M.M., Farber, E., Qiao, X., Peale, F., Bunting, S., Walzem, R.L., Wong, J.S., et al. 2007. Glycosylphosphatidylinositol-anchored high-density lipoprotein-binding protein 1 plays a critical role in the lipolytic processing of chylomicrons. *Cell Metab* 5:279-291.

2. Havel, R.J., and Hamilton, R.L. 2004. Hepatic catabolism of remnant lipoproteins: where the action is. *Arterioscler Thromb Vasc Biol* 24:213-215.

3. Trigatti, B.L., Krieger, M., and Rigotti, A. 2003. Influence of the HDL receptor SR-BI on lipoprotein metabolism and atherosclerosis. *Arterioscler Thromb Vasc Biol* 23:1732-1738.

4. Brown, M.S., and Goldstein, J.L. 1986. A receptor-mediated pathway for cholesterol homeostasis. *Science* 232:34-47.

5. Ishibashi, S., Brown, M.S., Goldstein, J.L., Gerard, R.D., Hammer, R.E., and Herz, J. 1993. Hypercholesterolemia in low density lipoprotein receptor knockout mice and its reversal by adenovirus-mediated gene delivery. *J Clin Invest* 92:883-893.

6. Rubinsztein, D.C., Cohen, J.C., Berger, G.M., van der Westhuyzen, D.R., Coetzee, G.A., and Gevers, W. 1990. Chylomicron remnant clearance from the plasma is normal in familial hypercholesterolemic homozygotes with defined receptor defects. *J Clin Invest* 86:1306-1312.

7. Kita, T., Brown, M.S., Bilheimer, D.W., and Goldstein, J.L. 1982. Delayed clearance of very low density and intermediate density lipoproteins with enhanced conversion to low density lipoprotein in WHHL rabbits. *Proc Natl Acad Sci USA* 79:5693-5697.

8. Kowal, R.C., Herz, J., Goldstein, J.L., Esser, V., and Brown, M.S. 1989. Low density lipoprotein receptor-related protein mediates uptake of cholesteryl esters derived from apoprotein E-enriched lipoproteins. *Proc Natl Acad Sci USA* 86:5810-5814.

9. Herz, J., Hamann, U., Rogne, S., Myklebost, O., Gausepohl, H., and Stanley, K.K. 1988. Surface location and high affinity for calcium of a 500-kd liver membrane protein closely related to the LDL-receptor suggest a physiological role as lipoprotein receptor. *EMBO J* 7:4119-4127.

10. Beisiegel, U., Weber, W., Ihrke, G., Herz, J., and Stanley, K.K. 1989. The LDL-receptor-related protein, LRP, is an apolipoprotein E-binding protein. *Nature* 341:162-164.

11. May, P., Woldt, E., Matz, R.L., and Boucher, P. 2007. The LDL receptor-related protein (LRP) family: an old family of proteins with new physiological functions. *Ann Med* 39:219-228.

12. Kim, D.H., Inagaki, Y., Suzuki, T., Ioka, R.X., Yoshioka, S.Z., Magoori, K., Kang, M.J., Cho, Y., Nakano, A.Z., Liu, Q., et al. 1998. A new low density lipoprotein receptor related protein, LRP5, is expressed in hepatocytes and adrenal cortex, and recognizes apolipoprotein E. *J Biochem* 124:1072-1076.

13. Herz, J., Clouthier, D.E., and Hammer, R.E. 1992. LDL receptor-related protein internalizes and degrades uPA-PAI-1 complexes and is essential for embryo implantation. *Cell* 71:411-421.

14. Rohlmann, A., Gotthardt, M., Hammer, R.E., and Herz, J. 1998. Inducible inactivation of hepatic LRP gene by cre-mediated recombination confirms role of LRP in clearance of chylomicron remnants. *J Clin Invest* 101:689-695.

15. Fujino, T., Asaba, H., Kang, M.J., Ikeda, Y., Sone, H., Takada, S., Kim, D.H., Ioka, R.X., Ono, M., Tomoyori, H., et al. 2003. Low-density lipoprotein receptor-related protein 5 (LRP5) is essential for normal cholesterol metabolism and glucose-induced insulin secretion. *Proc Natl Acad Sci USA* 100:229-234.

16. Sakai, J., Hoshino, A., Takahashi, S., Miura, Y., Ishii, H., Suzuki, H., Kawarabayasi, Y., and Yamamoto, T. 1994. Structure, chromosome location, and expression of the human very low density lipoprotein receptor gene. *J Biol Chem* 269:2173-2182.

17. Frykman, P.K., Brown, M.S., Yamamoto, T., Goldstein, J.L., and Herz, J. 1995. Normal plasma lipoproteins and fertility in gene-targeted mice homozygous for a disruption in the gene encoding very low density lipoprotein receptor. *Proc Natl Acad Sci USA* 92:8453-8457.

18. Goudriaan, J.R., Espirito Santo, S.M., Voshol, P.J., Teusink, B., van Dijk, K.W., van Vlijmen, B.J., Romijn, J.A., Havekes, L.M., and Rensen, P.C. 2004. The VLDL receptor plays a major role in chylomicron metabolism by enhancing LPL-mediated triglyceride hydrolysis. *J Lipid Res* 45:1475-1481.

19. Espirito Santo, S.M., Rensen, P.C., Goudriaan, J.R., Bensadoun, A., Bovenschen, N., Voshol, P.J., Havekes, L.M., and van Vlijmen, B.J. 2005.

Triglyceride-rich lipoprotein metabolism in unique VLDL receptor, LDL receptor, and LRP triple-deficient mice. *J Lipid Res* 46:1097-1102.

20. Mann, C.J., Khallou, J., Chevreuil, O., Troussard, A.A., Guermani, L.M., Launay, K., Delplanque, B., Yen, F.T., and Bihain, B.E. 1995. Mechanism of activation and functional significance of the lipolysis-stimulated receptor. Evidence for a role as chylomicron remnant receptor. *Biochemistry* 34:10421-10431.

21. Bihain, B.E., and Yen, F.T. 1992. Free fatty acids activate a high-affinity saturable pathway for degradation of low-density lipoproteins in fibroblasts from a subject homozygous for familial hypercholesterolemia. *Biochemistry* 31:4628-4636.

22. Narvekar, P., Berriel Diaz, M., Krones-Herzig, A., Hardeland, U., Strzoda, D., Stohr, S., Frohme, M., and Herzig, S. 2009. Liver-specific loss of lipolysis-stimulated lipoprotein receptor triggers systemic hyperlipidemia in mice. *Diabetes* 58:1040-1049.

23. Yen, F.T., Roitel, O., Bonnard, L., Notet, V., Pratte, D., Stenger, C., Magueur, E., and Bihain, B.E. 2008. Lipolysis stimulated lipoprotein receptor: a novel molecular link between hyperlipidemia, weight gain, and atherosclerosis in mice. *J Biol Chem* 283:25650-25659.

24. Mesli, S., Javorschi, S., Berard, A.M., Landry, M., Priddle, H., Kivlichan, D., Smith, A.J., Yen, F.T., Bihain, B.E., and Darmon, M. 2004. Distribution of the lipolysis stimulated receptor in adult and embryonic murine tissues and lethality of LSR-/- embryos at 12.5 to 14.5 days of gestation. *Eur J Biochem* 271:3103-3114.

25. Out, R., Hoekstra, M., de Jager, S.C., de Vos, P., van der Westhuyzen, D.R., Webb, N.R., Van Eck, M., Biessen, E.A., and Van Berkel, T.J. 2005. Adenovirus-mediated hepatic overexpression of scavenger receptor class B type I accelerates chylomicron metabolism in C57BL/6J mice. *J Lipid Res* 46:1172-1181.

26. Out, R., Kruijt, J.K., Rensen, P.C., Hildebrand, R.B., de Vos, P., Van Eck, M., and Van Berkel, T.J. 2004. Scavenger receptor BI plays a role in facilitating chylomicron metabolism. *J Biol Chem* 279:18401-18406.

27. Van Eck, M., Hoekstra, M., Out, R., Bos, I.S., Kruijt, J.K., Hildebrand, R.B., and Van Berkel, T.J. 2008. Scavenger receptor BI facilitates the metabolism of VLDL lipoproteins in vivo. *J Lipid Res* 49:136-146.

28. Krieger, M. 2001. Scavenger receptor class B type I is a multiligand HDL receptor that influences diverse physiologic systems. *J Clin Invest* 108:793-797.

29. Ji, Z.S., Pitas, R.E., and Mahley, R.W. 1998. Differential cellular accumulation/retention of apolipoprotein E mediated by cell surface heparan sulfate proteoglycans. Apolipoproteins E3 and E2 greater than e4. *J Biol Chem* 273:13452-13460.

30. Al-Haideri, M., Goldberg, I.J., Galeano, N.F., Gleeson, A., Vogel, T., Gorecki, M., Sturley, S.L., and Deckelbaum, R.J. 1997. Heparan sulfate proteoglycan-mediated uptake of apolipoprotein E-triglyceride-rich lipoprotein particles: a major pathway at physiological particle concentrations. *Biochemistry* 36:12766-12772.

31. Feussner, G., Scharnagl, H., Scherbaum, C., Acar, J., Dobmeyer, J., Lohrmann, J., Wieland, H., and März, W. 1996. Apolipoprotein E5 (Glu_{212}-->Lys): Increased binding to cell surface proteoglycans but decreased uptake and lysosomal degradation in cultured fibroblasts. *J Lipid Res* 37:1632-1645.

32. Krapp, A., Ahle, S., Kersting, S., Hua, Y., Kneser, K., Nielsen, M., Gliemann, J., and Beisiegel, U. 1996. Hepatic lipase mediates the uptake of chylomicrons and β-VLDL into cells via the LDL receptor-related protein (LRP). *J Lipid Res* 37:926-936.

33. Williams, K.J., Fless, G.M., Petrie, K.A., Snyder, M.L., Brocia, R.W., and Swenson, T.L. 1992. Mechanisms by which lipoprotein lipase alters cellular metabolism of lipoprotein(a), low density lipoprotein, and nascent lipoproteins. Roles for low density lipoprotein receptors and heparan sulfate proteoglycans. *J Biol Chem* 267:13284-13292.

34. Ji, Z.S., Brecht, W.J., Miranda, R.D., Hussain, M.M., Innerarity, T.L., and Mahley, R.W. 1993. Role of heparan sulfate proteoglycans in the binding and uptake of apolipoprotein E-enriched remnant lipoproteins by cultured cells. *J Biol Chem* 268:10160-10167.

35. Huff, M.W., Miller, D.B., Wolfe, B.M., Connelly, P.W., and Sawyez, C.G. 1997. Uptake of hypertriglyceridemic very low density lipoproteins and their remnants by HepG2 cells: the role of lipoprotein lipase, hepatic triglyceride lipase, and cell surface proteoglycans. *J Lipid Res* 38:1318-1333.

36. Seo, T., Al-Haideri, M., Treskova, E., Worgall, T.S., Kako, Y., Goldberg, I.J., and Deckelbaum, R.J. 2000. Lipoprotein lipase-mediated selective uptake from low density lipoprotein requires cell surface proteoglycans and is independent of scavenger receptor class B type 1. *J Biol Chem* 275:30355-30362.

37. Medh, J.D., Fry, G.L., Bowen, S.L., Ruben, S., Wong, H., and Chappell, D.A. 2000. Lipoprotein lipase- and hepatic triglyceride lipase- promoted very low density lipoprotein degradation proceeds via an apolipoprotein E-dependent mechanism. *J Lipid Res* 41:1858-1871.

38. Ji, Z.S., Sanan, D.A., and Mahley, R.W. 1995. Intravenous heparinase inhibits remnant lipoprotein clearance from the plasma and uptake by the liver: in vivo role of heparan sulfate proteoglycans. *J Lipid Res* 36:583-592.

39. Mortimer, B.C., Beveridge, D.J., Martins, I.J., and Redgrave, T.G. 1995. Intracellular localization and metabolism of chylomicron remnants in the livers of low density lipoprotein receptor-deficient mice and apoE-deficient mice. Evidence for slow metabolism via an alternative apoE-dependent pathway. *J Biol Chem* 270:28767-28776.

40. Windler, E., Greeve, J., Robenek, H., Rinninger, F., Greten, H., and Jackle, S. 1996. Differences in the mechanisms of uptake and endocytosis of small and large chylomicron remnants by rat liver. *Hepatology* 24:344-351.

41. Hayashi, K., Hayashi, M., Jalkanen, M., Firestone, J.H., Trelstad, R.L., and Bernfield, M. 1987. Immunocytochemistry of cell surface heparan sulfate proteoglycan in mouse tissues. A light and electron microscopic study. *J Histochem Cytochem* 35:1079-1088.

42. Roskams, T., Moshage, H., De Vos, R., Guido, D., Yap, P., and Desmet, V. 1995. Heparan sulfate proteoglycan expression in normal human liver. *Hepatology* 21:950-958.

43. Fuki, I.V., Kuhn, K.M., Lomazov, I.R., Rothman, V.L., Tuszynski, G.P., Iozzo, R.V., Swenson, T.L., Fisher, E.A., and Williams, K.J. 1997. The syndecan family of proteoglycans. Novel receptors mediating internalization of atherogenic lipoproteins in vitro. *J Clin Invest* 100:1611-1622.

44. Fuki, I.V., Iozzo, R.V., and Williams, K.J. 2000. Perlecan heparan sulfate proteoglycan - A novel receptor that mediates a distinct pathway for ligand catabolism. *J Biol Chem* 275:25742-25750.

45. Zeng, B.J., Mortimer, B.C., Martins, I.J., Seydel, U., and Redgrave, T.G. 1998. Chylomicron remnant uptake is regulated by the expression and function of heparan sulfate proteoglycan in hepatocytes. *J. Lipid Res.* 39:845-860.

46. Stanford, K.I., Bishop, J.R., Foley, E.M., Gonzales, J.C., Niesman, I.R., Witztum, J.L., and Esko, J.D. 2009. Syndecan-1 is the primary heparan sulfate

proteoglycan mediating hepatic clearance of triglyceride-rich lipoproteins in mice. *J Clin Invest* 119:3236-3245.

47. Cortes, V., Amigo, L., Donoso, K., Valencia, I., Quinones, V., Zanlungo, S., Brandan, E., and Rigotti, A. 2007. Adenovirus-mediated hepatic syndecan-1 overexpression induces hepatocyte proliferation and hyperlipidaemia in mice. *Liver Int* 27:569-581.

48. MacArthur, J.M., Bishop, J.R., Wang, L., Stanford, K.I., Bensadoun, A., Witztum, J.L., and Esko, J.D. 2007. Liver heparan sulfate proteoglycans mediate clearance of triglyceride-rich lipoproteins independently of LDL receptor family members. *J Clin Invest* 117:153-164.

49. Stanford, K.I., Wang, L., Castagnola, J., Song, D., Bishop, J.R., Brown, J.R., Lawrence, R., Bai, X., Habuchi, H., Tanaka, M., et al. 2010. Heparan sulfate 2-O-sulfotransferase is required for triglyceride-rich lipoprotein clearance. *J Biol Chem* 285:286-294.

50. Bernfield, M., Kokenyesi, R., Kato, M., Hinkes, M.T., Spring, J., Gallo, R.L., and Lose, E.J. 1992. Biology of the syndecans: a family of transmembrane heparan sulfate proteoglycans. *Annu Rev Cell Biol* 8:365-393.

51. Sanderson, R.D., and Bernfield, M. 1988. Molecular polymorphism of a cell surface proteoglycan: Distinct structures on simple and stratified epithelia. *Proc Natl Acad Sci USA* 85:9562-9566.

52. Kokenyesi, R., and Bernfield, M. 1994. Core protein structure and sequence determine the site and presence of heparan sulfate and chondroitin sulfate on syndecan-1. *J Biol Chem* 269:12304-12309.

53. Langford, J.K., Stanley, M.J., Cao, D.J., and Sanderson, R.D. 1998. Multiple heparan sulfate chains are required for optimal syndecan-1 function. *J Biol Chem* 273:29965-29971.

54. Rapraeger, A., Jalkanen, M., Endo, E., Koda, J., and Bernfield, M. 1985. The cell surface proteoglycan from mouse mammary epithelial cells bears chondroitin sulfate and heparan sulfate glycosaminoglycans. *J Biol Chem* 260:11046-11052.

55. Saunders, S., Jalkanen, M., O'Farrell, S., and Bernfield, M. 1989. Molecular cloning of syndecan, an integral membrane proteoglycan. *J Cell Biol* 108:1547-1556.

56. Xian, X., Gopal, S., and Couchman, J.R. 2010. Syndecans as receptors and organizers of the extracellular matrix. *Cell Tissue Res* 339:31-46.

57. Alexander, C.M., Reichsman, F., Hinkes, M.T., Lincecum, J., Becker, K.A., Cumberledge, S., and Bernfield, M. 2000. Syndecan-1 is required for Wnt-1-induced mammary tumorigenesis in mice. *Nat Genet* 25:329-332.

58. Park, P.W., Pier, G.B., Hinkes, M.T., and Bernfield, M. 2001. Exploitation of syndecan-1 shedding by Pseudomonas aeruginosa enhances virulence. *Nature* 411:98-102.

59. Wang, Z., Gotte, M., Bernfield, M., and Reizes, O. 2005. Constitutive and accelerated shedding of murine syndecan-1 is mediated by cleavage of its core protein at a specific juxtamembrane site. *Biochemistry* 44:12355-12361.

60. Jalkanen, M., Rapraeger, A., Saunders, S., and Benfield, M. 1987. Cell surface proteoglycan of mouse mammary epithelial cells is shed by cleavage of its matrix-binding ectodomain from its membrane-associated domain. *J Cell Biol* 105:3087-3096.

61. Varki, A., Cummings, R., Esko, J.D., Freeze, H., Stanley, P., Bertozzi, C.R., Hart, G.W., and Etzler, M.E. 2009. *Essentials of Glycobiology*. New York: Cold Spring Harbor Laboratories Press.

62. Mangelsdorf, D.J., Thummel, C., Beato, M., Herrlich, P., Schutz, G., Umesono, K., Blumberg, B., Kastner, P., Mark, M., Chambon, P., et al. 1995. The nuclear receptor superfamily: the second decade. *Cell* 83:835-839.

63. Anisfeld, A.M., Kast-Woelbern, H.R., Meyer, M.E., Jones, S.A., Zhang, Y., Williams, K.J., Willson, T., and Edwards, P.A. 2003. Syndecan-1 expression is regulated in an isoform-specific manner by the farnesoid-X receptor. *J Biol Chem* 278:20420-20428.

64. Kast, H.R., Nguyen, C.M., Sinal, C.J., Jones, S.A., Laffitte, B.A., Reue, K., Gonzalez, F.J., Willson, T.M., and Edwards, P.A. 2001. Farnesoid X-activated receptor induces apolipoprotein C-II transcription: a molecular mechanism linking plasma triglyceride levels to bile acids. *Mol Endocrinol* 15:1720-1728.

65. Mak, P.A., Kast-Woelbern, H.R., Anisfeld, A.M., and Edwards, P.A. 2002. Identification of PLTP as an LXR target gene and apoE as an FXR target gene reveals overlapping targets for the two nuclear receptors. *J Lipid Res* 43:2037-2041.

66. Edwards, I.J., Sun, H., Hu, Y., Berquin, I.M., O'Flaherty, J.T., Cline, J.M., Rudel, L.L., and Chen, Y.Q. 2008. In vivo and in vitro regulation of syndecan 1 in prostate cells by n-3 polyunsaturated fatty acids. *J Biol Chem* 283:18441-18449.

67. Sun, H., Berquin, I.M., Owens, R.T., O'Flaherty, J.T., and Edwards, I.J. 2008. Peroxisome proliferator-activated receptor gamma-mediated up-regulation of syndecan-1 by n-3 fatty acids promotes apoptosis of human breast cancer cells. *Cancer Res* 68:2912-2919.

68. Chen, P., Abacherli, L.E., Nadler, S.T., Wang, Y., Li, Q., and Parks, W.C. 2009. MMP7 shedding of syndecan-1 facilitates re-epithelialization by affecting alpha(2)beta(1) integrin activation. *PLoS One* 4:e6565.

69. Brule, S., Charnaux, N., Sutton, A., Ledoux, D., Chaigneau, T., Saffar, L., and Gattegno, L. 2006. The shedding of syndecan-4 and syndecan-1 from HeLa cells and human primary macrophages is accelerated by SDF-1/CXCL12 and mediated by the matrix metalloproteinase-9. *Glycobiology* 16:488-501.

70. Endo, K., Takino, T., Miyamori, H., Kinsen, H., Yoshizaki, T., Furukawa, M., and Sato, H. 2003. Cleavage of syndecan-1 by membrane type matrix metalloproteinase-1 stimulates cell migration. *J Biol Chem* 278:40764-40770.

71. Subramanian, S.V., Fitzgerald, M.L., and Bernfield, M. 1997. Regulated shedding of syndecan-1 and -4 ectodomains by thrombin and growth factor receptor activation. *J Biol Chem* 272:14713-14720.

72. Popova, T.G., Millis, B., Bradburne, C., Nazarenko, S., Bailey, C., Chandhoke, V., and Popov, S.G. 2006. Acceleration of epithelial cell syndecan-1 shedding by anthrax hemolytic virulence factors. *BMC Microbiol* 6:8.

73. Fitzgerald, M.L., Wang, Z.H., Park, P.W., Murphy, G., and Bernfield, M. 2000. Shedding of syndecan-1 and-4 ectodomains is regulated by multiple signaling pathways and mediated by a TIMP-3-sensitive metalloproteinase. *J Cell Biol* 148:811-824.

74. Hayashida, K., Parks, W.C., and Park, P.W. 2009. Syndecan-1 shedding facilitates the resolution of neutrophilic inflammation by removing sequestered CXC chemokines. *Blood* 114:3033-3043.

75. Deng, Y., Foley, E.M., Gonzales, J.C., Gordts, P.L., Li, Y., and Esko, J.D. Shedding of syndecan-1 from human hepatocytes alters very low density lipoprotein clearance. *Hepatology* 55:277-286.

76. Tkachenko, E., Rhodes, J.M., and Simons, M. 2005. Syndecans: new kids on the signaling block. *Circ Res* 96:488-500.

77. Dews, I.C., and Mackenzie, K.R. 2007. Transmembrane domains of the syndecan family of growth factor coreceptors display a hierarchy of homotypic and heterotypic interactions. *Proc Natl Acad Sci USA* 104:20782-20787.

78. Carey, D.J., Bendt, K.M., and Stahl, R.C. 1996. The cytoplasmic domain of syndecan-1 is required for cytoskeleton association but not detergent insolubility. Identification of essential cytoplasmic domain residues. *J Biol Chem* 271:15253-15260.

79. Grootjans, J.J., Zimmermann, P., Reekmans, G., Smets, A., Degeest, G., Durr, J., and David, G. 1997. Syntenin, a PDZ protein that binds syndecan cytoplasmic domains. *Proc Natl Acad Sci U S A* 94:13683-13688.

80. Gao, Y., Li, M., Chen, W., and Simons, M. 2000. Synectin, syndecan-4 cytoplasmic domain binding PDZ protein, inhibits cell migration. *J Cell Physiol* 184:373-379.

81. Ott, V.L., and Rapraeger, A.C. 1998. Tyrosine phosphorylation of syndecan-1 and -4 cytoplasmic domains in adherent B82 fibroblasts. *J Biol Chem* 273:35291-35298.

82. Reiland, J., Ott, V.L., Lebakken, C.S., Yeaman, C., McCarthy, J., and Rapraeger, A.C. 1996. Pervanadate activation of intracellular kinases leads to tyrosine phosphorylation and shedding of syndecan-1. *Biochem J* 319:39-47.

83. Hayashida, K., Stahl, P.D., and Park, P.W. 2008. Syndecan-1 ectodomain shedding is regulated by the small GTPase Rab5. *J Biol Chem* 283:35435-35444.

84. Lyon, M., Deakin, J.A., and Gallagher, J.T. 1994. Liver heparan sulfate structure. A novel molecular design. *J Biol Chem* 269:11208-11215.

85. Gallagher, J.T., and Walker, A. 1985. Molecular distinctions between heparan sulphate and heparin. Analysis of sulphation patterns indicates that heparan sulphate and heparin are separate families of N-sulphated polysaccharides. *Biochem J* 230:665-674.

86. Lawrence, R., Lu, H., Rosenberg, R.D., Esko, J.D., and Zhang, L. 2008. Disaccharide structure code for the easy representation of constituent oligosaccharides from glycosaminoglycans. *Nat Methods* 5:291-292.

87. Oldberg, Å., Kjellén, L., and Höök, M. 1979. Cell-surface heparan sulfate. Isolation and characterization of a proteoglycan from rat liver membranes. *J Biol Chem* 254:8505-8510.

88. Ringvall, M., Ledin, J., Holmborn, K., Van Kuppevelt, T., Ellin, F., Eriksson, I., Olofsson, A.M., Kjellén, L., and Forsberg, E. 2000. Defective heparan sulfate biosynthesis and neonatal lethality in mice lacking N-deacetylase/N-sulfotransferase-1. *J Biol Chem* 275:25926-25930.

89. Fan, G., Xiao, L., Cheng, L., Wang, X., Sun, B., and Hu, G. 2000. Targeted disruption of NDST-1 gene leads to pulmonary hypoplasia and neonatal respiratory distress in mice. *FEBS Lett* 467:7-11.

90. Grobe, K., Inatani, M., Pallerla, S.R., Castagnola, J., Yamaguchi, Y., and Esko, J.D. 2005. Cerebral hypoplasia and craniofacial defects in mice lacking heparan sulfate Ndst1 gene function. *Development* 132:3777-3786.

91. Esko, J.D., and Lindahl, U. 2001. Molecular diversity of heparan sulfate. *J.Clin.Invest.* 108:169-173.

92. Habuchi, H., Nagai, N., Sugaya, N., Atsumi, F., Stevens, R.L., and Kimata, K. 2007. Mice deficient in heparan sulfate 6-O-sulfotransferase-1 exhibit defective heparan sulfate biosynthesis, abnormal placentation, and late embryonic lethality. *J Biol Chem* 282:15578-15588.

93. Williams, K.J., and Chen, K. 2010. Recent insights into factors affecting remnant lipoprotein uptake. *Curr Opin Lipidol* 21:218-228.

94. Libeu, C.P., Lund-Katz, S., Phillips, M.C., Wehrli, S., Hernaiz, M.J., Capila, I., Linhardt, R.J., Raffai, R.L., Newhouse, Y.M., Zhou, F., et al. 2001. New insights into the heparan sulfate proteoglycan-binding activity of apolipoprotein E. *J Biol Chem* 276:39138-39144.

95. Dong, J., Peters-Libeu, C.A., Weisgraber, K.H., Segelke, B.W., Rupp, B., Capila, I., Hernaiz, M.J., LeBrun, L.A., and Linhardt, R.J. 2001. Interaction of the N-terminal domain of apolipoprotein E4 with heparin. *Biochemistry* 40:2826-2834.

96. Parthasarathy, N., Goldberg, I.J., Sivaram, P., Mulloy, B., Flory, D.M., and Wagner, W.D. 1994. Oligosaccharide sequences of endothelial cell surface heparan sulfate proteoglycan with affinity for lipoprotein lipase. *J Biol Chem* 269:22391-22396.

97. Spillmann, D., Lookene, A., and Olivecrona, G. 2006. Isolation and characterization of low sulfated heparan sulfate sequences with affinity for lipoprotein lipase. *J Biol Chem* 281:23405-23413.

98. Bazin, H.G., Marques, M.A., Owens, A.P., 3rd, Linhardt, R.J., and Crutcher, K.A. 2002. Inhibition of apolipoprotein E-related neurotoxicity by glycosaminoglycans and their oligosaccharides. *Biochemistry* 41:8203-8211.

99. Cardin, A.D., and Weintraub, H.J. 1989. Molecular modeling of protein-glycosaminoglycan interactions. *Arteriosclerosis.* 9:21-32.

100. Flood, C., Gustafsson, M., Richardson, P.E., Harvey, S.C., Segrest, J.P., and Boren, J. 2002. Identification of the proteoglycan binding site in apolipoprotein B48. *J Biol Chem* 277:32228-32233.

101. Goldberg, I.J., Wagner, W.D., Pang, L., Paka, L., Curtiss, L.K., DeLozier, J.A., Shelness, G.S., Young, C.S., and Pillarisetti, S. 1998. The NH2-terminal region of apolipoprotein B is sufficient for lipoprotein association with glycosaminoglycans. *J Biol Chem* 273:35355-35361.

102. Borén, J., Olin, K., Lee, I., Chait, A., Wight, T.N., and Innerarity, T.L. 1998. Identification of the principal proteoglycan-binding site in LDL - A single-point mutation in apo-B100 severely affects proteoglycan interaction without affecting LDL receptor binding. *J.Clin.Invest.* 101:2658-2664.

103. Merchant, Z.M., Erbe, E.E., Eddy, W.P., Patel, D., and Linhardt, R.J. 1986. Effect of very low molecular weight heparin-derived oligosaccharides on lipoprotein lipase release in rabbits. *Atherosclerosis* 62:151-158.

104. Yu, W., and Hill, J.S. 2006. Mapping the heparin-binding domain of human hepatic lipase. *Biochem Biophys Res Commun* 343:659-665.

105. Sendak, R.A., Berryman, D.E., Gellman, G., Melford, K., and Bensadoun, A. 2000. Binding of hepatic lipase to heparin: identification of specific heparin-binding residues in two distinct positive charge clusters. *J.Lipid Res.* 41:260-268.

106. Larnkjaer, A., Nykjaer, A., Olivecrona, G., Thogersen, H., and Ostergaard, P.B. 1995. Structure of heparin fragments with high affinity for lipoprotein lipase and inhibition of lipoprotein lipase binding to alpha 2-macroglobulin-receptor/low-density-lipoprotein-receptor-related protein by heparin fragments. *Biochem J* 307 (Pt 1):205-214.

107. Jaye, M., Lynch, K.J., Krawiec, J., Marchadier, D., Maugeais, C., Doan, K., South, V., Amin, D., Perrone, M., and Rader, D.J. 1999. A novel endothelial-derived lipase that modulates HDL metabolism. *Nat Genet* 21:424-428.

108. Fuki, I.V., Blanchard, N., Jin, W., Marchadier, D.H., Millar, J.S., Glick, J.M., and Rader, D.J. 2003. Endogenously produced endothelial lipase enhances

binding and cellular processing of plasma lipoproteins via HSPG-mediated pathway. *J Biol Chem* 278:34331-34338.

109. Lookene, A., Beckstead, J.A., Nilsson, S., Olivecrona, G., and Ryan, R.O. 2005. Apolipoprotein A-V-heparin interactions: implications for plasma lipoprotein metabolism. *J Biol Chem* 280:25383-25387.

110. Fuki, I.V., Meyer, M.E., and Williams, K.J. 2000. Transmembrane and cytoplasmic domains of syndecan mediate a multi-step endocytic pathway involving detergent-insoluble membrane rafts. *Biochem J* 351:607-612.

111. Mahley, R.W., Ji, Z.S., Brecht, W.J., Miranda, R.D., and He, D. 1994. Role of heparan sulfate proteoglycans and the LDL receptor-related protein in remnant lipoprotein metabolism. *Ann N Y Acad Sci* 737:39-52.

112. Ishibashi, S., Herz, J., Maeda, N., Goldstein, J.L., and Brown, M.S. 1994. The two-receptor model of lipoprotein clearance: tests of the hypothesis in "knockout" mice lacking the low density lipoprotein receptor, apolipoprotein E, or both proteins. *Proc Natl Acad Sci USA* 91:4431-4435.

113. Farese, R.V., Jr., Veniant, M.M., Cham, C.M., Flynn, L.M., Pierotti, V., Loring, J.F., Traber, M., Ruland, S., Stokowski, R.S., Huszar, D., et al. 1996. Phenotypic analysis of mice expressing exclusively apolipoprotein B48 or apolipoprotein B100. *Proc Natl Acad Sci USA* 93:6393-6398.

114. Heeren, J., Niemeier, A., Merkel, M., and Beisiegel, U. 2002. Endothelial-derived lipoprotein lipase is bound to postprandial triglyceride-rich lipoproteins and mediates their hepatic clearance in vivo. *J Mol Med* 80:576-584.

115. Beisiegel, U., Weber, W., and Bengtsson-Olivecrona, G. 1991. Lipoprotein lipase enhances the binding of chylomicrons to low density lipoprotein receptor-related protein. *Proc Natl Acad Sci USA* 88:8342-8346.

116. Eisenberg, S., Sehayek, E., Olivecrona, T., and Vlodavsky, I. 1992. Lipoprotein lipase enhances binding of lipoproteins to heparan sulfate on cell surfaces and extracellular matrix. *J.Clin.Invest.* 90:2013-2021.

117. Bishop, J.R., Passos-Bueno, M.R., Fong, L., Stanford, K.I., Gonzales, J.C., Yeh, E., Young, S.G., Bensadoun, A., Witztum, J.L., Esko, J.D., et al. 2010. Deletion of the basement membrane heparan sulfate proteoglycan type XVIII collagen causes hypertriglyceridemia in mice and humans. *PLoS ONE* 5:e13919.

118. Roskams, T., Rosenbaum, J., De Vos, R., David, G., and Desmet, V. 1996. Heparan sulfate proteoglycan expression in chronic cholestatic human liver diseases. *Hepatology* 24:524-532.

119. Kovalszky, H., Gallai, M., Armbrust, T., and Ramadori, G. 1994. Syndecan-1 gene expression in isolated rat liver cells (hepatocytes, Kupffer cells, endothelial and Ito cells). *Biochem Biophys.Res.Commun.* 204:944-949.

120. Weiner, O.H., Zoremba, M., and Gressner, A.M. 1996. Gene expression of syndecans and betaglycan in isolated rat liver cells. *Cell Tissue Res.* 285:11-16.

121. de Faria, E., Fong, L.G., Komaromy, M., and Cooper, A.D. 1996. Relative roles of the LDL receptor, the LDL receptor-like protein, and hepatic lipase in chylomicron remnant removal by the liver. *J Lipid Res* 37:197-209.

122. Brown, M.S., Anderson, R.G., and Goldstein, J.L. 1983. Recycling receptors: the round-trip itinerary of migrant membrane proteins. *Cell* 32:663-667.

123. Tkachenko, E., Lutgens, E., Stan, R.V., and Simons, M. 2004. Fibroblast growth factor 2 endocytosis in endothelial cells proceed via syndecan-4-dependent activation of Rac1 and a Cdc42-dependent macropinocytic pathway. *J Cell Sci* 117:3189-3199.

124. Wilsie, L.C., Gonzales, A.M., and Orlando, R.A. 2006. Syndecan-1 mediates internalization of apoE-VLDL through a low density lipoprotein receptor-related protein (LRP)-independent, non-clathrin-mediated pathway. *Lipids Health Dis* 5:23.

125. Thankamony, S.P., and Knudson, W. 2006. Acylation of CD44 and its association with lipid rafts are required for receptor and hyaluronan endocytosis. *J Biol Chem* 281:34601-34609.

126. Mahley, R.W., and Ji, Z.S. 1999. Remnant lipoprotein metabolism: key pathways involving cell-surface heparan sulfate proteoglycans and apolipoprotein E. *J Lipid Res* 40:1-16.

127. Wilsie, L.C., and Orlando, R.A. 2003. The low density lipoprotein receptor-related protein complexes with cell surface heparan sulfate proteoglycans to regulate proteoglycan-mediated lipoprotein catabolism. *J Biol Chem* 278:15758-15764.

128. Williams, K.J., and Fuki, I.V. 1997. Cell-surface heparan sulfate proteoglycans: dynamic molecules mediating ligand catabolism. *Curr Opin Lipidol* 8:253-262.

129. Belting, M. 2003. Heparan sulfate proteoglycan as a plasma membrane carrier. *Trends Biochem Sci* 28:145-151.

130. Elson-Schwab, L., Garner, O.B., Schuksz, M., Crawford, B.E., Esko, J.D., and Tor, Y. 2007. Guanidinylated neomycin delivers large, bioactive cargo into cells through a heparan sulfate-dependent pathway. *J Biol Chem* 282:13585-13591.

131. Warshawsky, I., Herz, J., Broze, G.J., Jr., and Schwartz, A.L. 1996. The low density lipoprotein receptor-related protein can function independently from heparan sulfate proteoglycans in tissue factor pathway inhibitor endocytosis. *J Biol Chem* 271:25873-25879.

132. Stalenhoef, A.F., and de Graaf, J. 2008. Association of fasting and nonfasting serum triglycerides with cardiovascular disease and the role of remnant-like lipoproteins and small dense LDL. *Curr Opin Lipidol* 19:355-361.

133. Yuan, G., Al-Shali, K.Z., and Hegele, R.A. 2007. Hypertriglyceridemia: its etiology, effects and treatment. *Cmaj* 176:1113-1120.

134. Nordestgaard, B.G., Benn, M., Schnohr, P., and Tybjaerg-Hansen, A. 2007. Nonfasting triglycerides and risk of myocardial infarction, ischemic heart disease, and death in men and women. *Jama* 298:299-308.

135. Bansal, S., Buring, J.E., Rifai, N., Mora, S., Sacks, F.M., and Ridker, P.M. 2007. Fasting compared with nonfasting triglycerides and risk of cardiovascular events in women. *Jama* 298:309-316.

136. Langsted, A., Freiberg, J.J., and Nordestgaard, B.G. 2008. Fasting and nonfasting lipid levels: influence of normal food intake on lipids, lipoproteins, apolipoproteins, and cardiovascular risk prediction. *Circulation* 118:2047-2056.

137. Fujioka, Y., and Ishikawa, Y. 2009. Remnant lipoproteins as strong key particles to atherogenesis. *J Atheroscler Thromb*.

CHAPTER 2

Identification and characterization of syndecan-1 as a clearance receptor for triglyceride-rich lipoproteins.

2.1 Summary

We have previously shown that, under normal physiological conditions, hepatic heparan sulfate proteoglycans play a crucial role in the clearance of both intestinally derived and hepatic lipoprotein particles in mice (1). To set the stage for further mechanistic studies of TRL uptake and processing, we endeavored to determine whether one specific heparan sulfate proteoglycan is specialized to mediate clearance. The purpose of this chapter is to describe the identification of syndecan-1 as the primary proteoglycan receptor in mice, and to discuss various avenues through which we have characterized the function of syndecan-1 in this context. The data in this chapter demonstrates the contribution of syndecan-1 to clearance in mice and in primary and immortalized human hepatocytes. Next, this chapter explains our preliminary structure/function studies of syndecan-1 as a TRL clearance receptor. Finally, the influence of syndecan-1 in hypertriglyceridemia associated with diabetes and sepsis is discussed.

2.2 Syndecan-1 is the primary proteoglycan receptor in mice

Inactivation of the heparan sulfate biosynthetic enzyme GlcNAc *N*-deacetylase/*N*-sulfotransferase 1 (Ndst1) in the liver using the Cre-LoxP system ($Ndst1^{f/f}AlbCre^{+}$) leads to elevated fasting triglycerides and persistence of postprandial

triglycerides in mice (1). Triglyceride-rich lipoprotein (TRL) synthesis is not affected in these mice, and hypertriglyceridemia results from a defect in hepatic clearance. The identity of the physiologically relevant hepatic heparan sulfate proteoglycan (HSPG) that mediates TRL remnant particle clearance cannot be determined by studies of *Ndst1*$^{f/f}$*AlbCre*$^{+}$ mice, however, because this mutation affects the sulfation of all hepatic proteoglycans. By quantitative real-time PCR, we determined that freshly isolated murine hepatocytes express the membrane proteoglycans syndecans-1, -2, and -4, and glypicans-1 and -4 (Figure 2-1) and the extracellular matrix proteoglycans collagen-18 and perlecan. Thus, to identify the relevant receptor, we examined mice lacking individual proteoglycans. Of the available mutants, only collagen-18 and syndecan-1 deficient mice accumulate triglycerides (Figure 2-1). Syndecan-3 is not expressed in the liver, but it serves as a control. Collagen-18 is a basement membrane proteoglycan found in vascular tissues. Mice lacking collagen-18 have mild hyperchylomicronemia, resulting not from hepatic clearance defects, but instead from altered secretion of LPL and altered lipolysis in the periphery (2). Thus, syndecan-1 emerged as a candidate receptor for TRL clearance, and this protein became the focus of the following studies.

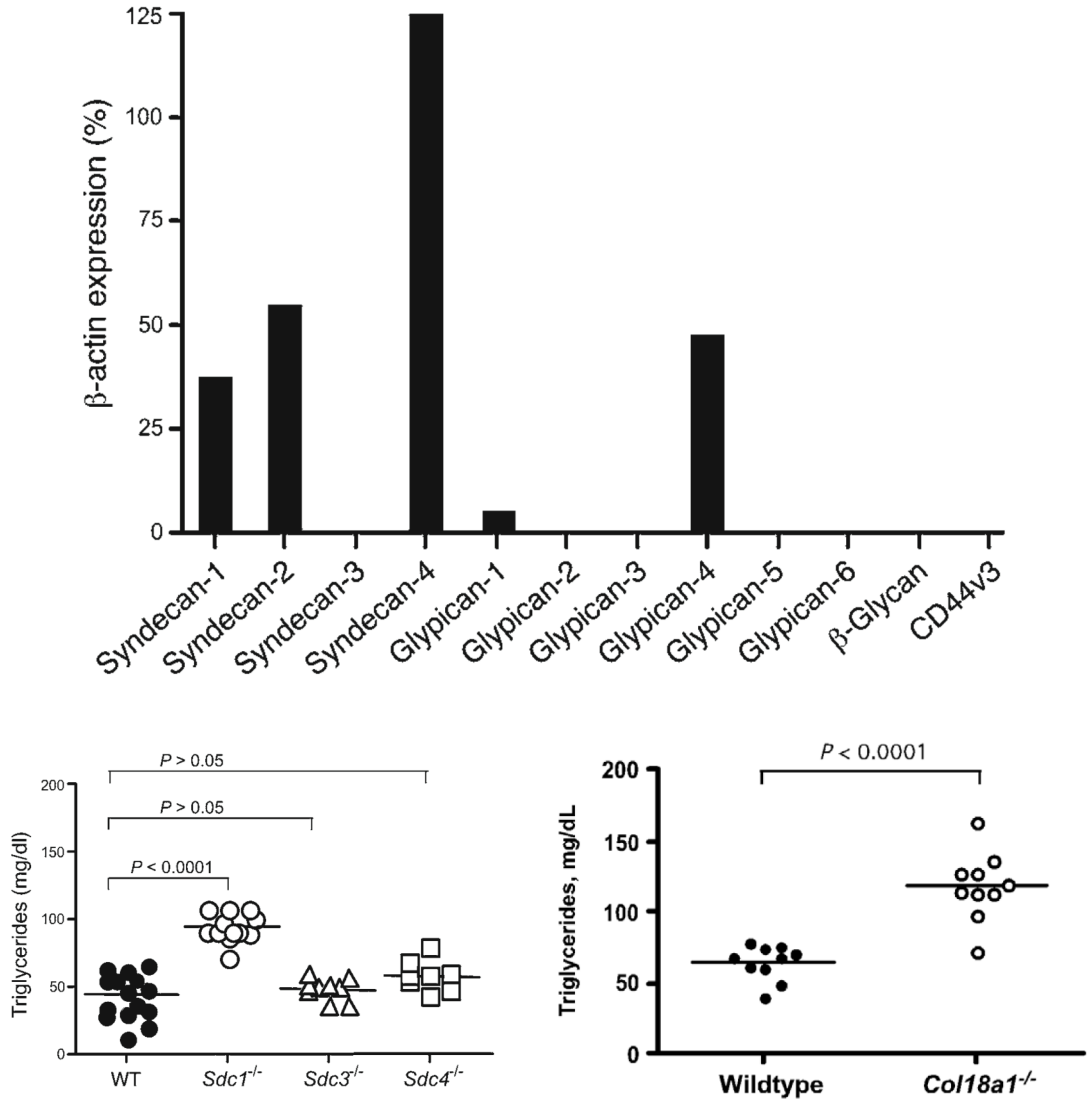

Figure 2-1: *RT-PCR analysis of membrane HSPGs and hypertriglyceridemia in* Sdc1$^{-/-}$ *mice.* (*top*) Transcript levels of the membrane proteoglycan core proteins were measured in isolated hepatocytes. The numbers represent the level of expression compared with the housekeeping gene β-actin using C_T values from triplicate assays according to the Stratagene manual. Error bars are not shown because they are factored into the final calculation. Comparable results were obtained in 2 independent preparations of RNA. (*bottom left*) Triglycerides were measured in plasma samples from fasted male and female mice of indicated genotypes. Wildtype (n = 14), *Sdc1*$^{-/-}$(n = 13), *Sdc3*$^{-/-}$ (n = 10), *Sdc4*$^{-/-}$ (n = 8). Horizontal bars indicate mean values. (*bottom right*) Retro-orbital sinus blood was taken from wild-type and collagen 18 knockout (*Col18a*$^{-/-}$) mice after fasting the animals for 4 hrs in the morning. Total plasma triglycerides were compared between mutant and wild-type (n = 10 mice, unpaired t-test, $P < 0.0001$) and results were repeated. This figure is reproduced from (2).

Like *Ndst1*$^{f/f}$*AlbCre*$^{+}$ mice, *Sdc1*$^{-/-}$ mice exhibited prolonged circulation of injected human VLDL and intestinally derived chylomicrons. Crossbreeding mutants defective in syndecan-1 and Ndst1 (*Sdc1*$^{-/-}$*Ndst1*$^{f/f}$*AlbCre*$^{+}$) did not accentuate triglyceride accumulation beyond the level observed in each single mutant (Figure 2-2), indicating that syndecan-1 is, in fact, the primary proteoglycan clearance receptor in the liver. Immunoelectron microscopy showed expression of syndecan-1 on the microvilli of hepatocyte basal membranes facing the space of Disse where lipoprotein uptake occurs (3). We also showed that syndecan-1 receptors on hepatocytes exhibit saturable binding and inhibition by heparin, and facilitate degradation of labeled VLDL *in vitro*. This study provided the first genetic evidence that syndecan-1 is the primary proteoglycan clearance receptor in the liver.

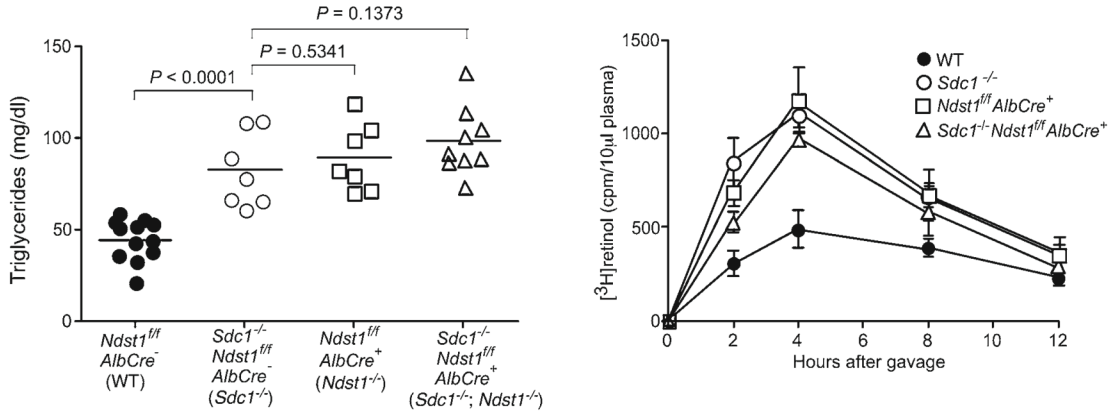

Figure 2-2: *Hypertriglyceridemia and delayed clearance of dietary lipids in $Sdc1^{-/-}$ and $Ndst1^{f/f}AlbCre^{+}$ mice are not additive traits.* (*left panel*) Plasma triglycerides were measured in plasma samples from fasted mice. There was no difference in plasma triglycerides in $Sdc1^{-/-}Ndst1^{f/f}AlbCre^{+}$ (triangles, n = 9), $Sdc1^{-/-}Ndst1^{f/f}AlbCre^{-}$ (open circles, n = 7), and $Ndst1^{f/f}AlbCre^{+}$ (squares, n = 7) mice, although all 3 genotypes were significantly elevated above the wildtype, $Ndst1^{f/f}AlbCre^{-}$ (closed circles, n = 13). Horizontal bars indicate mean values. (*right panel*) Retinol ester excursions were measured at the times indicated in wildtype (filled circles, n = 3), $Sdc1^{-/-}$ (open circles, n = 3), $Ndst1^{f/f}AlbCre^{+}$ (squares, n = 3), and $Sdc1^{-/-}Ndst1^{f/f}AlbCre^{+}$ (triangles, n = 3) mice. Animals were fasted for 4 hours in the morning and given 200 µl of corn oil containing [^{3}H]retinol by oral gavage. Blood samples were taken at the indicated times, and radioactivity remaining in 10 µl of serum was determined by scintillation counting. The values are expressed as mean ± SD. The areas under the curves were 4100 ± 1200 for wildtype, 8400 ± 300 for $Sdc1^{-/-}$, 8300 ± 400 for $Ndst1^{f/f}AlbCre^{+}$ and 6900 ± 1000 for $Sdc1^{-/-}Ndst1^{f/f}AlbCre^{+}$ mice. Clearance was significantly delayed in the $Sdc1^{-/-}$ mice compared with wildtype ($P < 0.01$), whereas the difference observed between $Sdc1^{-/-}$ and $Sdc1^{-/-}Ndst1^{f/f}AlbCre^{+}$ animals was not significant (P = 0.1373).

2.3 Syndecan-1 mediates clearance of TRLs in human hepatocytes

After we identified syndecan-1 as the primary proteoglycan receptor in mice, we explored whether it contributes to clearance of TRLs in human hepatocytes. To this end, we silenced syndecan-1 expression in Hep3B cells, a cell line derived from a well-differentiated human hepatocellular carcinoma (4), using specific siRNAs. We then used these cells to measure binding and uptake of VLDL labeled with DiD (1,1'-dioctadecyl-3,3,3',3'-tetramethylindodicarbocyanide perchlorate), a fluorescent tracer.

DiD-VLDL binding at 4°C and uptake at 37°C was reduced in cells treated with syndecan-1 siRNAs compared to cells treated with a scrambled siRNA (Figure 2-3). Binding and uptake were diminished to a greater extent by heparin lyase digestion, suggesting that either the extent of syndecan-1 silencing was incomplete or that other HSPGs in human hepatocytes also can mediate binding and uptake. In addition to syndecan-1, human hepatocytes express the membrane proteoglycans syndecan-2 and -4, and glypican-1 and -4, and the extracellular matrix proteoglycans perlecan, collagen-18, and agrin (5, 6). Silencing of syndecan-4 did not result in reduction of binding, but other proteoglycans have not been examined. The residual heparin lyase-insensitive component of binding/uptake presumably reflects other receptors, most likely LDL receptors and one or more members of the family of LDLR-related proteins.

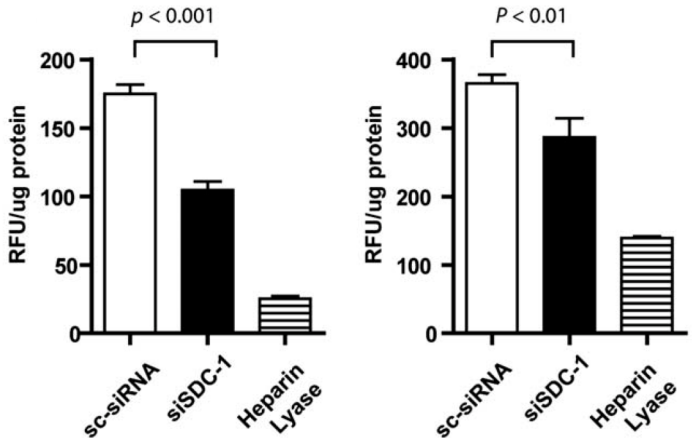

Figure 2-3: *VLDL binding and uptake by human Hep3B hepatoma cells after siRNA-mediated knockdown of Sdc1.* Cells were treated with a scrambled siRNA (sc-siRNA, open bars), siRNA to syndecan-1 (siSDC-1, filled bars), or heparin lyase (hatched bars). Binding (left panel) and binding/uptake (right panel) were measured by incubating treated cells with 100 µg/mL DiD-VLDL for 1 hour (n=4). The values represent the average fluorescence intensity normalized to cell protein. Error bars indicate standard deviation.

We further examined the role of syndecan-1 in TRL clearance in normal primary human hepatocytes, which also bind DiD-VLDL in a heparan lyase-sensitive manner (Figure 2-4). In primary human hepatocytes, as in other cell types, syndecan-1 ectodomains are released from the cell surface via proteolytic shedding, resulting in the appearance in the medium of the extracellular domains of the protein containing the ligand-binding heparan sulfate chains. Shedding occurs constitutively from human hepatocytes, but can also be induced using phorbol myristic acid (PMA) (7). Given that syndecan-1 mediates TRL binding and uptake in Hep3B cells (Figure 2-3), we predicted that PMA-induced syndecan-1 shedding would affect VLDL binding and uptake in primary human hepatocytes. In primary human hepatocytes, PMA treatment reduced VLDL binding and uptake by approximately 50% compared to untreated cells (Figure 2-4). Treatment with heparin lyases reduced VLDL binding and uptake to a greater extent, most likely because of incomplete removal of proteoglycan receptors from the cell surface by PMA-induced shedding. Shed ectodomains did not inhibit binding when purified and added to fresh cells at their original concentration. PMA can also induce shedding of LRP1, another TRL receptor, which might account for some decrease in binding (8, 9).

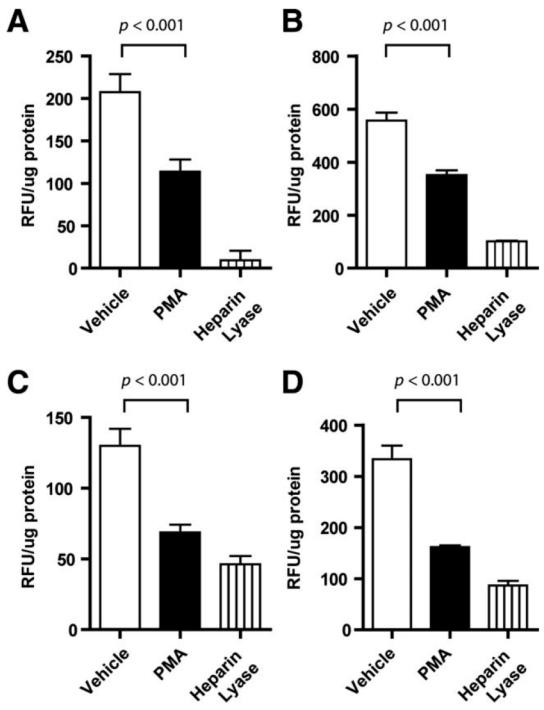

Figure 2-4: *PMA-induced shedding reduces VLDL binding and uptake.* Hep3B cells (*A,B*) and primary human hepatocytes (*C,D*) were treated with 0.25 μM PMA for 1 hour (filled bars) or heparin lyase for 30 minutes (hatched bars) and then incubated with DiD-VLDL (100 μg/ mL) for 1 hour at 4°C for binding (*A,C*) or at 37°C for binding and uptake (*B,D*). The fluorescence intensity was quantitated and normalized to cell protein. Control cells were not treated with PMA (open bars). All values represent the average ± standard deviation (n = 3).

Because syndecan-1 interacts with ligands via its heparan sulfate chains, we predicted that shed syndecan-1 ectodomains from hepatocytes would retain the capacity to bind VLDL. To test this hypothesis, we incubated hepatoma cells with $[^{35}S]O_4$ to radiolabel the heparan sulfate chains on syndecan-1, triggered shedding with PMA, and purified the ^{35}S-labeled ectodomains from the medium by anion exchange chromatography. The ^{35}S-labeled ectodomains were then mixed with VLDL, placed at the bottom of centrifuge tubes, and overlaid with a solution of iodixanol (δ =

1.019 g/mL). Ultracentrifugation resulted in the appearance of ~65% of counts in the top four fractions, whereas in the absence of VLDL, less than 5% of the counts were found in the top fractions (Figure 2-5). Dot blot analysis of the pooled top four fractions showed syndecan-1 ectodomains were present in samples containing VLDL (Figure 2-5, inset). Inclusion of 50 μg of heparin in the binding solution reduced the recovery of ^{35}S-labeled ectodomains in the top fractions, consistent with the idea that heparin prevented the association of the particles with the heparan sulfate chains on the ectodomains. Interestingly, when the mixture of VLDL and ^{35}S-labeled ectodomains was overlaid with a lower density solution (δ = 1.006 g/mL), flotation of [^{35}S]ectodomains did not occur (data not shown), consistent with the idea that the association of ectodomains with VLDL caused a shift in the buoyant density of the complex.

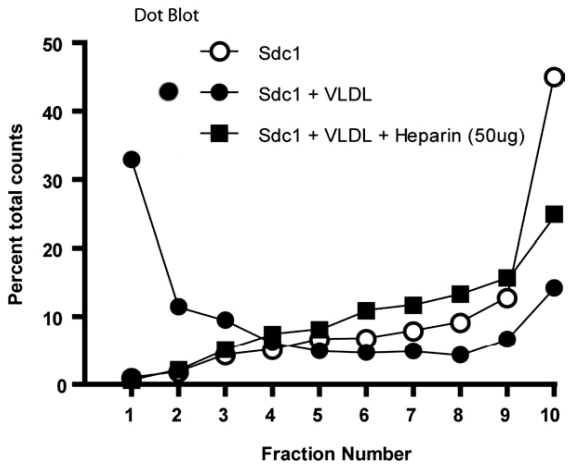

Figure 2-5: *Shed syndecan-1 binds VLDL.* [^{35}S]-Labeled syndecan-1 ectodomains were combined with 50 μg of human VLDL in the presence (squares) or absence (filled circles) of 50 μg of heparin. A sample of ectodomains was incubated with buffer alone as a control (open circles). The samples were then adjusted to δ = 1.019 g/mL with iodixanol and centrifuged. Fractions taken sequentially from the top of the tubes were assayed for radioactivity and syndecan-1 ectodomains (embedded dot blot figure).

Taken together, the experiments revealed an important role for syndecan-1 as a clearance receptor for TRLs in human hepatocytes, and showed that syndecan-1 shedding in these cells abrogates syndecan-1-mediated binding and uptake.

2.4 Structure/function analysis of syndecan-1

We know that TRLs bind to the heparan sulfate chains on syndecan-1 because primary mouse hepatocytes treated with heparan lyases bind and internalize significantly less DiD-VLDL than untreated cells (Figure 2-3), and shed syndecan-1 ectodomains fail to bind VLDLs in the presence of heparin (Figure 2-5). However, because syndecan-1 is unique among HSPGs in its ability to mediate clearance of TRLs, we wondered whether any syndecan-1-specific protein domains or features were also essential for clearance. To this end, we embarked on a structure/function analysis of syndecan-1.

2.4.1 Rationale and Design

In this study, wildtype and mutant syndecan-1 cDNA constructs were created and packaged into adenoviral vectors. These vectors were then used to reconstitute *Sdc1*$^{-/-}$ mice. Mutant viral constructs that failed to restore TRL clearance to wildtype levels were considered to bear mutations in regions of the protein relevant to its function as a clearance receptor. The various mutants, described in Table 2-1, were planned to test fairly simple hypotheses. The rationale behind each construct design is described below.

Table 2-1: *Mutant syndecan-1 cDNAs for structure/function analysis.*

Name of construct	Description
Sdc1	Full length cDNA for wild-type syndecan-1
S37A S45A S47A	Lacking individual heparan sulfate attachment sites
S45,47A S37,45A S37,47A	Lacking two heparan sulfate attachment sites
S37,45,47A	Lacking all heparan sulfate attachment sites
GAG-null	Lacking all heparan sulfate and chondroitin sulfate attachment sites
Cyto-null	All but one amino acid of the C-terminal cytoplasmic domain deleted
Ecto-only	Lacks transmembrane and cytoplasmic domain
No-cleavage	Lacks cleavage site, preventing shedding
Sdc4	Full length cDNA for wild-type syndecan-4
Ecto-swap	Consists of the ectodomain from syndecan-4 fused to the transmembrane and cytoplasmic domains from syndecan-1

Syndecan-1 is a 311-amino acid single-pass transmembrane protein. Its ectodomain contains three attachment sites for heparan sulfate distal from the membrane (amino acids 37, 45, and 47), two sites for chondroitin sulfate attachment more proximal to the membrane (amino acids 217 and 227), as well as one N-glycosylation site (10, 11). Syndecan-1 constructs lacking one, two, or all three sites for heparan sulfate attachment (e.g. S37A, S45,47A, S37,45,47A, etc) test whether multiple chains are required for binding. The GAG-null construct tests the importance of the chondroitin sulfate chains.

The cytoplasmic domain of syndecan-1 contains two “constant” regions that bear sequence homology with other members of the syndecan family (12). The constant regions flank a “variable” region that is syndecan-1 specific. The cytoplasmic

domain also includes four invariant tyrosine residues, which may be phosphorylated on syndecan-1 and other members of the syndecan family (13). The syndecan-1 amino acid sequence terminates in an EYFA domain, allowing the C-terminal region of this protein to interact with other proteins containing PDZ domains (14). Cyto-null tests the role of the cytoplasmic domain in internalization.

Syndecan-1 ectodomain shedding occurs after proteolytic cleavage of the protein at a specific juxtamembrane site (15). Shed ectodomains may act to sequester lipoprotein particles in the space of Disse prior to clearance by receptors on hepatocytes. Thus, Ecto-only tests if the ectodomain is sufficient to drive clearance and No-cleavage prevents shedding from occurring. In this construct, the stem region from the Fc receptor replaces the sequence between the membrane spanning domain and the chondroitin sulfate attachment sites (16).

By immunofluorescence and immunoelectron microscopy, we have observed syndecan-1 localization in the space of Disse, specifically on the microvilli of hepatocytes (2). Antibody to syndecan-4 also stained this perisinusoidal space (unpublished findings), but *Sdc4*$^{-/-}$ mice do not accumulate plasma triglycerides (Figure 2-1) nor does its inactivation further enhance TRL accumulation on a *Sdc1*$^{-/-}$ background. Thus, we predict either the localization of syndecan-1 or its level of expression is the key determinant of its ability to act as an endocytic receptor for TRLs. To examine this issue, the Ecto-swap construct (syndecan-4 ectodomain fused to the syndecan-1 cytoplasmic domain) and an adenovirus containing full length syndecan-4 to enhance its level of expression were created. An important control is to

inject AdSdc1 into wild-type animals to determine if augmenting its expression enhances turnover or whether the system is saturated.

2.4.2 Creation of wildtype and mutant syndecan-1 adenoviral vectors

The murine syndecan-1 cDNA was packaged into human adenovirus type 5 particles using the ViraPower Adenoviral Expression System (Invitrogen). Briefly, syndecan-1 cDNA was reverse transcribed from isolated hepatocyte mRNA and inserted into the pENTR-D-TOPO entry vector. This vector was recombined with the pAD/CMV/V5-DEST adenovirus vector using LR clonase. The adenovirus vector containing snydecan-1 cDNA was transfected into HEK 293A cells, which stably express the adenoviral E1 proteins required to make recombinant adenovirus. After approximately two weeks, a crude lysate containing virus was obtained. Adenovirus was amplified and purified using CsCl gradient ultracentrifugation according to established protocols (17). Purified viral stocks were titered for plaque forming ability using the AdenoX Rapid Titer system (Clontech) and for particle number by measuring OD260 in SDS buffer.

2.4.3 Syndecan-1 is expressed in hepatocytes following adenovirus-mediated transduction

To validate our experimental system, freshly isolated primary *Sdc1*$^{-/-}$ hepatocytes were infected with the various AdSdc1 constructs in culture, and syndecan-1 expression was detected by western blot. Syndecan-1 was expressed abundantly in the cells, and expression peaked at 48 hours post-transduction (Figure 2-

6). To insure that the syndecan-1 constructs were also expressed in vivo, hepatocytes were isolated from mice that had been injected 14 days prior with wildtype AdSdc1. A separate set of mice were injected with AdGFP as a control. As expected, syndecan-1 expression was seen in AdSdc1-transduced knockouts by western blot, but no expression was observed in the AdGFP-infected mice.

It has previously been shown that under similar experimental conditions, more than 95% of injected adenovirus is cleared by the liver, leading to hepatic-specific expression of syndecan-1 (18). Adenoviruses have been used extensively to introduce genes into the liver, however several studies have shown that the vector alone causes liver damage and may independently impact triglyceride and cholesterol levels (8, 19). To address these concerns, we carefully determined optimal time post infection (14 days) and optimal viral dose (2×10^{11} viral particles/mouse) to minimize unwanted side effects on liver function and clearance. Throughout these experiments, adenovirus containing wild-type syndecan-1 cDNA and green fluorescent protein (AdGFP) served as positive and negative controls, respectively.

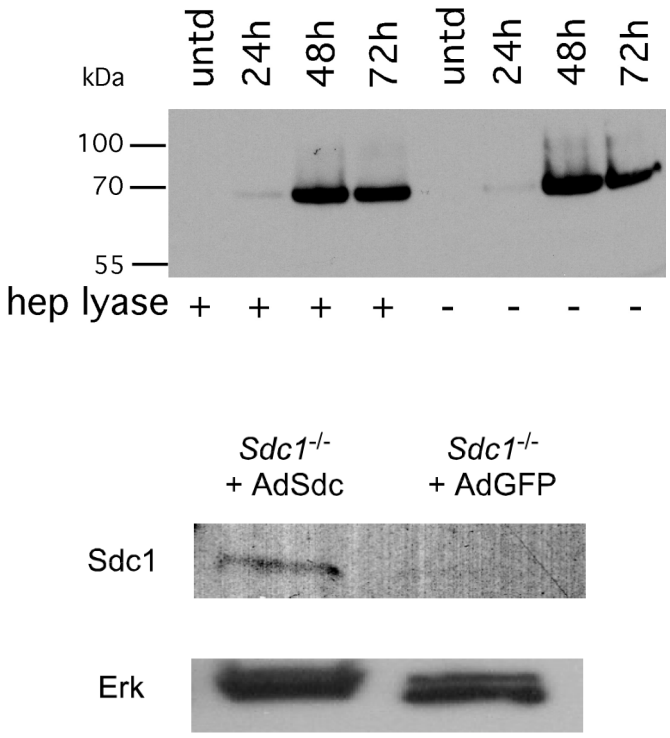

Figure 2-6: *Adenoviral-mediated syndecan-1 expression.* (*top panel*) Isolated primary *Sdc1*$^{-/-}$ hepatocytes were infected with AdGAG mutant syndecan-1 adenovirus (multiplicity of infection = 1). Protein expression was visualized by western blot using mAB 281-2 (1:500, BD Pharmingen) at 24, 48, and 72 hours post infection. Heparan lyase treatment had no effect on the bands, indicating that AdGAG was, in fact, translated without GAG chains. Samples labeled "untd " were not treated with virus. Samples labeled "hep lyase" were treated with a mixture of heparin lyases I, II, and II as well as chondroitinase ABC before electrophoresis. (*bottom panel*) Hepatocytes were isolated from Sdc1$^{-/-}$ mice two weeks post-transduction with AdSdc1. Protein expression of syndecan-1 was visualized as in the top panel. Erk expression was measured as a loading control.

2.4.4 Structure/function analysis of syndecan-1 *in vivo*

Once we had designed and produced the syndecan-1 constructs, verified their expression *in vivo*, and determined optimal dose and timing, we were ready to assess the behavior of the wildtype and mutant syndecan-1 constructs in live animals. To evaluate the ability of syndecan-1 constructs to restore clearance in mice, *Sdc1*$^{-/-}$ mice were injected with live virions via the tail vein. Two weeks post-injection, animals were subjected to a vitamin A fat tolerance test. Fasted mice were given a bolus mixture of [^{3}H]retinol and corn oil by oral gavage, and blood was sampled at various time points to determine the plasma level of ^{3}H-counts. In the intestine, [^{3}H]retinol is converted to fatty acid esters and incorporated into newly made chylomicrons, and its only route of removal is through clearance in the liver.

Infection with adenovirus containing wildtype syndecan-1 cDNA (AdSdc1) normalized clearance compared to *Sdc1*$^{-/-}$ mice infected with AdGFP ($P = 0.0037$), and the excursion curve was similar to that of wild-type mice (Figure 2-7). These findings show that hepatic syndecan-1 is both necessary and sufficient to clear plasma triglycerides. They contrast the results of a previous study, which showed that syndecan-1 overexpression leads to hypertriglyceridemia (20). This may reflect differences in viral load, timing of the lipid analyses relative to viral infection, or acute liver injury in the earlier study.

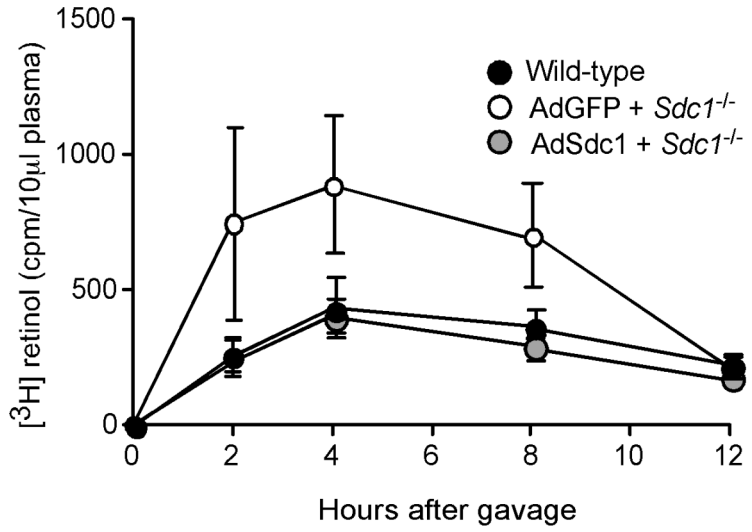

Figure 2-7: *AdSdc1 restores postprandial clearance to wildtype levels in* Sdc1$^{-/-}$ *mice.* *Sdc1*$^{-/-}$ mice were injected with AdSdc1 (n = 6 mice) or AdGFP (n = 6 mice). Plasma retinol ester levels were measured as described above and compared with wild-type mice (filled circles). The areas under the curve were 3,700 ± 1,100 for wild-type, 7,400 ± 2,600 for AdGFP *Sdc1*$^{-/-}$, and 3,200 ± 900 for AdSdc1 *Sdc1*$^{-/-}$. Animals treated with AdSdc1 demonstrated clearance similar to that wild-type animals (gray circles, P = 0.1272) and significantly faster clearance than *Sdc1*$^{-/-}$ mice treated with AdGFP (P = 0.0037).

Next, *Sdc1*$^{-/-}$ mice were injected with adenovirus containing the various mutant syndecan-1 constructs. These mice were subjected to the same vitamin A fat tolerance test as described above, and a bar graph representing counts remaining in 10 μL of plasma at the four-hour time point is presented in Figure 2-8. Overexpression of syndecan-4 (AdSdc4) in *Sdc1*$^{-/-}$ mice did not rescue clearance to wildtype levels. Additionally, clearance was not rescued in mice lacking all but one amino acid of the intracellular domain of syndecan-1 (AdDeltaC). As expected, mice expressing a syndecan-1 construct lacking all three heparan sulfate attachment sites (AdHS) did not restore clearance. Interestingly, however, adenovirus encoding a syndecan-1 construct

lacking only one heparan sulfate attachment site (Ad45) was also unable to rescue clearance.

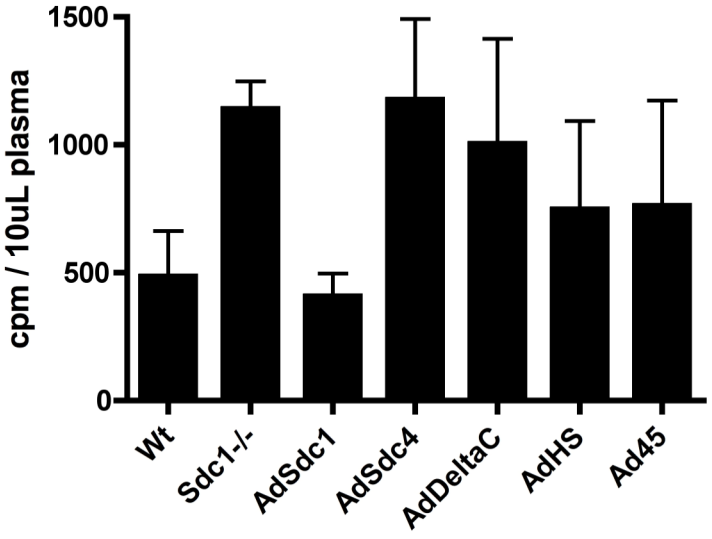

Figure 2-8: *Syndecan-1 mutant adenoviruses do not rescue clearance in* Sdc1$^{-/-}$ *mice* in vivo. *Sdc1*$^{-/-}$ mice were injected with 2 x 10^{11} viral particles of AdSdc1, AdSdc4, AdDeltaC, AdHS, or Ad45. Two weeks later, the mice were subjected to a vitamin A fat tolerance test. Counts remaining in 10 μL of plasma at four hours post-gavage is shown. Data from wildtype and *Sdc1*$^{-/-}$ mice injected with PBS is shown for reference.

2.5 Syndecan-1 as a clearance receptor: Implications for disease-associated hypertriglyceridemia

Hypertriglyceridemia, characterized by the accumulation of triglyceride-rich lipoproteins in the blood, affects 10-20% of the population in western countries and increases the risk of atherosclerosis and coronary artery disease in patients (21-25). While some cases arise from genetic defects (such as mutations in LPL, APOE, or LDLR), many cases are associated with disease states such as hypothyroidism, pancreatitis, nephrotic syndrome, obesity, diabetes, and sepsis (26-28). Because

syndecan-1 mediates clearance of TRLs in human hepatocytes, it is possible that syndecan-1 dysfunction plays a role in the hypertriglyceridemia associated with these various disease states. This section describes studies that address the contribution of syndecan-1 to the dyslipidemia associated with diabetes and sepsis.

2.5.1 Neither changes in syndecan-1 expression nor heparan sulfate fine structure are observed in hepatocytes from diabetic mice

Hypertriglyceridemia is a significant complication of insulin-dependent diabetes mellitus (IDDM) that likely contributes to cardiovascular disease in affected individuals, but its cause remains unknown (29-31). Insulin deficiency suppresses hepatic triglyceride production (32, 33), suggesting that diabetes-associated hyperlipidemia is due to reduced clearance of plasma lipoproteins, especially remnant lipoproteins enriched in cholesterol and triglycerides. This led us to examine hepatic syndecan-1 levels and heparan sulfate composition in a mouse model of IDDM.

In this study, mice were made diabetic by administering 50 mg/kg body weight of streptozotocin (STZ) intraperitoneally for 5 consecutive days. Mice developed hypertriglyceridemia (>400 mg/dL blood glucose) 6-8 weeks post treatment, and approximately 50% of diabetic mice showed a mild elevation of fasting triglyceride levels (51 ± 13 mg/dL in control mice versus 81 ± 20 mg/dL in streptozotocin treated mice, n = 12 per strain, $P < 0.003$) with no significant change in plasma cholesterol. The diabetic mice also showed significantly delayed clearance of postprandial triglycerides.

To examine whether changes in hepatocyte syndecan-1 were responsible for the delayed postprandial clearance observed in IDDM mice, we examined syndecan-1 expression in freshly isolated hepatocytes. We did not detect any differences in syndecan-1 core protein levels by western blotting of hepatocyte extracts from IDDM mice (Figure 2-9). Similar results were also observed at the mRNA level as determined by qPCR (data not shown). Thus, altered syndecan-1 expression did not account for the delayed clearance of plasma triglycerides in IDDM mice.

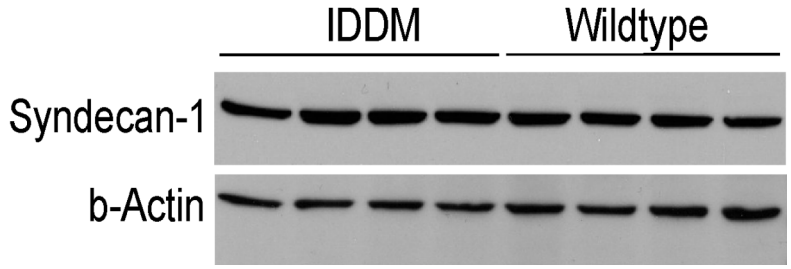

Figure 2-9: *Western blot analysis of syndecan-1 expression in IDDM hepatocytes.* Proteoglycans were isolated from hepatocyte cell pellets according to a protocol adapted from Reizes *et al* (34) and collected by anion exchange chromatography (DEAE-Sephacel). Samples were digested for 1 h with a mixture of 2 milliunits/mL heparin lyases I and II and 5 milliunits/mL heparin lyase III and 10 mU/mL chondroitinase ABC. The deglycosylated core proteins were separated by SDS-PAGE (NuPage 4-12% BisTris gel, Invitrogen) and transferred to nitrocellulose. Syndecan-1 was detected with mAb 281-2 (BD Pharmingen) and corresponding horseradish peroxidase-conjugated secondary antibody. One band was detected at 140 kDa, and this band likely represents a syndecan-1 oligomer (35-37). Beta actin was detected with an anti-β-actin antibody (Cell Signaling Technologies) and a horseradish peroxidase-conjugated secondary. Each lane represents a different mouse (n=4 per group).

It is possible that syndecan-1 mediated clearance is impaired in IDDM due to changes in heparan sulfate fine structure, as the interaction between triglyceride-rich lipoproteins and hepatocyte heparan sulfate depends on the presence of *N*- and *2-O*-

sulfate modified disaccharides (1, 38). Previous studies have suggested that expression of NDST1, the major heparan sulfate sulfating enzyme, is reduced in IDDM (39-44). To address this issue, we measured both the amount of liver heparan sulfate present in IDDM livers and its composition. Heparan sulfate fine structure was determined quantitatively by glycan reductive isotope labeling-liquid chromatography/mass spectroscopy (GRIL-LC/MS) as described (45). The amount of heparan sulfate was expressed relative to liver wet weight. Interestingly, no change in heparan sulfate amount or fine structure was observed in IDDM mice (Figure 2-10). As a control, disaccharide composition was analyzed in Ndst1 deficient mice (*Ndst1*$^{f/f}$*AlbCre*$^{+}$), which show statistically significant decreases in *N*-, *2-O*- and *6-O*-sulfation. Taken together, these data show that hypertriglyceridemia associated with streptozotocin-induced diabetes mellitus is not due to deficient syndecan-1-mediated clearance.

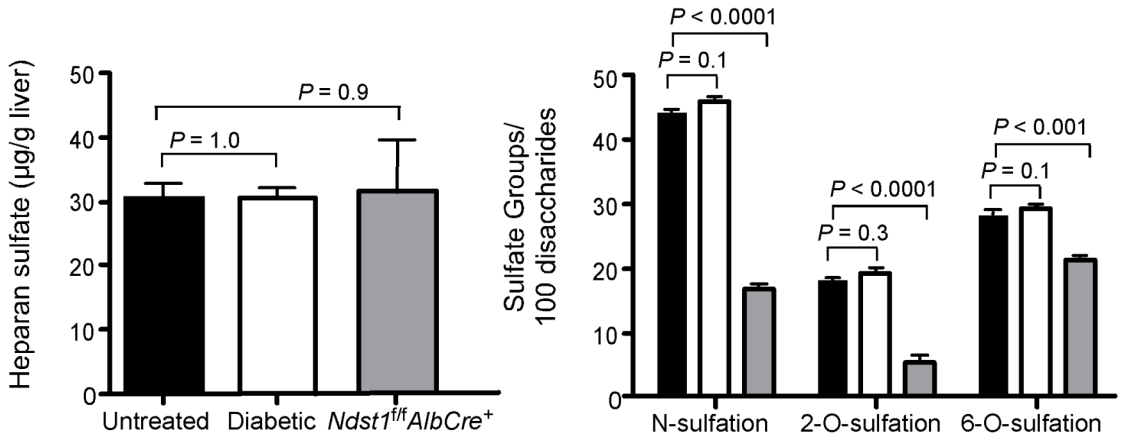

Figure 2-10: *Analysis of liver heparan sulfate amount and disaccharide composition.* (*left panel*) Liver heparan sulfate was purified from untreated (n = 9) and STZ treated hyperglycemic diabetic (n = 9) wild-type mice and Ndst1 mutant mice (n = 4). The mass of heparan sulfate purified from each animal was determined by GRIL-LC/MS. Results were normalized to the amount of liver that had been analyzed (wet weight). (*right panel*) The disaccharide composition of liver heparan sulfate was determined by GRIL-LC/MS. *N*-sulfate and *6-O*-sulfate groups in glucosamine moieties and *2-O*-sulfate groups in uronic acids were calculated from the recovery of the individual disaccharides.

Our results contradict previous studies suggesting that hypertriglyceridemia observed in IDDM is due to altered heparan sulfate composition (39, 41-44, 46, 47). The conclusions of these studies were based on the finding that, in IDDM mice and rats, there is a ~50% decreased incorporation of [^{35}S]sulfate into liver heparan sulfate chains *in vivo*. Similarly, we observed a reduction (57 ± 27%) in the amount of [^{35}S]heparan sulfate produced in diabetic mouse liver compared with controls. A similar level of reduction was also observed in *Ndst1$^{f/f}$AlbCre^{+}* mice, which produce undersulfated heparan sulfate chains (50 ± 13%). What is the explanation for the decrease in [^{35}S]O_4 incorporation observed here and in prior studies? Earlier work suggested that diabetes can result in alteration of plasma and tissue sulfate pools (48-

51). Thus, the decrease in ^{35}S-labeling might have resulted simply from differences in the radiospecific activity of the $^{35}SO_4$ in the plasma or in the liver. Indeed, endogenous plasma sulfate concentration in diabetic mice was ~3-fold greater than in wild-type mice or *Ndst1*$^{f/f}$*AlbCre*$^{+}$ mice (Figure 2-11). The source of elevated plasma sulfate could be caused by altered anion filtration by the kidney due to diabetic nephropathy. Alternatively, IDDM is also known to induce gluconeogenesis, which could lead to the increased conversion of cysteine and methionine to pyruvate causing the release of inorganic sulfate from these amino acids. The release of inorganic sulfate from sulfur containing amino acids can be significant, providing all of the sulfate needed for glycosaminoglycan biosynthesis in cultured cells (52).

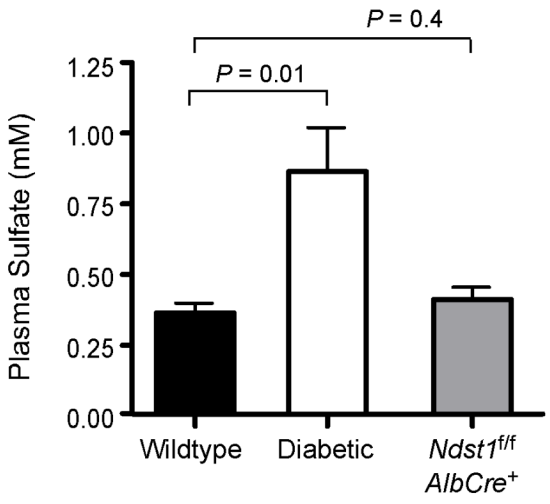

Figure 2-11: *Plasma sulfate levels in IDDM mice.* Sulfate levels were measured in untreated, diabetic, and Ndst1-mutant plasma samples (n = 6, respectively) by high performance liquid chromatography.

2.5.2 Sepsis

Sepsis, a potentially fatal medical condition, is often triggered by bacterial infection and is characterized by a whole-body inflammatory state. Sepsis patients suffer from hyperlipidemia of unknown etiology (27, 28). Hayashida *et al* recently showed that, in mice, injection of bacterial LPS induces syndecan-1 shedding in the liver (53). We predicted that induction of syndecan-1 shedding by treatment with LPS would affect VLDL binding and uptake in this model of septic shock.

To examine this possibility, we injected mice with 4.5 mg LPS/kg body weight. We found that 24 hours after injection, significantly more syndecan-1 ectodomain had accumulated in the plasma compared to mice injected with PBS alone. LPS injection also resulted in dramatic loss of synecan-1 in the liver, as measured by immunohistochemistry. Analysis of fasting plasma lipids showed that triglyceride levels increased two-fold in mice injected with LPS, whereas plasma total cholesterol did not change (Figure 2-12). The accumulation of plasma lipids was greatly accentuated under these conditions by deletion of the LDL receptor, which resembles the phenotype of compound mutants lacking hepatic heparan sulfate and LDL receptors (1). When the animals were challenged with human VLDL, the injected particles cleared less extensively in the LPS-injected mice (Figure 2-12c, area under the curve = 9200 ± 400 for LPS-injected mice versus 7000 ± 400 for the control), consistent with a loss of syndecan-1 clearance from the liver.

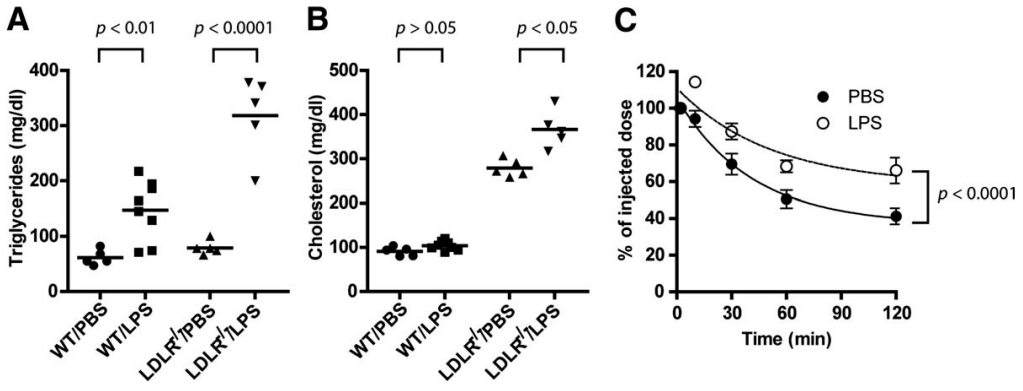

Figure 2-12: *LPS increases plasma triglycerides in mice.* Wild-type (WT) or *Ldlr*$^{-/-}$ mice were injected intraperitoneally with 4.5 mg LPS/kg body weight or phosphate-buffered saline as control. Eighteen hours later, the animals were fasted for 6 hours, and (*A*) plasma triglycerides and (*B*) total cholesterol were determined. In (*C*), similarly treated animals were injected with 20 µg of human VLDL, and the amount of remaining human apolipoprotein B was determined by ELISA at the indicated times. Each value represents the average ± standard deviation (n = 3 mice).

The observation that LPS induces shedding, elevates plasma TRLs and reduces VLDL clearance suggests that syndecan-1 shedding might be responsible in part for the elevation of plasma triglycerides in bacterial sepsis. Further studies are planned to determine whether syndecan-1 shedding contributes to the hyperlipidemia of sepsis in human patients and whether it might explain other idiopathic forms of hypertriglyceridemia, a common side effect of many drugs (26).

2.6 Discussion

Several studies that characterize syndecan-1's function as a TRL clearance receptor have been presented in this chapter. We have shown that syndecan-1 is the primary proteoglycan receptor in mice, and that syndecan-1 on primary human hepatocytes as well as Hep3B cells can bind and take up native TRL particles derived

from fasted donors. These findings suggest that changes in the expression of syndecan-1 or the assembly of heparan sulfate chains might explain some forms of human dyslipidemias. Though IDDM-induced hypertriglyceridemia in mice is not associated with any obvious changes in syndecan-1 expression or alteration of liver heparan sulfate content or composition, LPS-mediated syndecan-1 shedding may contribute to hyperlipidemia of sepsis. Further studies are necessary to determine if syndecan-1 plays a role in the other forms of disease-associated hypertriglyceridemia or hypertriglyceridemia of unknown etiology.

A step-wise mechanism of binding remnants by syndecan-1 and hand-off to LDLR or LRP receptors has been proposed (54-56). However, in the present study, a mutant lacking all but one amino acid of the cytoplasmic domain (AdDeltaC) was unable to rescue clearance in *Sdc1*$^{-/-}$ mice. As endocytosis of syndecan-1 depends on its cytoplasmic domain (16), this data indicates that syndecan-1 endocytosis is necessary for its function in TRL clearance and suggests that syndecan-1 is an independent endocytic receptor for TRLs. Syndecan-1 is endocytosed via a clathrin- and caveolin-independent route that is preceded by clustering and translocation to lipid rafts (16, 57-59), while endocytosis of LDLR and LRP1 is known to occur through classical clathrin-mediated endocytosis. This observation further argues against the possibility that syndecan-1 acts in concert with either of these receptors to mediate clearance. The path of syndecan-1 after endocytosis has not been well characterized, although there is evidence that a portion may be recycled to the cell surface like other endocytic receptors (60) and that it is eventually degraded in lysosomes (61).

The binding of TRLs to heparan sulfate chains presumably occurs through electrostatic interactions between negatively charged sulfate and carboxyl groups with complementary positively charged domains in the apolipoproteins (APOB, APOE, etc.) or lipases (lipoprotein lipase or hepatic lipase) associated with the particles. It has recently been shown that the interaction between triglyceride-rich lipoproteins and hepatocyte heparan sulfate depends on the presence of *N*- and *2*-*O*-sulfate modified disaccharides (1, 38). Both murine and human hepatocytes express multiple heparan sulfate proteoglycans, however, and it remains unclear why syndecan-1 is the primary proteoglycan receptor. Syndecan-1 is localized to hepatocyte microvilli lining the space of Disse, and is thus poised to mediate clearance (3). It is likely, however, that syndecan-1 possesses unique structural features that facilitate its function in TRL clearance, as overexpression of syndecan-4, a structurally related but distinct protein, did not rescue clearance. However, care must be taken when interpreting these preliminary data, as we did not verify the location of the overexpressed syndecan-4. It may be expressed on the basolateral surface of the cells, and therefore would not come into contact with TRLs in the space of Disse.

One unique feature of syndecan-1 is that it contains sites for attachment of up to three heparan sulfate chains. TRL binding and internalization might depend on multiple interactions with one or more chains on individual syndecan-1 molecules or clustered multimers. Interestingly, mice expressing the Ad45 syndecan-1 mutant (lacking only one heparan sulfate attachment site) were unable to clear particles efficiently, which would support the hypothesis that all three chains are required to engage lipoproteins and stabilize the lipoprotein-proteoglycan complex before

endocytosis. Previous studies have suggested that syndecan-1 is most active when all three heparan sulfate sites are occupied, and that certain chains may be more important for ligand binding than others (62). Further study of the other mutants lacking combinations of heparan sulfate chains (Ad35,47, etc.) is necessary to fully understand the interaction between TRLs and syndecan-1.

The syndecan-1 structure/function study presented here is still ongoing. Evaluation of the other mutant constructs, including ecto-only, ecto-swap, and no-cleavage, will need to be completed. There are several important controls that also need to be done. These include histology of livers from adenovirus-infected mice to verify localization of the mutant syndecan-1 constructs on hepatocyte cell surfaces in the space of Disse, and confirmation of the data using a cell culture model of VLDL binding and uptake post-AdSdc1 infection. Finally, we need to assess the role of chondroitin sulfate chains in syndecan-1 binding to TRLs.

2.7 Acknowledgements

Section 2.2 and section 2.4 contain material reprinted from The Journal of Clinical Investigation, Volume 119, Issue 11, Kristin I. Stanford, Joseph R. Bishop, Erin M. Foley, Jon C. Gonzales, Ingrid R. Niesman, Joseph L. Witztum, Jeffrey D. Esko, “Syndecan-1 is the primary heparan sulfate proteoglycan mediating hepatic clearance of triglyceride-rich lipoproteins in mice”, Pages 3236-45, Copyright © (2009), The American Society for Clinical Investigation.

Sections 2.3 and section 2.5 contain material reprinted from Hepatology, Volume 55, Issue 1, Yiping Deng, Erin M. Foley, Jon C. Gonzales, Philip Gordts,

Yulin Li, and Jeffrey D. Esko, "Shedding of syndecan-1 from human hepatocytes alters VLDL clearance", Pages 277-86, Copyright © (2012) with permission from John Wiley and Sons.

Section 2.5 contains material reprinted from The Journal of Biological Chemistry, Volume 285, Issue 19, Joseph R. Bishop, Erin Foley, Roger Lawrence, and Jeffrey D. Esko, "Insulin-dependent diabetes mellitus in mice does not alter liver heparan sulfate", Pages 14658-62, Copyright © (2010), American Society for Biochemistry and Molecular Biology.

Together with her coauthors, the author would like to thank Dr. Pyong Park for assistance with adenovirus creation, and Dr. Anne Zaiss for technical assistance with adenovirus purification. The author would also like to acknowledge Patrick Secrest, David Ditto, and Qiongyu Chen for their kind assistance with tail-vein injections and serum chemistry analysis. The author would additionally like to thank Dr. Adam Cadwallader for cloning assistance. Work was conducted within the department of Cellular and Molecular Medicine, and the Glycobiology Research and Training Center, University of California, San Diego, La Jolla, California.

2.8 References

1. MacArthur, J.M., Bishop, J.R., Wang, L., Stanford, K.I., Bensadoun, A., Witztum, J.L., and Esko, J.D. 2007. Liver heparan sulfate proteoglycans mediate clearance of triglyceride-rich lipoproteins independently of LDL receptor family members. *J Clin Invest* 117:153-164.

2. Bishop, J.R., Passos-Bueno, M.R., Fong, L., Stanford, K.I., Gonzales, J.C., Yeh, E., Young, S.G., Bensadoun, A., Witztum, J.L., Esko, J.D., et al. 2010. Deletion of the basement membrane heparan sulfate proteoglycan type XVIII collagen causes hypertriglyceridemia in mice and humans. *PLoS ONE* 5:e13919.

3. Stanford, K.I., Bishop, J.R., Foley, E.M., Gonzales, J.C., Niesman, I.R., Witztum, J.L., and Esko, J.D. 2009. Syndecan-1 is the primary heparan sulfate proteoglycan mediating hepatic clearance of triglyceride-rich lipoproteins in mice. *J Clin Invest* 119:3236-3245.

4. Mann, W.A., Meyer, N., Berg, D., Greten, H., and Beisiegel, U. 1999. Lipoprotein lipase compensates for the defective function of apo E variants in vitro by interacting with proteoglycans and lipoprotein receptors. *Atherosclerosis* 145:61-69.

5. Roskams, T., De Vos, R., David, G., Van Damme, B., and Desmet, V. 1998. Heparan sulphate proteoglycan expression in human primary liver tumours. *J Pathol* 185:290-297.

6. Roskams, T., Moshage, H., De Vos, R., Guido, D., Yap, P., and Desmet, V. 1995. Heparan sulfate proteoglycan expression in normal human liver. *Hepatology* 21:950-958.

7. Manon-Jensen, T., Itoh, Y., and Couchman, J.R. 2010. Proteoglycans in health and disease: the multiple roles of syndecan shedding. *Febs J* 277:3876-3889.

8. Rohlmann, A., Gotthardt, M., Hammer, R.E., and Herz, J. 1998. Inducible inactivation of hepatic LRP gene by cre-mediated recombination confirms role of LRP in clearance of chylomicron remnants. *J Clin Invest* 101:689-695.

9. Basford, J.E., Wancata, L., Hofmann, S.M., Silva, R.A., Davidson, W.S., Howles, P.N., and Hui, D.Y. 2011. Hepatic deficiency of low density lipoprotein receptor-related protein-1 reduces high density lipoprotein secretion and plasma levels in mice. *J Biol Chem*.

10. Saunders, S., Jalkanen, M., O'Farrell, S., and Bernfield, M. 1989. Molecular cloning of syndecan, an integral membrane proteoglycan. *J Cell Biol* 108:1547-1556.

11. Kokenyesi, R., and Bernfield, M. 1994. Core protein structure and sequence determine the site and presence of heparan sulfate and chondroitin sulfate on syndecan-1. *J Biol Chem* 269:12304-12309.

12. Bernfield, M., Kokenyesi, R., Kato, M., Hinkes, M.T., Spring, J., Gallo, R.L., and Lose, E.J. 1992. Biology of the syndecans: a family of transmembrane heparan sulfate proteoglycans. *Annu Rev Cell Biol* 8:365-393.

13. Rousselle, P., and Letourneur, F. 2009. Mysterious tasks of tyrosines in syndecan-1 cytoplasmic tail. *ScientificWorldJournal* 9:629-632.

14. Zimmermann, P., and David, G. 1999. The syndecans, tuners of transmembrane signaling. *FASEB J* 13:S91-S100.

15. Wang, Z., Gotte, M., Bernfield, M., and Reizes, O. 2005. Constitutive and accelerated shedding of murine syndecan-1 is mediated by cleavage of its core protein at a specific juxtamembrane site. *Biochemistry* 44:12355-12361.

16. Fuki, I.V., Meyer, M.E., and Williams, K.J. 2000. Transmembrane and cytoplasmic domains of syndecan mediate a multi-step endocytic pathway involving detergent-insoluble membrane rafts. *Biochem J* 351:607-612.

17. Green, M., and Loewenstein, P.M. 2006. Human adenoviruses: propagation, purification, quantification, and storage. *Curr Protoc Microbiol* Chapter 14:Unit 14C 11.

18. Rohlmann, A., Gotthardt, M., Willnow, T.E., Hammer, R.E., and Herz, J. 1996. Sustained somatic gene inactivation by viral transfer of Cre recombinase. *Biotechnology* 14:1562-1565.

19. Hu, L., van der Hoogt, C.C., Espirito Santo, S.M., Out, R., Kypreos, K.E., van Vlijmen, B.J., Van Berkel, T.J., Romijn, J.A., Havekes, L.M., van Dijk, K.W., et al. 2008. The hepatic uptake of VLDL in lrp-ldlr-/-vldlr-/- mice is regulated by LPL activity and involves proteoglycans and SR-BI. *J Lipid Res* 49:1553-1561.

20. Cortes, V., Amigo, L., Donoso, K., Valencia, I., Quinones, V., Zanlungo, S., Brandan, E., and Rigotti, A. 2007. Adenovirus-mediated hepatic syndecan-1 overexpression induces hepatocyte proliferation and hyperlipidaemia in mice. *Liver Int* 27:569-581.

21. Stalenhoef, A.F., and de Graaf, J. 2008. Association of fasting and nonfasting serum triglycerides with cardiovascular disease and the role of remnant-like lipoproteins and small dense LDL. *Curr Opin Lipidol* 19:355-361.

22. Nordestgaard, B.G., Benn, M., Schnohr, P., and Tybjaerg-Hansen, A. 2007. Nonfasting triglycerides and risk of myocardial infarction, ischemic heart disease, and death in men and women. *Jama* 298:299-308.

23. Bansal, S., Buring, J.E., Rifai, N., Mora, S., Sacks, F.M., and Ridker, P.M. 2007. Fasting compared with nonfasting triglycerides and risk of cardiovascular events in women. *Jama* 298:309-316.

24. Langsted, A., Freiberg, J.J., and Nordestgaard, B.G. 2008. Fasting and nonfasting lipid levels: influence of normal food intake on lipids, lipoproteins, apolipoproteins, and cardiovascular risk prediction. *Circulation* 118:2047-2056.

25. Fujioka, Y., and Ishikawa, Y. 2009. Remnant lipoproteins as strong key particles to atherogenesis. *J Atheroscler Thromb*.

26. Yuan, G., Al-Shali, K.Z., and Hegele, R.A. 2007. Hypertriglyceridemia: its etiology, effects and treatment. *Cmaj* 176:1113-1120.

27. Evans, R.D., and Williamson, D.H. 1991. Signals, mechanisms, and function of the acute lipid response to sepsis. *Biochem Cell Biol* 69:320-321.

28. Mizock, B.A. 2000. Metabolic derangements in sepsis and septic shock. *Crit Care Clin* 16:319-336, vii.

29. Haffner, S.M. 1998. The importance of hyperglycemia in the nonfasting state to the development of cardiovascular disease. *Endocr Rev* 19:583-592.

30. Reusch, J.E. 2003. Diabetes, microvascular complications, and cardiovascular complications: what is it about glucose? *J Clin Invest* 112:986-988.

31. Goldberg, R.B. 2003. Cardiovascular disease in patients who have diabetes. *Cardiol Clin* 21:399-413.

32. Bar-On, H., Roheim, P.S., and Eder, H.A. 1976. Hyperlipoproteinemia in streptozotocin-treated rats. *Diabetes* 25:509-515.

33. Ebara, T., Hirano, T., Mamo, J.C., Sakamaki, R., Furukawa, S., Nagano, S., and Takahashi, T. 1994. Hyperlipidemia in streptozocin-diabetic hamsters as a model for human insulin-deficient diabetes: comparison to streptozocin-diabetic rats. *Metabolism* 43:299-305.

34. Reizes, O., Lincecum, J., Wang, Z., Goldberger, O., Huang, L., Kaksonen, M., Ahima, R., Hinkes, M.T., Barsh, G.S., Rauvala, H., et al. 2001. Transgenic expression of syndecan-1 uncovers a physiological control of feeding behavior by syndecan-3. *Cell* 106:105-116.

35. Choi, S., Lee, E., Kwon, S., Park, H., Yi, J.Y., Kim, S., Han, I.O., Yun, Y., and Oh, E.S. 2005. Transmembrane domain-induced oligomerization is crucial for the functions of syndecan-2 and syndecan-4. *J Biol Chem* 280:42573-42579.

36. Asundi, V.K., and Carey, D.J. 1995. Self-association of N-syndecan (syndecan-3) core protein is mediated by a novel structural motif in the transmembrane domain and ectodomain flanking region. *J Biol Chem* 270:26404-26410.

37. Miettinen, H.M., and Jalkanen, M. 1994. The cytoplasmic domain of syndecan-1 is not required for association with Triton X-100-insoluble material. *J Cell Sci* 107:1571-1581.

38. Stanford, K.I., Wang, L., Castagnola, J., Song, D., Bishop, J.R., Brown, J.R., Lawrence, R., Bai, X., Habuchi, H., Tanaka, M., et al. 2010. Heparan sulfate 2-O-sulfotransferase is required for triglyceride-rich lipoprotein clearance. *J Biol Chem* 285:286-294.

39. Williams, K.J. 2008. Molecular processes that handle -- and mishandle -- dietary lipids. *J Clin Invest* 118:3247-3259.

40. Goldberg, I.J., Hu, Y., Noh, H.L., Wei, J., Huggins, L.A., Rackmill, M.G., Hamai, H., Reid, B.N., Blaner, W.S., and Huang, L.S. 2008. Decreased lipoprotein clearance is responsible for increased cholesterol in LDL receptor knockout mice with streptozotocin-induced diabetes. *Diabetes* 57:1674-1682.

41. Williams, K.J., Liu, M.L., Zhu, Y., Xu, X., Davidson, W.R., McCue, P., and Sharma, K. 2005. Loss of heparan N-Sulfotransferase in diabetic liver: role of angiotensin II. *Diabetes* 54:1116-1122.

42. Kofoed-Enevoldsen, A., and Eriksson, U.J. 1991. Inhibition of N-acetylheparosan deacetylase in diabetic rats. *Diabetes* 40:1449-1452.

43. Kofoed-Enevoldsen, A. 1992. Inhibition of glomerular glucosaminyl N-deacetylase in diabetic rats. *Kidney Int* 41:763-767.

44. Kjellen, L., Bielefeld, D., and Hook, M. 1983. Reduced sulfation of liver heparan sulfate in experimentally diabetic rats. *Diabetes* 32:337-342.

45. Lawrence, R., Olson, S.K., Steele, R.E., Wang, L., Warrior, R., Cummings, R.D., and Esko, J.D. 2008. Evolutionary differences in glycosaminoglycan fine structure detected by quantitative glycan reductive isotope labeling. *J Biol Chem* 283:33674-33684.

46. Goldberg, M., Rapoport, O., Septier, D., Palmier, K., Hall, R., Embery, G., Young, M., and Ameye, L. 2003. Proteoglycans in predentin: the last 15 micrometers before mineralization. *Connect Tissue Res* 44 Suppl 1:184-188.

47. Ebara, T., Conde, K., Kako, Y., Liu, Y., Xu, Y., Ramakrishnan, R., Goldberg, I.J., and Shachter, N.S. 2000. Delayed catabolism of apoB-48 lipoproteins due to decreased heparan sulfate proteoglycan production in diabetic mice. *J Clin Invest* 105:1807-1818.

48. Blezquez-Medela, A.M., Lopez-Novoa, J.M., and Martinez-Salgado, C. 2009. Mechanisms involved in the genesis of diabetic nephropathy. *Curr Diabetes Rev*.

49. Fan, M.Y., and Templeton, D.M. 1992. Sulfate metabolism in experimental diabetes. *Diabete Metab* 18:98-103.

50. Spiro, M.J. 1987. Sulfate metabolism in the alloxan-diabetic rat: relationship of altered sulfate pools to proteoglycan sulfation in heart and other tissues. *Diabetologia* 30:259-267.

51. Cohen, M.P., and Surma, M.L. 1984. Effect of diabetes on in vivo metabolism of [35S]-labeled glomerular basement membrane. *Diabetes* 33:8-12.

52. Esko, J.D., Elgavish, A., Prasthofer, T., Taylor, W.H., and Weinke, J.L. 1986. Sulfate transport-deficient mutants of Chinese hamster ovary cells. Sulfation of glycosaminoglycans dependent on cysteine. *J Biol Chem* 261:15725-15733.

53. Hayashida, K., Parks, W.C., and Park, P.W. 2009. Syndecan-1 shedding facilitates the resolution of neutrophilic inflammation by removing sequestered CXC chemokines. *Blood* 114:3033-3043.

54. Mahley, R.W., and Ji, Z.S. 1999. Remnant lipoprotein metabolism: key pathways involving cell-surface heparan sulfate proteoglycans and apolipoprotein E. *J Lipid Res* 40:1-16.

55. Mahley, R.W., and Huang, Y. 2007. Atherogenic remnant lipoproteins: role for proteoglycans in trapping, transferring, and internalizing. *J Clin Invest* 117:94-98.

56. Wilsie, L.C., and Orlando, R.A. 2003. The low density lipoprotein receptor-related protein complexes with cell surface heparan sulfate proteoglycans to regulate proteoglycan-mediated lipoprotein catabolism. *J Biol Chem* 278:15758-15764.

57. Fuki, I.V., Kuhn, K.M., Lomazov, I.R., Rothman, V.L., Tuszynski, G.P., Iozzo, R.V., Swenson, T.L., Fisher, E.A., and Williams, K.J. 1997. The syndecan family of proteoglycans. Novel receptors mediating internalization of atherogenic lipoproteins in vitro. *J Clin Invest* 100:1611-1622.

58. Wilsie, L.C., Gonzales, A.M., and Orlando, R.A. 2006. Syndecan-1 mediates internalization of apoE-VLDL through a low density lipoprotein receptor-

related protein (LRP)-independent, non-clathrin-mediated pathway. *Lipids Health Dis* 5:23.

59. Schmid, S.L. 1997. Clathrin-coated vesicle formation and protein sorting: an integrated process. *Annu Rev Biochem* 66:511-548.

60. Zimmermann, P., Zhang, Z., Degeest, G., Mortier, E., Leenaerts, I., Coomans, C., Schulz, J., N'Kuli, F., Courtoy, P.J., and David, G. 2005. Syndecan recycling [corrected] is controlled by syntenin-PIP2 interaction and Arf6. *Dev Cell* 9:377-388.

61. Burbach, B.J., Friedl, A., Mundhenke, C., and Rapraeger, A.C. 2003. Syndecan-1 accumulates in lysosomes of poorly differentiated breast carcinoma cells. *Matrix Biol* 22:163-177.

62. Langford, J.K., Stanley, M.J., Cao, D.J., and Sanderson, R.D. 1998. Multiple heparan sulfate chains are required for optimal syndecan-1 function. *J Biol Chem* 273:29965-29971.

CHAPTER 3

Heparan sulfate proteoglycans mediate hepatic clearance of triglyceride-rich lipoproteins of unique size and composition

3.1 Summary

Several hepatic receptors clear chylomicron and very low-density lipoprotein remnants from the circulation, but the relative contribution of each class of receptors remains unknown. In the present study, we characterized the relative contribution to clearance of the low-density lipoprotein receptor (Ldlr), Ldlr-related protein-1 (Lrp1), and heparan sulfate proteoglycan (HSPG) receptors by analyzing mice in which we inactivated Ldlr, Lrp1, HSPG receptors and various combinations of all three receptors. Fasting triglyceride data in single and double mutant mice showed that HSPGs and the Ldlr dominate the receptor landscape, while Lrp1 contributes significantly to clearance when the Ldlr is absent. Mice lacking hepatic expression of all three receptors (*AlbCre*$^{+}$*Ndst1*$^{f/f}$*Lrp1*$^{f/f}$*Ldlr*$^{-/-}$*)* displayed massive hyperlipidemia (triglyceride: 874 ± 270 mg/dL; total cholesterol: 1308 ± 346 mg/dL) and exhibited persistent elevated postprandial triglyceride levels and reduced liver clearance. Analysis of the particles accumulating in mutants showed that HSPGs preferentially clear a subset of smaller triglyceride-rich lipoproteins (~20-40 nm diameter) enriched in ApoE and ApoAV, while Ldlr and Lrp1 clear a larger subset of particles (~40-60 nm diameter) containing ApoB100, ApoB48, ApoE, and ApoCs. Taken together, these data show that HSPGs, Ldlr, and Lrp1 clear distinct subsets of particles; that HSPGs

work independently from Ldlr and Lrp1; and that Ldlr, Lrp1, and HSPGs are the three major hepatic TRL clearance receptors in mice.

3.2 Introduction

Hypertriglyceridemia increases the risk of atherosclerosis, coronary artery disease, and pancreatitis (1-6). This condition, which affects 10–20% of the population in western countries, is characterized by the accumulation of triglyceride-rich lipoproteins (TRLs) in the blood. TRLs consist of intestinal chylomicrons derived from dietary fats and very low density lipoproteins (VLDL) from the liver, as well as remnant particles resulting from the lipolytic processing of these lipoproteins in the peripheral circulation. These remnant particles are cleared in the liver by multiple receptors. Genetic defects in TRL synthesis, processing and clearance result in accumulation of plasma triglycerides, but account only for a small fraction of the patients presenting with hypertriglyceridemia.

Clearance of TRL remnants occurs in the liver via a multi-step process. The particles first pass through the fenestrated endothelium of the liver sinusoids and are sequestered in the perisinusoidal space of Disse. Here, remnants undergo further processing by lipoprotein lipase (Lpl) and hepatic lipase, which may remain associated with the particles. Particles are then cleared by endocytic receptors on the surface of hepatocytes, leading to their lysosomal catabolism. Several receptors for remnant lipoproteins have been identified, including the low-density lipoprotein receptor (Ldlr) (7), members of the Ldlr-related protein family (Lrp1 and Lrp5) (8, 9), the very low density lipoprotein receptor (Vldlr) (11, 12), scavenger receptor B1 (SR-B1) (13, 14),

the lipolysis stimulated receptor (Lsr) (15), and syndecan-1 (10), a type of heparan sulfate proteoglycan (HSPG). The relative contribution of these receptors to clearance remains controversial.

In the present study, we sought to understand the relative contribution of Ldlr, Lrp1, and HSPGs to clearance of remnant lipoproteins using a genetic approach. To this end, we interbred mice lacking *Ndst1*, *Ldlr* and *Lrp1*, producing double and triple mutants lacking all three receptors. Based on analysis of fasting lipid levels, we found that HSPGs and the Ldlr are the two dominant receptors mediating clearance, although Lrp contributes to clearance in the absence of the other two receptors. Our findings show that HSPGs, Ldlr, and Lrp1 preferentially bind and internalize distinct subsets of particles, that HSPGs work independently from Ldlr and Lrp1, and that Ldlr, Lrp1, and HSPGs account for the majority of TRL clearance in the liver in mice.

3.3 Results

3.3.1 Inactivation of *Ldlr, Lrp1* and *Ndst1*

We previously described mice in which the Cre transgene under control of the albumin promoter was used to inactivate the heparan sulfate biosynthetic enzyme GlcNAc *N*-deacetlyase *N*-sulfotransferase-1 (Ndst1) selectively in hepatocytes (16). Ndst1 affects the sulfation of all HSPGs including syndecan-1, the primary hepatic proteoglycan receptor (10). Like $Sdc1^{-/-}$ mice, $Cre^{+}Ndst1^{f/f}$ mice have delayed clearance of postprandial triglycerides and display a two-fold accumulation of fasting triglycerides due to loss of sulfation of the HS chains located on syndecan-1. Syndecan-1 knockout mice were not used in this study because a conditional mutant

has not been described, but the phenotype of Ndst1-deficient mice is identical to that of syndecan-1 knockout mice.

$Cre^{+}Ndst1^{f/f}$ mice were bred with *Ldlr* systemic knockout mice *($Ldlr^{-/-}$)* or mice bearing a floxed allele of *Lrp1* (*$Lrp1^{f/f}$*) to produce all combinations of double and triple receptor mutant mice. The compound mutant mice were viable and fertile, and produced litters of normal size and the expected Mendelian ratios of genotypes.

To verify that the Cre transgene under control of the albumin promoter was sufficient to mediate recombination of two separate floxed genes (*Ndst1* and *Lrp1*) in the *$Cre^{+}Ndst1^{f/f}Lrp1^{f/f}Ldlr^{-/-}$* mouse, we analyzed hepatic HS disaccharide composition using mass spectroscopy. We found that *N*-sulfation was decreased from 43 N-sulfate groups/100 disaccharides in wildtype hepatocytes to 19 N-sulfates/100 disaccharides in *$Cre^{+}Ndst1^{f/f}Lrp1^{f/f}Ldlr^{-/-}$* hepatocytes. The reduction in sulfation was similar to that observed in hepatocytes from the *$Cre^{+}Ndst1^{f/f}$* mouse (Table 3-1 and (16)). This finding indicates that *Ndst1* was efficiently deleted in the *$Cre^{+}Ndst1^{f/f}Lrp1^{f/f}Ldlr^{-/-}$* mice. Deletion of *Ndst1* in hepatocytes does not fully eliminate *N*-sulfation because these cells express another *Ndst* isoform, *Ndst2*. To verify that hepatic Lrp1 expression was also ablated in the *$Cre^{+}Ndst1^{f/f}Lrp1^{f/f}Ldlr^{-/-}$ mice*, we examined the level of Lrp1 protein in isolated hepatocytes by Western blotting. Lrp1 protein was not detectable in both *$Cre^{+}Ndst1^{f/f}Lrp1^{f/f}Ldlr^{-/-}$* and *$Cre^{+}Lrp1^{f/f}Ldlr^{-/-}$* mice (Figure 3-1a). Though Lrp1 and Ldlr expression exhibited some variability among wildtype and *$Cre^{+}Ndst1^{f/f}$* mice, there was no statistically significant difference when expression was normalized to β-actin ($P > 0.05$, Figures 3-1b and 3-1c). Moreover, the expression of Ldlr and Lrp1 was not affected by inactivation of Ndst1.

Table 3-1: *Disaccharide analysis of hepatocyte heparan sulfate.*

	Disaccharides (mole %)							
	D0A0	**D0S0**	**D0A6**	**D0S6**	**D2A0**	**D2S0**	**S2A6**	**D2S6**
Cre^{-}Ndst1$^{f/f}$	40.1	16.5	15.9	9.6	0.8	6.3	0.1	10.7
Cre^{+}Ndst1$^{f/f}$	63.3	3.9	17.8	11.6	0.1	1.5	0.0	1.9
Cre^{+}Lrp1$^{f/f}$Ldlr$^{-/-}$	43.8	18.7	14.7	7.9	0.7	6.5	0.0	7.7
Cre^{+}Ndst1$^{f/f}$Lrp1$^{f/f}$Ldlr$^{-/-}$	65.1	3.2	16.1	13.9	0.1	0.6	0.1	1.1

HS chains from isolated hepatocytes were digested with heparin lyases I, II, and III, and the disaccharides were derivatized with isotopically labeled aniline and quantified by mass spectrometry (see methods). Disaccharides are designated using the code established in (51). *D0A0*, ΔUA-GlcNAc; *D0S0*, ΔUA-GlcNS; *D0A6*, ΔUA-GlcNAc6S; *D0S6*, ΔUA-GlcNS6S; *D2A0*, ΔUA2S-GlcNAc; *D2S0*, ΔUA2S-GlcNS; *D2A6*, ΔUA2S-GlcNAc6S; *D2S6*, ΔUA2S-GlcNS6S.

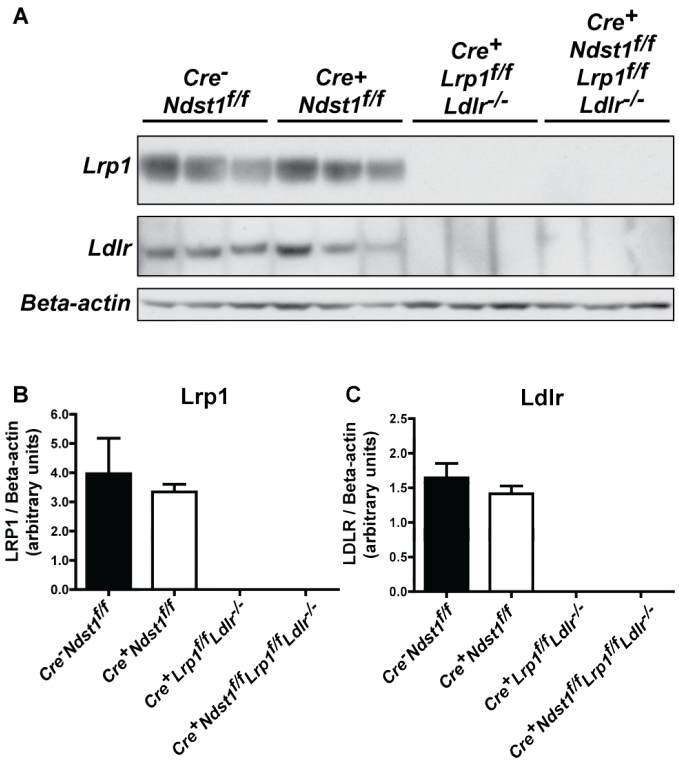

Figure 3-1: *Inactivation of Ldlr and Lrp1 in compound mutant mice.* (A) Fresh hepatocytes were isolated from 12 week-old male mice, and protein was solubilized in RIPA buffer. Samples were separated by gradient SDS-PAGE and transferred to PVDF. The membrane was probed with antibodies against Ldlr, Lrp1, and β-actin. Each lane represents a different mouse (n=3 per genotype). Lrp1 and Ldlr protein expression is undetectable in $Cre^{+}Lrp1^{f/f}Ldlr^{-/-}$ and $Cre^{+}Ndst1^{f/f}Lrp1^{f/f}Ldlr^{-/-}$ mice. (B, C) Densitometry analysis of the western blots presented in A is shown.

3.3.2 Hyperlipidemia in compound mutant mice

To study the relative contribution of the three receptors to clearance of TRLs, we analyzed fasting lipid levels. Plasma triglyceride and cholesterol were measured in blood drawn from 12 week-old overnight-fasted animals raised on a normal chow diet (Figure 3-2a and 3-2b, and Table 3-2). $Cre^{+}Ndst1^{f/f}$ accumulated triglycerides compared to wildtype animals (Figure 3-2a, 43 ± 10 mg/dL in wildtype [n = 12] vs. 69 ± 26 mg/dL in $Cre^{+}Ndst1^{f/f}$ [n = 13], $P < 0.01$), as shown previously (16). In contrast,

mice with a hepatocyte-specific ablation of Lrp1 ($Cre^{+}Lrp1^{f/f}$) did not accumulate plasma triglycerides (33 ± 5 mg/dL [n =7]) beyond the wildtype. Double mutant mice deficient for both the HSPG receptor and Lrp1 ($Cre^{+}Ndst1^{f/f}Lrp1^{f/f}$) also did not accumulate fasting triglycerides (66 ± 20 mg/dL [n = 19]) compared to the level observed in $Cre^{+}Ndst1^{f/f}$ mice ($P = 0.7$). Thus, these findings suggests that Lrp1 does not play a major role in TRL clearance when Ldlr is present.

We next analyzed mice lacking the Ldlr. Mice lacking only Ldlr ($Ldlr^{-/-}$) accumulated triglycerides (Figure 3-2b, 181 ± 59 mg/dL [n = 9]) approximately 4-fold over wildtype ($P < 0.0001$). Mice lacking both Ldlr and Lrp1 (i.e., expressing only HSPG receptors) exhibited elevated plasma triglycerides (548 ± 148 mg/dL [n = 9]) over $Ldlr^{-/-}$ mice ($P < 0.0001$). Mice lacking Ndst1 and Ldlr (i.e., expressing only Lrp1) ($Cre^{+}Ndst1^{f/f}Ldlr^{-/-}$) also had elevated triglyceride levels (415 ± 218 mg/dL [n = 9]) compared to either $Ldlr^{-/-}$ or $Ndst1^{-/-}$. $Cre^{+}Ndst1^{f/f}Lrp1^{f/f}Ldlr^{-/-}$ accumulated even greater levels of triglycerides (874 ± 270 mg/dL for $Cre^{+}Ndst1^{f/f}Lrp1^{f/f}Ldlr^{-/-}$ [n = 14], $P < 0.001$ compared to $Cre^{+}Ndst1^{f/f}Ldlr^{-/-}$ or $Cre^{+}Lrp1^{f/f}Ldlr^{-/-}$). These data suggest that Lrp1 contributes significantly to clearance when Ldlr is absent, consistent with previous studies (21, 22).

Heparan sulfate proteoglycans do not contribute to clearance of cholesterol-rich lipoprotein particles (16), as $Cre^{+}Ndst1^{f/f}$ do not have elevated cholesterol levels over wildtype mice (Figure 3-2c, 67 ± 9 mg/dL in wildtype [n = 12] vs. 71 ± 22 mg/dL in $Cre^{+}Ndst1^{f/f}$ [n = 13], $P = 0.6$). Lrp1 deficient mice ($Cre^{+}Lrp1^{f/f}$) also did not show cholesterol accumulation (71 ± 15 mg/dL [n = 7]) over wildtype ($P = 0.5$). Mice lacking the HSPG receptor and Lrp1 ($Cre^{+}Ndst1^{f/f}Lrp1^{f/f}$) had somewhat reduced

cholesterol levels (52 ± 7 mg/dL [n = 12]) compared to wildtype ($P < 0.001$), which may be due to upregulation of Ldlr (22). Surprisingly, mice lacking the HSPG receptor and Ldlr (*Cre*$^{+}$*Ndst1*$^{f/f}$*Ldlr*$^{-/-}$) had approximately 2-fold higher cholesterol levels (Figure 3-2d, 477 ± 160 mg/dL [n = 10]) than *Ldlr*$^{-/-}$ mice (291 ± 63 mg/dL, $P < 0.01$), and *Cre*$^{+}$*Ndst1*$^{f/f}$*Lrp1*$^{f/f}$*Ldlr*$^{-/-}$ mice exhibited higher fasting cholesterol levels (1308 ± 346 mg/dL [n = 6]) than *Cre*$^{+}$*Lrp1*$^{f/f}$*Ldlr*$^{-/-}$ mice (779 ± 149 mg/dL [n = 9], $P < 0.01$). Taken together, this data suggests that HSPGs also mediate clearance of cholesterol-rich lipoproteins in the absence of Ldlr family members.

Table 3-2: *Fasting lipid levels.*

Genotype	Triglyceride		Cholesterol	
	Concentration (mg/dL)	***P* value relative to wildtype**	**Concentration (mg/dL)**	***P* value relative to wildtype**
***Cre*$^{-}$*Ndst1*$^{f/f}$**	43 ± 10	--	67 ± 9	--
***Cre*$^{+}$*Ndst1*$^{f/f}$**	69 ± 26	< 0.01	71 ± 22	*n.s.*
***Cre*$^{+}$*Lrp1*$^{f/f}$**	33 ± 5	< 0.05	71 ± 15	*n.s.*
***Ldlr*$^{-/-}$**	181 ± 59	< 0.0001	291 ± 63	< 0.0001
***Cre*$^{+}$*Ndst1*$^{f/f}$*Lrp1*$^{f/f}$**	66 ± 20	< 0.01	52 ± 7	< 0.001
***Cre*$^{+}$*Ndst1*$^{f/f}$*Ldlr*$^{-/-}$**	415 ± 218	< 0.0001	477 ±160	< 0.0001
***Cre*$^{+}$*Lrp1*$^{f/f}$*Ldlr*$^{-/-}$**	548 ± 148	< 0.0001	779 ± 149	< 0.0001
***Cre*$^{+}$*Ndst1*$^{f/f}$*Lrp1*$^{f/f}$*Ldlr*$^{-/-}$**	874 ± 270	< 0.0001	1308 ± 346	< 0.0001

All values are expressed as average ± standard deviation. Statistical significance was determined by two-tailed *t*-test. *n.s.,* not significant

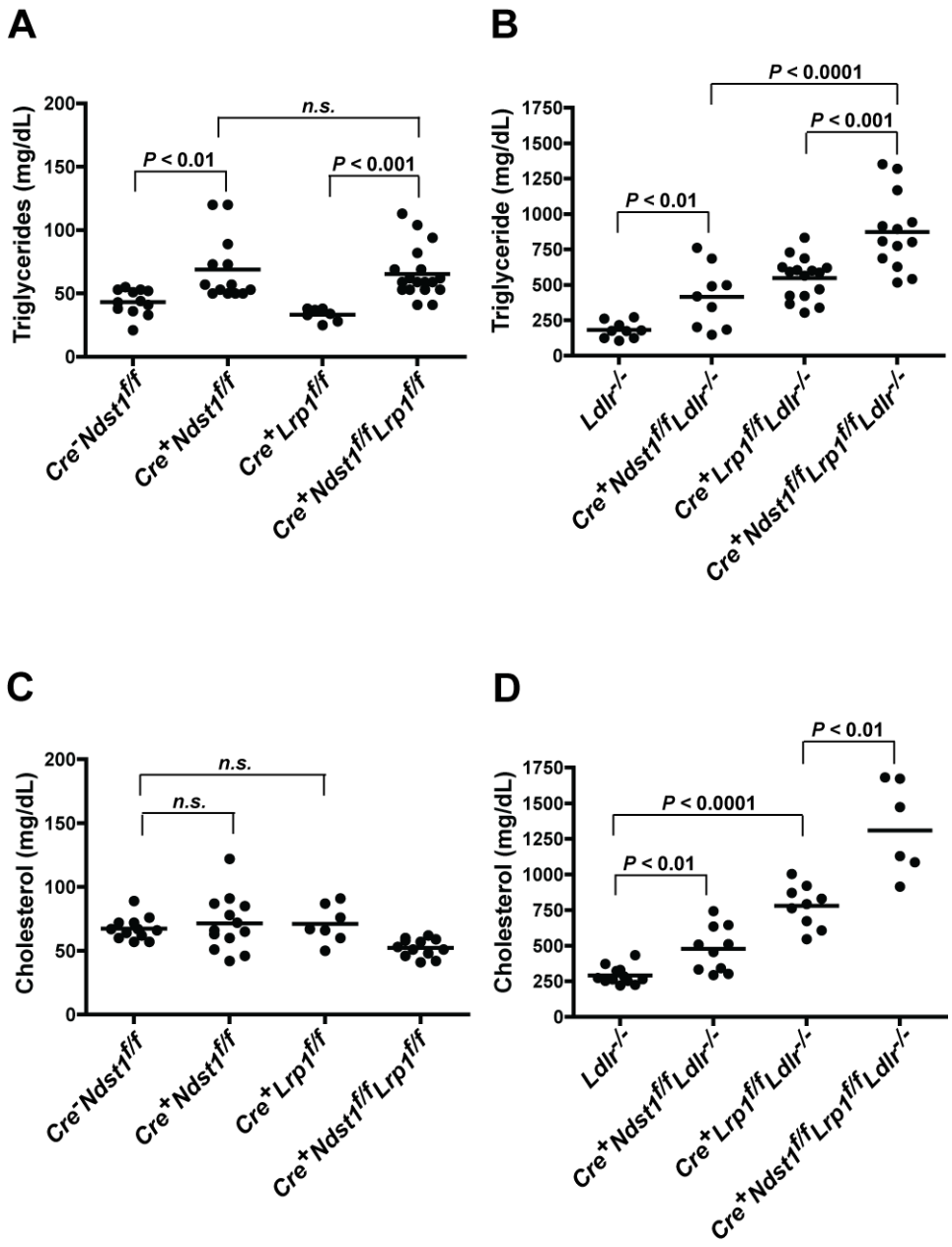

Figure 3-2: *Fasting lipids in compound mutant mice*. After a 12-hour fast (10 pm – 10 am), blood was drawn from 12 week-old mice via retroorbital sinus. Fasting triglycerides (A, B) and cholesterol (C, D) were measured in plasma from the various mutant mice (n = 6-19 per genotype, see text). Horizontal bars indicate mean values. Statistical significance was determined by t-test, $P < 0.05$.

3.3.3 Postprandial triglyceride clearance and liver uptake is significantly delayed in compound mutant mice

To differentiate between the contribution of the Ldlr family of receptors and HSPGs to hepatic TRL clearance we chose to focus on four genotypes for the remainder of the study: *Cre*$^{-}$*Ndst1*$^{f/f}$ (wildtype), *Cre*$^{+}$*Ndst1*$^{f/f}$, *Cre*$^{+}$*Lrp1*$^{f/f}$*Ldlr*$^{-/-}$, and *Cre*$^{+}$*Ndst1*$^{f/f}$*Lrp1*$^{f/f}$*Ldlr*$^{-/-}$. We first examined clearance of postprandial triglycerides. Fasted mice were given a bolus of corn oil by oral gavage. Blood was sampled at various time points post-gavage to measure appearance of and disappearance of triglycerides in the circulation. As shown in Figure 3-3a, *Cre*$^{+}$*Ndst1*$^{f/f}$ mice had delayed clearance of postprandial triglycerides compared to wildtype (AUC: 2244 vs. 864 respectively). *Cre*$^{+}$*Lrp1*$^{f/f}$*Ldlr*$^{-/-}$ mice had an even greater delay in clearance (AUC: 5406). *Cre*$^{+}$*Ndst1*$^{f/f}$*Lrp1*$^{f/f}$*Ldlr*$^{-/-}$ mice had severely impaired clearance (AUC: 11033), and triglyceride levels remained high at 8 hours post-gavage.

To verify that this delay in postprandial clearance was due to altered liver clearance and not caused by defects in peripheral clearance, we performed a separate study that measured uptake of radioactive triglyceride into the organs of the various mutant mice. Mice were given a bolus of [^{3}H]retinol mixed with corn oil by oral gavage. In the intestine, [^{3}H]retinol is packaged into chylomicrons and these radioactive particles are subsequently cleared from the circulation in a time-dependent manner. At 8-hours post-gavage, the animals were sacrificed and their tissues were assayed for radioactivity. At this time point, counts remained high in plasma from the *Cre*$^{+}$*Ndst1*$^{f/f}$ mice and even greater in *Cre*$^{+}$*Lrp1*$^{f/f}$*Ldlr*$^{-/-}$ and *Cre*$^{+}$*Ndst1*$^{f/f}$*Lrp1*$^{f/f}$*Ldlr*$^{-/-}$ animals (Figure 3-3b). In a separate experiment, counts remained significantly

elevated in plasma from the *Cre*$^{+}$*Ndst1*$^{f/f}$*Lrp1*$^{f/f}$*Ldlr*$^{-/-}$ mice even 24 hours post-gavage (data not shown).

Correspondingly, liver uptake of the radioactive TRLs was decreased compared to wildtype among mutant mice, with very low uptake occurring in livers from *Cre*$^{+}$*Ndst1*$^{f/f}$*Lrp1*$^{f/f}$*Ldlr*$^{-/-}$ mice (Figure 3-3c). There was no statistically significant difference in uptake of radioactive counts into skeletal muscle or heart between mutant and wildtype mice (Figures 3-3d and 3-3e), confirming that there was no difference in peripheral triglyceride clearance among these mutant mice, and that the observed persistence of postprandial triglycerides is due to defective clearance by liver receptors.

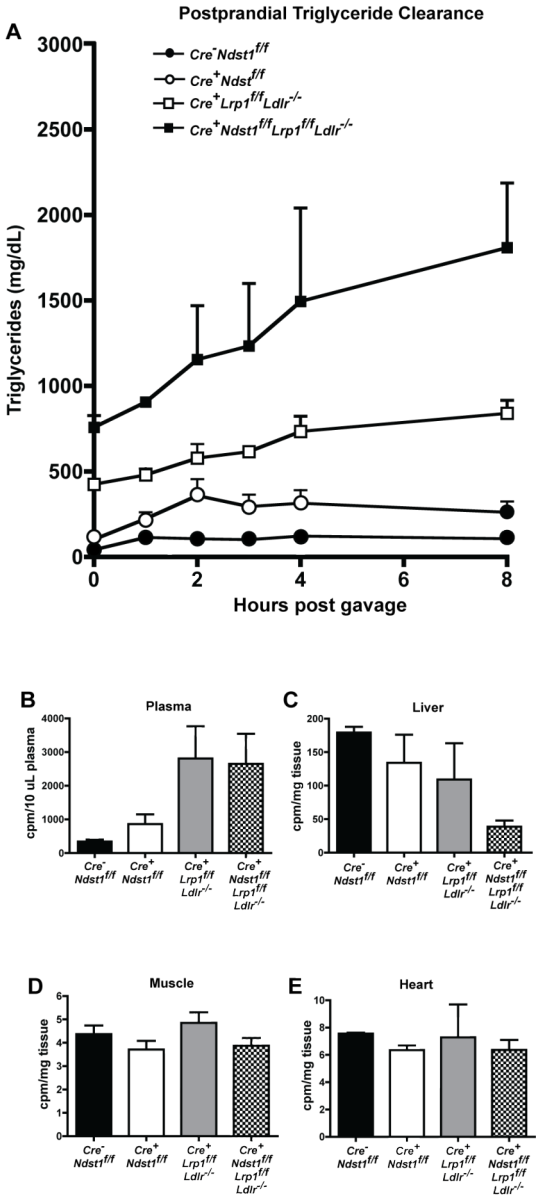

Figure 3-3: *Postprandial clearance and organ uptake in compound mutant mice.* (A) To measure triglyceride clearance rates in mutants, overnight fasted mice were given 200 µL of corn oil by oral gavage. At 0, 1, 2, 3, 4, and 8 hours post-gavage, mice were bled via the tail vein and triglyceride concentration in plasma was measured. (B-E) Overnight fasted mice were given a bolus of 27 µCi [^{3}H]retinol mixed with corn oil by oral gavage. At 8 hours post-gavage, blood was obtained by cardiac puncture and plasma was assayed for radioactivity by liquid scintillation counting in duplicate (B). Subsequently, the mice were sacrificed and dissected. Organs were weighed, homogenized in SOLVABLE, and assayed for radioactivity. Counts per milligram of tissue are reported for (C) liver, (D) muscle, and (E) heart. No statistically significant difference in uptake was observed in muscle or heart uptake among the mutants, n = 3 mice per genotype.

3.3.4 Heparan sulfate proteoglycans and LDL receptor family members mediate clearance of TRLs of unique size

To further characterize the accumulated particles, whole plasma lipoprotein profiles were determined by gel filtration fast-phase liquid chromatography (FPLC). In *Cre*$^{+}$*Ndst1*$^{f/f}$, *Cre*$^{+}$*Lrp1*$^{f/f}$*Ldlr*$^{-/-}$, and *Cre*$^{+}$*Ndst1*$^{f/f}$*Lrp1*$^{f/f}$*Ldlr*$^{-/-}$ mice, we documented the accumulation of large TRLs consistent in size with chylomicron remnants (CR), VLDL, and intermediate density lipoproteins (IDL), with no change in HDL levels (Figures 3-4a and 3-4b). The cholesterol profile of *Cre*$^{+}$*Lrp1*$^{f/f}$*Ldlr*$^{-/-}$ mice showed that these mutants have increased accumulation of IDL/LDL cholesterol compared to wildtype and *Cre*$^{+}$*Ndst1*$^{f/f}$ mice, and this accumulation was even greater in *Cre*$^{+}$*Ndst1*$^{f/f}$*Lrp1*$^{f/f}$*Ldlr*$^{-/-}$ mice.

Next, we isolated TRLs using buoyant density ultracentrifugation ($d < 1.006$ g/mL), and analyzed lipoprotein samples using non-denaturing agarose gel electrophoresis. In this assay, migration of lipoprotein particles is dependent on both their size and charge. Surprisingly, the accumulated TRLs from each mouse had distinct migration properties (Figure 3-4c). Wildtype TRLs migrated furthest, while the migration of TRLs that accumulated in *Cre*$^{+}$*Ndst1*$^{f/f}$ mice was retarded. The migration of TRLs from *Cre*$^{+}$*Lrp1*$^{f/f}$*Ldlr*$^{-/-}$ animals was even more delayed. Migration of TRLs from *Cre*$^{+}$*Ndst1*$^{f/f}$*Lrp1*$^{f/f}$*Ldlr*$^{-/-}$ mice was intermediate between that observed in samples from the *Cre*$^{+}$*Ndst1*$^{f/f}$ and *Cre*$^{+}$*Lrp1*$^{f/f}$*Ldlr*$^{-/-}$ mice. Taken together, this data suggests that particles with unique size and charge properties are accumulating in each mutant.

To analyze if the migration shifts could be explained by differences in the size of the accumulated particles, TRLs from each mutant ($d < 1.006$ g/mL) were visualized by electron microscopy (Figure 3-4d). Small particles (~20-40 nm in diameter) accumulated in mice lacking the HSPG receptor. In contrast, larger particles accumulated (~40-60 nm diameter) in mutants lacking Ldlr family members. The altered distribution of particle size was significant between all groups (Kruskal-Wallis test, $P < 0.001$).

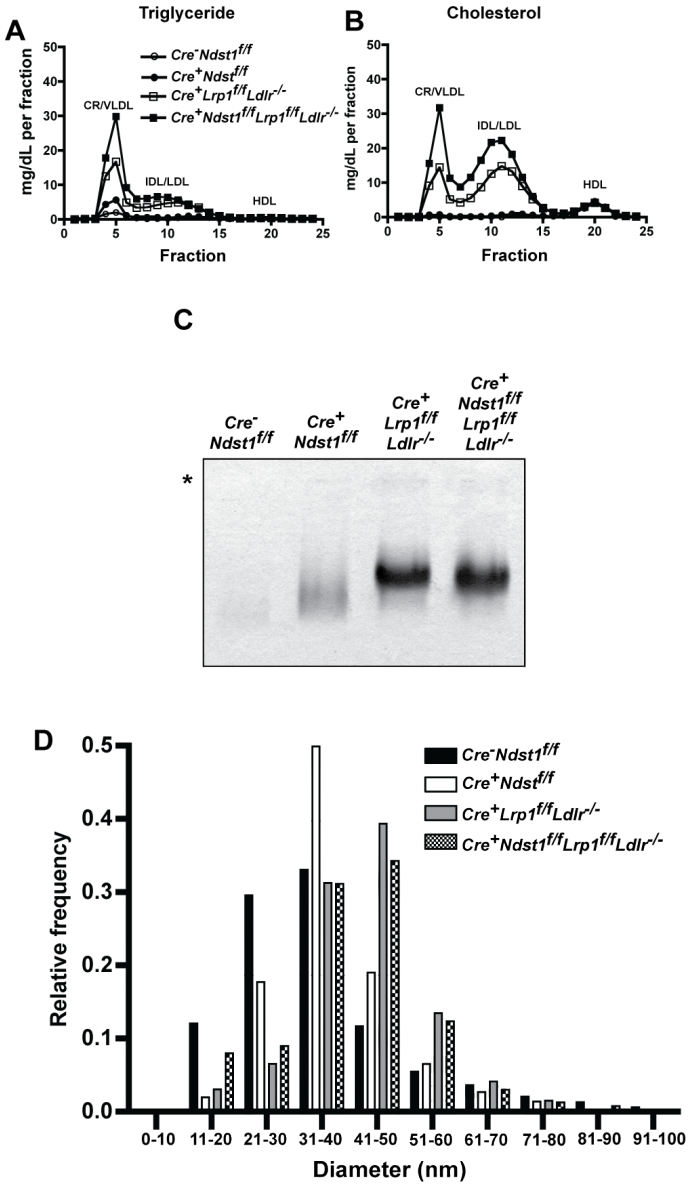

Figure 3-4: *Sizing of accumulated particles.* Lipoproteins were analyzed by gel filtration FPLC, and the amount of (A) triglyceride and (B) cholesterol in each fraction was measured. Plasma was pooled from three mice of each genotype. The elution positions of human CR/VLDL, IDL/LDL, and HDL are indicated. (C) Lipoproteins of $d < 1.006$ g/mL (pooled from n = 3 mice per each genotype) were isolated by buoyant density ultracentrifugation) and were analyzed by non-denaturing agarose electrophoresis using a kit. Asterisk indicates location of the origin. (D) TRLs ($d <$ 1.006 g/mL) were negatively stained with 1% uranyl acetate and analyzed transmission electron microscopy (18,500 x magnification). The diameters of particles present in 5-6 fields (approx. 1000-2000 particles per genotype) were measured using ImageJ software. Distribution of particle size was significant between all groups (Kruskal-Wallis test, $P < 0.001$).

3.3.5 Heparan sulfate proteoglycans and LDL receptor family members mediate clearance of TRLs of unique apolipoprotein composition

Samples of purified TRLs ($d < 1.006$ g/mL) were analyzed by gradient SDS-PAGE, and the individual apolipoproteins were visualized by silver staining. In all mutants, accumulated TRLs contained ApoB-48, ApoB-100, ApoE, and various ApoCs (Figure 3- 5a). In the *Cre*$^{+}$*Ndst1*$^{f/f}$ mutant, apoB-100 containing lipoproteins accumulated. In mutants lacking Ldlr (*Cre*$^{+}$*Lrp1*$^{f/f}$*Ldlr*$^{-/-}$ and *Cre*$^{+}$*Ndst1*$^{f/f}$*Lrp1*$^{f/f}$*Ldlr*$^{-/-}$), apoB-48-containing lipoproteins accumulated.

We further characterized the apolipoprotein composition of accumulated particles by western blot (Figures 3-5b and 3-5c). Recent studies have shown that lipoprotein particles containing ApoAV accumulate in *Cre*$^{+}$*Ndst1*$^{f/f}$ mice (J.C. Gonzales *et al*, in preparation). In our study, the *Cre*$^{+}$*Ndst1*$^{f/f}$ mutants accumulated ApoAV-containing lipoproteins, while *Cre*$^{+}$*Lrp1*$^{f/f}$*Ldlr*$^{-/-}$ mice did not. Particles containing apoE accumulated in *Cre*$^{+}$*Ndst1*$^{f/f}$, *Cre*$^{+}$*Lrp1*$^{f/f}$*Ldlr*$^{-/-}$, and *Cre*$^{+}$*Lrp1*$^{f/f}$*Ldlr*$^{-/-}$ mice. Taken together, these data suggest that members of the Ldlr family of receptors and the HSPG receptor each clear a distinctly different subset of remnant particles, and that the HSPG receptor clears particles enriched in ApoAV and ApoE.

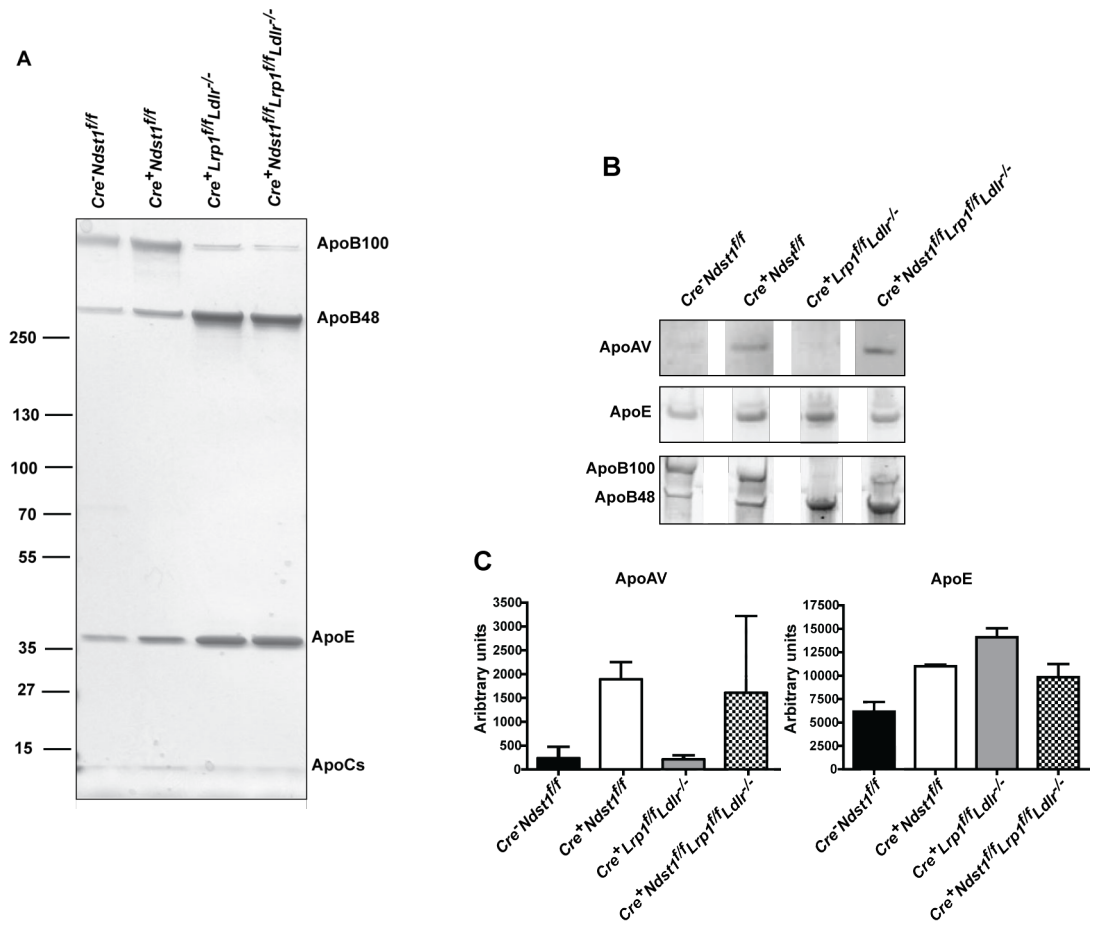

Figure 3-5: *Apolipoprotein composition of accumulated particles.* (A) Samples of pooled purified lipoproteins (d < 1.006 g/mL, pooled from n = 3 per genotype) were analyzed by gradient SDS-PAGE, and the individual lipoproteins were visualized by silver staining. The location of ApoB-48, ApoB-100, ApoE and ApoCs was deduced by M_r values. (B) Samples of purified lipoproteins (d < 1.006 g/mL) were analyzed by gradient SDS-PAGE, and the individual lipoproteins were visualized by western blotting using antibodies against ApoB, ApoE, and ApoAV. Representative images from the same gel are shown (n = 3 mice per genotype). (C) Densitometry analysis of the western blots presented in B is shown.

3.4 Discussion

A large body of work has established a role for HSPGs in the clearance of triglyceride-rich lipoproteins. HSPGs are composed of a core protein and one or more covalently attached chains of the glycosaminoglycan heparan sulfate (HS) (23). Early studies reported decreased lipoprotein uptake in hepatocytes treated with enzymes that degrade HS chains, pharmacological agents that manipulate glycosaminoglycan biosynthesis, or in Chinese hamster ovary (CHO) cell mutants lacking specific HS biosynthetic enzymes (24-30). Recently, our lab demonstrated that inactivation of the HS biosynthetic gene GlcNAc *N*-deacetylase/*N*-sulfotransferase 1 (*Ndst1*) in hepatocytes using the Cre-loxP system results in the accumulation of fasting triglycerides and delayed clearance of intestinally derived lipoproteins due to loss of sulfation of HS chains (16). Further, we identified syndecan-1 as the primary HSPG receptor for triglyceride-rich lipoproteins in the liver (10).

Members of the LDL receptor family have also has been well characterized as rapid, recycling clearance receptors for remnant lipoproteins. The primary role of Ldlr is in the clearance of cholesterol-rich ApoB100- and ApoE-containing particles such as low-density lipoproteins (LDLs). This conclusion is based on the observation that mice, rabbits, and humans deficient for the receptor have only modest accumulation of triglycerides (31-33). Lrp1, a member of the Ldlr family of receptors, is a multifunctional receptor that binds numerous ligands (34). *Lrp1* systemic knockout mice are not viable (35), but mice bearing floxed alleles of *Lrp1* are available (36). Mice with a liver-specific ablation of *Lrp1* do not accumulate fasting triglycerides or

cholesterol, but *Lrp1*$^{f/f}$*Ldlr*$^{-/-}$ mice in which *Lrp1* was inactivated by injection of AdCre have impaired clearance of triglycerides compared to control *Ldlr*$^{-/-}$ mice (22).

Our genetic analysis of the relative contribution of HS proteoglycans and members of the Ldlr family of receptors (Ldlr and Lrp1) to TRL clearance has several important implications. Based on fasting triglyceride data from double and triple mutant mice (Figure 3-2), we can conclude that Ldlr, Lrp1, and HSPGs are the major TRL clearance receptors in mice, though the role of Lrp1 only becomes apparent in the absence of Ldlr. These conclusions are also supported by postprandial clearance data (Figure 3-3). In the *Cre*$^{+}$*Ndst1*$^{f/f}$*Lrp1*$^{f/f}$*Ldlr*$^{-/-}$ mice, triglyceride levels remain elevated and liver uptake remains low even 8 hours post-gavage, suggesting that other TRL receptors cannot compensate for the absence of these three major receptors.

We further report that the receptor families clear distinct subsets of lipoprotein particles; that HSPGs clear a subset of small TRL particles enriched in ApoE and ApoAV, while members of the Ldlr family of receptors clear larger TRL particles lacking ApoAV (Figure 3-4 and 3-5). Though we and others have shown that HSPGs can act as independent endocytic receptors for numerous ligands (37-39), whether HSPGs act as independent receptors in the clearance of TRLs has been highly debated. Many people in the field have posited that HSPGs work in concert with Lrp1 to clear TRLs; that these two proteins either act as co-receptors for lipoprotein particles or participate in a “handoff” process whereby HSPGs trap lipoprotein particles in the space of Disse and subsequently transfer them to Lrp1 for endocytosis (40). Given our finding that the receptors clear different subsets of particles, it seems likely that each receptor family acts independently in its own non-redundant pathway.

The idea that particle size partially determines the affinity of lipoprotein particles for their receptors has been suggested (41), and may be a result of particle size dependent apolipoprotein conformation. In the present study, we found that HS proteoglycans preferentially clear smaller particles than those cleared by Ldlr family members. Chains of HS are highly flexible, however. It is feasible, therefore, that the HS chains on proteoglycans can change conformation to interact with particles of larger size as well. For instance, HS proteoglycans may display different particle size preference in the postprandial state when larger chylomicrons remnants are present. Apolipoprotein composition of larger particles may be different as well. Though only one molecule of ApoB is present per particle, the number of interchangeable apolipoproteins, such as ApoE, may increase as a function of size. This may change the affinity of the particles for the various receptors. Thus, further experiments are necessary to fully identify and characterize lipoprotein subsets and receptor preferences.

Though we focused on only three receptors in our genetic analysis, several other receptors for TRLs have been found, including the lipolysis stimulated receptor (Lsr), scavenger receptor B1 (Sr-b1), and Lrp5. The contribution of each of these receptors to TRL clearance remains unclear, however. Liver-specific knockdown of *Lsr* expression leads to hypertriglyceridemia in the fed state, but fasting triglyceride levels are normal (42). Heterozygous $Lsr^{+/-}$ mice have delayed postprandial clearance of triglyceride-rich lipoproteins (43), but systemic inactivation of Lsr leads to embryonic lethality (44), alluding to perhaps other roles for this protein. Though some evidence suggests that Sr-b1 can mediate clearance of VLDLs and chylomicrons *in*

vivo, its major role is in HDL clearance (13, 14, 45, 46). *Lrp5*$^{-/-}$ mice have normal fasting triglyceride levels, and the contribution of Lrp5 to TRL clearance only becomes apparent after high fat feeding (47). Our triple receptor mutant mouse has profound dyslipidemia and significantly delayed clearance of postprandial triglycerides, even 8 hours post-gavage, suggesting that little hepatic clearance is occurring in these mice and that Ldlr, Lrp1, and HS proteoglycans are the major receptors in the system. Given our other findings in this study, it is possible that Lsr, Sr-b1, and/or Lrp5 also recognize important and distinct subsets of particles. Thus, their contribution to clearance may not be apparent in our analysis.

Our *Cre*$^{+}$*Ndst1*$^{f/f}$*Lrp1*$^{f/f}$*Ldlr*$^{-/-}$ mouse is a unique system to tease apart the relative contribution of the various receptors to clearance. Though we have used Cre recombinase under control of the albumin promoter to selectively and irreversibly inactivate *Lrp1* and *Ndst1* in the liver, previous studies have employed other means to inactivate various TRL receptors. In one study, *in vivo* inhibition of Ldlr was achieved using tail vein injection of a blocking antibody (48). This treatment reduced plasma clearance of TRLs by approximately 45%, while injection of the receptor-associated protein (Rap), a selective inhibitor of Lrp1, reduced plasma clearance by 55%. When the Ldlr blocking antibody and Rap injection were administered together, plasma removal was only decreased by 60%, an incremental effect. This finding is consistent with our conclusions that HS proteoglycans are a major contributor to clearance in the liver, and that the two receptor families cannot fully compensate for one another. In a different study, mice with systemic deletions of the VLDL receptor (*Vldlr*) and the *Ldlr* were bred to mice with an ablation of *Lrp1* under control of an inducible Cre

(11). The Vldlr is not expressed in the liver, and has been shown to mediate TRL clearance in tissues active in fatty acid metabolism (heart, adipose, and skeletal muscle). Triple mutant mice deficient for *Ldlr, Lrp1,* and *Vldlr* accumulated fasting and postprandial TGs at a higher level than *Ldlr/Lrp-1* deficient mice. In these mice, notably, association of DiI-labeled lipoproteins to hepatocytes was inhibited by the addition of heparin. This again confirms our findings that HSPGs work independently from the other receptors.

Our $Cre^{+}Ndst1^{f/f}Lrp1^{f/f}Ldlr^{-/-}$ mouse represents a unique hyperlipidemic model that can be used to study triglyceride and cholesterol metabolism independent of clearance. For example, this model may be useful in understanding the mechanism of action of fenofibrate. Fenofibrate is a peroxisome proliferator-activated receptor alpha (PPARα) agonist, and has been shown to activate ApoAV expression (49). Treatment with fenofibrate decreases plasma triglycerides by both increasing clearance and decreasing VLDL production (50). Because clearance is significantly impaired in our $Cre^{+}Ndst1^{f/f}Lrp1^{f/f}Ldlr^{-/-}$ mouse, it may be a useful tool to study the clearance-independent effects of fenofibrate. Additionally, our $Cre^{+}Ndst1^{f/f}Lrp1^{f/f}Ldlr^{-/-}$ mice may prove to be a valuable tool for studying atherosclerosis. We have not yet performed controlled studies to examine plaque formation, or placed these mice on a high fat diet. Further characterization is necessary to determine how we may be able to use this model.

3.5 Materials and Methods

3.5.1 Mice and animal husbandry

Lrp1$^{f/f}$, *Ldlr*$^{-/-}$, and *AlbCre*$^{+}$ mice were purchased from The Jackson Laboratory. *Ndst1*$^{f/f}$*AlbCre*$^{+}$ mice (referred to as *Cre*$^{+}$*Ndst1*$^{f/f}$ mice in this study) were described by (16), and genotyping of these mice was performed as in (17). All mice were backcrossed more than 10 generations on a C57BL/6 background. All animals were housed and bred in vivaria approved by the Association for Assessment and Accreditation of Laboratory Animal Care located in the School of Medicine, UCSD, following standards and procedures approved by the UCSD Institutional Animal Care and Use Committee. Mice were weaned at 3 weeks, maintained on a 12-hour-light cycle, and fed *ad libitum* with water and standard rodent chow (Harlan Teklad).

3.5.2 Lipid analysis

Blood was drawn via retroorbital sinus from mice fasted for 12 hours overnight. Total cholesterol and triglyceride levels in plasma were determined using kits (Genzyme) against the Precipath L lipoprotein standard (Roche Diagnostics).

3.5.3 Ultracentrifugation studies

Blood was drawn via retroorbital sinus from mice fasted for 12 hours overnight, and plasma was pooled (70 μL per mouse, n = 3 mice per genotype). Lipoprotein fractions were separated by buoyant density ultracentrifugation according to established methods (18). Briefly, 210 μL of pooled plasma was loaded into micro-ultracentrifuge tubes (Beckman). The samples were centrifuged 12 hours in a 42.2 Ti

rotor at 38,000 rpm, 18°C. The top 50 μL containing VLDL and chylomicron remnants (d < 1.006 g/mL) was removed and used for analysis.

3.5.4 Heparan sulfate purification and disaccharide analysis

Hepatocytes were isolated as described (19) and allowed to recover in culture overnight. The cells were then treated overnight with Pronase (2 mg/mL; Roche Diagnostics) to degrade proteins, followed by purification of the glycopeptides by anion exchange chromatography using DEAE Sephacel (Amersham Biosciences). Columns were washed with low-salt buffer (0.15 M NaCl, 20 mM sodium acetate; pH 6.0) to retain low-sulfated chains and eluted with 1 M NaCl. Samples were desalted using PD-10 columns and then lyophilized. Chains were digested with heparin lyases I, II, and III. The resulting disaccharides were subsequently derivatized with isotopically labeled aniline and quantified by mass spectrometry as described previously (20). Molar percentages were calculated based on the relative area under each peak.

3.5.5 Electron microscopy

Lipoprotein particles isolated by buoyant density ultracentrifugation (d < 1.006 g/mL) were subjected to negative staining. Briefly, particles were diluted to a concentration of approximately 50-150 mg/dL triglyceride with water, and sucrose was added to a final concentration of 0.1%. The particles were then allowed to adhere to a Formvar carbon coated grid and stained with 1% uranyl acetate before visualization on a FEI Tecnai Spirit G2 BioTWIN transmission electron microscope

equipped with a 4K Eagle digital camera. Particle size was measured using ImageJ software (National Institutes of Health).

3.5.6 Fast performance liquid chromatography (FPLC)

Pooled plasma samples were separated by gel filtration FPLC. Samples were loaded on a GE Superose 6 10/30 GL column (Cat# 175172-01) in 0.15 M sodium chloride containing 1 mM ethylenediaminetetraacetic acid and 0.02% sodium azide, pH 7.4. 0.5 mL fractions were collected (0.5 mL/min). Total cholesterol and triglyceride levels were determined enzymatically using an automated reader (Cobas Mira; Roche Diagnostics) and kits: Cholesterol High-Performance Reagent (Roche Diagnostics) and Triglyceride-SL (Diagnostic Chemicals Ltd.).

3.5.7 Western blots

In Figure 3-1, isolated frozen hepatocytes were solubilized in RIPA buffer plus protease inhibitors (Sigma). For each sample, 20 μg protein was resolved on a 4-12% Bis-Tris NuPage gel (Invitrogen) and transferred to polyvinlyidene fluoride membrane (Bio-Rad Laboratories). The membrane was blocked with Super-Block buffer (Pierce). Blots were incubated with antibodies against Ldlr (AbCam), Lrp-1 (AbCam), or β-actin (Sigma) and appropriate HRP-conjugated secondaries (Santa Cruz). Reactive bands were visualized by chemiluminescence. In Figure 3-5, plasma was isolated from overnight-fasted mice by cardiac puncture (200 μL of plasma per mouse). TRLs were isolated by buoyant density ultracentrifugation. 5 μg of TRL protein was loaded in each lane, and samples were resolved by gradient SDS-PAGE and transferred to

PVDF as above. Blots were incubated with antibodies against ApoAV (Santa Cruz), ApoE (Meridian Life Sciences), and ApoB (AbCam), and appropriate secondary antibodies (Odyssey). Reactive bands were visualized on a LiCor fluorescence detection system.

3.5.8 Lipoprotein agarose

Lipoprotein samples (d < 1.006 g/mL) were loaded onto a TITAN Gel (Helena Laboratories), electrophoresed, and stained per the manufacturer's instructions.

3.5.9 Postprandial clearance studies

Mice were fasted for 12 hours overnight. At 10 am, mice were given a 200 μL bolus of corn oil (Sigma) by oral gavage. At the appropriate time points, mice were sedated with isofluorane and bled via the tail vein. Triglyceride and cholesterol levels were measured as described above.

3.5.10 [^{3}H]retinol organ uptake experiments

Clearance of chylomicrons derived from dietary triglyceride was measured by Vitamin A excursion essentially as described (10). Briefly, 27 μCi of [11,12-^{3}H]retinol (Perkin Elmer; 44 Ci/mmol) in ethanol was mixed with 1 mL of corn oil (Sigma-Aldrich) and administered to overnight fasted mice by oral gavage (200 μL/mouse). Blood was obtained 8-hours post-gavage by cardiac puncture and counts remaining in the serum were assayed in duplicate by liquid scintillation counting. The mice were dissected, and organs were removed. Approximately 100-200 mg of tissue was

solubilized in 1 mL of SOLVABLE (Perkin Elmer) at 55°C, and radioactive counts in the tissue were assayed by liquid scintillation counting.

3.5.11 Statistical analysis

Statistical analyses were performed using Prism 4.0c (GraphPad Software) using the indicated tests. Significance was taken as $P < 0.05$. Data are expressed as average ± standard deviation.

3.6 Acknowledgements

Work presented in this chapter will be submitted for publication to the Journal of Biological Chemistry with coauthors Kristin I. Stanford, Philip P.L.S.M Gordts, Jon C. Gonzales, Roger Lawrence, and Jeffrey D. Esko. The dissertation author was the primary author of this work. Together with her coauthors, the dissertation author would like to thank Jennifer Pattison and Joe Juliano for their assistance with FPLC and lipid analysis. We would also like to thank Timo Merloo and Marilyn Farquhar for technical assistance with electron microscopy. We acknowledge Carlos Lameda Diaz for his kind assistance with glycosaminoglycan isolation. We are grateful to Joe Witztum for helpful discussions. This work was supported by NIH grant GM33063 (to J.D. Esko) and training grant 5T32CA067754-17 (to E.M. Foley). Work was conducted within the department of Cellular and Molecular Medicine, and the Glycobiology Research and Training Center, University of California, San Diego, La Jolla, California.

3.7 References

1. Nordestgaard, B.G., Benn, M., Schnohr, P., and Tybjaerg-Hansen, A. 2007. Nonfasting triglycerides and risk of myocardial infarction, ischemic heart disease, and death in men and women. *Jama* 298:299-308.

2. Bansal, S., Buring, J.E., Rifai, N., Mora, S., Sacks, F.M., and Ridker, P.M. 2007. Fasting compared with nonfasting triglycerides and risk of cardiovascular events in women. *Jama* 298:309-316.

3. Yuan, G., Al-Shali, K.Z., and Hegele, R.A. 2007. Hypertriglyceridemia: its etiology, effects and treatment. *Cmaj* 176:1113-1120.

4. Langsted, A., Freiberg, J.J., and Nordestgaard, B.G. 2008. Fasting and nonfasting lipid levels: influence of normal food intake on lipids, lipoproteins, apolipoproteins, and cardiovascular risk prediction. *Circulation* 118:2047-2056.

5. Fujioka, Y., and Ishikawa, Y. 2009. Remnant lipoproteins as strong key particles to atherogenesis. *J Atheroscler Thromb*.

6. Stalenhoef, A.F., and de Graaf, J. 2008. Association of fasting and nonfasting serum triglycerides with cardiovascular disease and the role of remnant-like lipoproteins and small dense LDL. *Curr Opin Lipidol* 19:355-361.

7. Brown, M.S., and Goldstein, J.L. 1986. A receptor-mediated pathway for cholesterol homeostasis. *Science* 232:34-47.

8. Herz, J., Hamann, U., Rogne, S., Myklebost, O., Gausepohl, H., and Stanley, K.K. 1988. Surface location and high affinity for calcium of a 500-kd liver membrane protein closely related to the LDL-receptor suggest a physiological role as lipoprotein receptor. *EMBO J* 7:4119-4127.

9. Kowal, R.C., Herz, J., Goldstein, J.L., Esser, V., and Brown, M.S. 1989. Low density lipoprotein receptor-related protein mediates uptake of cholesteryl esters derived from apoprotein E-enriched lipoproteins. *Proc Natl Acad Sci USA* 86:5810-5814.

10. Stanford, K.I., Bishop, J.R., Foley, E.M., Gonzales, J.C., Niesman, I.R., Witztum, J.L., and Esko, J.D. 2009. Syndecan-1 is the primary heparan sulfate proteoglycan mediating hepatic clearance of triglyceride-rich lipoproteins in mice. *J Clin Invest* 119:3236-3245.

11. Espirito Santo, S.M., Rensen, P.C., Goudriaan, J.R., Bensadoun, A., Bovenschen, N., Voshol, P.J., Havekes, L.M., and van Vlijmen, B.J. 2005.

Triglyceride-rich lipoprotein metabolism in unique VLDL receptor, LDL receptor, and LRP triple-deficient mice. *J Lipid Res* 46:1097-1102.

12. Goudriaan, J.R., Espirito Santo, S.M., Voshol, P.J., Teusink, B., van Dijk, K.W., van Vlijmen, B.J., Romijn, J.A., Havekes, L.M., and Rensen, P.C. 2004. The VLDL receptor plays a major role in chylomicron metabolism by enhancing LPL-mediated triglyceride hydrolysis. *J Lipid Res* 45:1475-1481.

13. Out, R., Kruijt, J.K., Rensen, P.C., Hildebrand, R.B., de Vos, P., Van Eck, M., and Van Berkel, T.J. 2004. Scavenger receptor BI plays a role in facilitating chylomicron metabolism. *J Biol Chem* 279:18401-18406.

14. Out, R., Hoekstra, M., de Jager, S.C., de Vos, P., van der Westhuyzen, D.R., Webb, N.R., Van Eck, M., Biessen, E.A., and Van Berkel, T.J. 2005. Adenovirus-mediated hepatic overexpression of scavenger receptor class B type I accelerates chylomicron metabolism in C57BL/6J mice. *J Lipid Res* 46:1172-1181.

15. Mann, C.J., Khallou, J., Chevreuil, O., Troussard, A.A., Guermani, L.M., Launay, K., Delplanque, B., Yen, F.T., and Bihain, B.E. 1995. Mechanism of activation and functional significance of the lipolysis-stimulated receptor. Evidence for a role as chylomicron remnant receptor. *Biochemistry* 34:10421-10431.

16. MacArthur, J.M., Bishop, J.R., Wang, L., Stanford, K.I., Bensadoun, A., Witztum, J.L., and Esko, J.D. 2007. Liver heparan sulfate proteoglycans mediate clearance of triglyceride-rich lipoproteins independently of LDL receptor family members. *J Clin Invest* 117:153-164.

17. Wang, L., Fuster, M., Sriramarao, P., and Esko, J.D. 2005. Endothelial heparan sulfate deficiency impairs L-selectin- and chemokine-mediated neutrophil trafficking during inflammatory responses. *Nat Immunol* 6:902-910.

18. Kelley, J.L., and Kruski, A.W. 1986. Density gradient ultracentrifugation of serum lipoproteins in a swinging bucket rotor. *Methods Enzymol* 128:170-181.

19. Deng, Y., Foley, E.M., Gonzales, J.C., Gordts, P.L., Li, Y., and Esko, J.D. Shedding of syndecan-1 from human hepatocytes alters very low density lipoprotein clearance. *Hepatology* 55:277-286.

20. Lawrence, R., Olson, S.K., Steele, R.E., Wang, L., Warrior, R., Cummings, R.D., and Esko, J.D. 2008. Evolutionary differences in glycosaminoglycan fine structure detected by quantitative glycan reductive isotope labeling. *J Biol Chem* 283:33674-33684.

21. van Vlijmen, B.J., Rohlmann, A., Page, S.T., Bensadoun, A., Bos, I.S., van Berkel, T.J., Havekes, L.M., and Herz, J. 1999. An extrahepatic receptor-associated protein-sensitive mechanism is involved in the metabolism of triglyceride-rich lipoproteins. *J Biol Chem* 274:35219-35226.

22. Rohlmann, A., Gotthardt, M., Hammer, R.E., and Herz, J. 1998. Inducible inactivation of hepatic LRP gene by cre-mediated recombination confirms role of LRP in clearance of chylomicron remnants. *J Clin Invest* 101:689-695.

23. Esko, J.D., and Lindahl, U. 2001. Molecular diversity of heparan sulfate. *J.Clin.Invest.* 108:169-173.

24. Medh, J.D., Fry, G.L., Bowen, S.L., Ruben, S., Wong, H., and Chappell, D.A. 2000. Lipoprotein lipase- and hepatic triglyceride lipase- promoted very low density lipoprotein degradation proceeds via an apolipoprotein E-dependent mechanism. *J Lipid Res* 41:1858-1871.

25. Seo, T., Al-Haideri, M., Treskova, E., Worgall, T.S., Kako, Y., Goldberg, I.J., and Deckelbaum, R.J. 2000. Lipoprotein lipase-mediated selective uptake from low density lipoprotein requires cell surface proteoglycans and is independent of scavenger receptor class B type 1. *J Biol Chem* 275:30355-30362.

26. Ji, Z.S., Pitas, R.E., and Mahley, R.W. 1998. Differential cellular accumulation/retention of apolipoprotein E mediated by cell surface heparan sulfate proteoglycans. Apolipoproteins E3 and E2 greater than e4. *J Biol Chem* 273:13452-13460.

27. Huff, M.W., Miller, D.B., Wolfe, B.M., Connelly, P.W., and Sawyez, C.G. 1997. Uptake of hypertriglyceridemic very low density lipoproteins and their remnants by HepG2 cells: the role of lipoprotein lipase, hepatic triglyceride lipase, and cell surface proteoglycans. *J Lipid Res* 38:1318-1333.

28. Al-Haideri, M., Goldberg, I.J., Galeano, N.F., Gleeson, A., Vogel, T., Gorecki, M., Sturley, S.L., and Deckelbaum, R.J. 1997. Heparan sulfate proteoglycan-mediated uptake of apolipoprotein E-triglyceride-rich lipoprotein particles: a major pathway at physiological particle concentrations. *Biochemistry* 36:12766-12772.

29. Ji, Z.S., Brecht, W.J., Miranda, R.D., Hussain, M.M., Innerarity, T.L., and Mahley, R.W. 1993. Role of heparan sulfate proteoglycans in the binding and uptake of apolipoprotein E-enriched remnant lipoproteins by cultured cells. *J Biol Chem* 268:10160-10167.

30. Feussner, G., Scharnagl, H., Scherbaum, C., Acar, J., Dobmeyer, J., Lohrmann, J., Wieland, H., and März, W. 1996. Apolipoprotein E5 (Glu_{212}-->Lys):

Increased binding to cell surface proteoglycans but decreased uptake and lysosomal degradation in cultured fibroblasts. *J Lipid Res* 37:1632-1645.

31. Ishibashi, S., Perrey, S., Chen, Z., Osuga, J., Shimada, M., Ohashi, K., Harada, K., Yazaki, Y., and Yamada, N. 1996. Role of the low density lipoprotein (LDL) receptor pathway in the metabolism of chylomicron remnants. A quantitative study in knockout mice lacking the LDL receptor, apolipoprotein E, or both. *J Biol Chem* 271:22422-22427.

32. Kita, T., Goldstein, J.L., Brown, M.S., Watanabe, Y., Hornick, C.A., and Havel, R.J. 1982. Hepatic uptake of chylomicron remnants in WHHL rabbits: a mechanism genetically distinct from the low density lipoprotein receptor. *Proc Natl Acad Sci USA* 79:3623-3627.

33. Rubinsztein, D.C., Cohen, J.C., Berger, G.M., van der Westhuyzen, D.R., Coetzee, G.A., and Gevers, W. 1990. Chylomicron remnant clearance from the plasma is normal in familial hypercholesterolemic homozygotes with defined receptor defects. *J Clin Invest* 86:1306-1312.

34. May, P., Woldt, E., Matz, R.L., and Boucher, P. 2007. The LDL receptor-related protein (LRP) family: an old family of proteins with new physiological functions. *Ann Med* 39:219-228.

35. Herz, J., Clouthier, D.E., and Hammer, R.E. 1992. LDL receptor-related protein internalizes and degrades uPA-PAI-1 complexes and is essential for embryo implantation. *Cell* 71:411-421.

36. Rohlmann, A., Gotthardt, M., Willnow, T.E., Hammer, R.E., and Herz, J. 1996. Sustained somatic gene inactivation by viral transfer of Cre recombinase. *Biotechnology* 14:1562-1565.

37. Elson-Schwab, L., Garner, O.B., Schuksz, M., Crawford, B.E., Esko, J.D., and Tor, Y. 2007. Guanidinylated neomycin delivers large, bioactive cargo into cells through a heparan sulfate-dependent pathway. *J Biol Chem* 282:13585-13591.

38. Belting, M. 2003. Heparan sulfate proteoglycan as a plasma membrane carrier. *Trends Biochem Sci* 28:145-151.

39. Williams, K.J., and Fuki, I.V. 1997. Cell-surface heparan sulfate proteoglycans: dynamic molecules mediating ligand catabolism. *Curr Opin Lipidol* 8:253-262.

40. Mahley, R.W., and Huang, Y. 2007. Atherogenic remnant lipoproteins: role for proteoglycans in trapping, transferring, and internalizing. *J Clin Invest* 117:94-98.

41. Rensen, P.C., Herijgers, N., Netscher, M.H., Meskers, S.C., van Eck, M., and van Berkel, T.J. 1997. Particle size determines the specificity of apolipoprotein E-containing triglyceride-rich emulsions for the LDL receptor versus hepatic remnant receptor in vivo. *J Lipid Res* 38:1070-1084.

42. Narvekar, P., Berriel Diaz, M., Krones-Herzig, A., Hardeland, U., Strzoda, D., Stohr, S., Frohme, M., and Herzig, S. 2009. Liver-specific loss of lipolysis-stimulated lipoprotein receptor triggers systemic hyperlipidemia in mice. *Diabetes* 58:1040-1049.

43. Yen, F.T., Roitel, O., Bonnard, L., Notet, V., Pratte, D., Stenger, C., Magueur, E., and Bihain, B.E. 2008. Lipolysis stimulated lipoprotein receptor: a novel molecular link between hyperlipidemia, weight gain, and atherosclerosis in mice. *J Biol Chem* 283:25650-25659.

44. Mesli, S., Javorschi, S., Berard, A.M., Landry, M., Priddle, H., Kivlichan, D., Smith, A.J., Yen, F.T., Bihain, B.E., and Darmon, M. 2004. Distribution of the lipolysis stimulated receptor in adult and embryonic murine tissues and lethality of LSR-/- embryos at 12.5 to 14.5 days of gestation. *Eur J Biochem* 271:3103-3114.

45. Van Eck, M., Hoekstra, M., Out, R., Bos, I.S., Kruijt, J.K., Hildebrand, R.B., and Van Berkel, T.J. 2008. Scavenger receptor BI facilitates the metabolism of VLDL lipoproteins in vivo. *J Lipid Res* 49:136-146.

46. Krieger, M. 2001. Scavenger receptor class B type I is a multiligand HDL receptor that influences diverse physiologic systems. *J Clin Invest* 108:793-797.

47. Fujino, T., Asaba, H., Kang, M.J., Ikeda, Y., Sone, H., Takada, S., Kim, D.H., Ioka, R.X., Ono, M., Tomoyori, H., et al. 2003. Low-density lipoprotein receptor-related protein 5 (LRP5) is essential for normal cholesterol metabolism and glucose-induced insulin secretion. *Proc Natl Acad Sci USA* 100:229-234.

48. de Faria, E., Fong, L.G., Komaromy, M., and Cooper, A.D. 1996. Relative roles of the LDL receptor, the LDL receptor-like protein, and hepatic lipase in chylomicron remnant removal by the liver. *J Lipid Res* 37:197-209.

49. Mansouri, R.M., Bauge, E., Gervois, P., Fruchart-Najib, J., Fievet, C., Staels, B., and Fruchart, J.C. 2008. Atheroprotective effect of human apolipoprotein A5 in a mouse model of mixed dyslipidemia. *Circ Res* 103:450-453.

50. Bijland, S., Pieterman, E.J., Maas, A.C., van der Hoorn, J.W., van Erk, M.J., van Klinken, J.B., Havekes, L.M., van Dijk, K.W., Princen, H.M., and Rensen, P.C. Fenofibrate increases very low density lipoprotein triglyceride production

despite reducing plasma triglyceride levels in APOE*3-Leiden.CETP mice. *J Biol Chem* 285:25168-25175.

51. Lawrence, R., Lu, H., Rosenberg, R.D., Esko, J.D., and Zhang, L. 2008. Disaccharide structure code for the easy representation of constituent oligosaccharides from glycosaminoglycans. *Nat Methods* 5:291-292.

CHAPTER 4

Conclusions and future directions

4.1 Summary

The work described in this thesis characterizes the heparan sulfate proteoglycan syndecan-1 as a clearance receptor for triglyceride-rich lipoproteins. Several important conclusions can be drawn from this data. Syndecan-1 is the primary proteoglycan receptor for TRLs in mice, and also contributes to clearance in human hepatocytes. Syndecan-1 is an independent endocytic receptor, and binds to lipoproteins via its heparan sulfate chains. Defects in syndecan-1 mediated clearance do not appear to play a role in insulin-deficient diabetes mellitus, but syndecan-1 shedding abrogates clearance in a model of septic shock and thus may contribute to hypertriglyceridemia associated with other diseases.

We also characterized the relative contribution to clearance of the low density lipoprotein receptor (Ldlr), the low density lipoprotein receptor related protein-1 (Lrp1), and heparan sulfate (HS) proteoglycans using mice in which only HS proteoglycans, both Ldlr and Lrp1, or all three receptors were inactivated. We conclude that HS proteoglycans clear a distinct subset of particles from those cleared by Ldlr, and Lrp1; that HS proteoglycans work independently from Ldlr and Lrp1; and that Ldlr, Lrp1, and HS proteoglycans are the three major hepatic TRL clearance receptors in mice.

These studies have advanced our understanding of proteoglycan-mediated clearance of TRLs, but several facets of this work warrant further examination. The

purpose of this chapter is to review ongoing and future studies and to discuss the broader implications of our work.

4.2 Which lipoprotein ligands mediate physiologically relevant interactions with the heparan sulfate chains on syndecan-1?

Inactivation of Ndst1 selectively in the liver leads to ~50% overall reduction in sulfation of heparan sulfate in mice. Thus, the defects in TRL binding and uptake observed in the *Ndst1*$^{f/f}$*AlbCre*$^{+}$ mice could either be due to reduced overall charge of the chains or due to the absence of specific subclasses of sulfate groups. We have recently shown that the clearance of TRLs depends not on overall sulfation, but rather on the presence of *N*-sulfate and 2-*O*-sulfate modified disaccharides (1). This implies that a specific ligand on TRLs requires a particular sequence of sulfated sugars in heparan sulfate in order to be taken up into hepatocytes. The identity of the relevant ligand mediating syndecan-1/lipoprotein interactions has not been conclusively determined.

APOE is secreted into the space of Disse by hepatocytes. It has been suggested that*, in vivo*, lipoproteins in this space become enriched with APOE, possibly to increase the affinity of these particles for receptors (2). Though APOE is a ligand for both LDLR and LRP1, APOE binds to heparin *in vitro* (3-6), and isolated heparan sulfate chains from *Ndst1*$^{f/f}$*AlbCre*$^{+}$ mice show reduced binding to recombinant APOE in a filter-binding assay (7). In cultured cells, it has been shown that APOE plays an important role in binding and internalization via heparan sulfate proteoglycans (2, 8-10). *In vivo*, hepatic uptake and plasma clearance of β-VLDL

enriched in APOE was reduced after intravenous infusion of heparinase (11). Taken together, these studies support the conclusion that APOE might serve as a ligand for TRL clearance through syndecan-1.

APOAV is known to have an important role in triglyceride homeostasis. In humans, variations in the APOA5 gene are associated with increased levels of plasma triglycerides, and patients lacking APOAV expression have severe hypertriglyceridemia (12-18). Mice that overexpress ApoAV have reduced plasma triglyceride levels (19, 20). The mechanism by which APOAV regulates triglyceride levels is widely debated, however. APOAV may exert its effects on triglyceride levels by suppressing expression of the lipoprotein lipase inhibitor APOCIII (21), thereby enhancing lipolytic activity. Emerging evidence, however, suggests that APOAV acts as a ligand and directly enhances receptor-mediated lipoprotein particle uptake in the liver. APOAV interacts with heparan sulfate proteoglycans (22) and with LRP1 (23) via a known heparin binding domain. Further, APOAV deficient mice have reduced plasma remnant clearance and liver uptake after perfusion with radiolabeled chylomicrons and remnants (24). Thus, like APOE, APOAV is also a plausible candidate to mediate clearance of TRLs through syndecan-1.

Further experiments are underway to confirm the contribution of both APOAV and APOE to syndecan-1 mediated TRL clearance. Treatment with either APOAV- or APOE- blocking antibodies significantly reduces the binding of human VLDL to isolated syndecan-1 ectodomains (J. C. Gonzales and J. D. Esko, unpublished observations). Co-treatment with both blocking antibodies reduces binding to the same level observed when either antibody is used alone, and no inhibition of binding

is observed when either APOB-100 or APOB-48 antibodies are used. This suggests that simultaneous interactions with both APOE and APOAV are required for syndecan-1 binding. Study of these two ligands may lead to the identification of a heparan sulfate oligosaccharide sequence through which ligand binding occurs. Based on previous studies of heparan sulfate ligand binding, we predict that this sequence will be approximately 6-12 monosaccharides long (3, 5, 25, 26), and will contain *2-O-* and *N-* sulfated residues (1, 7).

4.3 How do lipoprotein ligands interact with syndecan-1?

The identification of APOE and APOAV as the relevant ligands for TRL binding leads to several additional questions. For instance, how does a lipoprotein containing ApoE and ApoAV interact with syndecan-1? When syndecan-1 deficient mice are bred to mice with a conditional ablation of liver Ndst1 (*Sdc1*$^{-/-}$ *Ndst1*$^{f/f}$*AlbCre*$^{+}$), there is neither an increase in fasting triglyceride levels nor an enhanced delay in clearance of postprandial lipoproteins in the double mutant mice compared to either single mutant (27). This data confirms that it is the heparan sulfate chains on hepatic syndecan-1 that are necessary for binding and uptake of TRLs in mice.

We have observed that approximately one third of beta-eliminated heparan sulfate chains removed from syndecan-1 ectodomains bind TRLs just as efficiently as entire ectodomains, suggesting that these single chains contain attachment sites for both APOE and APOAV (J.C. Gonzales and J.D. Esko, unpublished observations). Interestingly, syndecan-1 has attachment sites for three heparan sulfate chains.

Statistically, therefore, we would expect that nearly all syndecan-1 molecules would contain at least one chain capable of interacting with TRLs. Our data cannot rule out the possibility, however, that binding occurs when multiple chains simultaneously interact with TRLs – engaging the lipoproteins in a "proteoglycan hug" (Figure 1-1). This scenario would increase the probability of binding, as it would only require each chain to have a binding sequence for one ligand instead of two. Additionally, we cannot exclude the possibility that the chains responsible for binding are present on different syndecan-1 molecules. Indeed, syndecan-1 is known to multimerize (28), and clustering may be necessary for endocytosis (29, 30).

In our preliminary structure-function analysis of syndecan-1 presented in chapter 2, we found that removal of the attachment site for just one heparan sulfate chain (at amino acid 45, Figure 2-8) was enough to significantly reduce syndecan-1 mediated clearance. This finding can be interpreted in several ways. It is possible that the chains at the various attachment sites might vary in composition and capacity to interact with APOE and APOAV. However, no evidence exists for site-specific differences in chain composition in proteoglycans. Rather, the finding that the Ad45 mutant did not rescue clearance most likely represents the fact that interactions with multiple heparan sulfate chains are required for lipoprotein clearance. We predict that mutants lacking heparan sulfate attachment sites at either of the other two residues (amino acids 37 and 47) would show similar results, and that removal of just one chain at any location is enough to significantly reduce the ability of syndecan-1 to engage lipoproteins in a "proteoglycan hug".

4. 4 Is liver syndecan-1 uniquely able to mediate clearance?

In addition to syndecan-1, hepatocytes express other heparan sulfate proteoglycans, including syndecan-2, syndecan-4, glypican-4, collagen XVIII, agrin and perlecan (27). Inactivation of syndecan-4 does not result in hypertriglyceridemia, and adenovirus-mediated overexpression of this protein did not restore hepatic clearance of TRLs in *Sdc1*$^{-/-}$ mice, excluding its participation in hepatic clearance. It is possible that syndecan-4 is concentrated on the basolateral membrane of hepatocytes, and thus cannot interact with lipoprotein particles in the space of Disse. Collagen XVIII deficient mice suffer from mild chylomicronemia due to defects in peripheral lipolysis (31). Systemic loss-of-function alleles in perlecan and agrin are lethal in mice (32-34), and lipid clearance has not been analyzed in glypican-4 or syndecan-2 knockout mice. However, the lack of enhanced hypertriglyceridemia in *Sdc1*$^{-/-}$*Ndst1*$^{f/f}$*AlbCre*$^{+}$ mice would argue that other hepatic heparan sulfate proteoglycans do not contribute significantly to TRL clearance. Additionally, we and others have found, using immunoelectron microscopy, that syndecan-1 is concentrated on hepatocyte microvilli lining the hepatic space of Disse (27, 35). It is likely that unique conditions favoring TRL clearance exist in this space, such as a locally high concentration of lipoprotein ligands (including APOE, secreted by hepatocytes) or the presence of "trapped" lipoproteins that have been sequestered in this space by extracellular matrix proteoglycans or other factors. Thus, syndecan-1 may be uniquely poised to mediate clearance.

Does syndecan-1 in other tissues contribute to clearance of TRLs in the periphery? Syndecan-1 is expressed predominantly in epithelial cells and

subpopulations of leukocytes, but is also expressed at low levels in most tissues. Mice with an endothelial cell-specific ablation of heparan sulfate (*Ndst1$^{f/f}$Tie2Cre^{+}*) do not accumulate fasting or postprandial triglycerides, suggesting that endothelial syndecan-1 does not mediate clearance (7). The composition of liver syndecan-1 may be uniquely suited to facilitate lipoprotein binding and uptake. Liver heparan sulfate is highly sulfated. The chains contain approximately 1.34 sulfates per disaccharide (36), which is roughly twice the amount observed in other mouse and human tissues. Perhaps the core proteins are more highly substituted with heparan sulfate, on average, than syndecan-1 in other tissues. Furthermore, syndecan-1 expression appears to be quite high in hepatocytes, which might facilitate multimerization and multivalent interactions necessary for binding and/or endocytosis.

4.5 What is the endocytic route followed by syndecan-1 during TRL clearance?

To address this issue, uptake and degradation of radiolabeled lipoprotein particles in hepatocytes should be assessed after inhibition of the various endocytic routes. A panel of small molecule inhibitors with known inhibitory activities is commonly used in endocytosis studies. For example, monodansylcadaverine blocks clathrin-mediated endocytosis, methyl-β-clyclodextrin blocks caveolae/lipid-raft mediated endocytosis, and wortmannin blocks macropinocytosis (41). Though pharmacological inhibition is often informative, many of the agents affect more than one pathway. Thus, results should be confirmed genetically. Transfection with dominant negative Eps15 mutant constructs has been used to disrupt clathrin-mediated

endocytosis (42). Similar experiments can also be performed with dominant negative forms of caveolin-1, which have been successfully expressed in cells (43). Caveolin-1 deficient mice can also be used to test for defects in postprandial triglyceride-rich lipoprotein uptake *in vivo* (44).

Previous studies have attempted to characterize the pathway of syndecan-1 endocytosis in non-hepatic cell lines. Based on its primary sequence, syndecan-1 lacks the hallmarks of a classical clathrin-dependent receptor (39) and Wilsie *et al* showed that potassium depletion in syndecan-1-expressing human fibroblasts has no effect on ^{125}I-LDL uptake, confirming that uptake is not clathrin mediated (40). Endocytosis of DiI-labeled LDL in these cells was inhibited by nystatin, an agent known to block lipid raft/caveolae pathways. Fuki *et al* further showed that endocytosis of a syndecan-1/Fc receptor chimeric protein in transfected CHO cells was reduced by methyl-β-cyclodextrin (lipid raft/caveolae inhibitor) in a dose-dependent manner (30). The endocytic pathway followed by syndecan-1 in hepatocytes is unknown.

The fate of syndecan-1 after endocytosis is also unclear. Does this protein traffic to lysosomes with lipoprotein particles, or is it recycled to the cell surface like other endocytic receptors? Previous studies have begun to address these issues in other cell types (45, 46), but no careful study has been performed in hepatocytes. Intracellular trafficking of syndecan-1 can be easily observed using fluorescence microscopy, and localization of syndecan-1 in various intracellular organelles can be observed by co-staining for markers of those compartments. For instance, Rab7 and LAMP-1 are widely used as markers for late endosomes (47) and lysosomes (48)

respectively. Studies of endocytic routes followed by syndecan-1 are necessary to fully understand and characterize syndcan-1 as a receptor for triglyceride-rich lipoproteins.

4.6 Is syndecan-1 mediated clearance of TRLs atheroprotective?

Whether triglyceride levels can be correlated with cardiovascular disease has been a subject of intense debate. It remains a difficult issue to study, as hypertriglyceridemia is often associated with other cardiovascular risk factors such as metabolic syndrome, obesity, type 2 diabetes mellitus, and proinflammatory and pro-thrombotic biomarkers (49). However, several recent studies have suggested that hypertriglyceridemia is, in fact, an independent risk factor for cardiovascular disease (50-54). Though chylomicrons are not considered to be atherogenic, triglyceride rich remnant particles may contribute directly to foam cell formation in the arterial wall (55). Additionally, elevated triglycerides in the postprandial state has recently been named as an additional risk factor for cardiovascular disease (56).

The mutant mice that we have developed serve as a useful tool to evaluate the contribution of syndecan-1 mediated clearance to the development of atherosclerosis. To address this issue, wildtype, $Cre^{+}Ndst1^{f/f}$, $Cre^{+}Lrp1^{f/f}Ldlr^{-/-}$, and $Cre^{+}Ndst1^{f/f}Lrp1^{f/f}Ldlr^{-/-}$ mice should be subjected to high-fat feeding. Mice should then be sacrificed, and the abundance and relative size of aortic atherosclerotic lesions among the various genotypes should be compared. Additionally, stability of the lesions should be assessed by measuring smooth muscle cell infiltration and collagen deposition in the fibrous cap. Though mice of the C57BL/6 background are

significantly more susceptible to atherosclerosis than other strains of mice (57), wildtype mice only develop minimal lesions after western diet/high fat feeding, and these fatty streaks can only be seen at particular sites of the arterial tree. In contrast, *Ldlr*$^{-/-}$ mice develop lesions on a chow diet around six months of age (58), and form plaques more quickly with high fat feeding. Thus, given the role of syndecan-1 in TRL clearance, we predict that both lesion number and area will be enhanced in *Ndst1*$^{f/f}$*AlbCre*$^{+}$ mice compared to wildtype.

Syndecan-1 shedding reduces clearance of TRLs in primary human hepatocytes, suggesting that enhanced shedding may lead to the accumulation of pro-atherogenic particles in humans. Increased syndecan-1 shedding is observed *in vivo* in a number of pathological conditions, including hemorrhagic shock (59), pulmonary fibrosis (60), cancer (61), allergic inflammation (62), bacterial infection (63-67), and others (68, 69). Though it is unknown whether many drug treatments enhance syndecan-1 shedding, numerous inflammatory factors have been shown to stimulate this process (70-76). This could provide a partial explanation as to why patients with constant low-levels of inflammation have an increased risk of cardiovascular disease (77-81). Experiments should be performed to assess whether syndecan-1 shedding is related to the development of atherosclerosis in patients. This would require a long-term study to evaluate changes in syndecan-1 ectodomain levels in the plasma, and correlation of ectodomain levels with cardiovascular events.

4.7 Can polymorphisms in syndecan-1 or heparan sulfate biosynthetic enzyme genes explain human hyperlipidemias of unknown etiology?

Though elevation of plasma triglyceride levels is caused by a number of known genetic mutations (82) and disease states (83-85), hypertriglyceridemia in patients often has an unknown etiology. It is therefore possible that mutations in the syndecan-1 gene, or in any of the genes important for heparan sulfate biosynthesis, could be responsible for clinically relevant cases of hypertriglyceridemia. Genome-wide association studies (GWAS) have emerged as powerful tools to identify candidate genes associated with clinical traits. Several recent GWAS studies identified novel candidate gene loci contributing to plasma lipid and lipoprotein concentrations (86-88), but these studies failed to pick up any relevant polymorphisms in syndecan-1 or known HSPG-assembly genes. The polymorphisms that were positively identified, however, when combined with all other known polymorphisms, account for only 5-8% of interindividual variability after age, sex, and diabetic status are factored out (89). This suggests that there may be many more genes yet to be identified. These recent studies also focused on samples from type 2 diabetic and metabolic syndrome patients. Thus, GWAS studies specifically analyzing otherwise-healthy hypertriglyceridemic patients and normotriglyceridemic controls may be necessary to identify reasonable candidate loci.

The contribution of syndecan-1 to clearance in humans might be masked in healthy subjects due to the action of or compensation by other receptors. Thus, to tease apart the contribution of syndecan-1 polymorphisms to hypertriglyceridemia in humans, it may be necessary to look at a cohort of patients in which other TRL

receptors have been inactivated. Familial hypercholesterolemia (FH) patients who are homozygous for null alleles of LDLR have severely elevated cholesterol levels and modestly increased triglyceride levels. Heterozygous individuals, however, vary in their level of triglyceride accumulation. It is possible, therefore, that these patients have been "sensitized" to the effects of syndecan-1 polymorphisms due to partial inactivation of LDLR. In a preliminary study, we measured the concentration of syndecan-1 ectodomains in serum from FH heterozygotes. Though we did not observe any correlation between syndecan-1 ectodomain levels and triglyceride concentrations (Y. Deng and J.D. Esko, unpublished observations), the number of samples analyzed was relatively small. Thus, further study of these patients is necessary before any conclusions can be drawn.

4.8 Closing remarks

The incidence of hypertriglyceridemia continues to increase around the globe, and the clinical complications resulting from this condition are becoming increasingly apparent. A thorough understanding of the molecules involved in triglyceride homeostasis is critically important. The identification and characterization of syndecan-1 as the primary proteoglycan receptor that works independently from other known receptors opens up many new avenues for research and is likely to inspire numerous new studies among glycobiologists and lipoprotein researchers alike. As the nuances of syndecan-1's function in triglyceride clearance are elucidated, new treatments and prevention strategies are bound to emerge.

4.9 References

1. Stanford, K.I., Wang, L., Castagnola, J., Song, D., Bishop, J.R., Brown, J.R., Lawrence, R., Bai, X., Habuchi, H., Tanaka, M., et al. 2010. Heparan sulfate 2-O-sulfotransferase is required for triglyceride-rich lipoprotein clearance. *J Biol Chem* 285:286-294.

2. Ji, Z.S., Fazio, S., Lee, Y.L., and Mahley, R.W. 1994. Secretion-capture role for apolipoprotein E in remnant lipoprotein metabolism involving cell surface heparan sulfate proteoglycans. *J Biol Chem* 269:2764-2772.

3. Dong, J., Peters-Libeu, C.A., Weisgraber, K.H., Segelke, B.W., Rupp, B., Capila, I., Hernaiz, M.J., LeBrun, L.A., and Linhardt, R.J. 2001. Interaction of the N-terminal domain of apolipoprotein E4 with heparin. *Biochemistry* 40:2826-2834.

4. Cardin, A.D., and Weintraub, H.J. 1989. Molecular modeling of protein-glycosaminoglycan interactions. *Arteriosclerosis.* 9:21-32.

5. Libeu, C.P., Lund-Katz, S., Phillips, M.C., Wehrli, S., Hernaiz, M.J., Capila, I., Linhardt, R.J., Raffai, R.L., Newhouse, Y.M., Zhou, F., et al. 2001. New insights into the heparan sulfate proteoglycan-binding activity of apolipoprotein E. *J Biol Chem* 276:39138-39144.

6. Bazin, H.G., Marques, M.A., Owens, A.P., 3rd, Linhardt, R.J., and Crutcher, K.A. 2002. Inhibition of apolipoprotein E-related neurotoxicity by glycosaminoglycans and their oligosaccharides. *Biochemistry* 41:8203-8211.

7. MacArthur, J.M., Bishop, J.R., Wang, L., Stanford, K.I., Bensadoun, A., Witztum, J.L., and Esko, J.D. 2007. Liver heparan sulfate proteoglycans mediate clearance of triglyceride-rich lipoproteins independently of LDL receptor family members. *J Clin Invest* 117:153-164.

8. Ji, Z.S., Dichek, H.L., Miranda, R.D., and Mahley, R.W. 1997. Heparan sulfate proteoglycans participate in hepatic lipase- and apolipoprotein E-mediated binding and uptake of plasma lipoproteins, including high density lipoproteins. *J Biol Chem* 272:31285-31292.

9. Ji, Z.S., Brecht, W.J., Miranda, R.D., Hussain, M.M., Innerarity, T.L., and Mahley, R.W. 1993. Role of heparan sulfate proteoglycans in the binding and uptake of apolipoprotein E-enriched remnant lipoproteins by cultured cells. *J Biol Chem* 268:10160-10167.

10. Ji, Z.S., Fazio, S., and Mahley, R.W. 1994. Variable heparan sulfate proteoglycan binding of apolipoprotein E variants may modulate the expression of type III hyperlipoproteinemia. *J Biol Chem* 269:13421-13428.

11. Ji, Z.S., Sanan, D.A., and Mahley, R.W. 1995. Intravenous heparinase inhibits remnant lipoprotein clearance from the plasma and uptake by the liver: in vivo role of heparan sulfate proteoglycans. *J Lipid Res* 36:583-592.

12. Pennacchio, L.A., Olivier, M., Hubacek, J.A., Krauss, R.M., Rubin, E.M., and Cohen, J.C. 2002. Two independent apolipoprotein A5 haplotypes influence human plasma triglyceride levels. *Hum Mol Genet* 11:3031-3038.

13. Grallert, H., Sedlmeier, E.M., Huth, C., Kolz, M., Heid, I.M., Meisinger, C., Herder, C., Strassburger, K., Gehringer, A., Haak, M., et al. 2007. APOA5 variants and metabolic syndrome in Caucasians. *J Lipid Res* 48:2614-2621.

14. Wright, W.T., Young, I.S., Nicholls, D.P., Patterson, C., Lyttle, K., and Graham, C.A. 2006. SNPs at the APOA5 gene account for the strong association with hypertriglyceridaemia at the APOA5/A4/C3/A1 locus on chromosome 11q23 in the Northern Irish population. *Atherosclerosis* 185:353-360.

15. Lai, C.Q., Demissie, S., Cupples, L.A., Zhu, Y., Adiconis, X., Parnell, L.D., Corella, D., and Ordovas, J.M. 2004. Influence of the APOA5 locus on plasma triglyceride, lipoprotein subclasses, and CVD risk in the Framingham Heart Study. *J Lipid Res* 45:2096-2105.

16. Zhao, T., and Zhao, J. Association of the apolipoprotein A5 gene -1131 T>C polymorphism with fasting blood lipids: a meta-analysis in 37859 subjects. *BMC Med Genet* 11:120.

17. Johansen, C.T., Wang, J., Lanktree, M.B., Cao, H., McIntyre, A.D., Ban, M.R., Martins, R.A., Kennedy, B.A., Hassell, R.G., Visser, M.E., et al. Excess of rare variants in genes identified by genome-wide association study of hypertriglyceridemia. *Nat Genet* 42:684-687.

18. Kluger, M., Heeren, J., and Merkel, M. 2008. Apoprotein A-V: An important regulator of triglyceride metabolism. *J Inherit Metab Dis*.

19. Schaap, F.G., Rensen, P.C., Voshol, P.J., Vrins, C., van der Vliet, H.N., Chamuleau, R.A., Havekes, L.M., Groen, A.K., and van Dijk, K.W. 2004. ApoAV reduces plasma triglycerides by inhibiting very low density lipoprotein-triglyceride (VLDL-TG) production and stimulating lipoprotein lipase-mediated VLDL-TG hydrolysis. *J Biol Chem* 279:27941-27947.

20. Gerritsen, G., van der Hoogt, C.C., Schaap, F.G., Voshol, P.J., Kypreos, K.E., Maeda, N., Groen, A.K., Havekes, L.M., Rensen, P.C., and van Dijk, K.W. 2008. ApoE2-associated hypertriglyceridemia is ameliorated by increased levels of apoA-V but unaffected by apoC-III deficiency. *J Lipid Res* 49:1048-1055.

21. Staels, B., Vu-Dac, N., Kosykh, V.A., Saladin, R., Fruchart, J.C., Dallongeville, J., and Auwerx, J. 1995. Fibrates downregulate apolipoprotein C-III expression independent of induction of peroxisomal acyl coenzyme A oxidase. A potential mechanism for the hypolipidemic action of fibrates. *J Clin Invest* 95:705-712.

22. Lookene, A., Beckstead, J.A., Nilsson, S., Olivecrona, G., and Ryan, R.O. 2005. Apolipoprotein A-V-heparin interactions: implications for plasma lipoprotein metabolism. *J Biol Chem* 280:25383-25387.

23. Nilsson, S.K., Lookene, A., Beckstead, J.A., Gliemann, J., Ryan, R.O., and Olivecrona, G. 2007. Apolipoprotein A-V interaction with members of the low density lipoprotein receptor gene family. *Biochemistry* 46:3896-3904.

24. Grosskopf, I., Baroukh, N., Lee, S.J., Kamari, Y., Harats, D., Rubin, E.M., Pennacchio, L.A., and Cooper, A.D. 2005. Apolipoprotein A-V deficiency results in marked hypertriglyceridemia attributable to decreased lipolysis of triglyceride-rich lipoproteins and removal of their remnants. *Arterioscler Thromb Vasc Biol* 25:2573-2579.

25. Parthasarathy, N., Goldberg, I.J., Sivaram, P., Mulloy, B., Flory, D.M., and Wagner, W.D. 1994. Oligosaccharide sequences of endothelial cell surface heparan sulfate proteoglycan with affinity for lipoprotein lipase. *J Biol Chem* 269:22391-22396.

26. Spillmann, D., Lookene, A., and Olivecrona, G. 2006. Isolation and characterization of low sulfated heparan sulfate sequences with affinity for lipoprotein lipase. *J Biol Chem* 281:23405-23413.

27. Stanford, K.I., Bishop, J.R., Foley, E.M., Gonzales, J.C., Niesman, I.R., Witztum, J.L., and Esko, J.D. 2009. Syndecan-1 is the primary heparan sulfate proteoglycan mediating hepatic clearance of triglyceride-rich lipoproteins in mice. *J Clin Invest* 119:3236-3245.

28. Dews, I.C., and Mackenzie, K.R. 2007. Transmembrane domains of the syndecan family of growth factor coreceptors display a hierarchy of homotypic and heterotypic interactions. *Proc Natl Acad Sci USA* 104:20782-20787.

29. Fuki, I.V., Kuhn, K.M., Lomazov, I.R., Rothman, V.L., Tuszynski, G.P., Iozzo, R.V., Swenson, T.L., Fisher, E.A., and Williams, K.J. 1997. The syndecan family of proteoglycans. Novel receptors mediating internalization of atherogenic lipoproteins in vitro. *J Clin Invest* 100:1611-1622.

30. Fuki, I.V., Meyer, M.E., and Williams, K.J. 2000. Transmembrane and cytoplasmic domains of syndecan mediate a multi-step endocytic pathway involving detergent-insoluble membrane rafts. *Biochem J* 351:607-612.

31. Bishop, J.R., Passos-Bueno, M.R., Fong, L., Stanford, K.I., Gonzales, J.C., Yeh, E., Young, S.G., Bensadoun, A., Witztum, J.L., Esko, J.D., et al. 2010. Deletion of the basement membrane heparan sulfate proteoglycan type XVIII collagen causes hypertriglyceridemia in mice and humans. *PLoS ONE* 5:e13919.

32. Serpinskaya, A.S., Feng, G., Sanes, J.R., and Craig, A.M. 1999. Synapse formation by hippocampal neurons from agrin-deficient mice. *Dev Biol* 205:65-78.

33. Gautam, M., Noakes, P.G., Moscoso, L., Rupp, F., Scheller, R.H., Merlie, J.P., and Sanes, J.R. 1996. Defective neuromuscular synaptogenesis in agrin-deficient mutant mice. *Cell* 85:525-535.

34. Arikawa-Hirasawa, E., Watanabe, H., Takami, H., Hassell, J.R., and Yamada, Y. 1999. Perlecan is essential for cartilage and cephalic development. *Nat Genet* 23:354-358.

35. Soroka, C.J., and Farquhar, M.G. 1991. Characterization of a novel heparan sulfate proteoglycan found in the extracellular matrix of liver sinusoids and basement membranes. *J. Cell Biol.* 113:1231-1241.

36. Lyon, M., Deakin, J.A., and Gallagher, J.T. 1994. Liver heparan sulfate structure. A novel molecular design. *J Biol Chem* 269:11208-11215.

37. Gallagher, J.T., and Walker, A. 1985. Molecular distinctions between heparan sulphate and heparin. Analysis of sulphation patterns indicates that heparan sulphate and heparin are separate families of N-sulphated polysaccharides. *Biochem J* 230:665-674.

38. Oldberg, Å., Kjellén, L., and Höök, M. 1979. Cell-surface heparan sulfate. Isolation and characterization of a proteoglycan from rat liver membranes. *J Biol Chem* 254:8505-8510.

39. Schmid, S.L. 1997. Clathrin-coated vesicle formation and protein sorting: an integrated process. *Annu Rev Biochem* 66:511-548.

40. Wilsie, L.C., Gonzales, A.M., and Orlando, R.A. 2006. Syndecan-1 mediates internalization of apoE-VLDL through a low density lipoprotein receptor-related protein (LRP)-independent, non-clathrin-mediated pathway. *Lipids Health Dis* 5:23.

41. Ivanov, A.I. 2008. Pharmacological inhibition of endocytic pathways: is it specific enough to be useful? *Methods Mol Biol* 440:15-33.

42. Benmerah, A., Bayrou, M., Cerf-Bensussan, N., and Dautry-Varsat, A. 1999. Inhibition of clathrin-coated pit assembly by an Eps15 mutant. *J Cell Sci* 112 (Pt 9):1303-1311.

43. Lee, H., Park, D.S., Razani, B., Russell, R.G., Pestell, R.G., and Lisanti, M.P. 2002. Caveolin-1 mutations (P132L and null) and the pathogenesis of breast cancer: caveolin-1 (P132L) behaves in a dominant-negative manner and caveolin-1 (-/-) null mice show mammary epithelial cell hyperplasia. *Am J Pathol* 161:1357-1369.

44. Razani, B., Combs, T.P., Wang, X.B., Frank, P.G., Park, D.S., Russell, R.G., Li, M., Tang, B., Jelicks, L.A., Scherer, P.E., et al. 2002. Caveolin-1-deficient mice are lean, resistant to diet-induced obesity, and show hypertriglyceridemia with adipocyte abnormalities. *J Biol Chem* 277:8635-8647.

45. Burbach, B.J., Friedl, A., Mundhenke, C., and Rapraeger, A.C. 2003. Syndecan-1 accumulates in lysosomes of poorly differentiated breast carcinoma cells. *Matrix Biol* 22:163-177.

46. Zimmermann, P., Zhang, Z., Degeest, G., Mortier, E., Leenaerts, I., Coomans, C., Schulz, J., N'Kuli, F., Courtoy, P.J., and David, G. 2005. Syndecan recycling [corrected] is controlled by syntenin-PIP2 interaction and Arf6. *Dev Cell* 9:377-388.

47. Stenmark, H. 2009. Rab GTPases as coordinators of vesicle traffic. *Nat Rev Mol Cell Biol* 10:513-525.

48. Eskelinen, E.L. 2006. Roles of LAMP-1 and LAMP-2 in lysosome biogenesis and autophagy. *Mol Aspects Med* 27:495-502.

49. Hodis, H.N., Mack, W.J., Krauss, R.M., and Alaupovic, P. 1999. Pathophysiology of triglyceride-rich lipoproteins in atherothrombosis: clinical aspects. *Clin Cardiol* 22:II15-20.

50. Stalenhoef, A.F., and de Graaf, J. 2008. Association of fasting and nonfasting serum triglycerides with cardiovascular disease and the role of remnant-like lipoproteins and small dense LDL. *Curr Opin Lipidol* 19:355-361.

51. Nordestgaard, B.G., Benn, M., Schnohr, P., and Tybjaerg-Hansen, A. 2007. Nonfasting triglycerides and risk of myocardial infarction, ischemic heart disease, and death in men and women. *Jama* 298:299-308.

52. Bansal, S., Buring, J.E., Rifai, N., Mora, S., Sacks, F.M., and Ridker, P.M. 2007. Fasting compared with nonfasting triglycerides and risk of cardiovascular events in women. *Jama* 298:309-316.

53. Langsted, A., Freiberg, J.J., and Nordestgaard, B.G. 2008. Fasting and nonfasting lipid levels: influence of normal food intake on lipids, lipoproteins, apolipoproteins, and cardiovascular risk prediction. *Circulation* 118:2047-2056.

54. Fujioka, Y., and Ishikawa, Y. 2009. Remnant lipoproteins as strong key particles to atherogenesis. *J Atheroscler Thromb*.

55. Zilversmit, D.B. 1979. Atherogenesis: a postprandial phenomenon. *Circulation* 60:473-485.

56. Tushuizen, M.E., Diamant, M., and Heine, R.J. 2005. Postprandial dysmetabolism and cardiovascular disease in type 2 diabetes. *Postgrad Med J* 81:1-6.

57. Paigen, B., Morrow, A., Brandon, C., Mitchell, D., and Holmes, P. 1985. Variation in susceptibility to atherosclerosis among inbred strains of mice. *Atherosclerosis* 57:65-73.

58. Ishibashi, S., Goldstein, J.L., Brown, M.S., Herz, J., and Burns, D.K. 1994. Massive xanthomatosis and atherosclerosis in cholesterol-fed low density lipoprotein receptor-negative mice. *J Clin Invest* 93:1885-1893.

59. Haywood-Watson, R.J., Holcomb, J.B., Gonzalez, E.A., Peng, Z., Pati, S., Park, P.W., Wang, W., Zaske, A.M., Menge, T., and Kozar, R.A. Modulation of syndecan-1 shedding after hemorrhagic shock and resuscitation. *PLoS One* 6:e23530.

60. Kliment, C.R., Englert, J.M., Gochuico, B.R., Yu, G., Kaminski, N., Rosas, I., and Oury, T.D. 2009. Oxidative stress alters syndecan-1 distribution in lungs with pulmonary fibrosis. *J Biol Chem* 284:3537-3545.

61. Yang, Y., Yaccoby, S., Liu, W., Langford, J.K., Pumphrey, C.Y., Theus, A., Epstein, J., and Sanderson, R.D. 2002. Soluble syndecan-1 promotes growth of myeloma tumors in vivo. *Blood* 100:610-617.

62. Xu, J., Park, P.W., Kheradmand, F., and Corry, D.B. 2005. Endogenous attenuation of allergic lung inflammation by syndecan-1. *J Immunol* 174:5758-5765.

63. Park, P.W., Pier, G.B., Hinkes, M.T., and Bernfield, M. 2001. Exploitation of syndecan-1 shedding by Pseudomonas aeruginosa enhances virulence. *Nature* 411:98-102.

64. Hayashida, A., Bartlett, A.H., Foster, T.J., and Park, P.W. 2009. Staphylococcus aureus beta-toxin induces lung injury through syndecan-1. *Am J Pathol* 174:509-518.

65. Hayashida, A., Amano, S., and Park, P.W. 2011. Syndecan-1 promotes Staphylococcus aureus corneal infection by counteracting neutrophil-mediated host defense. *J Biol Chem* 286:3288-3297.

66. Hayashida, K., Parks, W.C., and Park, P.W. 2009. Syndecan-1 shedding facilitates the resolution of neutrophilic inflammation by removing sequestered CXC chemokines. *Blood* 114:3033-3043.

67. Haynes, A., 3rd, Ruda, F., Oliver, J., Hamood, A.N., Griswold, J.A., Park, P.W., and Rumbaugh, K.P. 2005. Syndecan 1 shedding contributes to Pseudomonas aeruginosa sepsis. *Infect Immun* 73:7914-7921.

68. Kainulainen, V., Wang, H.M., Schick, C., and Bernfield, M. 1998. Syndecans, heparan sulfate proteoglycans, maintain the proteolytic balance of acute wound fluids. *J Biol Chem* 273:11563-11569.

69. Kato, M., Wang, H., Kainulainen, V., Fitzgerald, M.L., Ledbetter, S., Ornitz, D.M., and Bernfield, M. 1998. Physiological degradation converts the soluble syndecan-1 ectodomain from an inhibitor to a potent activator of FGF-2. *Nat Med* 4:691-697.

70. Yang, Y., Macleod, V., Miao, H.Q., Theus, A., Zhan, F., Shaughnessy, J.D., Jr., Sawyer, J., Li, J.P., Zcharia, E., Vlodavsky, I., et al. 2007. Heparanase enhances syndecan-1 shedding: a novel mechanism for stimulation of tumor growth and metastasis. *J Biol Chem* 282:13326-13333.

71. Mahtouk, K., Hose, D., Raynaud, P., Hundemer, M., Jourdan, M., Jourdan, E., Pantesco, V., Baudard, M., De Vos, J., Larroque, M., et al. 2007. Heparanase influences expression and shedding of syndecan-1, and its expression by the bone marrow environment is a bad prognostic factor in multiple myeloma. *Blood* 109:4914-4923.

72. Chung, M.C., Popova, T.G., Millis, B.A., Mukherjee, D.V., Zhou, W., Liotta, L.A., Petricoin, E.F., Chandhoke, V., Bailey, C., and Popov, S.G. 2006. Secreted neutral metalloproteases of Bacillus anthracis as candidate pathogenic factors. *J Biol Chem* 281:31408-31418.

73. Brule, S., Charnaux, N., Sutton, A., Ledoux, D., Chaigneau, T., Saffar, L., and Gattegno, L. 2006. The shedding of syndecan-4 and syndecan-1 from HeLa cells and human primary macrophages is accelerated by SDF-1/CXCL12 and mediated by the matrix metalloproteinase-9. *Glycobiology* 16:488-501.

74. Charnaux, N., Brule, S., Chaigneau, T., Saffar, L., Sutton, A., Hamon, M., Prost, C., Lievre, N., Vita, C., and Gattegno, L. 2005. RANTES (CCL5) induces a CCR5-dependent accelerated shedding of syndecan-1 (CD138) and syndecan-4 from HeLa cells and forms complexes with the shed ectodomains

of these proteoglycans as well as with those of CD44. *Glycobiology* 15:119-130.

75. Park, P.W., Foster, T.J., Nishi, E., Duncan, S.J., Klagsbrun, M., and Chen, Y. 2004. Activation of syndecan-1 ectodomain shedding by Staphylococcus aureus alpha-toxin and beta-toxin. *J Biol Chem* 279:251-258.

76. Fitzgerald, M.L., Wang, Z.H., Park, P.W., Murphy, G., and Bernfield, M. 2000. Shedding of syndecan-1 and-4 ectodomains is regulated by multiple signaling pathways and mediated by a TIMP-3-sensitive metalloproteinase. *J Cell Biol* 148:811-824.

77. Lehr, H.A., Sagban, T.A., Ihling, C., Zahringer, U., Hungerer, K.D., Blumrich, M., Reifenberg, K., and Bhakdi, S. 2001. Immunopathogenesis of atherosclerosis: endotoxin accelerates atherosclerosis in rabbits on hypercholesterolemic diet. *Circulation* 104:914-920.

78. Kalayoglu, M.V., Libby, P., and Byrne, G.I. 2002. Chlamydia pneumoniae as an emerging risk factor in cardiovascular disease. *JAMA* 288:2724-2731.

79. Takaoka, N., Campbell, L.A., Lee, A., Rosenfeld, M.E., and Kuo, C.C. 2008. Chlamydia pneumoniae infection increases adherence of mouse macrophages to mouse endothelial cells in vitro and to aortas ex vivo. *Infect Immun* 76:510-514.

80. Scannapieco, F.A., Bush, R.B., and Paju, S. 2003. Associations between periodontal disease and risk for atherosclerosis, cardiovascular disease, and stroke. A systematic review. *Ann Periodontol* 8:38-53.

81. Pussinen, P.J., Tuomisto, K., Jousilahti, P., Havulinna, A.S., Sundvall, J., and Salomaa, V. 2007. Endotoxemia, immune response to periodontal pathogens, and systemic inflammation associate with incident cardiovascular disease events. *Arterioscler Thromb Vasc Biol* 27:1433-1439.

82. Hegele, R.A. 2001. Monogenic dyslipidemias: window on determinants of plasma lipoprotein metabolism. *Am J Hum Genet* 69:1161-1177.

83. Yuan, G., Al-Shali, K.Z., and Hegele, R.A. 2007. Hypertriglyceridemia: its etiology, effects and treatment. *Cmaj* 176:1113-1120.

84. Evans, R.D., and Williamson, D.H. 1991. Signals, mechanisms, and function of the acute lipid response to sepsis. *Biochem Cell Biol* 69:320-321.

85. Mizock, B.A. 2000. Metabolic derangements in sepsis and septic shock. *Crit Care Clin* 16:319-336, vii.

86. Kathiresan, S., Melander, O., Guiducci, C., Surti, A., Burtt, N.P., Rieder, M.J., Cooper, G.M., Roos, C., Voight, B.F., Havulinna, A.S., et al. 2008. Six new loci associated with blood low-density lipoprotein cholesterol, high-density lipoprotein cholesterol or triglycerides in humans. *Nat Genet* 40:189-197.

87. Kooner, J.S., Chambers, J.C., Aguilar-Salinas, C.A., Hinds, D.A., Hyde, C.L., Warnes, G.R., Gomez Perez, F.J., Frazer, K.A., Elliott, P., Scott, J., et al. 2008. Genome-wide scan identifies variation in MLXIPL associated with plasma triglycerides. *Nat Genet* 40:149-151.

88. Willer, C.J., Sanna, S., Jackson, A.U., Scuteri, A., Bonnycastle, L.L., Clarke, R., Heath, S.C., Timpson, N.J., Najjar, S.S., Stringham, H.M., et al. 2008. Newly identified loci that influence lipid concentrations and risk of coronary artery disease. *Nat Genet* 40:161-169.

89. Lusis, A.J., and Pajukanta, P. 2008. A treasure trove for lipoprotein biology. *Nat Genet* 40:129-130.

APPENDIX A

Syndecan-1 is the primary heparan sulfate proteoglycan mediating hepatic clearance of triglyceride-rich lipoproteins in mice

Syndecan-1 is the primary heparan sulfate proteoglycan mediating hepatic clearance of triglyceride-rich lipoproteins in mice

Kristin I. Stanford,[1,2] Joseph R. Bishop,[1] Erin M. Foley,[1,2] Jon C. Gonzales,[1,2] Ingrid R. Niesman,[1] Joseph L. Witztum,[3] and Jeffrey D. Esko[1,2]

[1]Department of Cellular and Molecular Medicine, [2]Biomedical Sciences Graduate Program, and [3]Department of Medicine, University of California, San Diego, La Jolla, California, USA.

Elevated plasma triglyceride levels represent a risk factor for premature atherosclerosis. In mice, accumulation of triglyceride-rich lipoproteins can occur if sulfation of heparan sulfate in hepatocytes is diminished, as this alters hepatic lipoprotein clearance via heparan sulfate proteoglycans (HSPGs). However, the relevant HSPG has not been determined. In this study, we found by RT-PCR analysis that mouse hepatocytes expressed the membrane proteoglycans syndecan-1, -2, and -4 and glypican-1 and -4. Analysis of available proteoglycan-deficient mice showed that only syndecan-1 mutants (*Sdc1*$^{-/-}$ mice) accumulated plasma triglycerides. *Sdc1*$^{-/-}$ mice also exhibited prolonged circulation of injected human VLDL and intestinally derived chylomicrons. We found that mice lacking both syndecan-1 and hepatocyte heparan sulfate did not display accentuated triglyceride accumulation compared with single mutants, suggesting that syndecan-1 is the primary HSPG mediating hepatic triglyceride clearance. Immunoelectron microscopy showed that syndecan-1 was expressed specifically on the microvilli of hepatocyte basal membranes, facing the space of Disse, where lipoprotein uptake occurs. Abundant syndecan-1 on wild-type murine hepatocytes exhibited saturable binding of VLDL and inhibition by heparin and facilitated degradation of VLDL. Furthermore, adenovirus-encoded syndecan-1 restored binding, uptake, and degradation of VLDL in isolated *Sdc1*$^{-/-}$ hepatocytes and the lipoprotein clearance defect in *Sdc1*$^{-/-}$ mice. These findings provide the first in vivo genetic evidence that syndecan-1 is the primary hepatocyte HSPG receptor mediating the clearance of both hepatic and intestinally derived triglyceride-rich lipoproteins.

Introduction

Because elevated plasma triglycerides constitute an independent risk factor for premature atherosclerosis, much interest exists in determining the factors that affect their synthesis and turnover (1, 2). Circulating triglyceride-rich lipoproteins (TRLs) arise from dietary fats in the intestine (chylomicrons) and de novo–synthesized lipids in the liver (VLDL). In the circulation, chylomicron and VLDL triglycerides undergo hydrolysis by lipoprotein lipase (LPL), which is immobilized on receptors on endothelial cells (3, 4). The surrounding tissues then take up the liberated free fatty acids for energy generation, membrane lipid synthesis, or storage as lipid droplets. Remnant lipoproteins arising from LPL-mediated lipolysis are cleared in the liver by multiple endocytic receptors, including the LDL receptor (LDLR) and heparan sulfate proteoglycans (HSPGs) (5–8). Recent genetic studies in mice have demonstrated the importance of these 2 classes of receptors in TRL clearance in vivo (9, 10).

The identity of the physiologically relevant HSPG in hepatocytes that mediates remnant particle clearance in vivo has not been determined. Animal cells express multiple HSPGs, including 4 transmembrane syndecans, 6 glycosylphosphatidylinositol-anchored glypicans, an alternatively spliced form of CD44 (v3), TGF-β type III receptors (betaglycan), neuropilin-1 (11), and 4 secreted proteoglycans, perlecan, agrin, collagen XVIII, and serglycin (12). Syndecans (13–16) and perlecan (14, 17, 18) have been shown to mediate the internalization of model remnant lipoproteins or TRL preparations enriched in LPL or apoE. Syndecan-1 can also mediate binding and uptake of chylomicron remnants by HepG2 liver cells in vitro based on antisense and antibody inhibition experiments (19). In vivo evidence pointing to specific hepatic proteoglycans mediating TRL clearance is more indirect. Yu et al. found that chylomicron remnants labeled with a fluorescent dye co-cluster with syndecan-1 on hepatocytes in the space of Disse (20), consistent with cell culture data indicating that clustering of syndecan may facilitate its internalization by endocytosis (13, 21). However, the authors opposed a functional role for syndecan-1 as a remnant receptor, suggesting that syndecan-1 acted merely as a chaperone to other receptors. As an added complication, overexpression of hepatic syndecan-1 in mice by infection with an adenoviral construct actually induced hyperlipidemia (22), but this may have reflected liver damage indicated by marked hepatocyte proliferation, apoptosis, and increased plasma alanine aminotransferase levels.

It is important to determine the relevant HSPG in the liver and its functional role in remnant clearance, because this would set the stage for further mechanistic studies of TRL uptake and processing and provide a candidate gene for allelic analysis in individuals with hypertriglyceridemia. In the current study, we examined available mutants in membrane HSPGs and found that mice deficient in syndecan-1 (*Sdc1*$^{-/-}$ mice) had elevated plasma triglycerides under fasting conditions and exhibited delayed hepatic clearance of dietary triglycerides and injected VLDL. Reconstitution of syndecan-1 expression in hepatocytes in vivo restored normal triglyceride metabolism. The absence of syndecan-1 also caused a decrease in the binding, uptake, and degradation of VLDL particles in isolated primary hepatocytes. Our findings show that syndecan-1 is the hepatic HSPG receptor involved in TRL clearance.

Conflict of interest: The authors have declared that no conflict of interest exists.

Citation for this article: *J. Clin. Invest.* **119**:3236–3245 (2009). doi:10.1172/JCI38251.

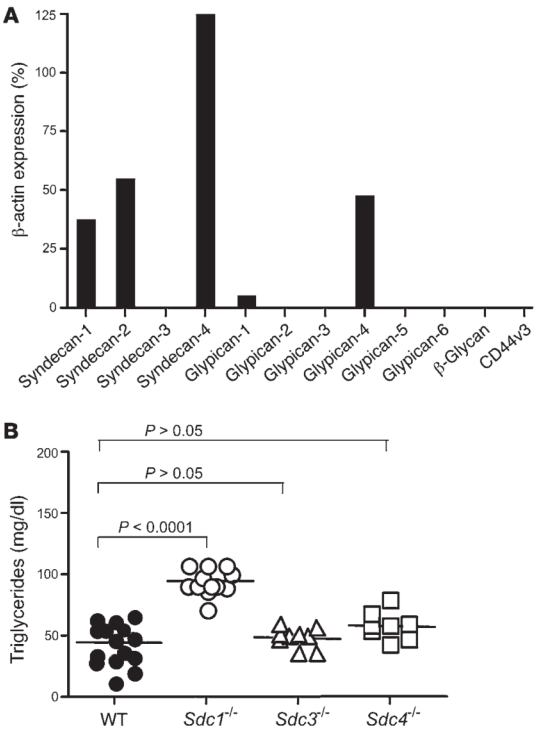

Figure 1
RT-PCR analysis of membrane HSPGs and hypertriglyceridemia in *Sdc1*$^{-/-}$ mice. (**A**) Transcript levels of the membrane proteoglycan core proteins were measured in isolated hepatocytes. The numbers represent the level of expression compared with the housekeeping gene β-actin, using C_T values from triplicate assays according to the Stratagene manual. Error bars are not shown because they are factored into the final calculation. Comparable results were obtained in 2 independent preparations of RNA. (**B**) Triglycerides were measured in plasma samples from fasted male and female mice of indicated genotypes. Wild-type (n = 14), *Sdc1*$^{-/-}$ (n = 13), *Sdc3*$^{-/-}$ (n = 10), *Sdc4*$^{-/-}$ (n = 8). Horizontal bars indicate mean values.

Results

Sdc1$^{-/-}$ *mice accumulate plasma triglycerides*. To identify the relevant HSPGs in hepatic clearance, we first determined the array of proteoglycan core proteins expressed by murine hepatocytes. Quantitative RT-PCR (qRT-PCR) using intron-spanning primers to all of the known membrane proteoglycans (Supplemental Table 1; supplemental material available online with this article; doi:10.1772/JCI38251DS1) showed that freshly purified hepatocytes expressed transcripts for syndecan-1, -2, and -4 and glypican-1 and -4 (n = 3) (Figure 1A). Since the probe sets were validated with preparations of RNA from other tissues, the absence of detectable mRNA for other proteoglycans (e.g., syndecan-3, other glypicans, betaglycan, and CD44v3) was judged important. A similar expression pattern for syndecans has been reported in rat hepatocytes (23).

Of the 5 membrane proteoglycan transcripts detected in hepatocytes, murine mutants containing systemic null alleles for syndecan-1 and -4 were available for further study. Analysis of fasted animals showed that only *Sdc1*$^{-/-}$ mice had elevated plasma triglyceride levels, which were approximately 2-fold higher than those of wild-type mice (95 ± 11 mg/dl in *Sdc1*$^{-/-}$ mice [n = 13] vs. 44 ± 19 mg/dl in wild-type mice [n = 14]; P < 0.0001). *Sdc4*$^{-/-}$ (and, as an added control, *Sdc3*$^{-/-}$ mice) had normal plasma triglyceride levels (n = 8) (Figure 1B). Plasma cholesterol levels were unaffected in *Sdc1*$^{-/-}$ mice (70 ± 1 mg/dl in *Sdc1*$^{-/-}$ [n = 13] vs. 74 ± 5 mg/dl in wild-type mice [n = 14]; P = 0.3782).

Buoyant density ultracentrifugation of fasting plasma lipoproteins from *Sdc1*$^{-/-}$ and wild-type mice showed that triglyceride accumulation occurred in particles of δ < 1.006 g/ml and δ = 1.006–1.019 g/ml, respectively, whereas LDL and HDL triglycerides were unaffected (Figure 2A). Only minor differences in the amounts of cholesterol in the separated lipoprotein classes were noted (Figure 2B). Analysis of lipoproteins of δ < 1.019 g/ml by SDS-PAGE showed that they had apoB-48, apoB-100, apoE, and apoC, characteristic of VLDL particles and chylomicron remnants (Figure 2C). Analysis of the lipoproteins by gel filtration fast-phase liquid chromatography (FPLC) showed that the triglyceride-rich particles eluted like chylomicron remnants and VLDL, with no obvious change in cholesterol content (Figure 2, D and E). A small decrease in cholesterol was noted in small, high-density particles, but we did not further investigate the characteristics of these particles. The lipoprotein phenotype of *Sdc1*$^{-/-}$ mice was virtually identical to that reported previously for *Ndst1*$^{f/f}$*AlbCre*$^{+}$ mice, which produce undersulfated heparan sulfate chains in hepatocyte proteoglycans (9).

Sdc1$^{-/-}$ *mice exhibit delayed plasma clearance of both VLDL and dietary triglycerides*. Prior studies showed that *Ndst1*$^{f/f}$*AlbCre*$^{+}$ mice displayed altered hepatic clearance of triglycerides, which suggested that *Sdc1*$^{-/-}$ mice might exhibit a similar phenotype (9). VLDL clearance was therefore measured by intravenous injection of a bolus of human VLDL and periodic blood sampling to determine human apoB-100 levels by ELISA using mAb MB47. As shown in Figure 3A, the initial rate of clearance of human VLDL was reduced about 2-fold in *Sdc1*$^{-/-}$ mice compared with the wild-type ($t_{1/2}$ = 92 ± 18 minutes in *Sdc1*$^{-/-}$ mice vs. 46 ± 7 minutes in wild-type mice, determined from linear regression of semi-log plots; P = 0.0009, n = 6). Although the absolute clearance rates differed from previous data obtained from studies of N-deacetylase/N-sulfotransferase-1–deficient (Ndst1-deficient) mice, the fold difference between mutant and wild-type mice was comparable (9).

The clearance rate of intestinally derived TRLs was also measured by vitamin A excursion studies. Fasted mice were given a bolus mixture of [^{3}H]retinol and corn oil by oral gavage, and blood was sampled at various time points to determine the plasma level of ^{3}H counts. In the intestine, [^{3}H]retinol is converted to fatty acid esters and incorporated into newly made chylomicrons, and its only route of removal is through clearance in the liver (24). As shown in Figure 3B, the area under the curve for *Sdc1*$^{-/-}$ mice was 2-fold greater than that for wild-type, indicating that the mutant cleared intestinally derived lipoproteins at a slower rate (P = 0.0034). After 12 hours, most of the tracer had been cleared in both mutant and wild-type animals, consistent with previous data showing that LDLRs also can clear plasma TRLs (9, 24, 25). Clearance of plasma triglycerides was similarly affected (Figure 3B, inset). The data presented in Figure 3, A and B, indicate that syndecan-1 plays a key role in the clearance of both hepatic (VLDL) and intestinally derived TRLs.

Since *Sdc1*$^{-/-}$ mice were created by conventional gene targeting methods (26), syndecan-1 expression was diminished in all tissues. Thus, other processes related to triglyceride synthesis, secre-

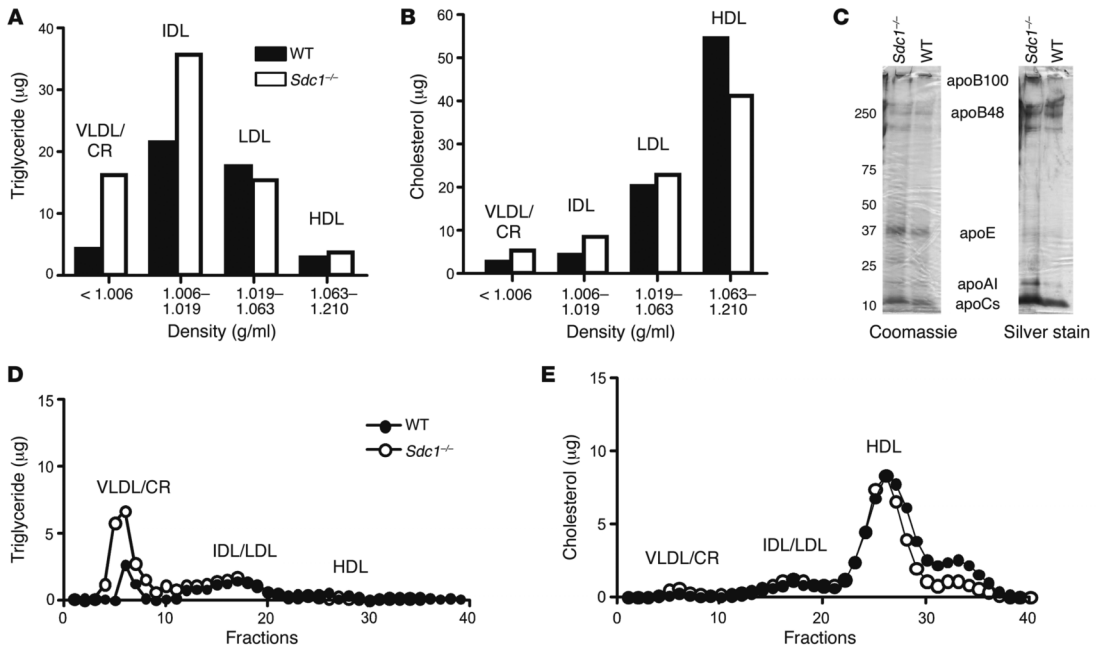

Figure 2

Hypertriglyceridemia in *Sdc1*$^{-/-}$ mice. (**A** and **B**) Triglyceride (**A**) and cholesterol (**B**) levels were measured in lipoprotein subclasses separated by preparative density ultracentrifugation. Each value is from pooled plasma derived from 10 mice. (**C**) Samples of purified lipoproteins (δ < 1.006 g/ml) were analyzed by gradient SDS-PAGE, and the individual apolipoproteins were visualized by Coomassie blue or silver staining. (**D** and **E**) Plasma triglycerides (**D**) and cholesterol (**E**) were analyzed by FPLC.

tion, or lipolysis in non-hepatic tissues could be affected in the mutant. To determine how the mutation affected overall synthesis and secretion of triglycerides, we injected the mice with Triton WR-1339, which inhibits lipolysis and lipoprotein clearance (27), and measured plasma triglycerides at various time points (Supplemental Figure 1). Analysis of the data showed that triglyceride secretion rates did not differ significantly between *Sdc1*$^{-/-}$ and wild-type mice (0.51 ± 0.11 mg/min vs. 0.38 ± 0.07 mg/min, respectively). To test whether lipolysis might be altered in tissues, we measured lipolytic activity in cell-free gonadal fat pad extracts. No difference in activity in extracts prepared from wild-type and *Sdc1*$^{-/-}$ mice was observed (Supplemental Figure 2A). Furthermore, syndecan-1 was not detected among the various HSPGs expressed in this tissue (Supplemental Figure 2B). We recently showed that altering sulfation of HSPGs in endothelial cells does not alter plasma triglyceride metabolism as well (28). Thus, these findings suggest that the hyperlipidemia associated with syndecan-1 deficiency was more likely due to defects in hepatic clearance than to non-hepatic processing of triglycerides.

Additional evidence was obtained by intravenously injecting *Sdc1*$^{-/-}$ mice with adenovirus containing either *Sdc1* or *GFP* cDNAs. Under these conditions, more than 95% of the adenovirus is cleared by the liver (29), leading to hepatic-specific expression of syndecan-1. Three weeks after infection, a bolus of [^{3}H]retinol and corn oil was administered by gavage and the rate of clearance was measured. Infection with adenovirus containing syndecan-1 cDNA (AdSdc1) partially restored expression of syndecan-1 (Supplemental Figure 3A), but nevertheless normalized clearance compared with *Sdc1*$^{-/-}$ mice infected with AdGFP (P = 0.0037), and the excursion curve was similar to that of wild-type mice (Figure 3C). These findings show that hepatic syndecan-1 is both necessary and sufficient to clear plasma triglycerides. They contrast the results of a previous study, which showed that syndecan-1 overexpression leads to hypertriglyceridemia, which may reflect differences in viral load, timing of the lipid analyses relative to viral infection, or acute liver injury in the earlier study (22).

Syndecan-1 is the primary HSPG mediating hepatic clearance. The data presented thus far show that the hyperlipidemia in *Sdc1*$^{-/-}$ mice resembles the phenotype of *Ndst1*$^{f/f}$*AlbCre*$^{+}$ mice, which produce undersulfated heparan sulfate chains in hepatocytes due to a deficiency of a specific sulfotransferase, Ndst1. To test whether other hepatocyte HSPGs can affect plasma triglyceride levels, *Sdc1*$^{-/-}$ mice were interbred with *Ndst1*$^{f/f}$*AlbCre*$^{+}$ mice, which resulted in undersulfation of heparan sulfate chains on syndecan as well as other hepatocyte-derived proteoglycans. Analysis of fasting plasma triglycerides showed that compounding the mutations did not result in accumulation of triglycerides to a greater extent than in either single mutant (Figure 4A; P = 0.1373). The double mutant also displayed delayed [^{3}H]retinol clearance to the same extent as *Sdc1*$^{-/-}$ and *Ndst1AlbCre*$^{+}$ mutants (Figure 4B). The slightly diminished effect in the double mutant was not significant (P = 0.6670). These data indicate that the heparan sulfate chains on syndecan-1 are responsible for plasma triglyceride clearance mediated by hepatic proteoglycans.

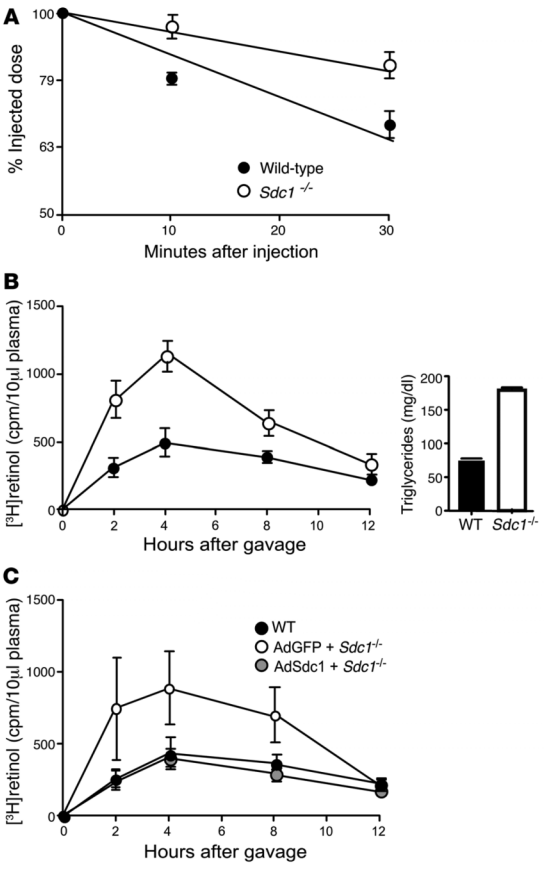

Figure 3
Sdc1$^{-/-}$ mice exhibit delayed plasma clearance of triglycerides and postprandial lipoproteins. (**A**) Clearance of human VLDL apoB-100 was measured by ELISA using human apoB-100–specific mAb MB47. Representative data from 3 different experiments is shown and plotted on a semi-log scale. Wild-type mice, $t_{1/2}$ = 46 ± 7 minutes (n = 6 mice); *Sdc1*$^{-/-}$ mice, $t_{1/2}$ = 92 ± 18 min (n = 6 mice). The difference in $t_{1/2}$ between the genotypes was significant (P = 0.0009). (**B**) Retinol ester clearance was measured in wild-type (filled circles, n = 3), and *Sdc1*$^{-/-}$ (open circles, n = 3) mice. Animals were fasted for 4 hours and given 200 μl of corn oil containing [^{3}H]retinol by gavage. Blood samples were taken and radioactivity remaining in 10 μl of serum was determined by scintillation counting. The values are expressed as mean ± SD. The areas under the curve were 4,100 ± 1,200 for the wild-type and 8,400 ± 30 for *Sdc1*$^{-/-}$ mice. Clearance was significantly delayed in *Sdc1*$^{-/-}$ mice compared with wild-type (P = 0.0034). Right: Triglyceride values were measured 4 hours after injection. (**C**) *Sdc1*$^{-/-}$ mice were injected with AdSdc1 (n = 6 mice) or AdGFP (n = 6 mice). Plasma retinol ester levels were measured as described above and compared with wild-type mice (filled circles). The areas under the curve were 3,700 ± 1,100 for wild-type, 7,400 ± 2,600 for AdGFP *Sdc1*$^{-/-}$, and 3,200 ± 900 for AdSdc1 *Sdc1*$^{-/-}$. Animals treated with AdSdc1 demonstrated clearance similar to that wild-type animals (gray circles, P = 0.1272) and significantly faster clearance than *Sdc1*$^{-/-}$ mice treated with AdGFP (P = 0.0037).

Syndecan-1 is localized on microvilli of hepatocytes in the space of Disse. Prior studies have shown that syndecan-1 is located on basal membrane of the hepatocytes facing the space of Disse (30, 31). To confirm these findings, we examined immunofluorescence micrographs of cryosections prepared from wild-type, *Sdc1*$^{-/-}$, and *Ndst1*$^{f/f}$*AlbCre*$^{+}$ livers. Sections prepared from wild-type mouse livers showed syndecan-1 localization around the sinusoids (Supplemental Figure 4A), whereas livers from *Sdc1*$^{-/-}$ mice did not stain, confirming the specificity of the antibody (Supplemental Figure 4B). Additionally, sections prepared from *Ndst1*$^{f/f}$*AlbCre*$^{+}$mice showed that syndecan-1 was localized around the sinusoids as in wild-type liver sections, indicating that altering the sulfation of the heparan sulfate chains had no effect on the distribution of syndecan-1 (Supplemental Figure 4C). In contrast to these findings, syndecan-2 was present mainly on sinusoidal endothelial cells, whereas syndecan-4 was ubiquitously expressed over the entire hepatocyte surface (data not shown). Electron microscopy of immunogold-labeled sections showed enrichment of syndecan-1 on the microvilli extending from the basal surface of the hepatocytes (Supplemental Figure 4D). Thus, syndecan-1 is positioned appropriately to encounter remnant TRLs entering the space of Disse.

Syndecan-1 can mediate binding, uptake, and degradation of VLDL. To determine whether syndecan-1 could directly mediate the binding of physiologically plausible concentrations of unmodified VLDL by primary hepatocytes, cells were isolated from wild-type mice and incubated with labeled and unlabeled native VLDL at 4°C. Normal primary hepatocytes bound ^{125}I-VLDL in a saturable manner, and the signal was reduced by the addition of heparin (Figure 5A). Specific binding was then determined by subtracting the counts obtained in the presence of heparin from the counts obtained in its absence (Figure 5A). Fitting the data to a conventional single-site binding equation yielded a B_{max} value of 8.2 ± 1.1 μg VLDL protein/mg cell protein and a K_D of 43 ± 10 μg/ml (~2.2 nM) (R^2 = 0.9760). From the B_{max} value, we calculated that hepatocytes expressed approximately 1.4 × 10^6 binding sites/cell, assuming that the average size particle had a diameter of 40 nm and a mass of 2 × 10^7 kDa, and that protein represented 1.8% of the mass. Binding was also sensitive to dilution with nonradioactive VLDL, yielding specific binding data comparable to that obtained by heparin inhibition (Figure 5B) (B_{max} value of 9.1 ± 1 μg VLDL protein/mg cell protein and a K_D of 51 ± 9 μg/ml; R^2 = 0.9871). Much of the binding depended on syndecan-1, since specific binding was reduced on average by 6-fold ± 1-fold in primary hepatocytes derived from *Sdc1*$^{-/-}$ mice compared with wild-type mice (Figure 5C). These findings are consistent with previous studies of other cell types and modified lipoproteins (13, 15, 19, 32, 33). Since the normal fasting plasma levels of VLDL in wild-type animals are lower than the calculated K_D values (8 ± 3 μg/ml plasma VLDL protein vs. 43–51 μg/ml K_D), we determined that only a portion of syndecan-1 is normally occupied under these conditions and the system is well poised to accommodate increased levels of remnants in the postprandial state.

Prior studies also have shown that syndecan-1 can mediate lipoprotein uptake and degradation (13, 21). Therefore, we examined uptake and degradation of VLDL by incubating wild-type and mutant hepatocytes with 20 μg/ml of ^{125}I-VLDL at 37°C. After 1 hour, wild-type cells bound and internalized 4.1 ± 0.4 μg VLDL/mg cell protein (Figure 6A), which was about 30% higher than the amount bound at 4°C (3.2 μg/mg cell protein at 20 μg/ml VLDL; Figure 5B). Uptake via syndecan-1 led to degradation of 2.4 μg/mg

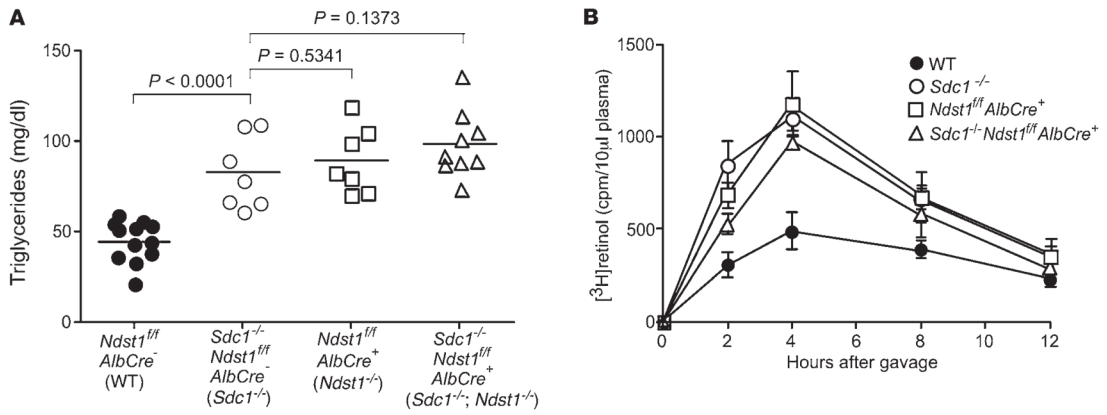

Figure 4

Hypertriglyceridemia and delayed clearance of dietary lipids in *Sdc1*$^{-/-}$ and *Ndst1*$^{f/f}$*AlbCre*$^{+}$ mice are not additive traits. (**A**) Plasma triglycerides were measured in plasma samples from fasted mice. There was no difference in plasma triglycerides in *Sdc1*$^{-/-}$*Ndst1*$^{f/f}$*AlbCre*$^{+}$ (triangles, $n = 9$), *Sdc1*$^{-/-}$*Ndst1*$^{f/f}$*AlbCre*$^{-}$ (open circles, $n = 7$), and *Ndst1*$^{f/f}$*AlbCre*$^{+}$ (squares, $n = 7$) mice, although all 3 genotypes were significantly elevated above the wild-type, *Ndst1*$^{f/f}$*AlbCre*$^{-}$ (closed circles, $n = 13$). Horizontal bars indicate mean values. (**B**) Retinol ester excursions were measured at the times indicated in wild-type (filled circles, $n = 3$), *Sdc1*$^{-/-}$ (open circles, $n = 3$), *Ndst1*$^{f/f}$*AlbCre*$^{+}$ (squares, $n = 3$), and *Sdc1*$^{-/-}$*Ndst1*$^{f/f}$*AlbCre*$^{+}$(triangles, $n = 3$) mice. Animals were fasted for 4 hours in the morning and given 200 μl of corn oil containing [^{3}H]retinol by gavage. Blood samples were taken at the indicated times, and radioactivity remaining in 10 μl of serum was determined by scintillation counting. The values are expressed as mean ± SD. The areas under the curves were 4,100 ± 1,200 for wild-type, 8,400 ± 300 for *Sdc1*$^{-/-}$, 8,300 ± 400 for *Ndst1*$^{f/f}$*AlbCre*$^{+}$, and 6,900 ± 1,000 for *Sdc1*$^{-/-}$*Ndst1*$^{f/f}$*AlbCre*$^{+}$ mice. Clearance was significantly delayed in the *Sdc1*$^{-/-}$ mice compared with wild-type ($P = 0.0034$), whereas the difference observed between *Sdc1*$^{-/-}$ and *Sdc1*$^{-/-}$*Ndst1*$^{f/f}$*AlbCre*$^{+}$ animals was not significant ($P = 0.1373$).

of cell protein in 1 hour, as measured by the appearance of acid-soluble, non-chloroform extractable ^{125}I counts in the growth medium. *Sdc1*$^{-/-}$ hepatocytes showed a dramatic decrease in both uptake (1.5 ± 0.4 μg VLDL/mg cell protein; $P < 0.005$) and degradation (0.4 ± 0.1 μg VLDL/mg cell protein; $P < 0.02$) under these conditions.

To confirm that altered uptake and degradation in *Sdc1*$^{-/-}$ hepatocytes resulted from loss of syndecan-1, we analyzed primary hepatocytes isolated from *Sdc1*$^{-/-}$ mice infected with AdSdc1 or AdGFP. AdSdc1-treated hepatocytes showed increased binding, uptake, and degradation of ^{125}I-VLDL compared with hepatocytes derived from mice treated with AdGFP (Figure 6B). Finally, we examined uptake and degradation in hepatocytes derived from mice deficient in LDLRs and in combination with a deficiency of Ndst1. As shown in Figure 6C, the LDLR contributes to binding and uptake, but to a lesser extent than syndecan-1. LDLR expression also was not altered in *Sdc1*$^{-/-}$ or *Ndst1*$^{f/f}$*AlbCre*$^{+}$ mice (Supplemental Figure 3B). Together, these data indicate that syndecan-1 accounts for the majority of ^{125}I-VLDL bound, taken up, and degraded by wild-type primary hepatic parenchymal cells.

Discussion

The major finding presented in this report is that syndecan-1 mediates hepatic clearance of TRLs in vivo. This conclusion is based on the observation that TRLs resembling VLDL and VLDL remnants accumulate in fasted *Sdc1*$^{-/-}$ mice (Figures 1 and 2) and that the mutant exhibits delayed clearance of TRLs derived from dietary fat (Figure 3). Importantly, syndecan-1 appears to be the principal hepatic HSPG involved in TRL clearance, since compounding the syndecan-1 deficiency with a mutation that affects sulfation of all heparan sulfate chains on hepatocyte HSPGs did not increase the extent of triglyceride accumulation (Figure 4). Syndecan-1, poised on the microvilli of hepatocytes (Supplemental Figure 4), can encounter circulating TRLs that enter the space of Disse. Binding to syndecan-1 showed saturability and inhibition by heparin (Figure 5), and increased expression of syndecan-1 by viral transduction corrected the deficiency in postprandial clearance in the mutant (Figure 3C) and enhanced the uptake and degradation of VLDL in isolated hepatocytes (Figure 6). Taken together, these data provide direct genetic evidence that syndecan-1 is the primary hepatic proteoglycan receptor mediating TRL clearance.

Our genetic studies of hepatic HSPGs extend previous observations showing that syndecans can mediate lipoprotein uptake in cultured cells. Fuki et al. introduced several syndecan core proteins into Chinese hamster ovary cells, which increased cell association and degradation of lipoproteins enriched in LPL, a protein that may mediate binding to the heparan sulfate chains on syndecan-1 (13). Subsequently, Zeng et al. showed by antisense and antibody inhibition that the uptake of chylomicron remnants by HepG2 liver cells was mediated in part by syndecan-1 (19). Uptake by cultured cells depends on the heparan sulfate chains, based on analysis of mutants altered in heparan sulfate biosynthesis, treatment of cells with heparinases that degrade the heparan sulfate chains, or pharmacological manipulation of glycosaminoglycan biosynthesis (34–42). Conversely, overexpression of human syndecan-1 increased binding and uptake of VLDL by human fibroblasts (15). The data presented here demonstrate that TRL binding and uptake in the liver occur by way of syndecan-1 and establish the physiologic relevance of those earlier findings.

Syndecan-1, first described by Bernfield and colleagues on mammary epithelial cells (43), is a transmembrane proteoglycan of

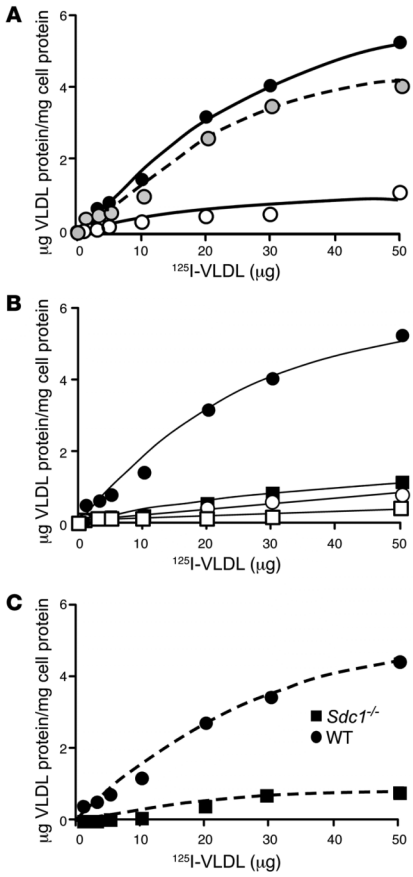

Figure 5
Syndecan-1 mediates binding of VLDL. (**A**) Wild-type cells were incubated with the indicated concentrations of ^{125}I-VLDL in the absence (filled circles) or presence (open circles) of 10 U heparin for 1 hour at 4°C. The amount of binding observed in the presence of heparin was subtracted from the total to obtain specific binding (dashed line, gray circles). (**B**) Wild-type (filled circles) and *Sdc1*$^{-/-}$ (filled squares) hepatocytes were incubated with the indicated concentrations of ^{125}I-VLDL for 1 hour at 4°C. A parallel set of cells was incubated under identical conditions with 250 μg/ml of non-radioactive VLDL. Addition of non-radioactive VLDL decreased binding in wild-type hepatocytes (open circles) to nearly the level measured in *Sdc1*$^{-/-}$ cells (open squares). (**C**) Deletion of syndecan-1 reduced maximal binding. The counts bound in the presence of excess non-radioactive VLDL in **B** were subtracted from the raw data, and the net counts were converted to μg VLDL protein bound/mg of cell protein, based on radiospecific activity of the particles (140 cpm/ng). Each data point represents the average of triplicate analyses, which varied by less than the height of the symbol.

diverse function that modulates cell adhesion and motility, growth factor activation, tumor growth, and microbial infection (43–49). Like other proteoglycans, syndecan undergoes endocytosis and degradation in lysosomes (50). Thus, ligands bound to the heparan sulfate chains can "piggy-back" into the cell (5), which operationally defines syndecan-1 as an endocytic receptor of broad specificity. Syndecan-1 also undergoes proteolytic processing, which results in shedding of ectodomains containing the attached glycosaminoglycan chains (51). Although, to our knowledge, the shedding process has not been studied in liver, cultured hepatocytes accumulate ectodomains in the conditioned medium (our unpublished observations). This finding raises the possibility that shed syndecan-1 ectodomains might bind plasma lipoproteins in the space of Disse and either prevent their escape back into the plasma or facilitate their further processing prior to uptake. The fact that compounding syndecan-1 deficiency with a mutation that affects all heparan sulfate chains produced by hepatocytes has no greater effect on lipoprotein clearance than either mutation alone (Figure 4) suggests that syndecan-1 might also be responsible for sequestration of lipoproteins in the space of Disse, as suggested previously (13, 19).

Syndecan-1 has 3 attachment sites for heparan sulfate clustered near its N terminus and up to 2 chondroitin sulfate chains located in the membrane proximal region, although the glycosaminoglycan content of liver syndecan-1 has not been determined. The binding of TRLs to the heparan sulfate chains presumably occurs through electrostatic interactions between negatively charged sulfate and carboxyl groups with complementary positively charged domains in the apolipoproteins (apoB and apoE) or lipases (LPL or hepatic lipase) associated with the particles. In general, only 8–12 monosaccharide residues are needed to bind to many proteins, including LPL and apoE (52–55), but the pattern of sulfate groups and uronic acids that mediate TRL binding is unknown. Liver heparan sulfate is unusual in that it is more highly sulfated than heparan sulfate in other tissues (54, 56, 57). Thus, the high degree of sulfation of the heparan sulfate chains in hepatocyte syndecan-1, compared with that of syndecan-1 in other tissues, might ensure selective binding of remnant lipoprotein particles to liver syndecan-1. Binding and/or internalization might depend on the multiple interactions between one or more chains on syndecan-1 or syndecan multimers with multiple protein ligands associated with the particles. Clustering of syndecan may in fact trigger internalization by endocytosis (13, 21).

The abundance of VLDL binding sites on isolated hepatocytes is also interesting. We estimate from saturation binding curves that wild-type cells express over 10^6 VLDL binding sites, and that syndecan-1 apparently accounts for the majority of them (Figure 5). At first glance, this finding would suggest that syndecan-1 should account for the majority of uptake and degradation of VLDL by hepatocytes. However, the rates of internalization of proteoglycans and other more classical receptors, such as LDLR, vary substantially. In cells that have been studied, endocytosis of syndecans occurs in a clathrin-independent manner with relatively slow kinetics ($t_{1/2}$ = 20–60 minutes) (15, 21, 58, 59) compared with clathrin-mediated uptake of ligands, e.g., uptake of lipoproteins by LDLRs ($t_{1/2}$ = 5–10 minutes) (60). LDLRs are much less abundant (~10^4 to 5×10^4 receptors/cell) than syndecan-1 receptors (~10^6 receptors/cell), but their faster rate of internalization might partially offset the higher level of expression of syndecan-1, resulting in perhaps comparable contribution to uptake and clearance. The fact that both *Ldlr*$^{-/-}$ and *Sdc1*$^{-/-}$ mice both accumulate plasma triglycerides suggests that neither receptor can fully compensate for each other (9), but the composition of the particles that accumulate in these mutants might differ. The quantitative contributions of these 2 receptors to clearance undoubtedly depends on the ligand (chylo-

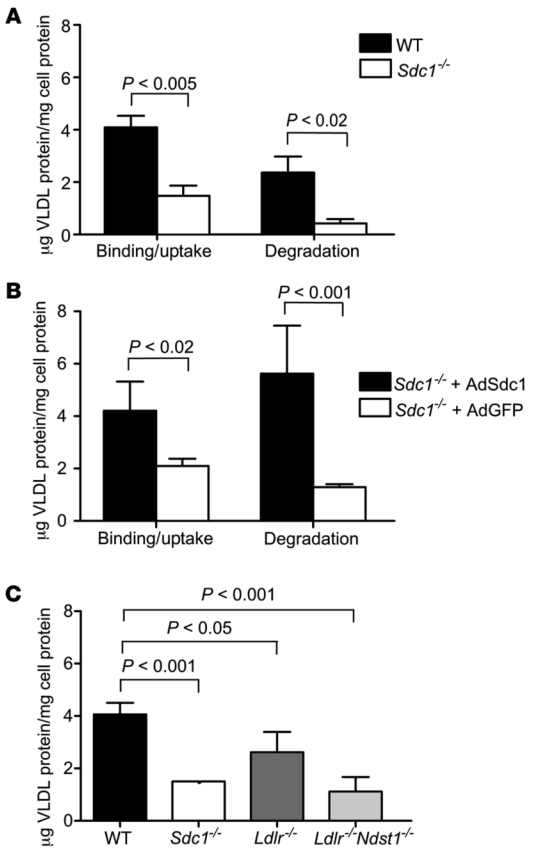

Figure 6
Binding, uptake, and degradation of VLDL at 37°C. (**A**) Uptake and degradation of VLDL was measured in wild-type and mutant hepatocytes after 1 hour of incubation with 20 μg/ml of ^{125}I-VLDL. The bars represent the sum of binding and internalization under these conditions, or the amount of degradation as determined by acid-soluble, non-chloroform–extractable counts in the medium. Binding plus uptake was reduced 2.7-fold in *Sdc1*$^{-/-}$ cells. Degradation was reduced by nearly 6-fold. (**B**) Hepatocytes isolated from *Sdc1*$^{-/-}$ mice treated with AdSdc1 showed enhanced binding and uptake and increased degradation of ^{125}I-VLDL compared with hepatocytes isolated from *Sdc1*$^{-/-}$ mice treated with AdGFP ($P < 0.02$). (**C**) Binding and uptake were also measured in hepatocytes isolated from wild-type, *Sdc1*$^{-/-}$, *Ldlr*$^{-/-}$, and *Ldlr*$^{-/-}$*Ndst1*$^{f/f}$*AlbCre*$^{+}$ mice. Uptake and binding were reduced 2-fold in the *Sdc1*$^{-/-}$ and *Ldlr*$^{-/-}$*Ndst1*$^{f/f}$*AlbCre*$^{+}$ hepatocytes compared with wild-type ($P < 0.001$), while a slight change was observed in *Ldlr*$^{-/-}$ compared with wild-type ($P < 0.05$).

micron remnants, VLDL, and LDL), their apolipoprotein compositions, their concentrations, and other factors. Additional studies of binding, uptake, and degradation in primary hepatocytes are underway to obtain more insight into this problem.

A third class of receptors, LDLR-related proteins (LRPs), have also been implicated in TRL clearance (61). LRP apparently can form a complex with HSPGs (62) and modulate their capacity to bind VLDL. However, inactivation of LRP1 or LRP5 in hepatocytes has no effect on fasting plasma triglyceride levels (61, 63), whereas inactivation of syndecan-1 increases plasma triglycerides, suggesting that syndecan-1 most likely acts independently of LRP receptors under these conditions. LRPs may aid in the metabolism of lipoproteins after dietary challenge or under conditions in which other receptors are occupied or rendered inoperative (61, 63). Sorting out the relative contribution of these receptors will require studies of various double mutants lacking syndecan-1, LDLR, and LRPs. It is also unknown whether these 3 receptors undergo coordinate regulation dependent on plasma triglyceride levels. Preliminary experiments show that the relative expression of mRNAs for LDLR and LRP1 in hepatocytes of *Sdc1*$^{-/-}$ mice is not elevated compared with transcripts in wild-type hepatocytes, and LDLR protein expression does not differ in wild-type, *Sdc1*$^{-/-}$, or *Ndst1*$^{f/f}$*AlbCre*$^{+}$ hepatocytes (Supplemental Figure 3B). However, this needs to be examined further in various paired mutants fed normal and high-fat diets.

A step-wise mechanism of binding remnants by syndecan-1 and hand-off to LDLR or LRP receptors has been proposed (6, 62). However, we showed previously that compounding *Ldlr*$^{-/-}$ with *Ndst1*$^{f/f}$*AlbCre*$^{+}$ mice causes an additive accumulation of plasma triglycerides and prolonged the delay in postprandial clearance manifested by each individual mutant (9). Compounding Ndst1 deficiency with *Sdc1*$^{-/-}$ does not result in additivity (Figure 4), which implies that the heparan sulfate chains on syndecan-1 are causally tied to the hyperlipidemia in *Sdc1*$^{-/-}$ mutants. By inference then, the heparan sulfate chains on syndecan-1 work independently of LDLR. Additional breeding experiments are underway to make *Ldlr*$^{-/-}$*Sdc1*$^{-/-}$ mice, to validate this interpretation of the data. At this time we cannot formally exclude a hand-off mechanism to LRPs, but inactivation of hepatic LRP1 in vivo does not result in reduced clearance of remnant lipoproteins (61), and preliminary data suggest that compounding mutations in Ndst1 and LRP1 does not cause higher plasma lipids than altering Ndst1 alone (our unpublished observations). Finally, a large body data indicates that proteoglycans can act as independent endocytic receptors for a variety of ligands, both natural and synthetic (5, 64, 65). Thus, we believe that the genetic data presented here and previously (9), coupled with numerous cell culture studies by other groups over the years (13–19, 21), argue for independent action of proteoglycans in the hepatic clearance of triglyceride-rich remnants.

In conclusion, we have determined that syndecan-1 acts as a primary receptor for remnant TRL clearance in the liver. While further work needs to be done to determine the relative contribution of syndecan-1 and other receptors to TRL clearance under different dietary conditions, the data presented here suggest that mutations affecting the expression of syndecan-1 or the assembly of the heparan sulfate chains might explain some forms of human dyslipidemias. Studies of patients with unexplained hypertriglyceridemia are underway to explore this possibility.

Methods

Mice and animal husbandry. Mice deficient in syndecan-1 (*Sdc1*$^{-/-}$, provided by P. Park, Harvard University, Cambridge, Massachusetts, USA), syndecan-3 (*Sdc3*$^{-/-}$, provided by P. Sanna, The Scripps Research Institute, La Jolla, California, USA), and syndecan–4 (*Sdc4*$^{-/-}$, provided by P. Goetinck, Harvard University, Cambridge, Massachusetts, USA) were described previously (26, 66–68). *Ndst1*$^{f/f}$*AlbCre*$^{+}$ mice were described by MacArthur et al. (9).

All mice were backcrossed more than 10 generations on a C57BL/6 background. All animals were housed and bred in vivaria approved by the Association for Assessment and Accreditation of Laboratory Animal Care located in the School of Medicine, UCSD, following standards and procedures approved by the UCSD IACUC. Mice were weaned at 3 weeks, maintained on a 12-hour-light/12-hour-dark cycle, and fed ad libitum with water and standard rodent chow (Harlan Teklad). Genotyping was performed as previously described (9, 66–68).

Hepatocyte isolation. Mouse hepatocytes were isolated essentially as previously described (69). Briefly, mice were anesthetized with isoflurane and perfused via cardiac puncture with 30 ml Krebs-Ringer solution containing 1 mM EDTA (37°C, 7.5 ml/min), followed by perfusion of 30 ml Krebs-Ringer containing 0.15 mM $CaCl_2$ and 0.5 mg/ml type I collagenase (Sigma-Aldrich). The liver was removed, cut into pieces, and chilled to 4°C in 40 ml of Krebs-Ringer solution. The tissue was dispersed by pipetting and filtered through a 70-μm nylon cell strainer (BD Falcon). The filtrate was centrifuged for 3 minutes at 50 *g* at 4°C, and the cell pellet was gently resuspended in fresh solution and centrifuged 2 more times. Cells were then resuspended in Williams media supplemented with 10% FBS and divided equally across the wells of a 6-well plate precoated with rat tail type I collagen (Sigma-Aldrich). After 3 hours, the medium was replaced with Williams medium supplemented with 10% FBS, 1% Insulin-Transferrin-Selenium (Gibco, Invitrogen), 10 μg/ml epidermal growth factor (Invitrogen), 0.1 μM dexamethazone, 4.4 μM nicotinamide, and 100 U/ml penicillin and 100 μg/ml streptomycin. All experiments with primary hepatocytes were completed within 48 hours of isolation.

Adenoviruses. AdSdc1 was a gift from Pyong Woo Park (Harvard Medical School, Cambridge, Massachusetts, USA) (70). AdSdc1 and AdGFP were amplified by the UCSD Vector Development Core Facility. Approximately 4×10^{11} particles in PBS (71) were injected via the tail vein (72). Mice were used after 3 weeks for the experimental procedures indicated in the text.

qRT-PCR of membrane HSPGs. Total RNAs from mouse, liver, heart, and brain were purchased from Ambion. RNA was isolated from purified hepatocytes from C57BL/6 mice as described previously (73). Samples were reverse transcribed (Superscript III; Invitrogen) and amplified using intron spanning primers (Supplemental Table 1). Quantitation was done by the $2^{-\Delta\Delta C_T}$ method using β-actin as control RNAs (74). C_T values from triplicate assays were used to calculate fold expression as compared with β-actin, according to the Stratagene manual. Results were verified in 3 independent assays.

Lipoprotein analysis. Plasma samples were prepared from blood drawn via retroorbital bleeding from mice fasted for 4–6 hours in the morning. Total cholesterol and triglyceride levels were determined enzymatically using an automated reader (Cobas Mira; Roche Diagnostics) and kits (Cholesterol High-Performance Reagent from Roche Diagnostics and Triglyceride-SL from Diagnostic Chemicals Ltd).

Lipoproteins were prepared from blood drawn by cardiac puncture using sequential preparative ultracentrifugation. TRLs (δ = 1.006 g/ml) were prepared from pooled plasma samples (n = 10 mice; volume, 5 ml) by centrifugation for 12 hours at 135,000 *g* in a Beckman 50.3Ti rotor. VLDL remnants and IDL were then collected as the δ = 1.006–1.019 g/ml fraction. LDL and HDL were subsequently collected as the δ = 1.019–1.063 and δ = 1.063–1.21 g/ml fractions, respectively. The isolated lipoproteins were dialyzed against PBS and analyzed for lipid content using kits. Plasma lipoproteins were also separated by gel filtration FPLC. Pooled plasma samples were loaded on a Superose 12 FPLC column (Amersham Biosciences) in 0.15 M sodium chloride containing 1 mM EDTA and 0.02% sodium azide, pH 7.4, and 0.25-ml fractions were collected (0.1 ml/min). Equal volumes of the δ < 1.006 g/ml float fraction were concentrated on the Microcon-30s (Millipore), and proteins were resolved by SDS-PAGE on 4%–15% Ready Gels (Bio-Rad). Proteins were visualized by Coomassie blue and silver staining.

VLDL plasma clearance. Human VLDL (δ < 1.006 g/ml) was isolated by ultracentrifugation from healthy, fasting volunteers. All volunteers gave informed consent, as required by the UCSD IACUC. Mice were fasted for 6 hours and injected with 10 μg human VLDL protein via the tail vein. Serial samples were taken by retroorbital bleeds at the indicated times. The amount of human VLDL remaining in the plasma was determined by sandwich ELISA, utilizing mAb MB47 specific for human apoB-100 (75). MB47 does not bind to murine apoB-100, and therefore it can be used to trace the clearance of injected human VLDL. U-bottom 96-well plates were coated overnight with MB47 at 5 μg/ml in Tris-buffered saline, followed by addition of nonsaturating amounts of plasma (typically, 1:100 dilution of mouse plasma) to capture human VLDL. Bound VLDL was detected using biotinylated goat anti-human apoB-100 (BIODESIGN International), followed by alkaline phosphatase–labeled neutrAvidin (Pierce Biotechnology). Plates were developed with Lumi-Phos 530 (Lumigen) and read in a DYNEX Technologies MLX Microtiter Plate Luminometer.

Vitamin A excursion studies. Clearance of chylomicrons derived from dietary triglyceride was measured by Vitamin A excursion essentially as described (24). Briefly, 27 μCi of [11,12-^{3}H]-retinol (PerkinElmer; 44.4 Ci/mmol) in ethanol was mixed with 1 ml of corn oil (Sigma-Aldrich) and administered by oral gavage (200 μl/mouse). Retroorbital sinus blood was sampled at the times indicated, and radioactivity was measured in triplicate (10 μl of serum) by scintillation counting. Triglycerides were measured enzymatically using a plate reader and kits.

Immunofluorescence microscopy. Livers were perfused at 7 ml/min with 30 ml of PBS/EDTA followed by 30 ml of 4% paraformaldehyde. Livers were snap-frozen, and 20-μm sections were cut on a cryostat. Sections were plated on glass coverslips precoated with laminin (2 μg/cm^2). They were then fixed with 2% paraformaldehyde in PBS for 10 minutes at room temperature, incubated for 10 minutes with 100 mM glycine, pH 7.4, to quench aldehyde groups, permeabilized in 0.1 % Triton X-100 for 10 minutes, blocked for 20 minutes with a solution of 1% BSA and 0.05% Tween in PBS, and then incubated for 2 hours at room temperature with primary antibodies (syndecan-1, 1:250; syndecan-2, 1:250; syndecan-4, 1:100) in blocking solution. Rabbit polyclonal antibodies raised against the various syndecans were a gift of A. Rapraeger (University of Wisconsin, Madison, Wisconsin, USA). Excess antibody was removed by incubation for 15 minutes with 0.1% Tween in PBS. Samples were then incubated for 1 hour with Alexa Fluor 594–conjugated goat anti-rabbit secondary antibody (1:250; Invitrogen) and then washed 6 times at 5-minute intervals with 0.1% Tween in PBS and incubated for 20 minutes with the nuclear stain DAPI (1:5,000) diluted in PBS. Images were captured with a DeltaVision Restoration microscope system (AppliedPrecision) using a Photometrics Sony CoolSAP HQ charge-coupled device camera system attached to an inverted, wide-field fluorescence microscope (Nikon TE200). Optical sections were acquired using a ×63 Nikon (NA 1.3) oil-immersion objective in 0.2-μm steps on the z axis. Fluorescence was detected using a standard DAPI and Texas Red filter set. Images were saved, processed, and analyzed on SGI workstations (O2; Octane) using the DeltaVision software package softWoRx (version 2.50). Quantification of fluorescence was accomplished using only the linear range of the digital camera.

Immunogold electron microscopy. Samples were fixed in 4% paraformaldehyde in 10 mM phosphate buffer, pH 7.4, cryoprotected, and frozen in liquid nitrogen. Ultrathin cryosections were cut at 4°C using a Leica Ultracut UCT Microtome with an EMFCS cryoattachment (Leica) and placed on glow-discharged nickel grids. Samples were stored on 2% gelatin in PBS at 4°C and incubated with rabbit anti-mouse syndecan-1 polyclonal antibody followed by goat anti-rabbit IgG conjugated to 5- or

10-nm gold particles (Amersham Biosciences) in PBS supplemented with 10% FBS. Grids were absorption-stained with 0.2% neutral uranyl acetate, 0.2% methylcellulose, and 3.2% polyvinyl alcohol. Images were obtained using a JEOL 1200EX II transmission electron microscope and photographed using a Gatan digital camera.

Lipoprotein binding and uptake by hepatocytes. Human VLDL (δ < 1.006 g/ml, ~1.1 mg protein) was iodinated using 3 mCi of $Na^{125}I$ (NEN, PerkinElmer) using Iodogen (76). Under these conditions, the final radiospecific activity was 1.4×10^2 cpm/ng and 13% of the label was lipid soluble. Isolated hepatocytes were treated with the indicated concentration of ^{125}I-VLDL in DMEM media with 2.5 mg/ml lipoprotein-free serum (Biomedical Technologies Inc.). Cells were incubated at 4°C or 37°C for 1 hour, rinsed 3 times with PBS, and then solubilized with 0.1 M sodium hydroxide. Protein concentration was determined by Bradford assay (BioRad), and radioactivity was measured by γ counting. Degradation of ^{125}I-VLDL was measured by precipitation of 0.25 ml of conditioned media with an equal volume of 50% trichloroacetic acid (16). After 30 minutes at 4°C, the samples were centrifuged for 30 minutes. The supernatant was placed in a fresh glass tube, and 5 μl of 40% potassium iodide was added as a carrier. Hydrogen peroxide (30%) was added, and lipid-soluble material was extracted by the addition of 2 ml of chloroform. An aliquot of the upper aqueous phase containing iodotyrosine was counted as measure of degradation.

Porcine intestinal heparin (M_r = 12,000–15,000, 180 U/mg) was a gift from P. Shaklee (Scientific Protein Laboratories Inc., Waunakee, Wisconsin, USA). In competition experiments, wild-type hepatocytes were treated simultaneously with varying concentrations of heparin and ^{125}I-VLDL and incubated at 4°C for 1 hour. The signal obtained in the presence of heparin was subtracted from the total binding in order to calculate specific binding.

Statistics. Statistical analyses were performed using PRISM (GraphPad Software). All data are expressed as mean values ± SD unless otherwise indicated. Significance was determined using an unpaired Student's (2-tailed) *t* test or ANOVA with Bonferroni post-hoc analysis. Significance was taken as $P < 0.05$.

Acknowledgments

We would like to thank Joseph Juliano, Fely Alamazen, and Jennifer Pattison at UCSD and David Ditto of the Hematology/Coagulation/Chemistry Core, UCSD, for excellent technical assistance. This work was supported by NIH grants GM33063 and HL57345 (to J.D. Esko) and HL088093 (to J.L. Witztum) and by the Leducq Foundation (to J.L. Witztum) and a Scientist Development Grant from the American Heart Association (to J.R. Bishop).

Received for publication December 5, 2008, and accepted in revised form July 29, 2009.

Address correspondence to: Jeffrey D. Esko, Department of Cellular and Molecular Medicine, University of California, San Diego, La Jolla, California 92093-0687, USA. Phone: (858) 822-1100; Fax: (858) 534-5611; E-mail: jesko@ucsd.edu.

1. Nordestgaard, B.G., Benn, M., Schnohr, P., and Tybjaerg-Hansen, A. 2007. Nonfasting triglycerides and risk of myocardial infarction, ischemic heart disease, and death in men and women. *JAMA.* **298**:299–308.
2. Bansal, S., et al. 2007. Fasting compared with nonfasting triglycerides and risk of cardiovascular events in women. *JAMA.* **298**:309–316.
3. Beigneux, A.P., et al. 2007. Glycosylphosphatidylinositol-anchored high-density lipoprotein-binding protein 1 plays a critical role in the lipolytic processing of chylomicrons. *Cell Metab.* **5**:279–291.
4. Young, S.G., et al. 2007. GPIHBP1: an endothelial cell molecule important for the lipolytic processing of chylomicrons. *Curr. Opin. Lipidol.* **18**:389–396.
5. Williams, K.J., and Fuki, I.V. 1997. Cell-surface heparan sulfate proteoglycans: dynamic molecules mediating ligand catabolism. *Curr. Opin. Lipidol.* **8**:253–262.
6. Mahley, R.W., and Ji, Z.S. 1999. Remnant lipoprotein metabolism: key pathways involving cell-surface heparan sulfate proteoglycans and apolipoprotein E. *J. Lipid Res.* **40**:1–16.
7. Mahley, R.W., and Huang, Y. 2007. Atherogenic remnant lipoproteins: role for proteoglycans in trapping, transferring, and internalizing. *J. Clin. Invest.* **117**:94–98.
8. Williams, K.J. 2008. Molecular processes that handle — and mishandle — dietary lipids. *J. Clin. Invest.* **118**:3247–3259.
9. MacArthur, J.M., et al. 2007. Liver heparan sulfate proteoglycans mediate clearance of triglyceride-rich lipoproteins independently of LDL receptor family members. *J. Clin. Invest.* **117**:153–164.
10. Bishop, J.R., Stanford, K.I., and Esko, J.D. 2008. Heparan sulfate proteoglycans and triglyceride-rich lipoprotein metabolism. *Curr. Opin. Lipidol.* **19**:307–313.
11. Shintani, Y., et al. 2006. Glycosaminoglycan modification of neuropilin-1 modulates VEGFR2 signaling. *EMBO J.* **25**:3045–3055.
12. Bishop, J.R., Schuksz, M., and Esko, J.D. 2007. Heparan sulphate proteoglycans fine-tune mammalian physiology. *Nature.* **446**:1030–1037.
13. Fuki, I.V., et al. 1997. The syndecan family of proteoglycans. Novel receptors mediating internalization of atherogenic lipoproteins in vitro. *J. Clin. Invest.* **100**:1611–1622.
14. Fuki, I.V., Iozzo, R.V., and Williams, K.J. 2000. Perlecan heparan sulfate proteoglycan - A novel receptor that mediates a distinct pathway for ligand catabolism. *J. Biol. Chem.* **275**:25742–25750.
15. Wilsie, L.C., Gonzales, A.M., and Orlando, R.A. 2006. Syndecan-1 mediates internalization of apoE-VLDL through a low density lipoprotein receptor-related protein (LRP)-independent, nonclathrin-mediated pathway. *Lipids Health Dis.* **5**:23.
16. Williams, K.J. 2001. Interactions of lipoproteins with proteoglycans. *Methods Mol. Biol.* **171**:457–477.
17. Ebara, T., et al. 2000. Delayed catabolism of apoB-48 lipoproteins due to decreased heparan sulfate proteoglycan production in diabetic mice. *J. Clin. Invest.* **105**:1807–1818.
18. Tran-Lundmark, K., et al. 2008. Heparan sulfate in perlecan promotes mouse atherosclerosis: roles in lipid permeability, lipid retention, and smooth muscle cell proliferation. *Circ. Res.* **103**:43–52.
19. Zeng, B.J., Mortimer, B.C., Martins, I.J., Seydel, U., and Redgrave, T.G. 1998. Chylomicron remnant uptake is regulated by the expression and function of heparan sulfate proteoglycan in hepatocytes. *J. Lipid Res.* **39**:845–860.
20. Yu, K.C., Chen, W., and Cooper, A.D. 2001. LDL receptor-related protein mediates cell-surface clustering and hepatic sequestration of chylomicron remnants in LDLR-deficient mice. *J. Clin. Invest.* **107**:1387–1394.
21. Fuki, I.V., Meyer, M.E., and Williams, K.J. 2000. Transmembrane and cytoplasmic domains of syndecan mediate a multi-step endocytic pathway involving detergent-insoluble membrane rafts. *Biochem. J.* **351**:607–612.
22. Cortes, V., et al. 2007. Adenovirus-mediated hepatic syndecan-1 overexpression induces hepatocyte proliferation and hyperlipidaemia in mice. *Liver Int.* **27**:569–581.
23. Weiner, O.H., Zoremba, M., and Gressner, A.M. 1996. Gene expression of syndecans and betaglycan in isolated rat liver cells. *Cell Tissue Res.* **285**:11–16.
24. Ishibashi, S., et al. 1996. Role of the low density lipoprotein (LDL) receptor pathway in the metabolism of chylomicron remnants. A quantitative study in knockout mice lacking the LDL receptor, apolipoprotein E, or both. *J. Biol. Chem.* **271**:22422–22427.
25. Horton, J.D., et al. 1999. Disruption of LDL receptor gene in transgenic SREBP-1a mice unmasks hyperlipidemia resulting from production of lipid-rich VLDL. *J. Clin. Invest.* **103**:1067–1076.
26. Alexander, C.M., et al. 2000. Syndecan-1 is required for Wnt-1-induced mammary tumorigenesis in mice. *Nat. Genet.* **25**:329–332.
27. Hirano, T., et al. 2001. Apoprotein C-III deficiency markedly stimulates triglyceride secretion in vivo: comparison with apoprotein E. *Am. J. Physiol. Endocrinol. Metab.* **281**:E665–E669.
28. Weinstein, M.M., et al. 2008. Abnormal patterns of lipoprotein lipase release into the plasma in GPIHBP1-deficient mice. *J. Biol. Chem.* **283**:34511–34518.
29. Ishibashi, S., et al. 1993. Hypercholesterolemia in low density lipoprotein receptor knockout mice and its reversal by adenovirus-mediated gene delivery. *J. Clin. Invest.* **92**:883–893.
30. Hayashi, K., et al. 1987. Immunocytochemistry of cell surface heparan sulfate proteoglycan in mouse tissues. A light and electron microscopic study. *J. Histochem. Cytochem.* **35**:1079–1088.
31. Roskams, T., et al. 1995. Heparan sulfate proteoglycan expression in normal human liver. *Hepatology.* **21**:950–958.
32. Higazi, A.A., et al. 2000. The alpha-defensins stimulate proteoglycan-dependent catabolism of low-density lipoprotein by vascular cells: a new class of inflammatory apolipoprotein and a possible contributor to atherogenesis. *Blood.* **96**:1393–1398.
33. Anisfeld, A.M., et al. 2003. Syndecan-1 expression is regulated in an isoform-specific manner by the farnesoid-X receptor. *J. Biol. Chem.* **278**:20420–20428.
34. Williams, K.J., et al. 1992. Mechanisms by which lipoprotein lipase alters cellular metabolism of lipoprotein(a), low density lipoprotein, and nascent lipoproteins. Roles for low density lipoprotein

receptors and heparan sulfate proteoglycans. *J. Biol. Chem.* **267**:13284–13292.
35. Ji, Z.S., et al. 1993. Role of heparan sulfate proteoglycans in the binding and uptake of apolipoprotein E-enriched remnant lipoproteins by cultured cells. *J. Biol. Chem.* **268**:10160–10167.
36. Feussner, G., et al. 1996. Apolipoprotein E5 (Glu_{212}-->Lys): Increased binding to cell surface proteoglycans but decreased uptake and lysosomal degradation in cultured fibroblasts. *J. Lipid Res.* **37**:1632–1645.
37. Krapp, A., et al. 1996. Hepatic lipase mediates the uptake of chylomicrons and β-VLDL into cells via the LDL receptor-related protein (LRP). *J. Lipid Res.* **37**:926–936.
38. Al-Haideri, M., et al. 1997. Heparan sulfate proteoglycan-mediated uptake of apolipoprotein E-triglyceride-rich lipoprotein particles: a major pathway at physiological particle concentrations. *Biochemistry.* **36**:12766–12772.
39. Huff, M.W., et al. 1997. Uptake of hypertriglyceridemic very low density lipoproteins and their remnants by HepG2 cells: the role of lipoprotein lipase, hepatic triglyceride lipase, and cell surface proteoglycans. *J. Lipid Res.* **38**:1318–1333.
40. Ji, Z.S., Pitas, R.E., and Mahley, R.W. 1998. Differential cellular accumulation/retention of apolipoprotein E mediated by cell surface heparan sulfate proteoglycans. Apolipoproteins E3 and E2 greater than e4. *J. Biol. Chem.* **273**:13452–13460.
41. Seo, T., et al. 2000. Lipoprotein lipase-mediated selective uptake from low density lipoprotein requires cell surface proteoglycans and is independent of scavenger receptor class B type 1. *J. Biol. Chem.* **275**:30355–30362.
42. Medh, J.D., et al. 2000. Lipoprotein lipase- and hepatic triglyceride lipase- promoted very low density lipoprotein degradation proceeds via an apolipoprotein E-dependent mechanism. *J. Lipid Res.* **41**:1858–1871.
43. Bernfield, M., et al. 1992. Biology of the syndecans: a family of transmembrane heparan sulfate proteoglycans. *Annu. Rev. Cell Biol.* **8**:365–393.
44. Bernfield, M., et al. 1999. Functions of cell surface heparan sulfate proteoglycans. *Annu. Rev. Biochem.* **68**:729–777.
45. Park, P.W., Reizes, O., and Bernfield, M. 2000. Cell surface heparan sulfate proteoglycans: Selective regulators of ligand-receptor encounters. *J. Biol. Chem.* **275**:29923–29926.
46. Bellin, R., et al. 2002. Unlocking the secrets of syndecans: Transgenic organisms as a potential key. *Glycoconj. J.* **19**:295–304.
47. Sanderson, R.D., and Yang, Y. 2008. Syndecan-1: a dynamic regulator of the myeloma microenvironment. *Clin. Exp. Metastasis.* **25**:149–159.
48. Bartlett, A.H., Hayashida, K., and Park, P.W. 2007. Molecular and cellular mechanisms of syndecans in tissue injury and inflammation. *Mol. Cells.* **24**:153–166.
49. Tumova, S., Woods, A., and Couchman, J.R. 2000. Heparan sulfate proteoglycans on the cell surface: versatile coordinators of cellular functions. *Int. J. Biochem. Cell Biol.* **32**:269–288.
50. Burbach, B.J., Friedl, A., Mundhenke, C., and Rapraeger, A.C. 2003. Syndecan-1 accumulates in lysosomes of poorly differentiated breast carcinoma cells. *Matrix Biol.* **22**:163–177.
51. Fitzgerald, M.L., Wang, Z.H., Park, P.W., Murphy, G., and Bernfield, M. 2000. Shedding of syndecan-1 and-4 ectodomains is regulated by multiple signaling pathways and mediated by a TIMP-3-sensitive metalloproteinase. *J. Cell Biol.* **148**:811–824.
52. Parthasarathy, N., et al. 1994. Oligosaccharide sequences of endothelial cell surface heparan sulfate proteoglycan with affinity for lipoprotein lipase. *J. Biol. Chem.* **269**:22391–22396.
53. Spillmann, D., Lookene, A., and Olivecrona, G. 2006. Isolation and characterization of low sulfated heparan sulfate sequences with affinity for lipoprotein lipase. *J. Biol. Chem.* **281**:23405–23413.
54. Libeu, C.P., et al. 2001. New insights into the heparan sulfate proteoglycan-binding activity of apolipoprotein E. *J. Biol. Chem.* **276**:39138–39144.
55. Dong, J., et al. 2001. Interaction of the N-terminal domain of apolipoprotein E4 with heparin. *Biochemistry.* **40**:2826–2834.
56. Lyon, M., Deakin, J.A., and Gallagher, J.T. 1994. Liver heparan sulfate structure. A novel molecular design. *J. Biol. Chem.* **269**:11208–11215.
57. Vongchan, P., et al. 2005. Structural characterization of human liver heparan sulfate. *Biochim. Biophys. Acta.* **1721**:1–8.
58. Thankamony, S.P., and Knudson, W. 2006. Acylation of CD44 and its association with lipid rafts are required for receptor and hyaluronan endocytosis. *J. Biol. Chem.* **281**:34601–34609.
59. Tkachenko, E., Lutgens, E., Stan, R.V., and Simons, M. 2004. Fibroblast growth factor 2 endocytosis in endothelial cells proceed via syndecan-4-dependent activation of Rac1 and a Cdc42-dependent macropinocytic pathway. *J. Cell Sci.* **117**:3189–3199.
60. Brown, M.S., Anderson, R.G., and Goldstein, J.L. 1983. Recycling receptors: the round-trip itinerary of migrant membrane proteins. *Cell.* **32**:663–667.
61. Rohlmann, A., Gotthardt, M., Hammer, R.E., and Herz, J. 1998. Inducible inactivation of hepatic LRP gene by cre-mediated recombination confirms role of LRP in clearance of chylomicron remnants. *J. Clin. Invest.* **101**:689–695.
62. Wilsie, L.C., and Orlando, R.A. 2003. The low density lipoprotein receptor-related protein complexes with cell surface heparan sulfate proteoglycans to regulate proteoglycan-mediated lipoprotein catabolism. *J. Biol. Chem.* **278**:15758–15764.
63. Magoori, K., et al. 2003. Severe hypercholesterolemia, impaired fat tolerance, and advanced atherosclerosis in mice lacking both low density lipoprotein receptor-related protein 5 and apolipoprotein E. *J. Biol. Chem.* **278**:11331–11336.
64. Belting, M. 2003. Heparan sulfate proteoglycan as a plasma membrane carrier. *Trends Biochem. Sci.* **28**:145–151.
65. Elson-Schwab, L., et al. 2007. Guanidinylated neomycin delivers large, bioactive cargo into cells through a heparan sulfate-dependent pathway. *J. Biol. Chem.* **282**:13585–13591.
66. Park, P.W., Pier, G.B., Hinkes, M.T., and Bernfield, M. 2001. Exploitation of syndecan-1 shedding by Pseudomonas aeruginosa enhances virulence. *Nature.* **411**:98–102.
67. Reizes, O., et al. 2001. Transgenic expression of syndecan-1 uncovers a physiological control of feeding behavior by syndecan-3. *Cell.* **106**:105–116.
68. Echtermeyer, F., et al. 2001. Delayed wound repair and impaired angiogenesis in mice lacking syndecan-4. *J. Clin. Invest.* **107**:R9–R14.
69. Seglen, P.O. 1976. Preparation of isolated rat liver cells. *Methods Cell Biol.* **13**:29–83.
70. Hayashida, K., Johnston, D.R., Goldberger, O., and Park, P.W. 2006. Syndecan-1 expression in epithelial cells is induced by transforming growth factor beta through a PKA-dependent pathway. *J. Biol. Chem.* **281**:24365–24374.
71. Dulbecco, R., and Vogt, M. 1954. Plaque formation and isolation of pure cell lines with poliomyelitis viruses. *J. Exp. Med.* **99**:167–182.
72. Rohlmann, A., Gotthardt, M., Willnow, T.E., Hammer, R.E., and Herz, J. 1996. Sustained somatic gene inactivation by viral transfer of Cre recombinase. *Nat. Biotechnol.* **14**:1562–1565.
73. Bishop, J.R., and Esko, J.D. 2005. The elusive role of heparan sulfate in Toxoplasma gondii infection. *Mol. Biochem. Parasitol.* **139**:267–269.
74. Livak, K.J., and Schmittgen, T.D. 2001. Analysis of relative gene expression data using real-time quantitative PCR and the 2(-Delta Delta C(T)) Method. *Methods.* **25**:402–408.
75. Young, S.G., Smith, R.S., Hogle, D.M., Curtiss, L.K., and Witztum, J.L. 1986. Two new monoclonal antibody-based enzyme-linked assays of apolipoprotein B. *Clin. Chem.* **32**:1484–1490.
76. Salacinski, P.R., McLean, C., Sykes, J.E., Clement-Jones, V.V., and Lowry, P.J. 1981. Iodination of proteins, glycoproteins, and peptides using a solid-phase oxidizing agent, 1,3,4,6-tetrachloro-3 alpha,6 alpha-diphenyl glycoluril (Iodogen). *Anal. Biochem.* **117**:136–146.

Supplemental Table S1. Primers used for qPCR analysis

HSPG	Primer Sequence
Syndecan 1	5′ A G G A T G G A A C T G C C A A T C A G 3′ A T C C G G T A C A G C A T G A A A G C
Syndecan 2	5′ T C T G A G G C A G A A G A G A A G C T G 3′ A G G A T G A G G A A A A T G G C A A A
Syndecan 3	5′ A T A C T G G A G C G G A A G G A G G T 3′ T T T C T G G T A C G T G A C G C T T G
Syndecan 4	5′ A A C C A C A T C C C T G A G A A T G C 3′ A G G A A A A C G G C A A A G A G G A T
Glypican 1	5′ G G C C A T C A T G A A G T T G G T C T 3′ A C A C C G C C A A T G A C A C T C T C
Glypican 2	5′ T G A A T G A G C A G C T C C A C A A A C 3′ T C G T C T G C A T A C T G C T G T C C
Glypican 3	5′ T G T G C C C A A G G G T A A A G T T C 3′ A G G T G G T G A T C T C G T T G T C C
Glypican 4	5′ C G T T T G C A A T G A T G A G A G G A 3′ G C C A T G A T C T G A C G A A G G A T
Glypican 5	5′ A G A T G G C T G T G G A G G A T C A G 3′ G A C T C A G T T C C T G A C G C A C A
Glypican 6	5′ G T G C C A C G G A A A C T G A A G A T 3′ G G C C G A A G A T T C C T C T T C T C
Betaglycan	5′ G C A G A A T A A G A A G A C 3′ C T T G C T G C C T T C G T G C
CD44	5′ G C C T C A A C T G T G C A C T C A A A 3′ C A G C C T G T T G G G T T G G G T A T T 5′ G A T G A C C A C C C C T G A A A C A C 3′ T C A T C A A T G C C T G A T C C A G A

Supplemental Figure Legends

Supplemental Figure S1. Triglyceride Secretion. After a 6 hour fast, triglyceride secretion rate (TGSR) was determined by the method described by Hirano et al. (1). Briefly, Triton WR-1339 (0.5 mg per gm body weight of (Sigma) was injected via tail vein, and triglyceride concentrations were measured in plasma samples taken pre-injection, and 0.5, 1, 1.5, 2, and 24 hours post-injection. TGSR was calculated from the increment in triglyceride concentration per min multiplied by the plasma volume of the mouse (estimated by 0.035% of body weight in g) and expressed in mg/min. The rates did not differ significantly between *Sdc1*$^{-/-}$ (0.51 $\pm$ 0.11 mg/min; n = 3) and wild-type (0.38 $\pm$ 0.07; n = 3), P = 0.63.

Supplemental Figure S2. Syndecan-1 expression and lipolytic activity in adipose tissue. **(A)** Lipolytic activity was measured as previously described (4) in extracts of gonadal adipose tissue (5) homogenized in RIPA buffer. Samples were centrifuged at 4^{o}C for 10 min at 1000 x g on a tabletop centrifuge. An aliquot of the supernatant was mixed with 100 µL of [^{3}H]triolein. Samples were then incubated at 37^{o}C for 30 min. The reaction was stopped by the addition of 3.25 mL of methanol/chloroform/heptane (1.4:1.25:1, v/v). Free fatty acids were extracted through addition of 0.1M borate-potassium carbonate buffer (pH 10.5). After centrifugation, the upper phase (1 mL) was removed and counted. Activity was determined as units of activity per gram of wet weight of the tissue (1 U = 1 µmol/min). No difference in activity was observed (P = 0.37). **(B)** Proteoglycans were isolated from gonadal fat pads according to a protocol adapted from Reizes et al (2). Proteoglycans in the supernatants were collected by anion-exchange chromatography (DEAE-Sephacel) and digested for 1 hr with a mixture of 2 mU/ml of heparin lyases I and II and 5 mU/ml of heparin lyase III and chondroitinase ABC. Syndecan-1 was detected with mAb 281-2 and goat anti-rat IgG conjugated to HRP. Two bands were detected as indicated by the arrows, a 69 kDa form representing syndecan-1 and a 140 kDa band

representing most likely a dimer (3). The membrane was stripped and reprobed with mAb 3G10, which reacts with the glycan stubs remaining after heparinase digestion. mAb 3G10 was detected with a goat anti-rat !gG conjugated to HRP.

Supplemental Figure S3. Syndecan-1 and LDLR expression. (A) Syndecan-1 expression in control and AdSdc1 infected livers. Hepatocytes were isolated from *Sdc1*$^{-/-}$ mice treated with AdSdc1 or AdGFP three weeks after intravenous virus injection. Equal volumes of hepatocyte lysate were loaded on NuPAGE gradient gels (4-15%). Western blots were performed by transfer of the gel to 0.45 μm nitrocellulose (NuPAGE) using a wet transfer apparatus in NuPAGE transfer buffer. Membranes were blocked in Superblock (Pierce) for 1 hour, then incubated overnight at 4°C with mAb 281-2 or rabbit polyclonal anti-ERK (1:1000, Cell Signaling Technology). Membranes were washed and incubated with HRP-conjugated secondary antibody, washed and developed with ECL West Pico SuperSignal Reagents (Pierce). **(B) LDLR expression.** Equal volumes of hepatocyte lysate from wild-type, *Ndst1*$^{f/f}$*AlbCre*$^{+}$, *Sdc1*$^{-/-}$, and *Ldlr*$^{-/-}$ mice were separated by SDS-PAGE and Western blotted as described in panel A, using rabbit polyclonal anti-LDLR (1:2500, a kind gift from Dr. Jay Horton, University of Texas, Southwestern) or rabbit polyclonal anti-β-actin (1:1000, Cell Signaling Technology).

Supplemental Figure S4. Syndecan-1 localization in the liver. (A) Immunofluorescence micrographs of wild-type and **(B)** *Sdc1*$^{-/-}$ livers stained with rabbit polyclonal antibody to syndecan-1 and goat anti-rabbit secondary antibody conjugated to Alexa fluor-594 (red). Nuclei were stained with DAPI (blue). Syndecan-1 was localized around the sinusoids (H, hepatocytes, S, sinusoid). The antiserum was specific for syndecan-1 based on the absence of staining in sections from *Sdc1*$^{-/-}$ livers. Images were captured with a DeltaVision Restoration microscope system (AppliedPrecision) using a Photometrics Sony CoolSAP HQ charge-coupled device

(CCD) camera system attached to an inverted, wide-field fluorescence microscope (Nikon TE200). Optical sections were acquired using a 63x Nikon (NA 1.3) oil immersion objective in 0.2-μm steps in the *z*-axis. (**C)** The pattern of staining was similar in wild-type and *Ndst1*$^{f/f}$*AlbCre*$^{+}$ mice, indicating that alteration of the sulfation pattern on the chains did not affect syndecan-1 expression or localization. **(D)** Electron microscopy of immunogold-labeled sections revealed syndecan-1 on the microvilli extending from the basal surface of the hepatocytes. Bar = 0.5 μ. The area outlined by the box in the center was magnified 1.8X in the inset in the lower right. The images shows syndecan-1 expression restricted to the microvilli of the basal membrane facing the space of Disse, as observed previously (6,7).

References

1. Hirano, T., Takahashi, T., Saito, S., Tajima, H., Ebara, T., and Adachi, M. 2001. Apoprotein C-III deficiency markedly stimulates triglyceride secretion in vivo: comparison with apoprotein E. *Am J Physiol Endocrinol Metab* 281:E665-669.
2. Reizes, O., Lincecum, J., Wang, Z., Goldberger, O., Huang, L., Kaksonen, M., Ahima, R., Hinkes, M.T., Barsh, G.S., Rauvala, H., et al. 2001. Transgenic expression of syndecan-1 uncovers a physiological control of feeding behavior by syndecan-3. *Cell* 106:105-116.
3. Sanderson, R.D., Hinkes, M.T., and Bernfield, M. 1992. Syndecan-1, a cell-surface proteoglycan, changes in size and abundance when keratinocytes stratify. *J Invest Dermatol* 99:390-396.
4. Briquet-Laugier, V., Ben-Zeev, O., and Doolittle, M.H. 1999. Determining lipoprotein lipase and hepatic lipase activity using radiolabeled substrates. *Methods Mol Biol* 109:81-94.
5. Bergo, M., Olivecrona, G., and Olivecrona, T. 1996. Forms of lipoprotein lipase in rat tissues: in adipose tissue the proportion of inactive lipase increases on fasting. *Biochem J* 313 (Pt 3):893-898.
6. Hayashi, K., Hayashi, M., Jalkanen, M., Firestone, J.H., Trelstad, R.L., and Bernfield, M. 1987. Immunocytochemistry of cell surface heparan sulfate proteoglycan in mouse tissues. A light and electron microscopic study. *J.Histochem.Cytochem.* 35:1079-1088.
7. Roskams, T., Moshage, H., De Vos, R., Guido, D., Yap, P., and Desmet, V. 1995. Heparan sulfate proteoglycan expression in normal human liver. *Hepatology* 21:950-958.

Stanford et al. Supplemental Fig. S1

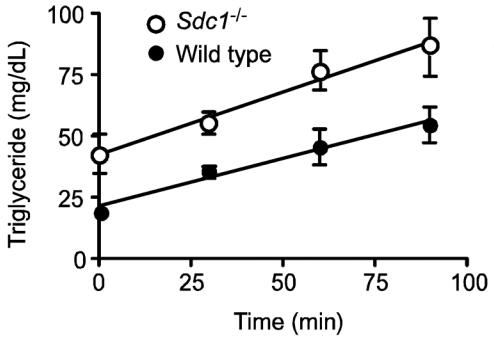

Stanford et al. Supplemental Fig. S2

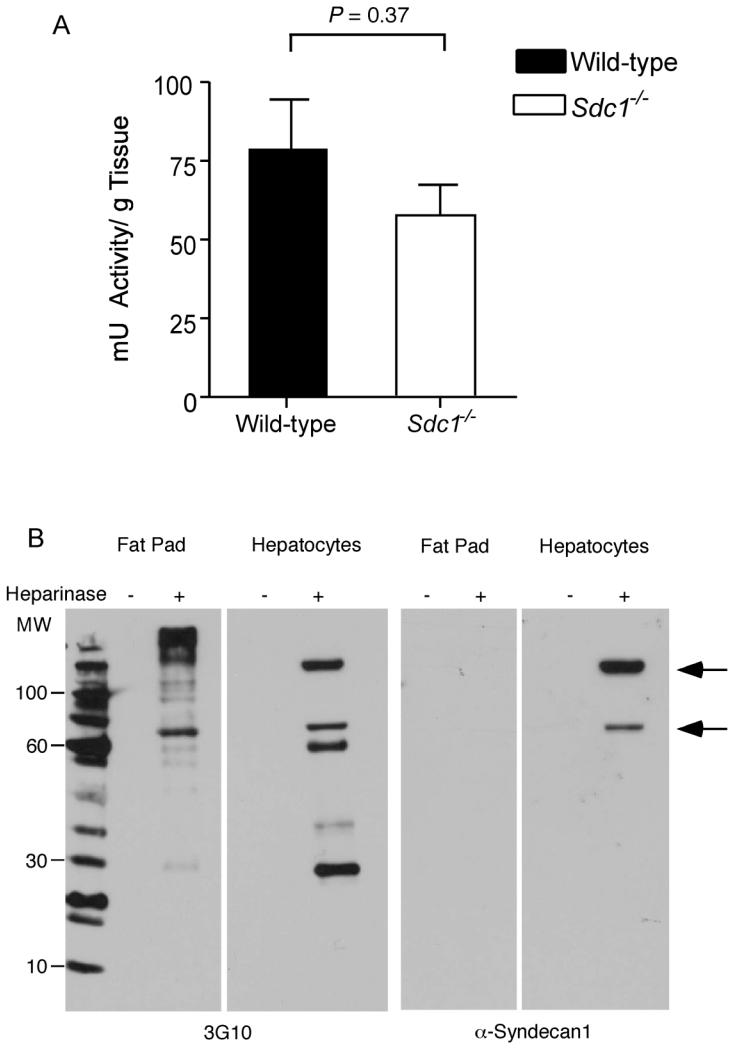

Stanford et al. Supplemental Fig. S3

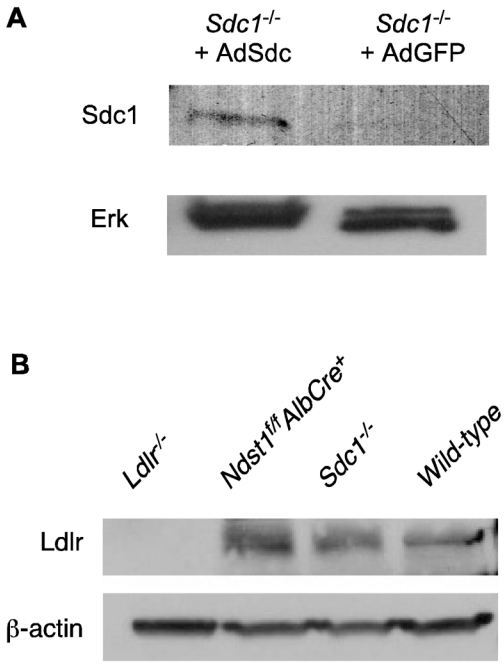

Stanford et al. Supplemental Fig. S4

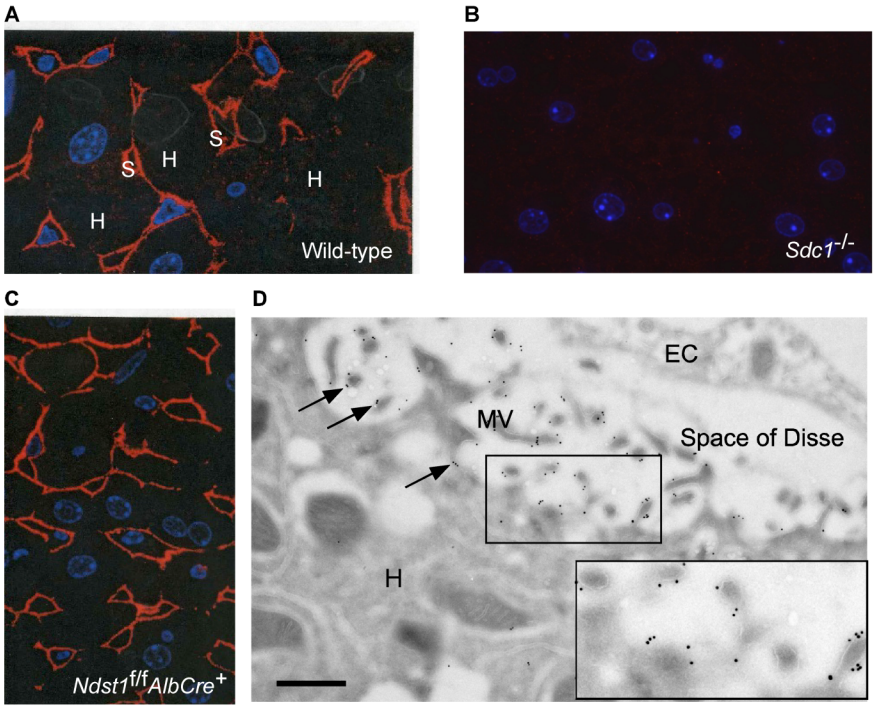

APPENDIX B

Insulin deficient diabetes mellitus in mice does not alter liver heparan sulfate

This chapter is reprinted from The Journal of Biological Chemistry, Volume 285, Issue 19, Joseph R. Bishop, Erin Foley, Roger Lawrence, and Jeffrey D. Esko, "Insulin-dependent diabetes mellitus in mice does not alter liver heparan sulfate", Pages 14658-62, Copyright © (2010), American Society for Biochemistry and Molecular Biology.

Insulin-dependent Diabetes Mellitus in Mice Does Not Alter Liver Heparan Sulfate*

Received for publication, February 8, 2010, and in revised form, March 15, 2010 Published, JBC Papers in Press, March 17, 2010, DOI 10.1074/jbc.M110.112391

Joseph R. Bishop[‡], **Erin Foley**[‡§], **Roger Lawrence**[‡], **and Jeffrey D. Esko**[‡1]

From the [‡]*Department of Cellular and Molecular Medicine, Glycobiology Research and Training Center, and* [§]*Biomedical Sciences Graduate Program, University of California, San Diego, La Jolla, California 92093*

Diabetes -associated hyperlipidemia is generally attributed to reduced clearance of plasma lipoproteins, especially remnant lipoproteins enriched in cholesterol and triglycerides. Hepatic clearance of remnants occurs via low density lipoprotein receptors and the heparan sulfate proteoglycan, syndecan-1. Previous studies have suggested alterations in heparan sulfate proteoglycan metabolism in rat and mouse diabetic models, consistent with the idea that diabetic dyslipidemia might be caused by alterations in proteoglycan expression in the liver. In this study we analyzed the content and composition of liver heparan sulfate in streptozotocin-induced insulin-deficient diabetic mice that displayed fasting hypertriglyceridemia and delayed clearance of dietary triglyceride-rich lipoproteins. No differences between normal and diabetic littermates in liver heparan sulfate content, sulfation, syndecan-1 protein levels, or affinity for heparin-binding ligands, such as apolipoprotein E or fibroblast growth factor-2, were noted. Decreased incorporation of [^{35}S]sulfate in insulin-deficient mice *in vivo* was observed, but the decrease was due to increased plasma inorganic sulfate, which reduced the efficiency of labeling of liver heparan sulfate. These results show that hyperlipidemia in insulin-deficient mice is not due to changes in hepatic heparan sulfate composition.

Hypertriglyceridemia is a significant complication of insulin-dependent diabetes mellitus (IDDM)[2] that likely contributes to cardiovascular disease in affected individuals, but its cause remains unknown (1–3). Insulin deficiency suppresses hepatic triglyceride production (4, 5), suggesting that increased plasma triglyceride levels might result from decreased catabolism of triglyceride-rich lipoproteins (TRL). In various diabetic models delayed TRL remnant clearance has been attributed to altered expression of heparan sulfate proteoglycans (HSPGs) in the liver (6–14).

We recently showed that mutant mice lacking the plasma membrane HSPG, syndecan-1, exhibit hypertriglyceridemia due to delayed clearance of TRL remnants from the circulation associated with reduced VLDL binding, uptake, and degradation in isolated hepatocytes (15). Furthermore, mice with undersulfated liver heparan sulfate have the same phenotype (16, 17). One of mutants lacked the enzyme *N*-acetylglucosamine *N*-deacetylase/*N*-sulfotransferase 1 (Ndst1), a biosynthetic enzyme that regulates the overall level of sulfation of heparan sulfate glycosaminoglycans. *In vivo* studies have suggested that IDDM causes reduced expression of Ndst1 (6, 10, 11, 13, 14, 18), leading to the hypothesis that hypertriglyceridemia was caused by undersulfated heparan sulfate in the liver.

In this work, we show that mice with IDDM exhibit reduced [^{35}S]sulfate incorporation into hepatic heparan sulfate. However, the reduction was caused by changes in plasma sulfate concentration after the onset of diabetes rather than any change in heparan sulfate biosynthesis. The application of mass spectrometry showed that hepatic heparan sulfate did not change in content and composition in diabetic mice, and the binding of apolipoprotein E (apoE) and fibroblast growth factor-2 was unaltered. Similarly, no alteration of syndecan-1 protein level was observed in freshly isolated hepatocytes from diabetic mice. Thus, fasting and postprandial hypertriglyceridemia in IDDM does not correlate with altered hepatic heparan sulfate in mice.

EXPERIMENTAL PROCEDURES

Mice and Induction of Diabetes—Male C57BL/6 mice (4 weeks of age) were purchased from Jackson Laboratory and maintained in a temperature-controlled (25 °C) facility with a 12-h light/dark cycle. The derivation and genotyping of *Ndst1*$^{f/f}$*AlbCre*$^{+}$ mice have been described previously (16). Mice were fed laboratory rodent chow (Harlan-Teklad) *ad libitum* except when fasting blood specimens were obtained. Mice were made diabetic by administering 50 mg/kg body weight of streptozotocin (STZ; Sigma) intraperitoneally for 5 consecutive days. Because of variations in plasma triglycerides in females, only male mice were used in this study.

Plasma Glucose and Lipid Measurements—Animals were fasted for 4 h in the morning. Blood glucose levels were monitored using a glucose monitor (Abbott) and test strips after a small tail nick. All experiments were carried out in animals with blood glucose levels between 400 and 500 mg/dl. Prior to experiments, plasma was prepared from retroorbital sinus bleeds to analyze glucose, cholesterol, and triglyceride levels enzymatically (Wako kits).

* This was supported by National Institutes of Health Grant GM33063 (to J. D. E.). This work was also supported by an American Heart Association scientist development grant (to J. R. B.).

[1] To whom correspondence should be addressed. Tel.: 858-822-1100; E-mail: jesko@ucsd.edu.

[2] The abbreviations used are: IDDM, insulin-dependent diabetes mellitus; TRL, triglyceride-rich lipoprotein; HSPG, heparan sulfate proteoglycan; Ndst1, *N*-acetylglucosamine *N*-deacetylase/*N*-sulfotransferase 1; STZ, streptozotocin; GRIL-LC/MS, glycan reductive isotope labeling-liquid chromatography/mass spectrometry; BisTris, 2-[bis(2-hydroxyethyl)amino]-2-(hydroxymethyl)propane-1,3-diol; apoE, apolipoprotein E; FGF-2, fibroblast growth factor-2.

Fat Tolerance Test—Vitamin A fat tolerance was measured essentially as described in Ref. 19. Briefly, 27 μCi of [11,12-^{3}H]retinol (44.4 Ci/mmol; PerkinElmer Life Sciences) in ethanol was mixed with 1 ml of corn oil (Sigma). Each mouse received 200 μl of the emulsion directly into the stomach by gavage. Blood was sampled at the times indicated by retroorbital sinus bleedings, and circulating radioactivity in 10 μl of plasma was measured in triplicate by scintillation counting.

Liver Heparan Sulfate Purification and Analysis—Heparan sulfate was isolated from whole livers, essentially as described (20). After cutting the portal vein, mice were perfused through the left ventricle with 50 ml of phosphate-buffered saline, pH 8, at 7 ml/min with a syringe pump to remove blood from the liver. Livers were excised, homogenized with a razor blade, and digested overnight with Pronase (2 mg/ml; Roche Applied Science) to degrade proteins, followed by purification of glycopeptides by anion exchange chromatography using DEAE-Sephacel (GE Healthcare). The columns (0.5 ml) were washed with low salt buffer (0.3 M NaCl in 20 mM sodium acetate, pH 6, 10 ml) to remove contaminants, and the glycosaminoglycan fraction was eluted with 2.5 ml of 2 M NaCl. Finally, the glycosaminoglycan preparation was treated with chondroitinase ABC to depolymerize chondroitin sulfate chains, and the heparan sulfate fraction was purified by a second round of anion exchange chromatography.

Heparan sulfate fine structure was determined quantitatively by glycan reductive isotope labeling-liquid chromatography/mass spectrometry (GRIL-LC/MS) as described (21). The amount of heparan sulfate was expressed relative to liver wet weight. The molar percentage of each disaccharide was calculated based on the total recovery. In some cases, mice were injected intraperitoneally with 1 mCi of $Na^{35}SO_{44}$ (25 mCi/ml; PerkinElmer Life Sciences), and liver [^{35}S]heparan sulfate was isolated after 2 h.

Analysis of Hepatocyte Syndecan-1—Primary hepatocytes were isolated from wild-type and diabetic mice as described (15, 22). Proteoglycans were isolated from the cell pellets according to a protocol adapted from Reizes *et al.* (23) and collected by anion exchange chromatography (DEAE-Sephacel). Samples were digested for 1 h with a mixture of 2 milliunits/ml heparin lyases I and II and 5 milliunits/ml heparin lyase III and chondroitinase ABC. The deglycosylated core proteins were separated by SDS-PAGE (NuPage 4–12% BisTris gel; Invitrogen) and transferred to nitrocellulose. Syndecan-1 was detected with mAb 281-2 (BD Pharmingen) and horseradish peroxidase-conjugated goat anti-rat IgG (Santa Cruz). One band was detected at 140 kDa. This band likely represents a syndecan-1 oligomer (24–26). β-Actin was detected with an anti-β-actin antibody (Cell Signaling Technologies) and a horseradish peroxidase-conjugated anti-rabbit IgG (Cell Signaling Technologies). Quantitative reverse transcription PCR was performed exactly as described previously (15).

Analysis of Plasma Sulfate Concentration—Inorganic sulfate was determined in plasma samples from wild-type and diabetic mice through the University of California San Diego Glycotechnology Core. Samples, blank and standards were hydrolyzed in 0.03 N HCl at 150 °C for 1 h and dried. Each sample was pyrolyzed in an open flame for about 15 s, cooled, and redissolved in water. Sulfate and phosphate anions were separated by a Dionex IonPac AS11HC column, eluted with a gradient mobile phase (2–50 mM KOH at 1 ml/min for 30 min), and quantified by conductivity detection relative to standard solutions.

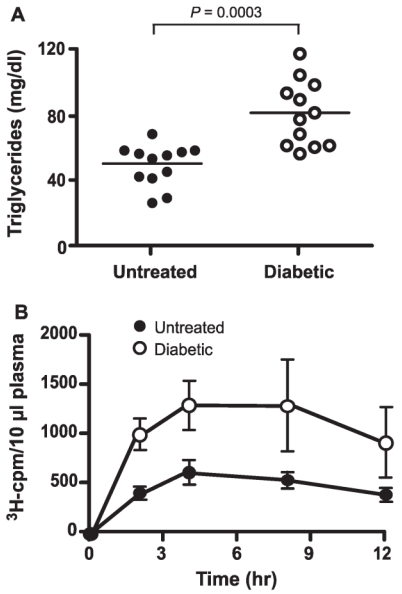

FIGURE 1. **Hypertriglyceridemia in IDDM mice.** *A*, total fasting plasma triglycerides. STZ-treated diabetic (*open circles*) or untreated control (*filled circles*) C57BL/6 mice were fasted for 4 h in the morning, and blood was taken from the retroorbital sinus for triglyceride analysis. Average values ± S.D. were 50 ± 12 mg/dl in control mice *versus* 81 ± 19 mg/dl in STZ-treated animals, respectively (n = 12). *B*, chylomicron clearance measurement by retinyl ester excursion. Fasted control mice (*closed circles*, n = 4) and IDDM mice (*open circles*, n = 4) were given 200 μl of corn oil containing [^{3}H]retinol by oral gavage. Blood samples were taken at the indicated times, and radioactivity remaining in plasma samples (10 μl) was determined by liquid scintillation counting. The values are expressed as mean ± S.D. (*error bars*) of three samples and are representative of at least three separate experiments.

Liver Heparan Sulfate-Protein Interaction—Samples of purified [^{35}S]heparan sulfate (10^4 cpm) were incubated for 20 min with 10 μg of recombinant apoE (Invitrogen) or fibroblast growth factor-2 (Selective Genetics) in physiological saline with and without 100 μg/ml unfractionated heparin (SPL). Bound material was collected on nitrocellulose membranes by fast vacuum filtration as described (27).

Statistics—Statistical analyses were performed using PRISM software (GraphPad Software). All data are expressed as mean values ± S.D. unless otherwise indicated. Significance was determined using an unpaired Student's (two-tailed) t test. Significance was taken as $p < 0.05$.

RESULTS AND DISCUSSION

Recent studies linking hypertriglyceridemia to altered hepatocyte heparan sulfate chains and expression of the proteoglycan syndecan-1 led us to investigate hepatocyte heparan sulfate in a mouse model of IDDM (15–17). Prior studies have suggested that insulin deficiency causes alterations in heparan sul-

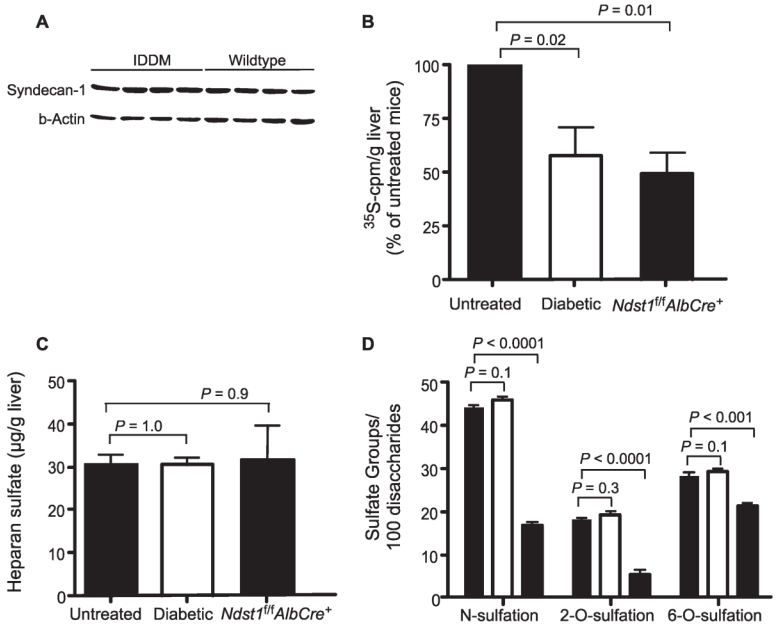

FIGURE 2. **Analysis of liver heparan sulfate in IDDM mice.** *A*, Western blot analysis of syndecan-1 expression in IDDM hepatocytes. Syndecan-1 was detected with mAb 281-2 in freshly prepared hepatocytes from untreated and STZ-treated hypertriglyceridemic diabetic mice ($n = 4$/strain). β-Actin was used as a loading control. *B*, analysis of endogenous liver [^{35}S]heparan sulfate. Untreated ($n = 3$) and STZ-treated hypertriglyceridemic diabetic ($n = 3$) wild-type mice and mutant mice bearing a hepatocyte specific deletion of *Ndst1* ($n = 3$) were given [^{35}S]sulfate intraperitoneally to radiolabel newly made heparan sulfate chains *in vivo*. Two hours later [^{35}S]heparan sulfate was purified from the liver and quantified by liquid scintillation counting. Results were normalized/g of liver and are presented as a percentage of labeling in untreated control mice ($1 \pm 0.05 \times 10^5$ cpm/g). The values are expressed as mean ± S.D. (*error bars*) and are representative of three separate studies ($n = 9$ mice). *C*, liver heparan sulfate measured chemically. Liver heparan sulfate was purified from untreated ($n = 9$) and STZ-treated hypertriglyceridemic diabetic ($n = 9$) wild-type mice and Ndst1 mutant mice ($n = 4$). The mass of heparan sulfate purified from each animal was determined by GRIL-LC/MS (see "Experimental Procedures"). Results were normalized to the amount of liver that had been analyzed (wet weight). *D*, sulfation of liver heparan sulfate. The disaccharide composition of liver heparan sulfate isolated in *C* was determined by GRIL-LC/MS. *N*-Sulfate and 6-*O*-sulfate groups in glucosamine moieties and 2-*O*-sulfate groups in uronic acids were calculated from the recovery of the individual disaccharides (see "Experimental Procedures").

fate in STZ-induced diabetes (6–14, 28). To study this problem further, IDDM was induced in C57BL/6 mice by low dose injection of STZ on 5 consecutive days. In a typical study group, STZ-treated mice developed hyperglycemia (>400 mg/dl blood glucose) 6–8 weeks after treatment. Approximately 50% of the diabetic mice exhibited mildly elevated fasting plasma triglycerides (Fig. 1*A*, 51 ± 13 mg/dl in control mice *versus* 81 ± 20 mg/dl in STZ-treated mice, $n = 12$/strain, $p < 0.003$) with no significant change in plasma cholesterol (data not shown). The majority of the triglycerides were present in lipoproteins of $d < 1.019$ g/ml, consistent with their identification as very low density lipoproteins and chylomicron remnants.

To examine the metabolism of dietary triglycerides, fasted mice were given a bolus of corn oil by gavage containing [^{3}H]retinol, which is converted into retinol esters and packaged into chylomicrons (vitamin A fat tolerance test). The amount of [^{3}H]retinol in the plasma was determined at various times (Fig. 1*B*). In untreated animals, plasma ^{3}H counts rose for 4 h and then decreased over the next 8 h as the retinyl esters containing lipoproteins were cleared in the liver. In STZ-treated animals, plasma counts behaved in a similar manner except the extent of accumulation was greater (Fig. 1*B*, *open circles*). The area under the curve was increased 2.3-fold for IDDM mice compared with the controls, indicating that diabetic animals cleared intestinally derived lipoproteins at a slower rate as previously observed (12). Similar results were obtained when plasma triglycerides were assayed (data not shown). Analysis of plasma lipoproteins by ultracentrifugation of samples drawn at 2 h after gavage showed that the majority of the counts and triglycerides were present in large buoyant lipoproteins of $d < 1.019$ g/ml (data not shown).

Analysis of Hepatocyte Syndecan-1 in IDDM Mice—The reduced clearance of plasma triglycerides might reflect decreased expression of syndecan-1 in IDDM mice compared with wild type. Analysis of syndecan-1 mRNA levels in IDDM liver as well as freshly isolated hepatocytes showed no difference compared with wild type (data not shown). Moreover, we did not detect any difference in syndecan core protein levels by Western blotting of extracts prepared from freshly isolated hepatocytes (Fig. 2*A*). Thus, altered syndecan-1 expression did not account for the delayed clearance of plasma triglycerides in IDDM mice.

Analysis of Liver Heparan Sulfate in IDDM Mice—Like diabetic mice, mutant mice lacking the heparan sulfate biosynthetic enzyme Ndst1 in hepatocytes (*Ndst1$^{f/f}$AlbCre$^+$* mice) exhibited delayed clearance of dietary triglycerides and fasting hypertriglyceridemia (16), suggesting that the hypertriglyceridemia observed in IDDM might be due to altered heparan sulfate composition. Previous studies have shown that IDDM leads to ~50% decreased incorporation of [^{35}S]sulfate into liver heparan sulfate chains *in vivo* (6, 10–14, 18). Similarly, we observed a reduction (57 ± 27%) in the amount of [^{35}S]heparan sulfate produced in diabetic mouse liver compared with controls (Fig. 2*B*). A similar level of reduction was also observed in *Ndst1$^{f/f}$AlbCre$^+$* mice, which produce undersulfated heparan sulfate chains (50 ± 13%).

To determine whether the composition of heparan sulfate was altered, we analyzed chemically heparan sulfate in normal and diabetic liver. Surprisingly, the mass of heparan sulfate

TABLE 1

Disaccharide analysis of heparan sulfate from wild-type, IDDM, and *Ndst1$^{f/f}$ AlbCre^{+}* mouse liver

Heparan sulfate chains were digested with heparin lyases I, II, and III, and the resulting disaccharides were resolved by GRIL-LC/MS (21). Disaccharides are designated by disaccharide structure code, in which D refers to a $\Delta^{4,5}$ unsaturated uronic acid derived from glucuronic acid or iduronic acid and whether sulfate groups are present at C2 of the uronic acid (0 or 2). The next letter designates whether the glucosamine residue is *N*-sulfated (S) or *N*-acetylated (A) and the presence or absence of 6-*O*-sulfate groups (0 or 6) (36). Thus, D0A0 = ΔUA-GlcNAc, D0S0 = ΔUA-GlcNS, D0A6 = ΔUA-GlcNAc6S, D0S6 = ΔUA-GlcNS6S, D2S0 = ΔUA2S-GlcNS, D2A6 = ΔUA2S-GlcNAc6S, and D2S6 = ΔUA2S-GlcNS6S.

Sample	Disaccharides[a]						
	D0A0	D0S0	D0A6	D0S6	D2S0	D2A6	D2S6
				mol %			
Wild type (n = 9)	40 ± 1	20 ± 1	11 ± 1	7 ± 1	7 ± 0	0.2 ± 0	12 ± 0
IDDM mouse (n = 9)	41 ± 1	20 ± 1	12 ± 1	7 ± 1	8 ± 1	0.2 ± 1	10 ± 1
Ndst1$^{f/f}$AlbCre^{+} (n = 4)	70 ± 3	6 ± 1	12 ± 1	5 ± 1	2 ± 1	0 ± 0	4 ± 0

[a] Values are expressed as the mole percent relative to the total amount of recovered disaccharides.

(micrograms of heparan sulfate/gram of liver) purified from IDDM mouse livers from animals with hypertriglyceridemia was equal to control (n = 9/strain) or Ndst1-deficient liver (n = 3) (Fig. 2*C*). To determine whether the extent of sulfation changed (glucosamine *N*-sulfation, uronyl 2-*O*-sulfation, or glucosamine 6-*O*-sulfation), we compared the disaccharide composition of the chains obtained from diabetic animals with wild type and *Ndst1$^{f/f}$AlbCre^{+}* mice using GRIL-LC/MS, a quantitative method for analyzing heparan sulfate composition. The total amount of *N*-sulfated, 2-*O*-sulfated, and 6-*O*-sulfated disaccharides derived from IDDM liver heparan sulfate appeared unchanged compared with heparan sulfate obtained from the wild type (Fig. 2*D*). Furthermore, the composition of individual disaccharides did not vary as well (Table 1). Similar findings were obtained in IDDM glomerular HSPGs as well (29). In contrast, Ndst1-deficient liver contained heparan sulfate chains with reduced *N*-sulfation and uronic acid 2-*O*-sulfation, as noted previously (17).

These findings contrast studies of experimentally diabetic rats in which insulin resistance was associated with production of HSPGs with reduced negative charge compared with HSPGs from control rats (6, 7). Subsequent studies suggested that reduced sulfation correlated with diminished GlcNAc *N*-deacetylase activity (7, 8, 10, 11, 13, 14). Although we have not measured Ndst1 expression or enzyme activity, the compositional studies demonstrate clearly that no change in sulfation occurred. The discrepancy between our findings and earlier studies may reflect the animal model under study (rats *versus* mice). How these results relate to type 1 and type 2 diabetes in humans remains to be determined.

Conceivably, the pattern of sulfated disaccharides might be altered in IDDM liver heparan sulfate in a way that might affect binding to protein ligands. [^{35}S]Heparan sulfate chains were purified from control and IDDM mice and incubated with apoE or fibroblast growth factor-2. The complexes that formed were collected on nitrocellulose membranes. The extent of binding of IDDM liver heparan sulfate to both proteins was equal to control liver heparan sulfate (Fig. 3). In contrast, the extent of binding to heparan sulfate from *Ndst1$^{f/f}$AlbCre^{+}* was dramatically reduced. Binding of these ligands to liver heparan sulfate was completely inhibited by the addition of exogenous heparin, demonstrating the specificity of the interaction (data not shown). Similarly, van den Born and co-workers (29) found that the protein binding properties as well as the disaccharide composition of heparan sulfate derived from control and diabetic glomeruli did not differ.

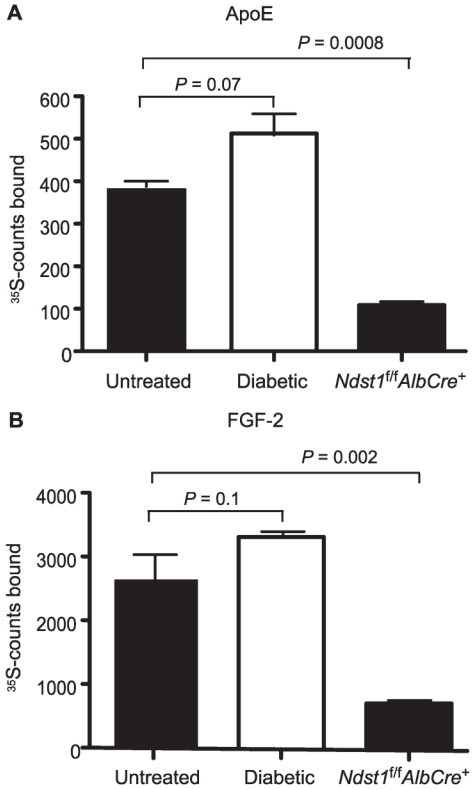

FIGURE 3. **Liver heparan sulfate binding to protein ligands.** Liver [^{35}S]heparan sulfate from diabetic, *Ndst1$^{f/f}$AlbCre^{+}*, and control mice (10^4 cpm) was incubated with 10 μg of recombinant apoE (*A*) or fibroblast growth factor-2 (*FGF-2*; *B*), and [^{35}S]heparan sulfate bound to the proteins was collected by membrane filtration (see "Experimental Procedures"). Unbound [^{35}S]heparan sulfate does not bind to the membrane. Each experiment was done in triplicate, and the average values are shown. The values are expressed as mean ± S.D. (*error bars*) and are representative of two separate experiments.

What is the explanation for the decrease in $^{35}SO_4$ incorporation observed here and in prior studies? Earlier work suggested that diabetes can result in alterations in plasma and tissue sulfate pools (30–32). Thus, the decrease in ^{35}S

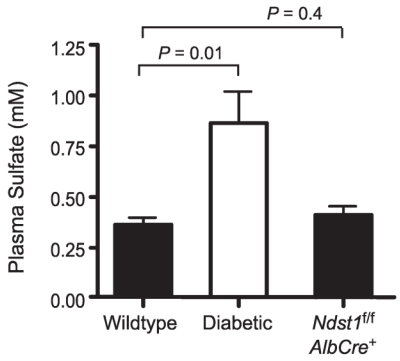

FIGURE 4. **Plasma sulfate levels in IDDM mice.** Sulfate levels were measured in untreated, diabetic, and Ndst1-mutant plasma samples (n = 6, respectively) by high performance liquid chromatography.

incorporation might have simply resulted from differences in the radiospecific activity of the $^{35}SO_4$ in the plasma or in the liver. Indeed, endogenous plasma sulfate concentration in diabetic mice was ~3-fold greater than in wild-type mice or *Ndst1$^{f/f}$AlbCre^{+}* mice (Fig. 4). The source of elevated plasma sulfate could be caused by altered anion filtration by the kidney due to diabetic nephropathy (33). Alternatively, IDDM is also known to induce gluconeogenesis, which could lead to the increased conversion of cysteine and methionine to pyruvate causing the release of inorganic sulfate from these amino acids. The release of inorganic sulfate from sulfur containing amino acids can be significant, providing all of the sulfate needed for glycosaminoglycan biosynthesis in cultured cells (34).

In summary, IDDM-induced hypertriglyceridemia in mice is not associated with any obvious changes in liver heparan sulfate content or composition. Although the affinity of the heparan sulfate chains for other factors involved in lipoprotein metabolism might be altered, we believe it more likely that IDDM induces changes in TRL composition that reduce the affinity of the particles for liver heparan sulfate. In support of this hypothesis, it has been shown that TRL in IDDM plasma exhibit reduced apoE and elevated apoC content potentially due to defects in lipoprotein lipase-mediated hydrolysis of triglycerides (35). Thus, we believe that the more likely explanation for elevated plasma triglycerides is a change in the processing of lipoproteins in the extrahepatic circulation rather than clearance mediated by HSPGs. Studies are currently under way to address whether these changes affect the affinity and uptake of lipoproteins by other liver receptors such as low density lipoprotein receptor or low density lipoprotein receptor-related protein.

REFERENCES

1. Haffner, S. M. (1998) *Endocr. Rev.* **19,** 583–592
2. Reusch, J. E. (2003) *J. Clin. Invest.* **112,** 986–988
3. Goldberg, R. B. (2003) *Cardiol. Clin.* **21,** 399–413
4. Bar-On, H., Roheim, P. S., and Eder, H. A. (1976) *Diabetes* **25,** 509–515
5. Ebara, T., Hirano, T., Mamo, J. C., Sakamaki, R., Furukawa, S., Nagano, S., and Takahashi, T. (1994) *Metabolism* **43,** 299–305
6. Kjellén, L., Bielefeld, D., and Hook, M. (1983) *Diabetes* **32,** 337–342
7. Unger, E., Pettersson, I., Eriksson, U. J., Lindahl, U., and Kjellén, L. (1991) *J. Biol. Chem.* **266,** 8671–8674
8. Oturai, P., Deckert, M., Rolin, B., Jensen, T., and Kofoed-Enevoldsen, A. (1999) *Exp. Clin. Endocrinol. Diabetes* **107,** 453–456
9. Olsson, U., Egnell, A. C., Lee, M. R., Lundén, G. O., Lorentzon, M., Salmivirta, M., Bondjers, G., and Camejo, G. (2001) *Diabetes* **50,** 2126–2132
10. Kofoed-Enevoldsen, A., and Eriksson, U. J. (1991) *Diabetes* **40,** 1449–1452
11. Kofoed-Enevoldsen, A. (1992) *Kidney Int.* **41,** 763–767
12. Ebara, T., Conde, K., Kako, Y., Liu, Y., Xu, Y., Ramakrishnan, R., Goldberg, I. J., and Shachter, N. S. (2000) *J. Clin. Invest.* **105,** 1807–1818
13. Williams, K. J., Liu, M. L., Zhu, Y., Xu, X., Davidson, W. R., McCue, P., and Sharma, K. (2005) *Diabetes* **54,** 1116–1122
14. Goldberg, I. J., Hu, Y., Noh, H. L., Wei, J., Huggins, L. A., Rackmill, M. G., Hamai, H., Reid, B. N., Blaner, W. S., and Huang, L. S. (2008) *Diabetes* **57,** 1674–1682
15. Stanford, K. I., Bishop, J. R., Foley, E. M., Gonzales, J. C., Niesman, I. R., Witztum, J. L., and Esko, J. D. (2009) *J. Clin. Invest.* **119,** 3236–3245
16. MacArthur, J. M., Bishop, J. R., Stanford, K. I., Wang, L., Bensadoun, A., Witztum, J. L., and Esko, J. D. (2007) *J. Clin. Invest.* **117,** 153–164
17. Stanford, K. I., Wang, L., Castagnola, J., Song, D., Bishop, J. R., Brown, J. R., Lawrence, R., Bai, X., Habuchi, H., Tanaka, M., Cardoso, W. V., Kimata, K., and Esko, J. D. (2010) *J. Biol. Chem.* **285,** 286–294
18. Williams, K. J. (2008) *J. Clin. Invest.* **118,** 3247–3259
19. Ishibashi, S., Perrey, S., Chen, Z., Osuga, J., Shimada, M., Ohashi, K., Harada, K., Yazaki, Y., and Yamada, N. (1996) *J. Biol. Chem.* **271,** 22422–22427
20. Grobe, K., Inatani, M., Pallerla, S. R., Castagnola, J., Yamaguchi, Y., and Esko, J. D. (2005) *Development* **132,** 3777–3786
21. Lawrence, R., Olson, S. K., Steele, R. E., Wang, L., Warrior, R., Cummings, R. D., and Esko, J. D. (2008) *J. Biol. Chem.* **283,** 33674–33684
22. Seglen, P. O. (1976) *Methods Cell Biol.* **13,** 29–83
23. Reizes, O., Lincecum, J., Wang, Z., Goldberger, O., Huang, L., Kaksonen, M., Ahima, R., Hinkes, M. T., Barsh, G. S., Rauvala, H., and Bernfield, M. (2001) *Cell* **106,** 105–116
24. Miettinen, H. M., and Jalkanen, M. (1994) *J. Cell Sci.* **107,** 1571–1581
25. Asundi, V. K., and Carey, D. J. (1995) *J. Biol. Chem.* **270,** 26404–26410
26. Choi, S., Lee, E., Kwon, S., Park, H., Yi, J. Y., Kim, S., Han, I. O., Yun, Y., and Oh, E. S. (2005) *J. Biol. Chem.* **280,** 42573–42579
27. Kreuger, J., Lindahl, U., and Jemth, P. (2003) *Methods Enzymol.* **363,** 327–339
28. Cohen, P. M., and Surma, M. L. (1981) *J. Lab. Clin. Med.* **98,** 715–722
29. van den Born, J., Pisa, B., Bakker, M. A., Celie, J. W., Straatman, C., Thomas, S., Viberti, G. C., Kjellen, L., and Berden, J. H. (2006) *J. Biol. Chem.* **281,** 29606–29613
30. Cohen, M. P., and Surma, M. L. (1984) *Diabetes* **33,** 8–12
31. Spiro, M. J. (1987) *Diabetologia* **30,** 259–267
32. Fan, M. Y., and Templeton, D. M. (1992) *Diabetes Metab.* **18,** 98–103
33. Blazquez-Medela, A. M., López-Novoa, J. M., and Martínez-Salgado, C. (2010) *Curr. Diabetes Rev.* **6,** 68–87
34. Esko, J. D., Elgavish, A., Prasthofer, T., Taylor, W. H., and Weinke, J. L. (1986) *J. Biol. Chem.* **261,** 15725–15733
35. Levy, E., Shafrir, E., Ziv, E., and Bar-On, H. (1985) *Biochim. Biophys. Acta* **834,** 376–385
36. Lawrence, R., Lu, H., Rosenberg, R. D., Esko, J. D., and Zhang, L. (2008) *Nat. Methods* **5,** 291–292

APPENDIX C

Shedding of syndecan-1 from human hepatocytes alters very low density lipoprotein clearance

This chapter is a reprint from Hepatology, Volume 55, Issue 1, Yiping Deng, Erin M. Foley, Jon C. Gonzales, Philip Gordts, Yulin Li, and Jeffrey D. Esko, "Shedding of syndecan-1 from human hepatocytes alters VLDL clearance", Pages 277-86,

Shedding of Syndecan-1 from Human Hepatocytes Alters Very Low Density Lipoprotein Clearance

Yiping Deng,[1,3] Erin M. Foley,[1,2] Jon C. Gonzales,[1,2] Philip L. Gordts,[1] Yulin Li,[3] and Jeffrey D. Esko[1,2]

We recently showed that the heparan sulfate proteoglycan syndecan-1 mediates hepatic clearance of triglyceride-rich lipoproteins in mice based on systemic deletion of syndecan-1 and hepatocyte-specific inactivation of sulfotransferases involved in heparan sulfate biosynthesis. Here, we show that syndecan-1 expressed on primary human hepatocytes and Hep3B human hepatoma cells can mediate binding and uptake of very low density lipoprotein (VLDL). Syndecan-1 also undergoes spontaneous shedding from primary human and murine hepatocytes and Hep3B cells. In human cells, phorbol myristic acid induces syndecan-1 shedding, resulting in accumulation of syndecan-1 ectodomains in the medium. Shedding occurs through a protein kinase C–dependent activation of ADAM17 (a disintegrin and metalloproteinase 17). Phorbol myristic acid stimulation significantly decreases DiD (1,1′-dioctadecyl-3,3,3′,3′-tetramethylindodicarbocyanine perchlorate)-VLDL binding to cells, and shed syndecan-1 ectodomains bind to VLDL. Although mouse hepatocytes appear resistant to induced shedding *in vitro*, injection of lipopolysaccharide into mice results in loss of hepatic syndecan-1, accumulation of ectodomains in the plasma, impaired VLDL catabolism, and hypertriglyceridemia. *Conclusion*: These findings suggest that syndecan-1 mediates hepatic VLDL turnover in humans as well as in mice and that shedding might contribute to hypertriglyceridemia in patients with sepsis. (HEPATOLOGY 2012;55:277-286)

Hypertriglyceridemia is a common disorder that results from the accumulation of triglyceride-rich lipoproteins (TRLs) in the circulation. TRLs include chylomicrons derived from dietary lipids, very low density lipoproteins (VLDLs) from the liver, and the remnant particles that remain after the action of lipoprotein lipase in the vasculature. These remnant lipoproteins are cleared from the circulation via endocytic receptors in the liver, including the low density lipoprotein receptor (LDLR),[1,2] the LDLR-related proteins (LRPs),[3,4] lipolysis stimulated receptor,[5] and one or more heparan sulfate proteoglycans.[6,7] The syndecans are type I transmembrane proteoglycans bearing up to three heparan sulfate chains and, in some family members, two chondroitin/dermatan sulfate chains.[8] Genetic studies in which heparan sulfate assembly was selectively altered in mouse hepatocytes by Cre-loxP targeting of two sulfotransferases demonstrated the importance of the heparan sulfate chains in hepatic TRL clearance.[9,10] Furthermore, direct genetic evidence has been provided showing that syndecan-1 is the primary heparan sulfate proteoglycan mediating hepatic clearance of TRLs in mice.[11] Its role in lipoprotein clearance in human hepatocytes is less clear, with some data suggesting that its primary role may be in binding of the remnants to the cell surface with subsequent transfer to other receptors.[12,13]

In many cultured cells, syndecan-1 is constitutively shed from the cell surface into the growth medium.[14]

Abbreviations: ADAM, a disintegrin and metalloproteinase; BIM I, bisindolylmaleimide I; DiD, 1,1′-dioctadecyl-3,3,3′,3′-tetramethylindodicarbocyanine perchlorate; ELISA, enzyme-linked immunosorbent assay; HSPG, heparan sulfate proteoglycan; LDLR, low density lipoprotein receptor; LPS, lipopolysaccharide; LRP, LDLR-related protein; PMA, phorbol myristic acid; siRNA, small interfering RNA; TNF-α, tumor necrosis factor-α; TRL, triglyceride-rich lipoprotein; VLDL, very low density lipoprotein.

From the [1]Department of Cellular and Molecular Medicine; and [2]Biomedical Sciences Graduate Program, University of California, San Diego, La Jolla, CA; and [3]The Key Laboratory of Pathobiology, Ministry of Education, Norman Bethune College of Medicine, Jilin University, Changchun, China.

Received July 16, 2011; accepted August 16, 2011.

This work was supported by a scholarship from the China Scholarship Council (to Y.D.), a Ruth L. Kirschstein National Research Service Award F31HL097721 (to J.C.G.), and National Institutes of Health grant GM33063 (to J.D.E.).

Address reprint requests to: Jeffrey D. Esko, Ph.D., Department of Cellular and Molecular Medicine, University of California, San Diego, La Jolla, CA 92093-0687. E-mail: jesko@ucsd.edu; fax: 858-534-5611.

View this article online at wileyonlinelibrary.com.

DOI 10.1002/hep.24626

Potential conflict of interest: Nothing to report.

Additional Supporting Information may be found in the online version of this article.

Inducers such as growth factors, bacterial virulence factors, ceramide, and the protein kinase C agonist phorbol myristic acid (PMA; phorbol-12-myristate-13-acetate) accelerate shedding by activation of one or more secreted or membrane-associated metalloproteinases including matrix metalloproteinase 7 (MMP7), MMP9, MMP14, and a disintegrin and metalloproteinase 17 (ADAM17).[14] Although the exact biological significance of syndecan-1 shedding is unclear in most cells, one important role appears to be in the regulation of chemokine activity during bacterial infection.[15-17] The role of syndecan-1 shedding in lipoprotein metabolism has not been studied.

Here, we examined the activity of syndecan-1 in TRL clearance in Hep3B human hepatoma cells and in primary human hepatocytes. We show that syndecan-1 is expressed by both human hepatoma cells and primary human hepatocytes and demonstrate its action as a TRL receptor. Syndecan-1 undergoes spontaneous proteolytic shedding from both human and mouse hepatocytes mediated by ADAM17. In mice, lipopolysaccharide (LPS) administration induces syndecan-1 shedding from the liver and reduces hepatic VLDL catabolism. These findings suggest that shedding of syndecan-1 may play a role in plasma lipid homeostasis.

Materials and Methods

Mice and Animal Husbandry. Wild-type C57BL/6 and *Ldlr*$^{-/-}$ mice on a C57BL/6 background were purchased from The Jackson Laboratory. All animals were housed and bred in vivaria approved by the Association for Assessment and Accreditation of Laboratory Animal Care located in the School of Medicine, University of California San Diego (UCSD), following standards and procedures approved by the UCSD Institutional Animal Care and Use Committee. Mice were maintained on a 12-hour-light/12-hour-dark cycle and provided *ad libitum* with water and standard rodent chow (Harlan Teklad).

Cell Culture. Hep3B hepatocarcinoma cells were obtained from the American Type Culture Collection (Manassas, VA) and cultured in minimum essential medium supplemented with 10% fetal bovine serum, nonessential amino acids, sodium pyruvate, penicillin, and streptomycin. Normal human hepatocytes were obtained through the Liver Tissue Cell Distribution System (Pittsburgh, PA) funded by NIH Contract N01-DK-7-0004/HHSN267200700004C. Primary mouse hepatocytes were isolated and cultured as described previously[11] and used within 2 days of isolation.

Syndecan-1 Shedding. To measure spontaneous syndecan-1 shedding, Hep3B cells were seeded in 12-well plates (3×10^5 cells) and incubated in serum-free medium. To induce shedding, cells were stimulated with 0.25 μM PMA (Sigma-Aldrich, St. Louis, MO) for 1 hour at 37°C. The effect of various metalloproteinase inhibitors and signaling pathway inhibitors was surveyed by pretreating cells for 1 hour with 10 μM Marimastat (Tocris bio, Ellisville, MO), GI254023 or GW280264 (provided by Dr. Andreas Ludwig, RWTH Aachen University, Aachen, Germany), bisindolylmaleimide I (BIM I), U0126 or SB 203580 (EMD, San Diego, CA), or vehicle only (dimethylsulfoxide; Sigma-Aldrich). In all shedding assays, conditioned media were collected and centrifuged to remove cell debris before further analysis.

Dot Blotting. Conditioned media or diluted plasma samples were applied to cationic polyvinylidene fluoride–based membranes (Hybond-N+; Amersham Biosciences, Piscataway, NJ) under mild vacuum in a bio-dot apparatus (Bio-Rad Laboratories, Hercules, CA). The membrane was blocked in 5% nonfat milk buffer and incubated with human syndecan-1 monoclonal antibody (mAb) B-A38 (AbD Serotec, Raleigh, NC) or mouse syndecan-1 mAb 281-2 (BD Biosciences, San Diego, CA) and a secondary horseradish peroxidase–conjugated anti-mouse immunoglobulin G (IgG; BD Bioscience, Franklin Lakes, NJ) or anti-rat IgG (Santa Cruz Biotechnology, Santa Cruz, CA). Blots were visualized by chemiluminescent substrate (Pierce, Rockford, IL) and analyzed with an Alpha Innotech Imager system (Cell Biosciences, Santa Clara, CA). All values were scaled relative to that obtained for the indicated control in each figure and expressed as a percentage.

Western Blotting. Hepatocytes were incubated with a mixture of 2 mU/mL of heparin lyase I and II and 5 mU/mL of heparin lyase III in serum-free medium at 37°C for 15 minutes. Cells were subsequently lysed in radioimmunoprecipitation assay buffer supplemented with 1× protease inhibitor cocktail (Sigma-Aldrich). Each sample (10 μg protein) was resolved on a 4%-12% Bis-Tris NuPage gel (Invitrogen) and transferred to polyvinylidene fluoride membrane (Bio-Rad Laboratories). The membrane was blocked with Super-Block buffer (Pierce). Blots were incubated with B-A38 (1:500) or anti-ADAM17 polyclonal antibody ab2051 (1:500) (Abcam, Cambridge, MA) and secondary antibodies (horseradish peroxidase–conjugated anti-mouse IgG; BD Biosciences). Reactive bands were visualized by chemiluminescence.

RNA Interference. Small interfering RNAs (siRNAs) specifically targeting human ADAM17 (5′-

AGAGAGUACAACUACAAA-3′, 5′-GCAGUAAA CAAUCAAUCU-3′, and 5′-GGAGAUUUGUUAAU GAUA-3′) and human syndecan-1(5′-AGAUAUCAC CUUGUCACA-3′, 5′-CCAGUAGACCUUGUUACU-3′, and 5′-GGAGACAGCAUCAGGGUU-3′) were obtained from Integrated DNA Technologies (Coralville, IA). A scrambled siRNA was used as a control. All siRNAs were transfected into cells by using Transfectin (Integrated DNA Technologies, San Diego, CA).

VLDL Binding and Uptake. Human VLDL (density $\delta < 1.006$ g/mL) was isolated from plasma by buoyant density ultracentrifugation as described[11] and quantified by BCA protein assay (Pierce). To label the particles, 1-2 mg of VLDL were combined with 100 μL of 3 mg/mL 1,1′-dioctadecyl-3,3,3′,3′-tetramethylindodicarbocyanine perchlorate (DiD; Invitrogen) in dimethylsufoxide and then reisolated by ultracentrifugation. After incubation with VLDL, cells were rinsed with phosphate-buffered saline and lysed by adding 0.1 M NaOH plus 0.1% sodium dodecyl sulfate for 40 minutes at room temperature.[18] Fluorescence intensity was measured with appropriate excitation and emission filters in a plate reader (TECAN GENios Pro; Tecan, Switzerland) and normalized to total cell protein. In some experiments, VLDL binding and uptake was measured by flow cytometry.

VLDL Plasma Clearance. Mice were fasted for 6 hours and injected via the tail vein with 20 μg human VLDL protein. Serial samples were taken by tail vein bleeds, and the amount of human VLDL remaining in the plasma was determined by sandwich enzyme-linked immunosorbent assay (ELISA) as previously described and plotted relative to VLDL detected at 2 minutes.[19]

Ectodomain Binding. To radiolabel glycosaminoglycans, hepatoma cells were incubated for 48 hours in growth medium supplemented with 10% dialyzed fetal bovine serum containing 100 μCi/mL Na[^{35}S]O_4 (PerkinElmer Life Science, Waltham, MA). Shed [^{35}S]syndecan-1 ectodomains were isolated from conditioned medium after incubation of cells with PMA. After 5 hours, proteoglycans were purified from the conditioned medium by anion exchange chromatography as described.[20] Approximately 125 ng syndecan-1 ectodomains (determined by Sdc-1 ELISA) were diluted in 200 μL of a solution of iodixanol ($\delta = 1.019$ g/mL; OptiPrep Density Gradient Medium; Sigma-Aldrich) at the bottom of an ultracentrifuge tube in the presence or absence of 50 μg VLDL with and without 50 μg heparin. The tubes were then carefully filled with a solution of iodixanol ($\delta = 1.019$ g/mL) and centrifuged at 45,000 rpm (250,000*g*) for 3 hours at 18°C in a Beckman 50.4 Ti rotor. Fractions were removed sequentially from the top of the tubes and assayed for radioactivity by liquid scintillation counting.

***Syndecan-1 Shedding* In Vivo.** C57Bl/6 mice, 8-10 weeks old, were injected intraperitoneally with 4.5 mg/kg *E. coli* LPS. Eighteen hours later, food was removed from the cages. After 6 hours of fasting, the animals were sacrificed, and their livers and blood were harvested. Syndecan-1 in plasma samples was measured by dot blotting. Syndecan-1 in liver sections was visualized using mAb 281-2 as described.[11] Plasma triglyceride was measured using Triglyceride-SL Reagent (Genzyme Diagnostics, Framingham, MA) and cholesterol via Roche Cobas C111 analyzer (Roche Diagnostics, Indianapolis, IN).

Statistical Analysis. All data were analyzed by unpaired one-tailed *t* tests. $P < 0.05$ was considered statistically significant.

Results

Human Hepatocytes Bind VLDL in a Heparan Sulfate-Dependent Manner. Binding of DiD-labeled VLDL (DiD-VLDL) at 4°C to Hep3B human hepatoma cells occurred in a saturable manner both with respect to time and concentration (Fig. 1A,C, respectively). Treatment of the cells with a mixture of heparin lyases reduced binding by 80%-90%, indicating that the majority of binding sites were attributable to heparan sulfate proteoglycans on the cell surface. Analysis of the binding curve in Fig. 1C by a conventional single-site binding equation yielded a maximum binding (B_{max}) value of 69 ± 12 μg VLDL/mg cell protein and a dissociation constant (K_D) of 8.8 ± 3.4 μg/mL ($R^2 = 0.9980$). Assuming that approximately 1.8% of the mass of VLDL particles is protein and an average molecular mass for VLDL of $\sim 2 \times 10^7$ Da,[21] we calculated that Hep3B cells express $\sim 7 \times 10^5$ binding sites/cell attributable to heparan sulfate, similar to previous studies of mouse hepatocytes.[11] Incubation of cells at 37°C increased the association of DiD-VLDL (Fig. 1B,D) because of internalization of the particles, as reported.[22] Inclusion of heparin (100 μg/mL) blocked binding and uptake five-fold as measured by flow cytometry (data not shown).

Human hepatocytes express multiple heparan sulfate proteoglycans, including the membrane proteoglycans syndecan-1, syndecan-2, and syndecan-4 and glypican-1 and glypican-4, and the extracellular matrix proteoglycans perlecan, collagen 18, and agrin[23,24] (Supporting Fig. 1). To examine the contribution of syndecan-1 to VLDL binding and uptake, we silenced its expression on Hep3B cells using specific siRNAs (Supporting

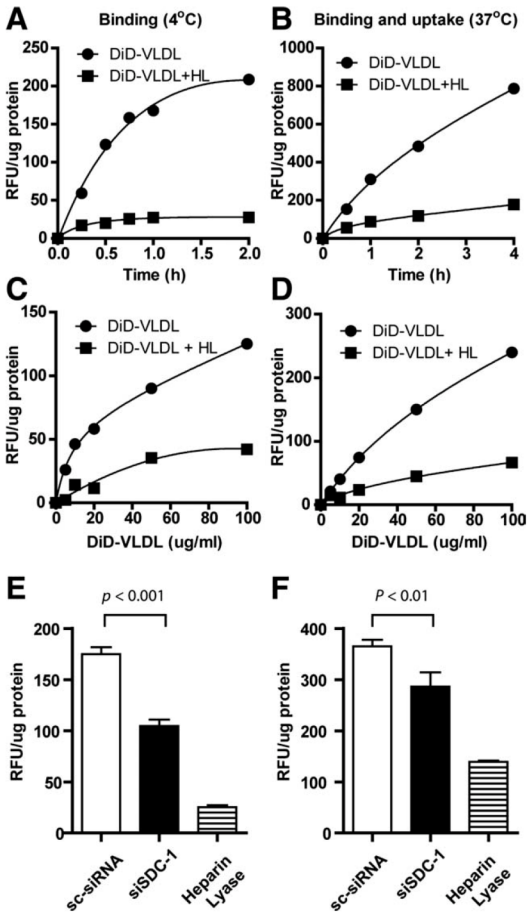

Fig. 1. VLDL binding and uptake by human Hep3B hepatoma cells. Binding and uptake of DiD-VLDL was measured at (A,C) 4°C and (B,D) 37°C, respectively, before (circles) or after (squares) treatment with heparin lyases. In (A) and (B), cells were incubated with 100 μg/mL DiD-VLDL for the indicated time. In (C) and (D), the cells were incubated with indicated concentration of DiD-VLDL for 1 hour ($n = 3$). In (E) and (F), cells were treated with a scrambled siRNA (sc-siRNA, open bars), siRNA to syndecan-1 (siSDC-1, filled bars), or heparin lyase (hatched bars). (E) Binding and (F) binding/uptake were measured by incubating treated cells with 100 μg/mL DiD-VLDL for 1 hour ($n = 4$). The values represent the average fluorescence intensity normalized to cell protein. Error bars indicate standard deviation.

Fig. 2). DiD-VLDL binding at 4°C (Fig. 1E) and uptake at 37°C (Fig. 1F) was reduced compared to cells treated with a scrambled siRNA. Binding and uptake were diminished to a greater extent by heparan lyase digestion (Fig. 1E,F), suggesting that either the extent of syndecan-1 silencing was incomplete or that other heparan sulfate proteoglycans can mediate binding and uptake.[6] Silencing of syndecan-4 did not result in reduction of binding, but other proteoglycans have not been examined (data not shown). The residual heparin lyase-insensitive component of binding/uptake presumably reflects other receptors, most likely LDL receptors and one or more members of the family of LDLR-related proteins.[3,4]

Hepatocytes Shed Syndecan-1. Syndecan-1 undergoes proteolytic shedding in many cells,[14] resulting in the appearance in the medium of the extracellular domains of the protein containing the ligand binding heparan sulfate chains. To investigate whether human hepatocytes spontaneously shed syndecan-1, we collected conditioned growth media from Hep3B cells (Fig. 2A) and primary human hepatocytes (Fig. 2B) and measured syndecan-1 ectodomains by dot blotting. Syndecan-1 ectodomains accumulated progressively in the conditioned media over time in both types of cells. The broad-spectrum metalloproteinase inhibitor Marimastat blocked spontaneous shedding of syndecan-1 (Fig. 2A,B), consistent with the idea that shedding depends on limited proteolysis.

Syndecan-1 shedding can be induced in cells by PMA.[14] In both Hep3B cells and primary human hepatocytes, PMA induced syndecan-1 shedding by ~10-fold (Fig. 2C,D). Induction of shedding was dependent on both time of incubation and the concentration of PMA added to the medium (Supporting Fig. 3). Syndecan-1 on the cell surface was diminished in a corresponding manner, consistent with shedding (Fig. 2E,F). PMA is known to stimulate endocytosis, which could account for some reduction in cell surface expression of syndecan-1 as well.[25] The protein kinase C inhibitor BIM I profoundly inhibited syndecan-1 ectodomain accumulation in conditioned media and prevented loss of syndecan-1 from the cell surface (Fig. 3A and Supporting Fig. 4A). In contrast, the MEK (MAPK/ERK kinase) inhibitor U0216 and the p38 mitogen-activated protein kinase (MAPK) inhibitor SB203580 failed to inhibit PMA-induced shedding of syndecan-1.

Marimastat blocked syndecan-1 shedding induced by PMA and spontaneous shedding (Fig. 2). To determine the relevant metalloproteinase(s), we tested two enzyme inhibitors on Hep3B cells. GW280264, which inhibits both ADAM17 and ADAM10, profoundly diminished the accumulation of syndecan-1 ectodomain in conditioned media (Fig. 3B) and prevented the PMA-induced loss of syndecan-1 from the cell surface (Supporting Fig. 4B). In contrast, the inhibitor GI254023, which preferentially blocks ADAM10 but not ADAM17, had no effect on PMA-induced shedding of syndecan-1. Silencing of ADAM17 expression in Hep3B cells by siRNA reduced ADAM17

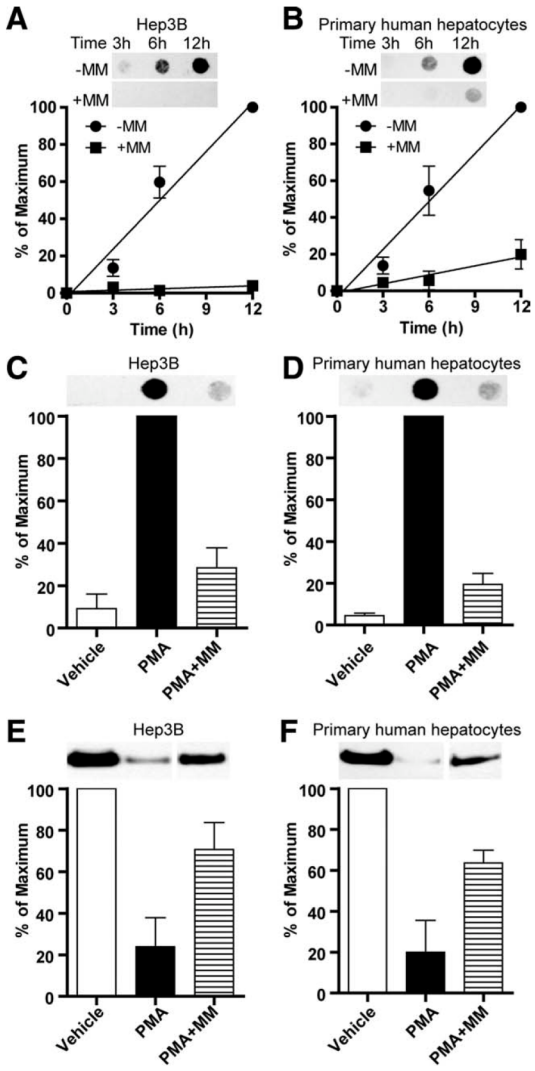

Fig. 2. Shedding of syndecan-1 from human hepatocytes. Conditioned medium was collected from (A) Hep3B human hepatoma cells and (B) primary human hepatocytes incubated with (squares) or without (circles) the metalloproteinase inhibitor Marimastat (MM). At the indicated time points, shed syndecan-1 was measured by dot blotting. (C,E) Hep3B cells and (D,F) primary human hepatocytes were treated with 0.25 μM PMA for 1 hour in the presence (shaded bars) or absence (filled bars) of Marimastat (MM). Conditioned media was collected and subjected to dot blotting for shed syndecan-1 (C,D) and cell lysates were prepared after treatment of the cells with heparin lyases in order to measure syndecan-1 core protein by western blotting (E,F). Each data point or bar represents the average $\pm$ standard deviation (n = 3).

expression approximately six-fold and prevented PMA-induced accumulation of syndecan-1 ectodomains in the conditioned medium (Fig. 3C) and prevented loss of syndecan-1 from the cell surface as compared to controls in which cells were treated with scrambled siRNA (Supporting Fig. 4C). Similar results were obtained with primary human hepatocytes (Fig. 4). These findings indicate that ADAM17 is the primary metalloproteinase responsible for PMA-induced syndecan-1 shedding in human hepatocytes.

Syndecan-1 Shedding Reduces VLDL Binding and Uptake. In view of the role for syndecan-1 in TRL binding and uptake (Figs. 1 and 2),[11] we predicted that PMA-induced syndecan-1 shedding would affect VLDL binding and uptake. In Hep3B cells, PMA reduced VLDL binding and uptake by ~50% compared to untreated cells (Fig. 5A,B). Treatment with heparin lyases reduced VLDL binding and uptake to a greater extent, most likely because of incomplete removal of proteoglycan receptors from the cell surface by PMA-induced shedding. Similar results were obtained in primary human hepatocytes (Fig. 5C,D). Shed ectodomains did not inhibit binding when purified and added to fresh cells at their original concentration. PMA can also induce shedding of LRP-1, another TRL receptor, which might account for some decrease in binding.[3,26] However, the major remnant receptor appears to bear heparan sulfate, on the basis of the large inhibitory effect of heparin lyase treatment (Fig. 1).

Although the ADAM17 cleavage site in syndecan-1 is unknown,[27] it presumably lies in the membrane proximal region, thus liberating the ectodomain with covalently attached heparan sulfate chains. Based on previous genetic studies of mouse syndecan-1,[11] the heparan sulfate chains make up the TRL-binding domain of the syndecan-1 receptors. Thus, we predicted that shed syndecan-1 ectodomains from hepatocytes would retain the capacity to bind VLDL. To test this hypothesis, we incubated hepatoma cells with $[^{35}S]O_4$ to radiolabel the heparan sulfate chains on syndecan-1, triggered shedding with PMA, and purified the $[^{35}S]$-labeled ectodomains from the medium by anion exchange chromatography. The $[^{35}S]$-labeled ectodomains were then mixed with VLDL, placed at the bottom of a centrifuge tubes, and overlaid with a solution of iodixanol (δ = 1.019 g/mL). Ultracentrifugation resulted in the appearance of ~65% of counts in the top four fractions, whereas in the absence of VLDL, less than 5% of the counts were found in the top fractions (Fig. 6). Dot blot analysis of the pooled top four fractions showed syndecan-1 ectodomains were present in samples containing VLDL (Fig. 6, inset). Inclusion of 50 μg of heparin in the binding solution reduced the recovery of $[^{35}S]$-labeled ectodomains in the top

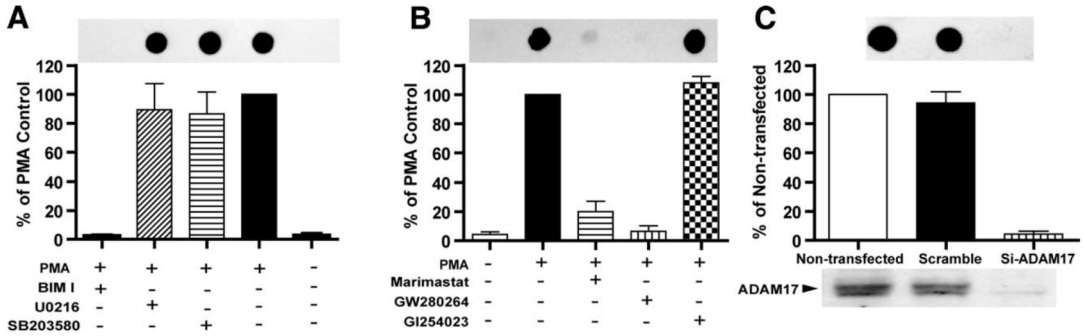

Fig. 3. ADAM17 mediates PMA-induced shedding of syndecan-1. (A) Different signaling pathway inhibitors were tested for their ability to inhibit syndecan-1 shedding induced by PMA. (B) Hep3B cells were pretreated with different metalloproteinase inhibitors and then stimulated with 0.25 μM PMA for 1 hour. Syndecan-1 shedding was measured by dot blotting of the medium. (C) ADAM17 was silenced by siRNA, and the extent of syndecan-1 shedding after PMA stimulation was measured. The extent of silencing of ADAM17 was measured by western blotting. All values represent the average $\pm$ standard deviation (n = 3).

fractions, consistent with the idea that heparin prevented the association of the particles with the heparan sulfate chains on the ectodomains. Interestingly, when the mixture of VLDL and [^{35}S]-labeled ectodomains was overlaid with a lower density solution ($\delta = 1.006$ g/mL), flotation of [^{35}S]-ectodomains did not occur (data not shown), consistent with the idea that the association of ectodomains with VLDL caused a shift in the buoyant density of the complex.

LPS Causes Syndecan-1 Shedding in Mice and Increases Plasma Triglycerides. On the basis of these findings, we predicted that the steady-state level of plasma triglycerides might depend on the extent of syndecan-1 shedding that occurs in the liver. To examine this possibility, we isolated hepatocytes from wild-type C57BL/6 mice and examined syndecan-1 shedding. Syndecan-1 was constitutively shed from the cells based on the appearance of ectodomains in the conditioned media (Fig. 7A). However, in

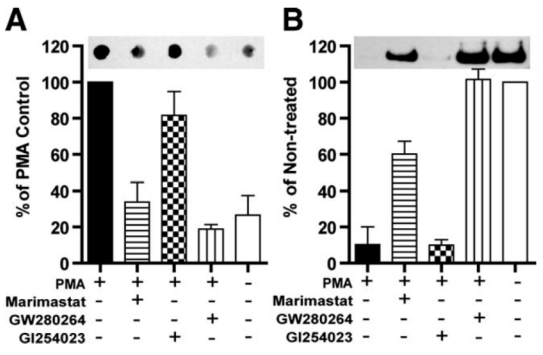

Fig. 4. PMA induces syndecan-1 shedding on primary human hepatocytes. Primary human hepatocytes cells were pretreated with different metalloproteinase inhibitors and then stimulated with 0.25 μM PMA for 1 hour. Syndecan-1 shedding was measured by dot blotting of the medium (A) and by western blotting of syndecan-1 in the cell lysate (B). All values represent the average $\pm$ standard deviation (n = 3).

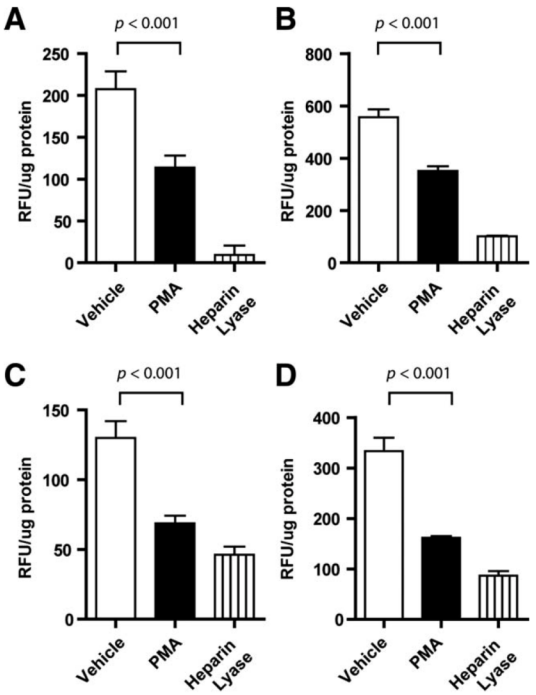

Fig. 5. PMA-induced shedding reduces VLDL binding and uptake. Hep3B cells (A,B) and primary human hepatocytes (C,D) were treated with 0.25 μM PMA for 1 hour (filled bars) or heparin lyase for 30 minutes (hatched bars) and then incubated with DiD-VLDL (100 μg/mL) for 1 hour at 4°C for binding (A,C) or at 37°C for binding and uptake (B,D). The fluorescence intensity was quantitated and normalized to cell protein. Control cells were not treated with PMA (open bars). All values represent the average $\pm$ standard deviation (n = 3).

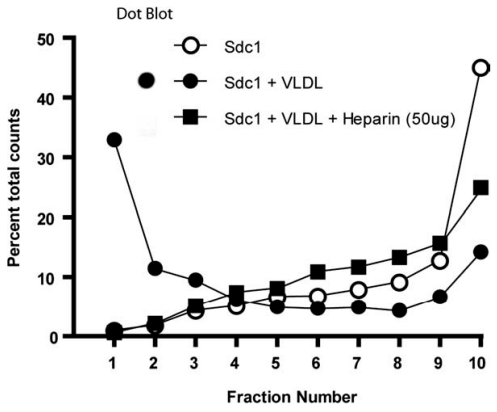

Fig. 6. Shed syndecan-1 binds VLDL. [^{35}S]-Labeled syndecan-1 ectodomains were combined with 50 μg of human VLDL in the presence (squares) or absence (filled circles) of 50 μg of heparin. A sample of ectodomains was incubated with buffer alone as a control (open circles). The samples were then adjusted to $\delta = 1.019$ g/mL with iodixanol and centrifuged. Fractions taken sequentially from the top of the tubes were assayed for radioactivity and syndecan-1 ectodomains (embedded dot blot figure).

Discussion

Here, we show that the heparan sulfate proteoglycan syndecan-1 mediates clearance of VLDL in human hepatoma cells and primary human hepatocytes. Furthermore, we demonstrate that shed syndecan-1 ectodomains from human hepatoma cells bind VLDL particles *in vitro* (Fig. 6), consistent with the idea that ectodomains contain the ligand binding site of the syndecan-1 receptor. Importantly, stimulation of shedding of syndecan-1 in mice was accompanied by an increase in fasting triglycerides (Fig. 8). Proteoglycan receptors appear to dominate the receptor landscape on human hepatocytes as on murine hepatocytes, representing at least 90% of the binding sites.[11]

Earlier studies of TRL uptake in human hepatocytes focused on hepatoma cell lines, such as HepG2 and Hep3B, that are derived from well-differentiated human hepatocellular carcinomas[12,31,32] or more rarely on primary hepatocytes.[33] The data demonstrated that the addition of apolipoprotein E and lipoprotein lipase to particles enhanced their uptake, and that under contrast to human hepatocytes, shedding was insensitive to Marimastat (or PMA stimulation; data not shown). Other factors previously shown to induce shedding in other cells types such as insulin, LPS, and tumor necrosis factor-α (TNF-α), also were without effect.[28-30]

Hayashida et al. recently showed that in mice, injection of LPS induces syndecan-1 shedding in liver.[16] We confirmed this finding by dot blotting of plasma samples 24 hours after injection of 4.5 mg LPS/kg body weight into mice, compared to the level in mice injected with vehicle (Fig. 7B). LPS injection also resulted in dramatic loss of syndecan-1 in the liver, as measured by immunohistochemistry (Fig. 7C). Analysis of fasting plasma lipids showed that triglyceride levels increased two-fold in mice injected with LPS (Fig. 8A), whereas plasma total cholesterol did not change (Fig. 8B). The accumulation of plasma lipids was greatly accentuated under these conditions by deletion of the LDL receptor, which resembles the phenotype of compound mutants lacking hepatic heparan sulfate and LDL receptors (Supporting Fig. 5).[9] When the animals were challenged with human VLDL, the injected particles cleared less extensively in the LPS-injected mice (Fig. 8C; area under the curve = 9200 ± 400 for LPS-injected mice versus 7000 ± 400 for the control), consistent with a loss of syndecan-1 clearance receptors in the liver.

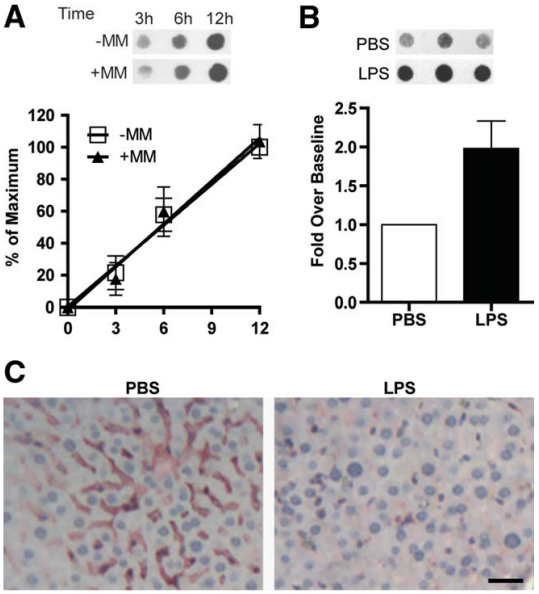

Fig. 7. LPS causes syndecan-1 shedding in the liver. Conditioned medium was collected from primary mouse hepatocytes incubated in the presence (triangles) or absence (squares) of Marimastat (MM). (A) Shed syndecan-1 was measured by dot blotting (n = 3). (B) Mice were injected intraperitoneally with 4.5 mg LPS/kg body weight or phosphate-buffered saline and plasma syndecan-1 was measured by dot blotting 24 hours later. All values represent the average ± standard deviation (n = 5). (C) The livers were harvested, fixed in paraformaldehyde, and immunostained for mouse syndecan-1 using mAb 281-2. Bar = 50 μm.

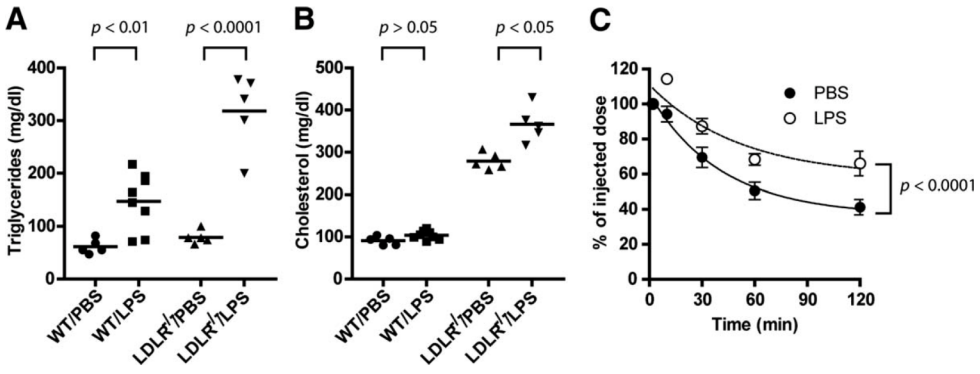

Fig. 8. LPS increases plasma triglycerides in mice. Wild-type (WT) or *Ldlr*$^{-/-}$ mice were injected intraperitoneally with 4.5 mg LPS/kg body weight or phosphate-buffered saline as control. Eighteen hours later, the animals were fasted for 6 hours, and (A) plasma triglycerides and (B) total cholesterol were determined. In (C), similarly treated animals were injected with 20 μg of human VLDL, and the amount of remaining human apolipoprotein B was determined by ELISA at the indicated times. Each value represents the average ± standard deviation (n = 3 mice).

these conditions, uptake occurred in a manner dependent on heparan sulfate. Similar observations were made using nonhepatic cell lines, which also suggested the participation of various syndecans[34-39] and perlecan.[34,35,37,40] Zeng et al. showed that syndecan-1 can mediate binding and uptake of chylomicron remnants by HepG2 liver cells *in vitro* based on antisense and antibody inhibition experiments.[12] In this report, we show that syndecan-1 on primary human hepatocytes as well as Hep3B cells can bind and take up native TRL particles derived from fasted donors. Prior genetic studies in mice and silencing experiments in human hepatocytes suggest that other heparan sulfate proteoglycans probably do not fulfill this role, emphasizing that syndecan-1 may be the dominant proteoglycan clearance receptor in humans as well as in mice.[11]

It has been estimated that as much as 4% of all cell-surface receptors undergo regulated proteolytic shedding.[41] Syndecan-1 also undergoes proteolytic processing, resulting in shedding of ectodomains containing the attached glycosaminoglycan chains.[42] The shedding process occurs in hepatocytes and appears to be mediated by ADAM17 both under basal conditions (data not shown) and after PMA stimulation (Figs. 3 and 4). The inducibility of syndecan-1 shedding by inflammation, ischemia, glucose, and insulin suggests that shed ectodomains might have functional significance.[28,43-46] Shed syndecan-1 ectodomains might bind plasma lipoproteins in the space of Disse and prevent their escape back into the plasma or facilitate their further processing prior to uptake. Because shedding of ectodomains increases plasma triglycerides (Fig. 8), shedding would appear to serve an alternative role, e.g., increasing the circulatory half-life of TRLs for more complete use of triglycerides in peripheral tissues. In order to study this question, studies are underway that use recombinant forms of syndecan-1 that fail to shed or which are shed constitutively.

Shedding of syndecan-1 in hepatocytes depends on ADAM17, which can be induced by treatment with PMA through a pathway dependent on protein kinase C. ADAM17, also known as TNF-α–converting enzyme, processes membrane-bound pro–TNF-α, releasing the soluble active form of TNF-α, as well as other factors involved in inflammation, including L-selectin,[46-48] LRP1,[43] TNF-α receptors TNFR1 and TNFR2,[49] CD30,[50] and interleukin-6 receptor IL-6R.[51] Park and colleagues have demonstrated that the role of syndecan-1 ectodomains in lung inflammation is to modulate the availability of chemokines.[52] It is also well known that LPS can bind to lipoproteins, which serves as a sink for this potent inflammatory mediator.[53] Thus, one can imagine that activation of shedding and the ensuing increase in plasma TRLs might serve a protective role during infection. The observation that LPS induces shedding, elevates plasma TRLs, and reduces VLDL clearance is consistent with this hypothesis and suggests that syndecan-1 shedding might be responsible in part for the elevation of plasma triglycerides in bacterial sepsis.[54,55] Further studies are planned to determine whether syndecan-1 shedding contributes to the hyperlipidemia of sepsis in human patients and whether it might explain other idiopathic forms of hypertriglyceridemia, a common side effect of many drugs.[56]

Acknowledgment: We thank Joe Juliano for performing lipid analyses, Andrea Garcia and Dr. Nissi Varki for their help on the syndecan-1 immunohistochemistry,

and Drs. Pyong Park and Joseph Witztum for many helpful discussions.

References

1. Kita T, Goldstein JL, Brown MS, Watanabe Y, Hornick CA, Havel RJ. Hepatic uptake of chylomicron remnants in WHHL rabbits: a mechanism genetically distinct from the low density lipoprotein receptor. Proc Natl Acad Sci U S A 1982;79:3623-3627.
2. Ishibashi S, Perrey S, Chen Z, Osuga J, Shimada M, Ohashi K, et al. Role of the low density lipoprotein (LDL) receptor pathway in the metabolism of chylomicron remnants. A quantitative study in knockout mice lacking the LDL receptor, apolipoprotein E, or both. J Biol Chem 1996;271:22422-22427.
3. Rohlmann A, Gotthardt M, Hammer RE, Herz J. Inducible inactivation of hepatic LRP gene by cre-mediated recombination confirms role of LRP in clearance of chylomicron remnants. J Clin Invest 1998;101: 689-695.
4. Fujino T, Asaba H, Kang MJ, Ikeda Y, Sone H, Takada S, et al. Low-density lipoprotein receptor-related protein 5 (LRP5) is essential for normal cholesterol metabolism and glucose-induced insulin secretion. Proc Natl Acad Sci U S A 2003;100:229-234.
5. Narvekar P, Berriel Diaz M, Krones-Herzig A, Hardeland U, Strzoda D, Stohr S, et al. Liver-specific loss of lipolysis-stimulated lipoprotein receptor triggers systemic hyperlipidemia in mice. Diabetes 2009;58: 1040-1049.
6. Williams KJ, Chen K. Recent insights into factors affecting remnant lipoprotein uptake. Curr Opin Lipidol 2010;21:218-228.
7. Foley EM, Esko JD. Hepatic heparan sulfate proteoglycans and endocytic clearance of triglyceride-rich lipoproteins. Prog Mol Biol Transl Sci 2010;93:213-233.
8. Bernfield M, Kokenyesi R, Kato M, Hinkes MT, Spring J, Gallo RL, et al. Biology of the syndecans: a family of transmembrane heparan sulfate proteoglycans. Annu Rev Cell Biol 1992;8:365-393.
9. MacArthur JM, Bishop JR, Wang L, Stanford KI, Bensadoun A, Witztum JL, et al. Liver heparan sulfate proteoglycans mediate clearance of triglyceride-rich lipoproteins independently of LDL receptor family members. J Clin Invest 2007;117:153-164.
10. Stanford KI, Wang L, Castagnola J, Song D, Bishop JR, Brown JR, et al. Heparan sulfate 2-O-sulfotransferase is required for triglyceride-rich lipoprotein clearance. J Biol Chem 2010;285:286-294.
11. Stanford KI, Bishop JR, Foley EM, Gonzales JC, Niesman IR, Witztum JL, et al. Syndecan-1 is the primary heparan sulfate proteoglycan mediating hepatic clearance of triglyceride-rich lipoproteins in mice. J Clin Invest 2009;119:3236-3245.
12. Zeng BJ, Mortimer BC, Martins IJ, Seydel U, Redgrave TG. Chylomicron remnant uptake is regulated by the expression and function of heparan sulfate proteoglycan in hepatocytes. J Lipid Res 1998;39: 845-860.
13. Wilsie LC, Orlando RA. The low density lipoprotein receptor-related protein complexes with cell surface heparan sulfate proteoglycans to regulate proteoglycan-mediated lipoprotein catabolism. J Biol Chem 2003;278:15758-15764.
14. Manon-Jensen T, Itoh Y, Couchman JR. Proteoglycans in health and disease: the multiple roles of syndecan shedding. FEBS J 2010;277: 3876-3889.
15. Hayashida A, Amano S, Park PW. Syndecan-1 promotes Staphylococcus aureus corneal infection by counteracting neutrophil-mediated host defense. J Biol Chem 2011;286:3288-3297.
16. Hayashida K, Parks WC, Park PW. Syndecan-1 shedding facilitates the resolution of neutrophilic inflammation by removing sequestered CXC chemokines. Blood 2009;114:3033-3043.
17. Hayashida A, Bartlett AH, Foster TJ, Park PW. Staphylococcus aureus beta-toxin induces lung injury through syndecan-1. Am J Pathol 2009; 174:509-518.
18. Teupser D, Thiery J, Walli AK, Seidel D. Determination of LDL- and scavenger-receptor activity in adherent and non-adherent cultured cells with a new single-step fluorometric assay. Biochim Biophys Acta 1996; 1303:193-198.
19. Young SG, Smith RS, Hogle DM, Curtiss LK, Witztum JL. Two new monoclonal antibody-based enzyme-linked assays of apolipoprotein B. Clin Chem 1986;32:1484-1490.
20. Esko JD. Special considerations for proteoglycans and glycosaminoglycans and their purification. Curr Protoc Mol Biol 2001;Chapter 17: Unit 17.2.
21. Gustafson A, Alaupovic P, Furman RH. Studies of the composition and structure of serum lipoproteins: isolation, purification, and characterization of very low density lipoproteins of human serum. Biochemistry 1965;4:596-605.
22. Krapp A, Zhang H, Ginzinger D, Liu MS, Lindberg A, Olivecrona G, et al. Structural features in lipoprotein lipase necessary for the mediation of lipoprotein uptake into cells. J Lipid Res 1995;36:2362-2373.
23. Roskams T, Moshage H, De Vos R, Guido D, Yap P, Desmet V. Heparan sulfate proteoglycan expression in normal human liver. HEPATOLOGY 1995;21:950-958.
24. Roskams T, De Vos R, David G, Van Damme B, Desmet V. Heparan sulphate proteoglycan expression in human primary liver tumours. J Pathol 1998;185:290-297.
25. Aballay A, Stahl PD, Mayorga LS. Phorbol ester promotes endocytosis by activating a factor involved in endosome fusion. J Cell Sci 1999; 112:2549-2557.
26. Basford JE, Wancata L, Hofmann SM, Silva RA, Davidson WS, Howles PN, et al. Hepatic deficiency of low density lipoprotein receptor-related protein-1 reduces high density lipoprotein secretion and plasma levels in mice. J Biol Chem 2011;286:13079-13087.
27. Pruessmeyer J, Martin C, Hess FM, Schwarz N, Schmidt S, Kogel T, et al. A disintegrin and metalloproteinase 17 (ADAM17) mediates inflammation-induced shedding of syndecan-1 and -4 by lung epithelial cells. J Biol Chem 2010;285:555-564.
28. Reizes O, Goldberger O, Smith AC, Xu Z, Bernfield M, Bickel PE. Insulin promotes shedding of syndecan ectodomains from 3T3-L1 adipocytes: a proposed mechanism for stabilization of extracellular lipoprotein lipase. Biochemistry 2006;45:5703-5711.
29. Andrian E, Grenier D, Rouabhia M. Porphyromonas gingivalis lipopolysaccharide induces shedding of syndecan-1 expressed by gingival epithelial cells. J Cell Physiol 2005;204:178-183.
30. Henry-Stanley MJ, Zhang B, Erlandsen SL, Wells CL. Synergistic effect of tumor necrosis factor-alpha and interferon-gamma on enterocyte shedding of syndecan-1 and associated decreases in internalization of Listeria monocytogenes and Staphylococcus aureus. Cytokine 2006;34: 252-259.
31. Huff MW, Miller DB, Wolfe BM, Connelly PW, Sawyez CG. Uptake of hypertriglyceridemic very low density lipoproteins and their remnants by HepG2 cells: the role of lipoprotein lipase, hepatic triglyceride lipase, and cell surface proteoglycans. J Lipid Res 1997;38:1318-1333.
32. Mann WA, Meyer N, Berg D, Greten H, Beisiegel U. Lipoprotein lipase compensates for the defective function of apo E variants in vitro by interacting with proteoglycans and lipoprotein receptors. Atherosclerosis 1999;145:61-69.
33. Mann WA, Meyer N, Weber W, Rinninger F, Greten H, Beisiegel U. Apolipoprotein E and lipoprotein lipase co-ordinately enhance binding and uptake of chylomicrons by human hepatocytes. Eur J Clin Invest 1995;25:880-882.
34. Williams KJ, Fuki IV. Cell-surface heparan sulfate proteoglycans: dynamic molecules mediating ligand catabolism. Curr Opin Lipidol 1997;8:253-262.
35. Williams KJ. Molecular processes that handle–and mishandle–dietary lipids. J Clin Invest 2008;118:3247-3259.
36. Fuki IV, Kuhn KM, Lomazov IR, Rothman VL, Tuszynski GP, Iozzo RV, et al. The syndecan family of proteoglycans. Novel receptors mediating internalization of atherogenic lipoproteins in vitro. J Clin Invest 1997;100:1611-1622.

37. Fuki IV, Iozzo RV, Williams KJ. Perlecan heparan sulfate proteoglycan: a novel receptor that mediates a distinct pathway for ligand catabolism. J Biol Chem 2000;275:25742-25750.
38. Wilsie LC, Gonzales AM, Orlando RA. Syndecan-1 mediates internalization of apoE-VLDL through a low density lipoprotein receptor-related protein (LRP)-independent, non-clathrin-mediated pathway. Lipids Health Dis 2006;5:23.
39. Williams KJ. Interactions of lipoproteins with proteoglycans. Methods Mol Biol 2001;171:457-477.
40. Ebara T, Conde K, Kako Y, Liu Y, Xu Y, Ramakrishnan R, et al. Delayed catabolism of apoB-48 lipoproteins due to decreased heparan sulfate proteoglycan production in diabetic mice. J Clin Invest 2000; 105:1807-1818.
41. Arribas J, Massague J. Transforming growth factor-alpha and beta-amyloid precursor protein share a secretory mechanism. J Cell Biol 1995; 128:433-441.
42. Wang Z, Götte M, Bernfield M, Reizes O. Constitutive and accelerated shedding of murine syndecan-1 is mediated by cleavage of its core protein at a specific juxtamembrane site. Biochemistry 2005;44: 12355-12361.
43. Gorovoy M, Gaultier A, Campana WM, Firestein GS, Gonias SL. Inflammatory mediators promote production of shed LRP1/CD91, which regulates cell signaling and cytokine expression by macrophages. J Leukoc Biol 2010;88:769-778.
44. Rehm M, Bruegger D, Christ F, Conzen P, Thiel M, Jacob M, et al. Shedding of the endothelial glycocalyx in patients undergoing major vascular surgery with global and regional ischemia. Circulation 2007; 116:1896-1906.
45. Zurhove K, Nakajima C, Herz J, Bock HH, May P. Gamma-secretase limits the inflammatory response through the processing of LRP1. Sci Signal 2008;1:ra15.
46. Wang Y, Herrera AH, Li Y, Belani KK, Walcheck B. Regulation of mature ADAM17 by redox agents for L-selectin shedding. J Immunol 2009;182:2449-2457.
47. Condon TP, Flournoy S, Sawyer GJ, Baker BF, Kishimoto TK, Bennett CF. ADAM17 but not ADAM10 mediates tumor necrosis factor-alpha and L-selectin shedding from leukocyte membranes. Antisense Nucleic Acid Drug Dev 2001;11:107-116.
48. Le Gall SM, Bobe P, Reiss K, Horiuchi K, Niu XD, Lundell D, et al. ADAMs 10 and 17 represent differentially regulated components of a general shedding machinery for membrane proteins such as transforming growth factor alpha, L-selectin, and tumor necrosis factor alpha. Mol Biol Cell 2009;20:1785-1794.
49. Bell JH, Herrera AH, Li Y, Walcheck B. Role of ADAM17 in the ectodomain shedding of TNF-alpha and its receptors by neutrophils and macrophages. J Leukoc Biol 2007;82:173-176.
50. Vahdat AM, Reiners KS, Simhadri VL, Eichenauer DA, Boll B, Chalaris A, et al. TNF-alpha-converting enzyme (TACE/ADAM17)-dependent loss of CD30 induced by proteasome inhibition through reactive oxygen species. Leukemia 2010;24:51-57.
51. Matthews V, Schuster B, Schutze S, Bussmeyer I, Ludwig A, Hundhausen C, et al. Cellular cholesterol depletion triggers shedding of the human interleukin-6 receptor by ADAM10 and ADAM17 (TACE). J Biol Chem 2003;278:38829-38839.
52. Li Q, Park PW, Wilson CL, Parks WC. Matrilysin shedding of syndecan-1 regulates chemokine mobilization and transepithelial efflux of neutrophils in acute lung injury. Cell 2002;111:635-646.
53. Barcia AM, Harris HW. Triglyceride-rich lipoproteins as agents of innate immunity. Clin Infect Dis 2005;41(suppl 7):S498-S503.
54. Mizock BA. Metabolic derangements in sepsis and septic shock. Crit Care Clin 2000;16:319-336.
55. Evans RD, Williamson DH. Signals, mechanisms, and function of the acute lipid response to sepsis. Biochem Cell Biol 1991;69:320-321.
56. Yuan G, Al-Shali KZ, Hegele RA. Hypertriglyceridemia: its etiology, effects and treatment. CMAJ 2007;176:1113-1120.

SUPPORTING EXPERIMENTAL PROCEDURES

RT-PCR of heparan sulfate proteoglycans. RNA was isolated from primary human hepatocytes (RNAqueous; Ambion, Austin, TX), reverse transcribed (Superscript II; Invitrogen) and amplified using intron spanning primers (Supporting Table 1). Power SYBR green (Applied Biosystems, Foster City, CA) was used to obtain C(T) values. Quantitation was done by the $2^{-\Delta\Delta C(t)}$ method using β-actin as a control (16). C(T) values from duplicate assays were used to calculate fold expression compared to β-actin.

Flow cytometry. Hepatocytes were harvested with Versene (Invitrogen), washed twice with cold PBS, and stained with Alexa Fluor 647-labeled syndecan-1 ectodomain monoclonal antibody (B-B4 clone; AbD Serotec, Oxford, UK) for 1 hr at 4^{o}C prior to analysis by flow cytometry (FACSCalibur, BD Biosciences).

SUPPORTING FIGURE LEGENDS

Supporting Fig. S1. qPCR analysis of HSPGs in primary human hepatocytes. RNA was extracted from primary human hepatocytes, reverse-transcribed, and amplified using gene-specific primers. The relative amount of RNA was determined by the $2^{-\Delta\Delta Ct}$ method, using β-actin as a control. Ct values for primary human hepatocytes were obtained from two independent RNA isolations from two human hepatocyte preparations assayed in duplicate. The values represent the mean expression compared to β-actin. Error bars represent the range.

Supporting Fig. S2. Syndecan-1 knockdown in Hep3B cells. Hep3B cells were transfected with syndecan-1 specific siRNAs and incubated for 72 hours. Cells were lifted with Versene and stained with Alexa Fluor 647-labeled syndecan-1 antibody. Cell surface syndecan-1 was measured by flow cytometry. Cells treated with syndecan-1 siRNAs (blue line) showed two populations, one representing ~70% of the cells exhibiting ~90% reduction of syndecan-1 staining and a second population (~30%) that had normal levels of syndecan-1. Another portion of cells were transfected with the scrambled siRNA (dark blue line). Wild-type Hep3B cells (red line).

Supporting Fig. S3. PMA induced syndecan-1 shedding. Hep3B cells were stimulated with the indicated concentration of PMA for 1 hour (A) or with 0.25 μM PMA for indicated time (B). Conditioned medium was collected and subjected to dot blotting for syndecan-1 ectodomains. The values represent the average amount of syndecan-1 after subtraction of the background (n = 3).

Supporting Fig. S4. ADAM-17 mediates PMA-induced shedding of syndecan-1. (A) Different signaling pathway inhibitors were tested for their ability to inhibit syndecan-1 shedding induced by PMA. (B) Hep3B cells were pretreated with different metalloproteinase inhibitors and then stimulated with 0.25 μM PMA for 1 hour. (C) ADAM-17 was silenced by siRNA. Cells were reacted with mAb 281-2 and analyzed by flow cytometry. The profiles represent a representative sample (n=4). Samples of the medium were also analyzed by dot blotting (cf. Fig. 3).

Supporting Fig. S5. Additive effects of altering heparan sulfate and Ldlr on plasma lipids. Plasma triglycerides and cholesterol were measured in wildtype mice, mice carrying a hepatocyte-specific deletion of the heparan sulfate biosynthetic gene, N-deacetylase-N-sulfotransferase (*Ndst1*$^{f/f}$*AlbCre*$^{+}$ = HS$^{-/-}$), LDL receptor-deficient mice *(Ldlr*$^{-/-}$), or mice carrying both mutations. Data was derived from Ref. (23) and presented for comparison to similar data obtained from wildtype or *Ldlr*$^{-/-}$ mice injected with LPS (cf. Fig. 8).

Sup. Fig. S1

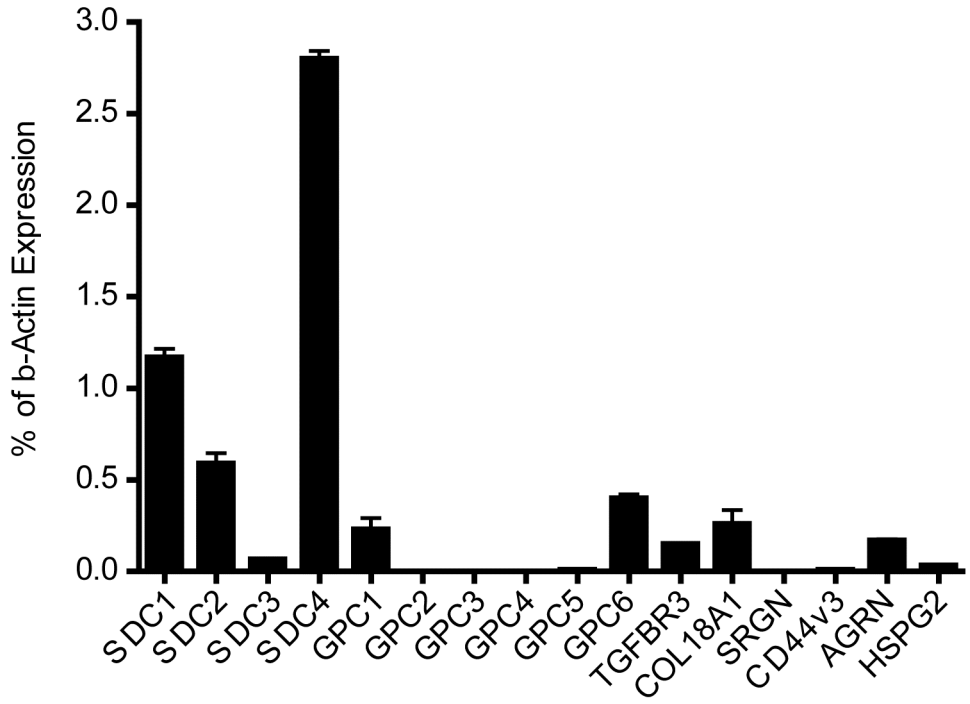
% of b-Actin Expression
3.0
2.5
2.0
1.5
1.0
0.5
0.0
SDC1
SDC2
SDC3
SDC4
GPC1
GPC2
GPC3
GPC4
GPC5
GPC6
TGFBR3
COL18A1
SRGN
CD44v3
AGRN
HSPG2

Sup. Fig. S2

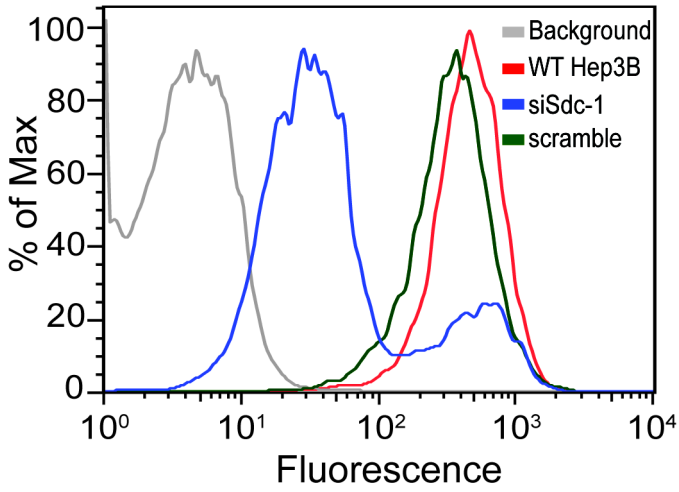
100
80
60
40
20
0
% of Max
10^0
10^1
10^2
10^3
10^4
Fluorescence
Background
WT Hep3B
siSdc-1
scramble

Sup. Fig. S3

A

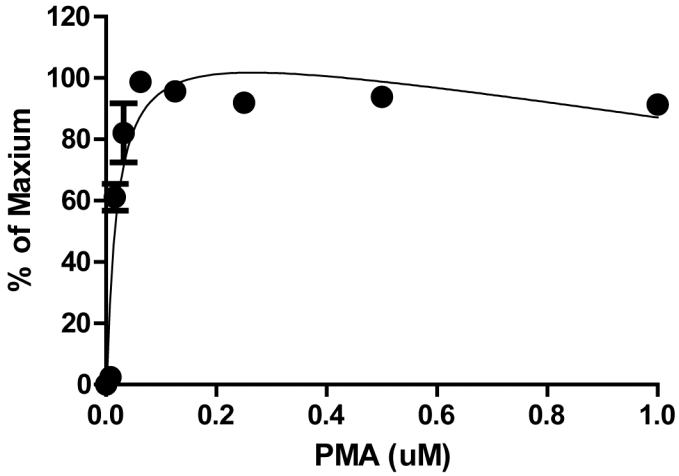
120
100
80
60
40
20
0
% of Maxium
0.0
0.2
0.4
0.6
0.8
1.0
PMA (uM)

B

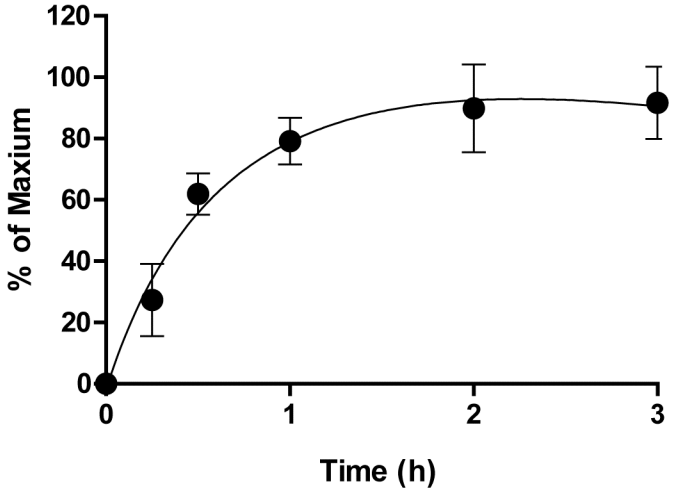
120
100
80
60
40
20
0
% of Maxium
0
1
2
3
Time (h)

Sup. Fig. S4

A

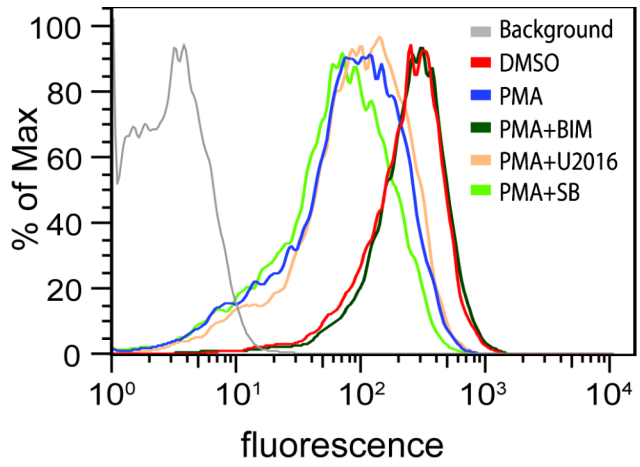

B

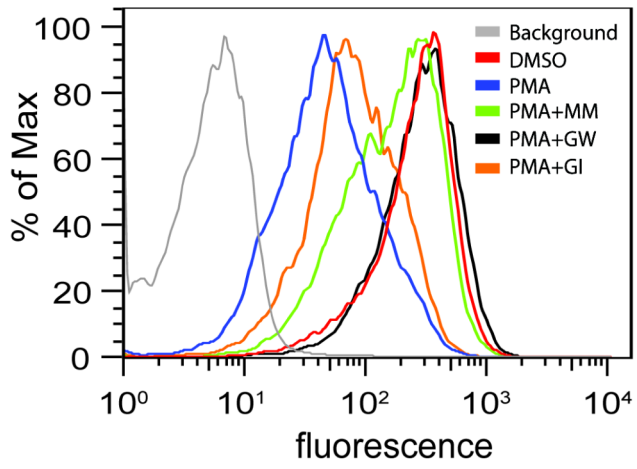

C

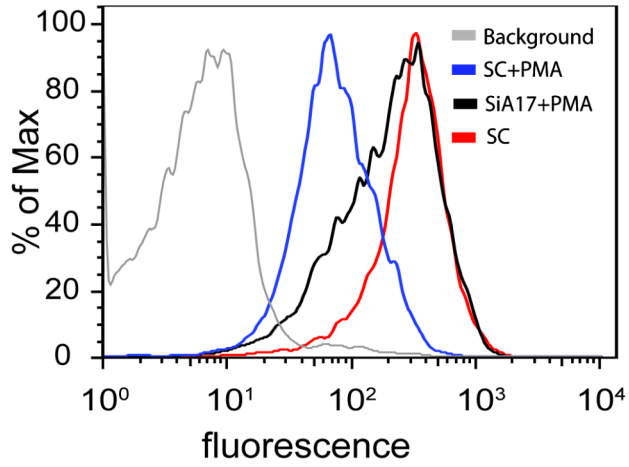

Sup. Fig. S5

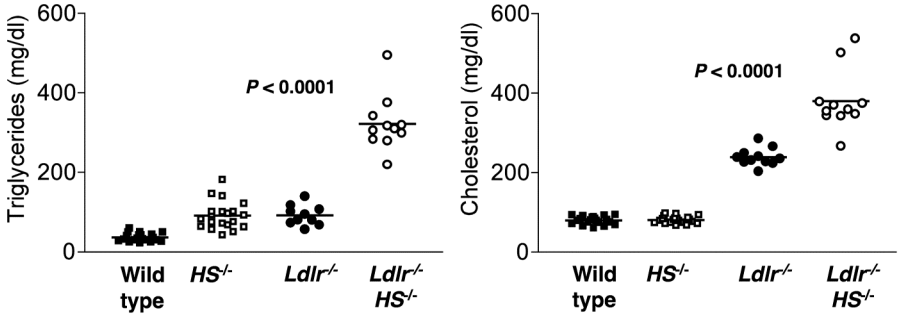
Triglycerides (mg/dl)
600
400
200
0
P < 0.0001
Wild type
HS-/-
Ldlr-/-
Ldlr-/- HS-/-
Cholesterol (mg/dl)
600
400
200
0
P < 0.0001
Wild type
HS-/-
Ldlr-/-
Ldlr-/- HS-/-